UNIVERSITAT
JAUME·I

TETRAMETALLIC (GOLD, IRIDIUM AND RHODIUM) COMPLEXES BASED

ON N-HETEROCYCLIC CARBENES. FROM LUMINESCENT PROPERTIES TO

SUPRAMOLECULAR ASSEMBLIES.

Ana Mª Gutiérrez Blanco

Supervisors: Prof. Dr. Eduardo Peris & Dr. Macarena Poyatos

Castellón de la Plana, Marzo de 2021

Programa de Doctorado en Ciencias

Escuela de Doctorado de la Universitat Jaume I

TETRAMETALLIC (GOLD, IRIDIUM AND RHODIUM) COMPLEXES BASED ON N-HETEROCYCLIC CARBENES. FROM LUMINESCENT PROPERTIES TO SUPRAMOLECULAR ASSEMBLIES.

Memoria presentada por Ana Gutiérrez Blanco para optar al grado de doctor/a por la Universidad Jaume I

Ana Mª Gutiérrez Blanco   **Eduardo Peris Fajarnés**

Macarena Poyatos de Lorenzo

Castellón de la Plana, Marzo de 2021

Scientific contribution

Publications included in this Thesis

1. Ana Gutiérrez-Blanco, Vanesa Fernández-Moreira, M. Concepción Gimeno, Eduardo Peris, and Macarena Poyatos. Tetra-Au(I) Complexes Bearing a Pyrene Tetraalkynyl Connector Behave as Fluorescence Torches, *Organometallics*, **2018**, 37, 1795-1800. (DOI: 10.1021/acs.organomet.8b00217).

   Impact factor 2018-19: 4.100 (Q1)

2. Ana Gutiérrez-Blanco, Eduardo Peris, and Macarena Poyatos. Pyrene-Connected Tetraimidazolylidene Complexes of Iridium and Rhodium. Structural Features and Catalytic Applications, *Organometallics*, **2018**, 37, 4070-4076. (DOI: 10.1021/acs.organomet.8b00633).

   Impact factor 2018-19: 4.100 (Q1)

3. Ana Gutiérrez-Blanco, Susana Ibáñez, F. Ekkehardt Hahn, Macarena Poyatos, and Eduardo Peris. A Twisted Tetragold Cyclophane from a Fused Bis-Imidazolindiylidene, *Organometallics*, **2019**, 38, 4565-4569. (DOI: 10.1021/acs.organomet.9b00719).

   Impact factor 2018-19: 4.100 (Q1)

Publications not included in this Thesis

Christian B. Dobbe, Ana Gutiérrez-Blanco, Tristan T. Y. Tan, Alexander Hepp, Macarena Poyatos, Eduardo Peris, and F. Ekkehardt Hahn. Template-Controlled Synthesis of Polyimidazolium Salts by Multiple [2+2] Cycloaddition Reactions, *Chemistry — A European Journal*, **2020**, 26, 11565-11570. (DOI: 10.1002/chem.202001515).

Participation in Conferences

o *NHC-based Au(I) complexes supported by 1,3,6,8-tetraethynylpyrene.* Ana Gutiérrez Blanco, Macarena Poyatos de Lorenzo, and Eduardo Peris Fajarnés. X International School on Organometallic Chemistry "Marcial Moreno Mañas", June 2017, Ciudad Real, Spain. (Flash presentation).

o *NHC-based Au(I) complexes supported by 1,3,6,8-tetraethynylpyrene.* Ana Gutiérrez Blanco, Eduardo Peris Fajarnés, and Macarena Poyatos de Lorenzo. XI International School of Organometallic Chemistry "ISOC", September 2017, San Benedetto del Tronto, Italy. (Flash presentation).

o *Tetranuclear Rhodium(I) and Iridium(I) complexes: synthesis, electronic properties, and catalytic studies.* Ana Gutiérrez Blanco, Eduardo Peris Fajarnés, and Macarena Poyatos de Lorenzo. XI International School on Organometallic Chemistry "Marcial Moreno Mañas", June 2018, Oviedo, Spain. (Flash presentation).

o *Tetra-Au(I) complexes bearing a pyrene-tetra-alkynyl connector behave as fluorescence torches.* Ana Gutiérrez Blanco, Vanesa Fernández Moreira, María Concepción Gimeno, Eduardo Peris Fajarnés, and Macarena Poyatos de Lorenzo. 28th International Conference on Organometallic Chemistry (ICOMC), July 2018, Florence, Italy. (Flash presentation).

o *Supramolecular self-assembly structures from a di-Au(I) complex with a hinge-shaped ligand.* Ana Gutiérrez Blanco, Susana Ibáñez Maella, Eduardo Peris Fajarnés, and Macarena Poyatos de Lorenzo. XXXVII Reunión Bienal de la Real Sociedad Española de Química, May 2019, San Sebastián, Spain. (Flash presentation).

o *Synthesis of three-dimensional NHC-based silver(I) cages.* Ana Gutiérrez Blanco, F. Ekkehardt Hahn, Eduardo Peris Fajarnés, and Macarena Poyatos de Lorenzo. XII International School on Organometallic Chemistry "Marcial Moreno Mañas", June 2019, Castellón, Spain. (Poster).

"This Thesis has been accepted by the co-authors of the publications listed above that have waved the right to present them as a part of another PhD thesis"

Acknowledgements

Desde aquel primer día hasta hoy ha habido tantos momentos y personas a las que agradecer que realmente no creo que sea capaz de llegar ni a una mínima parte de lo que todos ellos merecen.

Gracias Eduardo Peris, no sólo por ser mi director de tesis, no sólo por todas las correcciones y explicaciones durante todos estos años. El agradecimiento va más allá, va por todos esos proyectos que me has confiado, por todas esas ideas que con tanto entusiasmo me has transmitido, por darme la posibilidad de formar parte de este gran grupo y por mil cosas más que me hacen sentirme tan orgullosa de poder decir dónde he aprendido tanto. De la mano de todo esto van mis palabras para Macarena Poyatos, gracias por tanto Maca. Sí en este tiempo me llevo conmigo una milésima de todo lo que tú sabes ya he cumplido mi objetivo.

Thanks to Prof. Hahn for give me the opportunity to join his group and allow me the possibility to continue with my Ph.D. It has been a pleasure for me to listen all your advices and is amazing how much information you can transmit in such a short time.

A toda esa panda con la que he pasado tanto tiempo, ¿qué les voy a decir? Mi compi-trueno Víctor, por tantos ensayos, congresos, palabras de ánimo. A Goyo, que tantos consejos y unicornios me ha dado. A David, ese manojito de nervios como yo que es incapaz de parar ni un minuto. Carmencita, que te voy a tener conmigo de principio a fin, gran carácter y mejor persona. Andresito, igual te mato que te como, pero cuantos abrazos animosos me has dado. A Susana, vitrina con vitrina todos estos años. Al recién llegado César, ha sido breve pero intenso, no pierdas esas ganas de química que tienes. Al hijo pródigo Sergio, todo un placer poder coincidir contigo, aunque sea por poco tiempo. A Cristian, que ha traído con el mucha alegría, café y chocolate. Y a los babies Esteban y
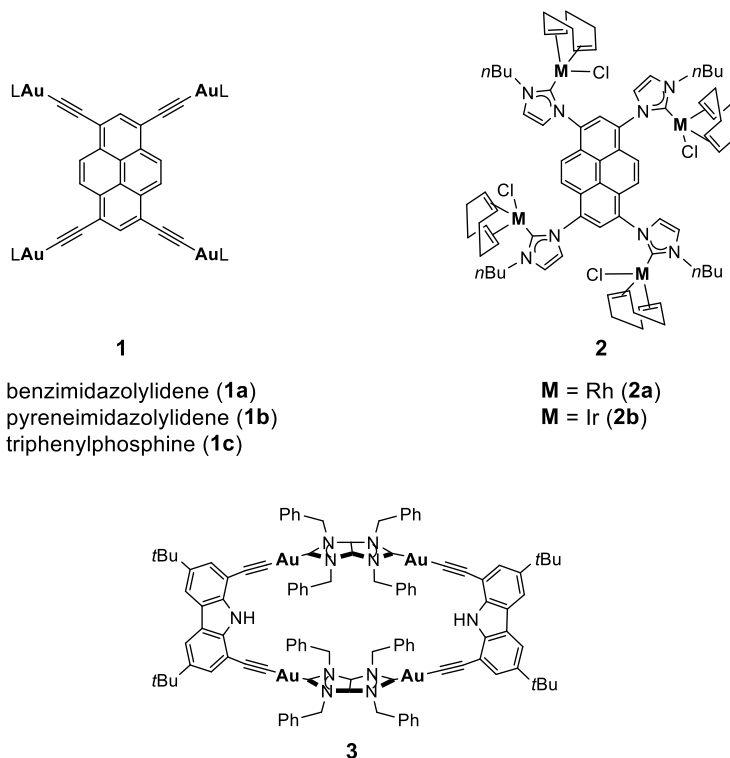
x

Abstract

This Doctoral Thesis has been developed in a collaboration between the Universitat Jaume I in Castellón (Spain) and the Westfälische Wilhelms-Universität in Münster (Germany).

The research deals with the preparation of different multimetallic complexes containing N-heterocylic carbene (NHC) ligands. In this aim, the main objective is to obtain new poly-NHC-based ligands with extended polyaromatic systems for the preparation of these complexes, which a combination of features that may give access to interesting photophysical and catalytic applications.

In the first part of the work a series of tetra-NHC gold(I) complexes with a central pyrene-tetra-alkynyl connector were synthesized (complexes **1a**-**1c** in Scheme 1). These complexes exhibited remarkably high fluorescent emission, with quantum yields that exceeded 90 %. It was found that the emission was mainly due to the presence of the pyrene central moiety, although the presence of the metal is key for reaching such large quantum yields. Confocal microscopy was used for studying the incorporation of the luminescent complexes into healthy cheek cells.

In the second part of the work, a pyrene-centred tetra-NHC ligand was prepared and coordinated to rhodium and iridium. The resulting tetra-metallic complexes were fully characterized. An interesting structural feature of these complexes is that they display axial chirality, giving rise to right- and left-handed conformations (clockwise conformation is shown for complex **2** in Scheme 1). The catalytic activity of the iridium and rhodium complexes was studied in the cyclization of acetylenic carboxylic acids and in the coupling of diphenylcyclopropenone with substituted phenylacetylenes. Interestingly, the tetra-iridium complex is the first iridium complex ever tested for this type of reaction.

In the final part of the work, an angular bridging bis-imidazolindiylidene ligand was used for the preparation of a supramolecular tetra-gold metallo-cyclophane (Scheme 1, complex **3**). The angular ligand was previously obtained by the QOMCAT group, but this is the first supramolecular organometallic complex obtained based on this type of ligand. The structure of the resulting metallo-cyclophane was determined by means of X-ray diffraction studies. The results obtained demonstrate that the rigid angular di-NHC ligand is a suitable scaffold for the reliable construction of organometallic-based metallosupramolecular assemblies.

L = benzimidazolylidene (**1a**)
L = pyreneimidazolylidene (**1b**)
L = triphenylphosphine (**1c**)

M = Rh (**2a**)
M = Ir (**2b**)

Scheme 1: Tetrametallic complexes synthesized during the Doctoral Thesis.

Resumen

Esta Tesis Doctoral ha sido desarrollada en colaboración entre la Universitat Jaume I en Castellón (España) y la Westfälische Wilhelms-Universität en Münster (Alemania).
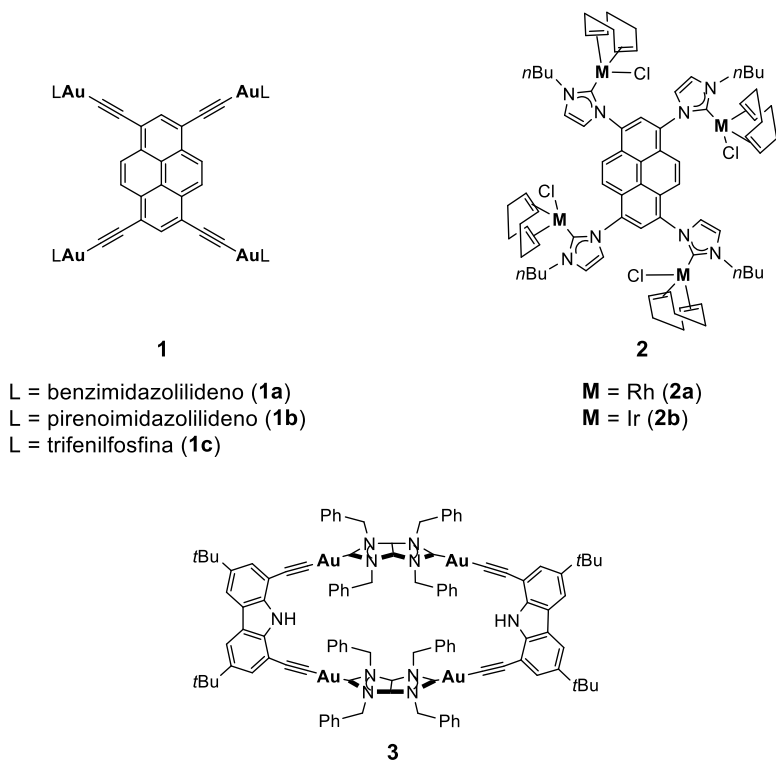
La investigación trata sobre la preparación de diferentes complejos multimetálicos que contienen ligandos carbeno N-heterocíclico (NHC). Con este propósito, el objetivo principal es la obtención de nuevos ligandos basados en poli-NHC con sistemas poliaromáticos extendidos para la preparación d estos complejos, con una combinación de características que pueden dar acceso a aplicaciones fotofísicas y catalíticas interesantes.

En la primera parte del trabajo fueron sintetizados una serie de complejos de oro(I) tetra-NHC con un conector central pireno tetra-alquino (complejos **1a**-**1c** en Esquema 1). Estos complejos exhibieron emisión fluorescente remarcablemente alta, con rendimientos cuánticos que excedieron el 90 %. Se supo que la emisión era principalmente debida a la presencia del fragmento central de pireno, aunque la presencia del metal es clave para alcanzar rendimientos cuánticos tan altos. Se utilizó microscopía confocal para estudiar la incorporación de los complejos luminiscentes en células sanas de la mejilla.

En la segunda parte del trabajo, se preparó un ligando tetra-NHC centrado en pireno y se coordinó a rodio e iridio. Los complejos tetra-metálicos resultantes fueron completamente caracterizados. Una característica estructural interesante de estos complejos es que muestran quiralidad axial, dando lugar a conformaciones con sentido derecho e izquierdo (se muestra la conformación en el sentido de las agujas del reloj para el complejo **2** en el Esquema 1). Se estudió la actividad catalítica de los complejos de rodio e iridio en la ciclación de ácidos carboxílicos acetilénicos y en el acoplamiento de difenilciclopropenona

con fenilacetilenos sustituidos. Curiosamente, el complejo de tetra-iridio es el primer complejo de iridio jamás testado para este tipo de reacción.

En la parte final del trabajo, fue usado un ligando angular bis-imidazolin-di-ilideno puente para la preparación de un metalo-ciclofano supramolecular de tetra-oro (Esquema 1, complejo **3**). El ligando angular fue obtenido previamente por el grupo QOMCAT, pero este es el primer complejo supramolecular organometálico obtenido basado en este tipo de ligando. La estructura del metalo-ciclofano resultante fue determinada por medio de estudios de difracción de Rayos-X. Los resultados obtenidos demuestran que el ligando angular di-NHC rígido es una base adecuada para la construcción fiable de estructuras metalo-supramoleculares con base organometálica.

1

L = benzimidazolilideno (**1a**)
L = pirenoimidazolilideno (**1b**)
L = trifenilfosfina (**1c**)

2

M = Rh (**2a**)
M = Ir (**2b**)

3

Esquema 1. Complejos tetrametálicos sintetizados durante la Tesis Doctoral.

List of abbreviations

Δ	Refluxing temperature
φ	Quantum yield
λ	Wavelength
ν	Frequency
AcOEt	Ethyl acetate
APT	Attached Proton Test
Bnz	Benzyl
carb	Carbazole
cat.	Catalyst
COD	1,5-Cyclooctadiene
Conv.	Conversion
COSY	Correlation Spectroscopy
DME	1,2-Dimethoxyethane
DMF	Dimethylformamide
DMSO	Dimethyl sulfoxide
DOSY	Diffusion-Ordered Spectroscopy
EA	Elemental Analysis
EtOH	Ethanol
Et_2O	Diethyl ether
ESI-MS	Electrospray Ionization Mass Spectrometry
h	Hour
HMBC	Heteronuclear Multiple-Bond Correlation Spectroscopy
HRMS	High Resolution Mass Spectrometry
HSQC	Heteronuclear Single-Quantum Correlation Spectroscopy
im	Imidazole
KHMDS	Potassium bis(trimethylsilyl)amide

L		Ligand
M		Metal
MeOH		Methanol
MeCN		Acetonitrile
*n*Bu		*normal*-Butyl
NHC		N-heterocyclic carbene
NMR		Nuclear Magnetic Resonance
	δ	Chemical shift
	br	Broad
	d	Doublet
	J	Coupling constant
	m	Multiplet
	ppm	Parts per million
	s	Singlet
	t	Triplet
*n*Oct		*n*-Octyl
NOESY		Nuclear Overhauser Effect Spectroscopy
NTCDI		*N,N'*-dimethyl-naphthalenecarboxydiimide
OAc		Acetate
O*t*Bu		*Tert*-butoxide
PAH		Polycyclic Aromatic Hydrocarbon
Ph		Phenyl
PLQY		Photoluminescence Quantum Yield
PPh$_3$		Triphenylphosphine
Pyr		Pyrene
QOMCAT		Organometallic Chemistry and Homogeneous Catalysis
RT		Room Temperature
s		Second

SEM	Scanning Electron Microscopy
SSC	Supramolecular Coordination Complex
SOC	Supramolecular Organometallic Complex
t	Time
T	Temperature
TBA	Tetrabutylammonium
*t*Bu	*Tert*-butyl
TEP	Tolman Electronic Parameter
Terp	Terphenyl
THF	Tetrahydrofuran
TMS	Tetramethylsilane
UV	Ultraviolet
Vis	Visible
VT	Variable Temperature

Index

1

Introduction

Inorganic chemistry Professor Malcolm Chisholm (1945-2015) once said that *'anything that one metal can do, two can do too – and it's more fun!'*.[1] This quote is actually a colloquial way of illustrating that compounds comprised of multiple metal centers are of interest for a number of potential properties, most of the times exceeding the possibilities of complexes with only a single metal center.[2] This is because the presence in a molecule of more than one metal center may confer a reactivity that is unique when compared to that of the related monometallic analogue. For example, high-density data storage devices have benefited from the study of the magnetic properties of multimetallic complexes. The lessons learned from enzymatic processes that work through the cooperation between two or more metal centers have given rise to a growing field of research in the area of biomimetic chemistry.[3]

The close proximity between two metal centers appears to provide favorable conditions for the occurrence of enhanced catalytic properties.[4] Such enhancement can be directly ascribed to the positive cooperativity that occurs when the affinity for binding of a substrate is increased upon fixation to another metal. In the case of heterodimetallic catalysts, each metal center may be responsible for facilitating distinct catalytic cycles, so that their combination may be used for designing sophisticated tandem processes that would not be imaginable for a monometallic-based catalyst.[5]

In addition, the inclusion of polyaromatic functionalities renders complexes furnished with properties that clearly differ from those shown by complexes lacking these polyaromatic moieties.[6] One of the reasons for this is that polyaromatic systems have the ability to participate in π-π stacking interactions, with other planar π-delocalized molecules. The incorporation of polyaromatic fragments to ligands has been particularly successful in the case of poly-*N*-heterocyclic carbenes (NHCs).[5d, 7] Some examples of interesting poly-NHC ligands

decorated with polyaromatic systems containing pyracene,[6b, 8] pyrene,[9] triphenylene,[6a, 10] triphenylbenzene,[11] quinoxalinophenanthrophenazine[12] or triptycene[13] are depicted in Scheme 2.
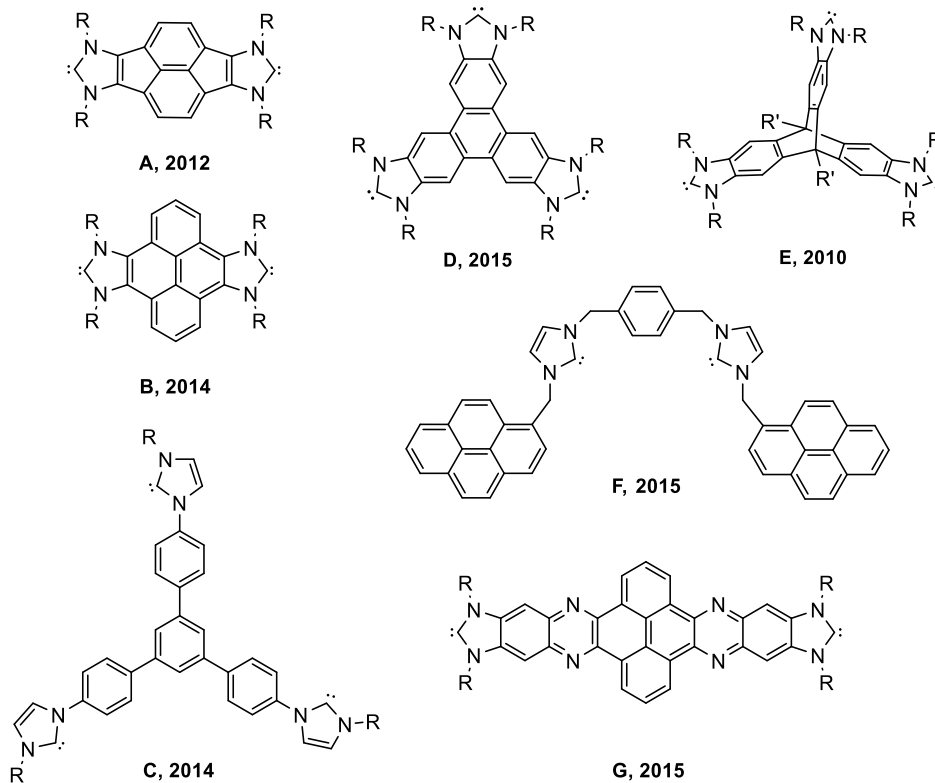
Scheme 2. Representative examples of poly-NHC ligands containing extended aromatic fragments (**A**,[8] **B**,[9c] **C**,[11] **D**,[6a] **E**,[13] **F**[14] and **G**[12]).

In this regard, transition metal complexes with poly-NHC ligands bearing polyaromatic systems are currently under great attention due to their potential in fields ranging from supramolecular chemistry,[7b, 15] catalysis[7b] or luminescence.[9c, 16] In the following sections, some of the most relevant examples that illustrate the influence of these metal complexes containing poly-conjugated aromatic systems will be described.

1. *Some basic concepts about supramolecular chemistry.*

Supramolecular chemistry deals with the study of non-covalent bonds between molecules and/or ionic species. These weak and reversible interactions, such as hydrogen bonding, hydrophobic forces, van der Waals forces, π-π stacking, etc., are key to understanding biological processes and self-assembling systems, and to constructing complex materials and molecular machinery.[17] In the several decades since its conception, supramolecular chemistry has become a truly interdisciplinary research area, providing insights into a large number of developments across biology, chemistry, nanotechnology, materials science, and physics.[18] This field of research was intensively developed in the last century by many researchers, who followed the steps of the 1987 Nobel Prize winners, C. J. Pedersen, D. J. Cram, and J. M. Lehn[18c, 19] *"for their development and use of molecules with structure-specific interactions of high selectivity"*.

Attracted by Nature's ability to obtain extremely sophisticated biomolecules by assembling simpler molecules, supramolecular chemistry attempts to mimic complex natural systems for obtaining abiotic molecules with similar properties.[20] In Nature, we can find numerous examples of self-assembly, such as protein folding, nucleic acid assembly and tertiary structure, phospholipid membranes, ribosomes and microtubules, etc., which are of vital importance to living organisms.[21] As an example, Figure 1 illustrates the folding of a polypeptide chain into the secondary structure of a protein by formation of a self-assembly architecture by H-bonding between hydrogen bond acceptors (electronegative O and N atoms with free lone pairs) and donors (H atoms attached to very electronegative atoms like O and N presenting a strong partial positive charge). As shown in the figure, adenine binds to thymine *via* two hydrogen bonds, while guanine forms three hydrogen bonds with cytosine. To achieve these structures, Nature's building blocks need to deliberately interact

through weak non-covalent interactions for facilitating the proper arrangements leading to complex architectures.[21b]

Figure 1. Formation of the secondary structure of a protein by intramolecular H-bonds between the complementary bases.

Inspired by these biological systems, synthetic receptors mimic biological recognition and regulation processes, and have revealed interesting applications in different fields such as catalysis[6a, 7b, 22] or molecular recognition.[23] These artificial supramolecular architectures result from the self-assembly of two or more chemical species by intermolecular forces and afford the creation of molecular assemblies with defined structures.

Related to all this, the following sections will be devoted to the synthesis and applications of metal-containing supramolecular systems.

1.1. *"Supermolecules" via coordination-driven self-assembly.*

In recent decades, Supramolecular Coordination Complexes (SCCs)[17b, 24] have emerged as a new branch of coordination chemistry that has given rise to diverse applications. Among the most attractive areas of applicability, catalysis,[25] sensing and molecular recognition[26] are the most widely explored ones. SCCs are discrete molecular systems, which are obtained by mixing the

metal centers of choice with the appropriate ligands that display relatively fixed angles and different binding sites. It needs to be noted that the complementarity between the building blocks is crucial in the design of discrete metallosupramolecular assemblies. The coordination geometry of the metal ions (nodes), as well as the geometry of the multidentate organic ligands (linkers), will determine the structure of the resulting materials. The mixture results in the spontaneous formation of metal-ligand bonds under self-assembly, rendering a thermodynamically stable product.

The number of supramolecular assemblies published increases progressively each year. These molecules are obtained based on different types of bonding interactions. Depending on the interactions used for the assembly, supramolecular chemistry can be broadly divided into 3 main branches:[24c]

I. Supramolecular architectures based on H-bonding motifs.

II. Systems obtained through ion-ion, ion-dipole, π-π stacking, cation-π, van der Waals, and hydrophobic interactions.

III. Assemblies that employ strong and directional metal-ligand bonds.

Coordination-driven self-assembly,[27] which is defined by the third approach, is considered the most widely used methodology for the construction of discrete SCCs. As shown in Figure 2, their structures range from 2D (rhomboids, squares, rectangles, triangles, etc.) to 3D systems (trigonal pyramids, trigonal prisms, cubes, cuboctahedra, double squares, adamantanoids, dodecahedra, and a variety of other cages).[24d, 25, 28]

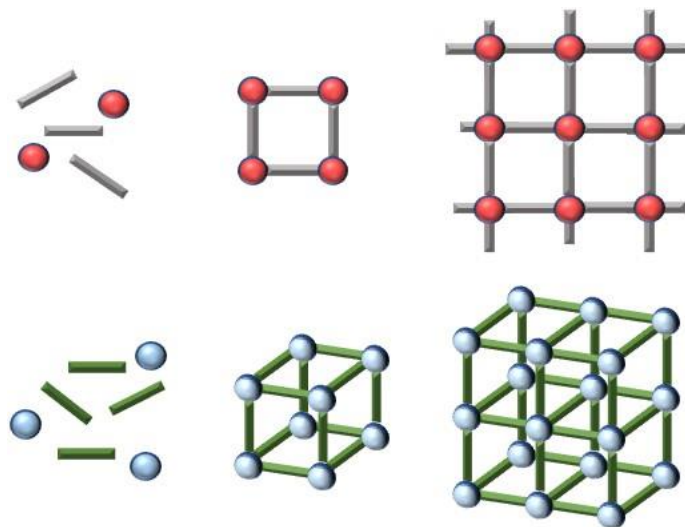**Figure 2.** Representation of 2D and 3D structures.

Lehn[29] and Sauvage[30] published their respective pioneering works on coordination-driven self-assembly for the construction of complex structures, which included infinite helicates, grids, ladders, racks, knots, rings, catenanes, rotaxanes, etc.. Since then, many other groups, such as those of Stang's,[27, 31] Raymond's,[24b, 32] Fujita's,[24f, 33] Mirkin's[24h, 34] and Cotton's[35] among others,[36] used the self-assembly methodology for the preparation of new discrete supramolecular architectures possessing cavities with well-defined shapes and sizes. The presence of these cavities, together with the geometries displayed by the supramolecular assemblies, allows these structures to behave as receptors for the selective encapsulation of guest molecules.[37] In this regard, host-guest chemistry, considered a sub-field within supramolecular chemistry, deals with the study of the selective interactions for which a smaller guest molecule becomes encapsulated within a larger molecular host (Scheme 3). Host-guest chemistry is considered as the most important feature of SCCs, due to the large number of applications that can be derived.[38]
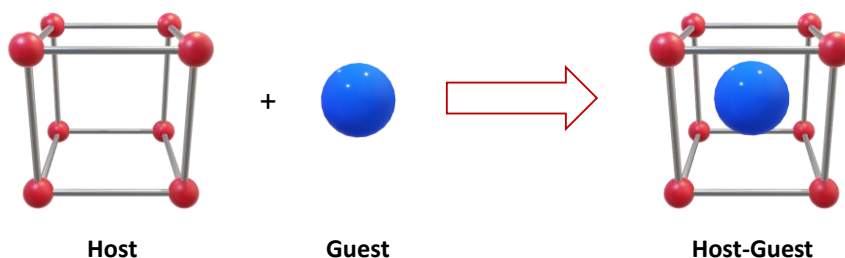
Scheme 3. Schematic representation of a Host-Guest system.

With regard to metal-containing supramolecular assemblies, most SCCs are built with O-, N-, and P-donor Werner-type linkers.[24d-g, 33a, 39] In the recent years, the use of carbon donor ligands is gaining popularity for the preparation of organometallic-based supramolecular hosts.[15a, 24d, 40] In fact, the term Supramolecular Organometallic Compounds (SOCs), was coined by Pöthig and Casini in 2019 to refer to all metal-containing supramolecular assemblies in which the linker-node connection is formed by M-C bonds.[41] This means that, for these organometallic assemblies, the carbon-metal bond is structurally decisive. Nowadays a large number of SOCs built with multidentate organometallic ligands, such as alkynyls,[42] arenes,[24c, 43] or *N*-heterocyclic carbenes (NHCs),[7a, 44] have been described. In particular, NHCs have proven to be promising scaffolds for the design of metallosupramolecular assemblies[15] and have undergone an enormous development in the past few years. In general, late transition metal NHC complexes are highly stable due to the stability of their M–C_{NHC} bond. This also accounts for NHC-based SOCs, which are generally more stable than supramolecular architectures derived from Werner-type ligands.[15, 45] This fact results in a significant difference between traditional SCCs and SOCs. While SCCs can be seen as "dynamic" assemblies (meaning that, in principle they can reversibly form and disintegrate), NHC-based SOCs can be regarded as "static" structures with an intrinsic irreversibility to assemble and disassemble.

Over the last 10 years, the number of metallosupramolecular assemblies featuring M−C$_{NHC}$ bonds has grown steadily. The first review on complexes from poly-NHC ligands was published by Peris and co-workers in 2009.[7a] Since then, different authors have focused their research on the development of supramolecular assemblies with poly-NHC ligands.[15] Among these ligands, the use of *Janus* di-NHCs[5c, 8, 9c, 12, 44a, 46] and threefold-symmetric tri-NHCs,[6a, 47] allowed the synthesis of organometallic-based assemblies with a large variety of topologies. In this context, it is convenient to recall that a *Janus*-head di-NHC contains two NHC units in a facially-opposed disposition and its denomination is attributed to its analogy with the representation of the Roman god *Janus* (Scheme 4, left). In particular, the benzo-bis-imidazolylidene ligand described by Bielawski in 2005[44a, 46] (Scheme 4, right) was the first example of a *Janus*-type bis-NHC ligand, and also the first one used for the preparation of NHC-based supramolecular assemblies.

Scheme 4. Roman god Janus (left) and benzo-bis-imidazolylidene ligand described by Bielawski[44a, 46] (right).

The Hahn's group was pioneer in the preparation of square- and rectangular-shaped assemblies, taking advantage of the linear arrangement of Bielawski's benzo-bis-imidazolylidene ligand. These organometallic-based assemblies included metals such as gold,[48] iridium,[49] platinum,[50] palladium,[49b] and nickel[51]. Hahn and co-workers also used a structurally similar di(NH,O)-NHC ligand together with the benzo-bis-imidazolylidene ligand for the preparation of a large number of molecular squares,[49a, 52] such as [**4**],[50] depicted in Scheme 5.
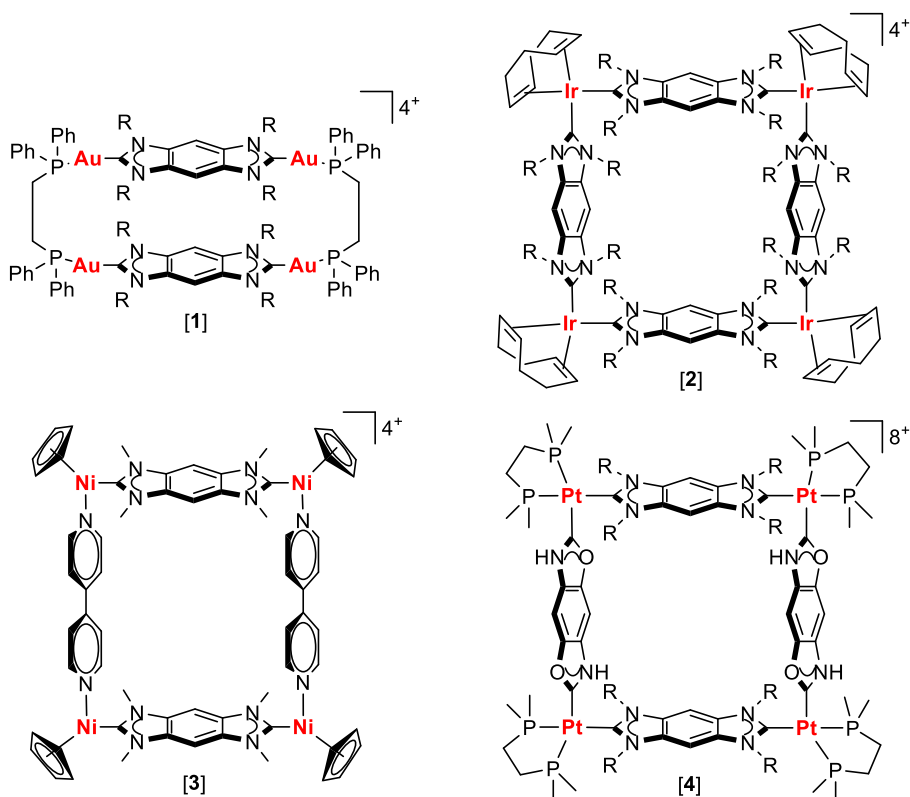
Scheme 5. NHC-Based metallosupramolecular assemblies described by Hahn and co-workers ([**1**],[48] [**2**],[49b] [**3**][51] and [**4**][50]).

In particular, NHC complexes of coinage metals have attracted a great deal of interest in the biomedical context.[41, 53] In this regard, silver NHC complexes are known to possess anti-microbial activity,[53b] and gold NHC compounds have shown interesting results as anti-cancer metallodrugs.[54] Just to name an example, a very recent study on the biological activity of pillarplex compounds[53c] based on a cyclic poly-NHC featuring different metals (Ag(I) or Au(I)) and anions (hexafluorophosphate or acetate), showed that the silver pillarplexes displayed antimicrobial (*B. subtilis, S. aureus, E. coli and P. aeruginosa*) and antifungal (*C. albicans*) activity, as well as moderate toxicity towards a human cell line (HepG2).

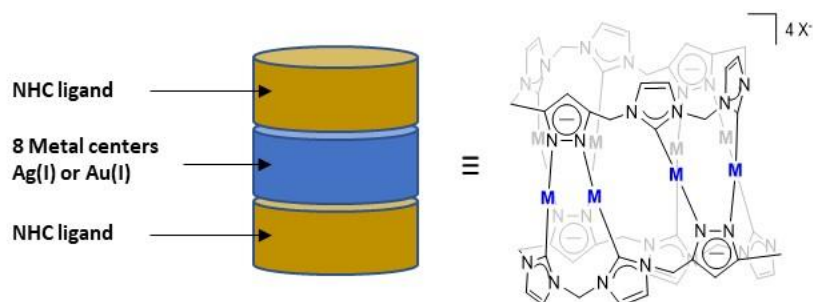**Figure 3.** Pillarplex: Metallocavitand with tubular cavity for supramolecular complexation.[55]

These Ag$_8$ and Au$_8$ metallosupramolecular assemblies also showed highly selective activity for the encapsulation of linear molecules, such as 1,8-diaminooctane (Scheme 6, left),[55] being one of the few SOCs used for host-guest chemistry so far. Additionally, these pillarplexes present unique properties allowing the synthesis of the first [2]rotaxane (Scheme 6, right) with a functional organometallic host framework. This system is pH-dependent and can be switched reversibly and quantitatively to its organic imidazolium-based [3]rotaxane *via* de-coordination of the involved metal ions.[56]
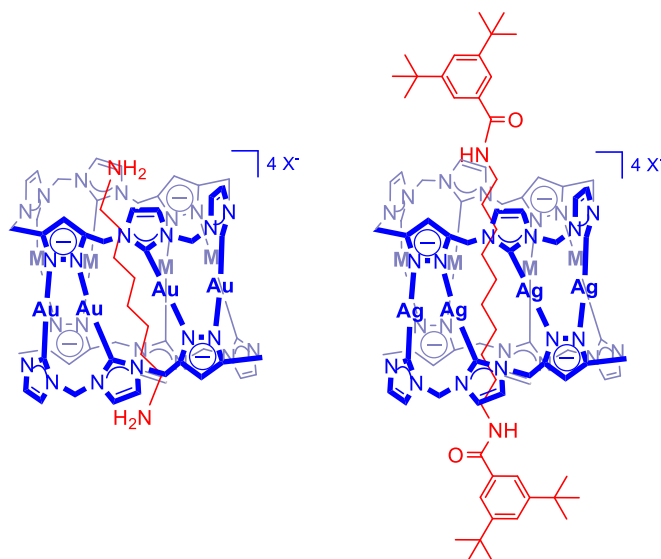

Scheme 6. Representation of the host-guest complex[55] (left) and the [2]rotaxane[56] (right) reported by Pöthig and co-workers.

1.1.1. *Development of NHC-based SOCs in the QOMCAT group.*

By benefiting by the experience obtained with the preparation of a series of planar extended π-conjugated poly-NHC ligands, such as those depicted in Scheme 2, the *Organometallic and Homogeneous Catalysis* group (QOMCAT) at Universitat Jaume I, developed several Ni-,[57] Pd-,[58] and Au-based metallorectangles,[59] metalloprisms,[60] and metallotweezers,[61] which showed different interesting properties. Among the ligands shown in Scheme 1, the pyrene-bis-imidazolylidene ligand **B**,[9] resulted particularly convenient for the preparation of metallosupramolecular structures, such as those depicted in Scheme 7.

By using the pyrene-bis-imidazolylidene ligand **B**, two nickel-cornered supramolecular coordination rectangles were synthesized ([**5**] and [**6**] in Scheme 7). The dimensions were modulated by using either pyrazine or 4,4'-bipyridine,[57b] so that pyrazine would afford a Pd-Pd distance of 7 Å, while bipyridine separates the two palladium centers at a distance of 11 Å. In the meantime, the metal-to-metal distance along the pyrene-bis-imidazolylidene ligand is fixed at ca. 13 Å (Scheme 7). The two rectangles were used as receptors for the recognition of polycyclic aromatic hydrocarbons (PAHs), which are considered hazardous materials.[62] Due to its dimensions, the bipyridine-containing rectangle [**6**] was able to host up to two guest molecules, while the pyrazine-containing rectangle [**5**] was capable to host only one molecule of the polyaromatic guest.
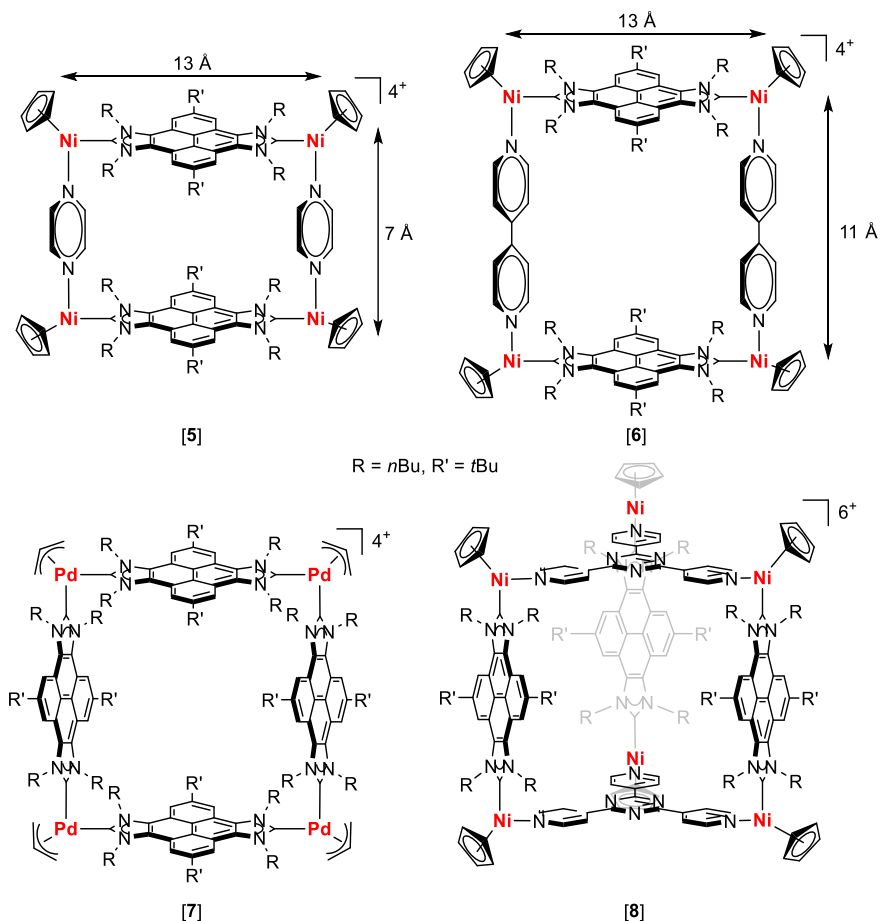
Scheme 7. Representative examples of supramolecular organometallic complexes based on the pyrene-bis-imidazolylidene ligand synthesized in the QOMCAT group.

To further explore the supramolecular assembly capabilities of the pyrene-based di-NHC ligand and using tripyridylpyrazine, Peris and co-workers obtained the trigonal prism [**8**] (Scheme 7),[57a] which was used for the encapsulation of large 3D-molecules, such as C_{60} and C_{70} fullerenes. The cage shows highly selective complexation of C_{70} over C_{60} (Scheme 8), a behaviour which can be potentially useful for fullerene separation and purification.
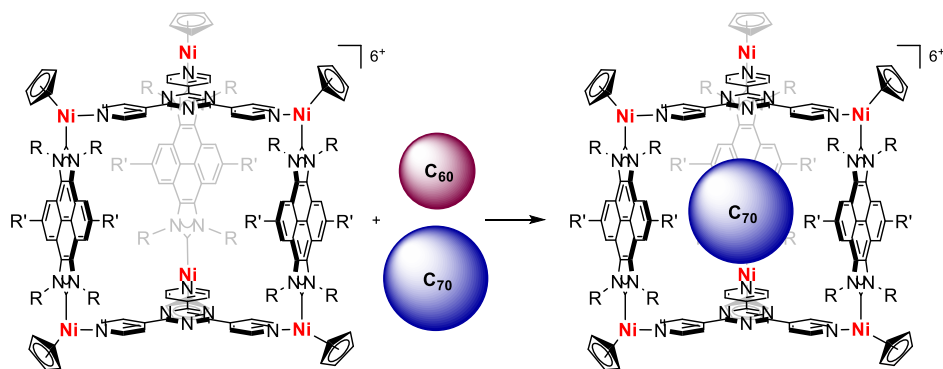
Scheme 8. Hexa-nickel metallocage [**8**] and representation of its ability to encapsulate C_{60} and C_{70} fullerenes.

Finally, by using the same pyrene-bis-imidazolylidene ligand, the palladium-conjoined molecular square [**7**] (Scheme 7) was prepared.[58a] This metallosquare showed incredible host-guest applicability summarized in Scheme 9. The presence of the four pyrene panels is a determining factor for the encapsulating properties of this metallosquare, which confers a 3-D shape to the compound. For example, the supramolecular assembly [**7**] was used for the encapsulation of C_{60} and C_{70}, showing a shape-adaptable conformation able to adjust its form to accommodate the size of the encapsulated fullerene and exhibiting a higher affinity for C_{70} over C_{60}.[36a] The final encapsulated host-guest complexes C_{60}@[**7**] and C_{70}@[**7**] present an important feature because both behaved as singlet oxygen photosensitizers. This made them suitable for oxidizing cyclic and acyclic alkenes at room temperature *via* visible-light-induced singlet oxygen generation. The results obtained by measuring the phosphorescence emission spectra of singlet oxygen generated by the two complexes upon irradiation with visible light represent a springboard towards the use of other fullerene-containing supramolecular systems for similar catalytic rractions.[36c]
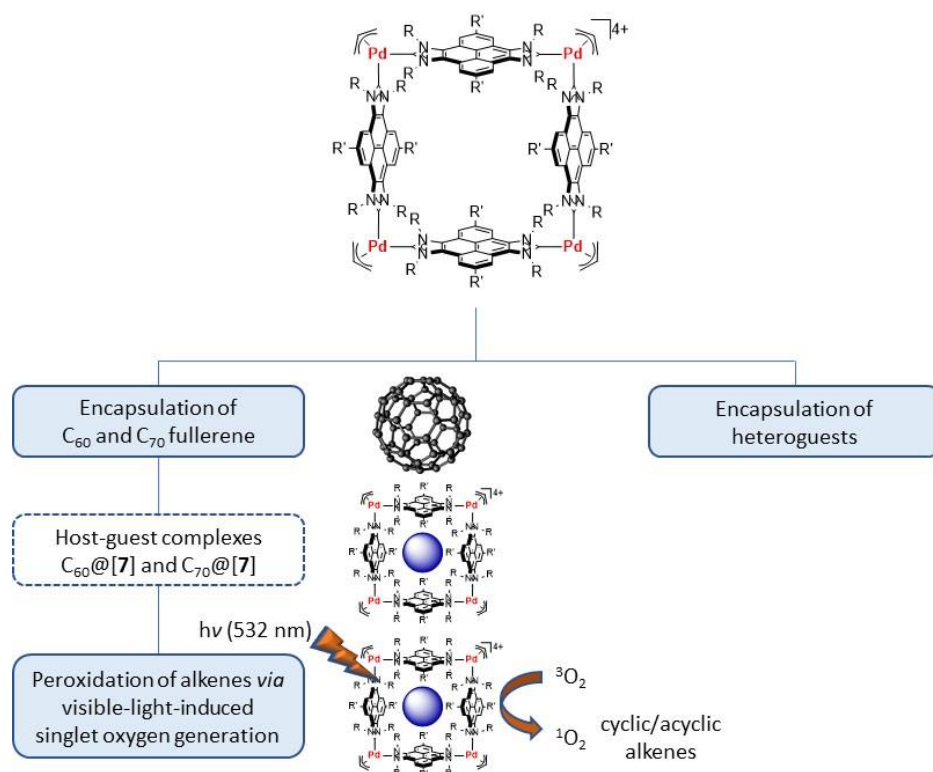
Scheme 9. Applicability areas shown for the metallosquare [**7**].

Another interesting feature is that [**7**] displays a metal-to-metal distance of 13 Å, which is perfect for the encapsulation of three polyaromatic guests, considering that is approximately 4 times the distance for an effective π-π stacking interaction (3.5 Å). The complex is able to encapsulate one molecule of an electron-rich PAH (pyrene, triphenylene or coronene) and two molecules of the electron deficient *N,N'*-dimethyl-naphthalenetetracarboxydiimide (NTCDI). This combination forms a quintuple π stack ordered in a donor–acceptor–donor–acceptor–donor (D–A–D–A–D) arrangement (Scheme 10), where the electron-rich pyrene fragments of the di-NHC ligand of the cage act as bookend donors.[58b] This metallosupramolecular assembly shows a very interesting feature, because it is the first "open" square structure used for the

encapsulation of heteroguests, while all other examples are based on "closed" trigonal-prismatic architectures.
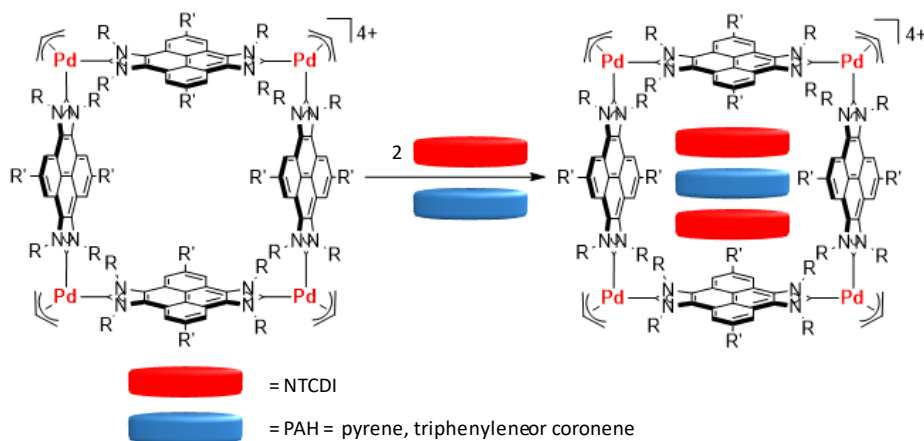
**Scheme 10.** Quintuple D−A−D−A−D π stack formed by heteroguest encapsulation based on an "open" square architecture.

The QOMCAT group also described a series of Au-based metallotweezers ([**9**]-[**11**] in Scheme 11),[61] metallorectangles ([**13**] in Scheme 11)[59] and metalloprisms ([**12**] in Scheme 11)[60] for the recognition of organic and inorganic substrates. A molecular tweezer is a type of molecular receptor containing two identical flat polyaromatic arms at the edges, which are bound by a more or less rigid tether.[63] In this regard, the next approach of the group was the preparation of different metallotweezers containing two Au(I) pyrene-imidazolylidene arms connected through different dialkynyl linkers (diethynylanthracene, bis(alkynyl)xanthene or bis(alkynyl)carbazole). Firstly, complex [**9**] (Scheme 11)[61d] was synthesized presenting a remarkably tendency to self-aggregate in nonpolar solvents, such as benzene, as well as in the presence of "nacked" metal cations, such as Cu$^+$, Ag$^+$, or Tl$^+$. The tendency to self-aggregate is explained because π-π stacking interactions are produced between the two pyrene polyaromatic arms and the anthracene linker.
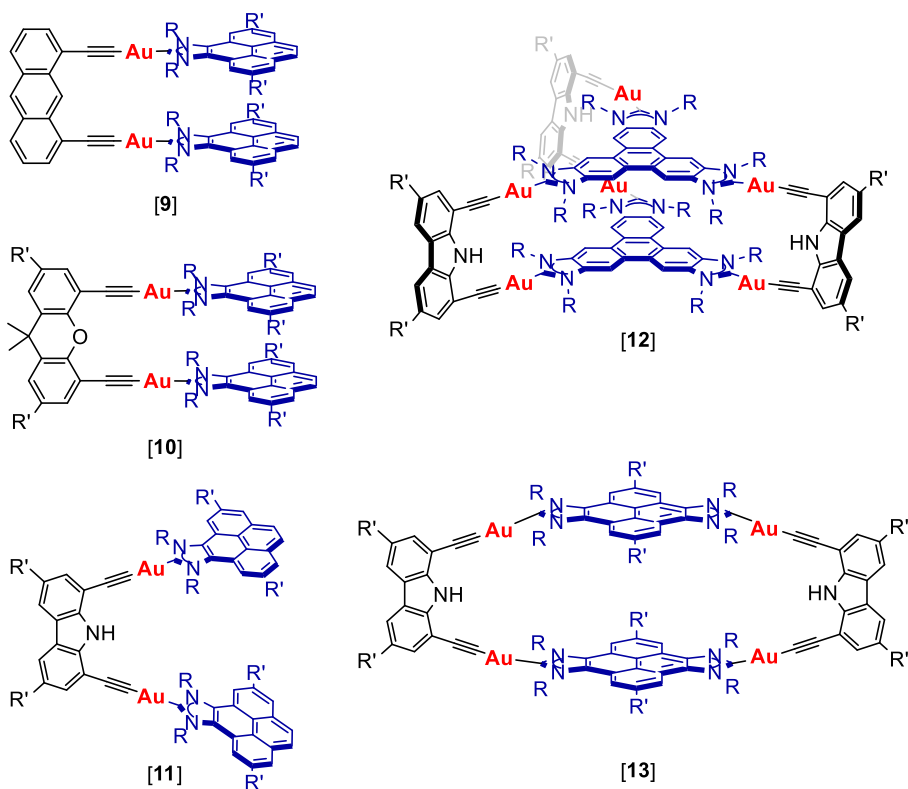
Scheme 11: Gold-based metallosupramolecular assemblies developed in the QOMCAT group.

In order to prepare metallotweezers for the recognition of aromatic substrates, it seemed necessary to minimize the self-aggregation tendency. For this, two strategies were applied, based on the use of linkers for which, (i) the π-extended system is disrupted, and (ii) the alkynyl groups present a diverging conformation. Using the first strategy, the U-shaped digold metallotweezer [**10**] (Scheme 11)[61c] with a bis(alkynyl)xanthene connector was prepared. This complex acts as metalloligand in the presence of "nacked" metal cations, showing a coordination ability highly cation-dependent. The second strategy enabled the synthesis of complex [**11**] (Scheme 11),[61a] with a bis(alkynyl)carbazole connector and two pyrene-imidazolylidne-Au(I) flexible arms. This metallotweezer was used for the recognition of PAHs and PAHs

functionalized with groups able to establish a hydrogen bond. It was found that the PAH guests featuring H-bonding groups showed binding affinities of about one order of magnitude larger than those for unfunctionalized PAHs, due to the hydrogen bonding interaction with the N-H group of the carbazole tether.

In parallel, the replacement of mono-NHC ligands by di- and tri-NHC ligands connected by extended π-conjugated systems allowed the preparation of trigonal-prismatic metallocages[60] ([**12**] in Scheme 11) and metallorectangles[59] ([**13**] in Scheme 11). The nanosized nature of these complexes, together with the presence of the two cofacial polycyclic-conjugated panels, made these assemblies remarkably effective for the encapsulation of PAHs. In particular, the hexagonal prismatic cage [**12**] showed a large binding affinity for coronene (Scheme 12, right), which makes it an excellent coronene scavenger.[60] And interestingly, the metallorectangle [**13**] is able to trap corannulene (Scheme 12, left), producing a significant flattening of these bowl-shaped guest molecules from 0.87 bowl-depth in Å (free corannulene) to 0.73 Å (encapsulated one).[59]
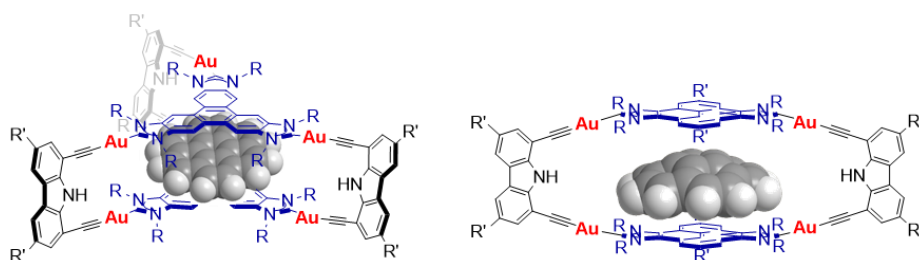
Scheme 12. Coronene@[**12**] (left) and corannulene@[**13**] (right) complexes obtained after the guest encapsulation.

1.2. *Supramolecular catalysis.*

Inspired by enzymatic catalysis, supramolecular catalysis appeared as a discipline that merges the principles of supramolecular chemistry with homogeneous catalysis, and therefore tries to benefit from the use of non-covalent interactions for achieving high reaction rates and good selectivities.

The term supramolecular catalysis was coined by Van Leeuwen in 2008,[64] and nowadays is a hot topic of research.[22, 25, 38a, 38b, 65]

Non-covalent interactions are reversible, and ultimately may allow the fine-tuning of the properties of a system accurately. Nevertheless, non-covalent interactions are hardly predictable, and for this reason, supramolecular effects that influence the catalytic performance of a catalytic process are often recognized *post-factum*. In general, supramolecular catalysts are recognized because they possess unique properties compared to analogues lacking the assembling properties.

According to the non-covalent interactions that can be established between the reaction partners during the catalytic process, Raynal and co-workers proposed a very useful classification for explaining how supramolecular interactions can influence a catalytic process.[65d] This classification is depicted in Scheme 13, and basically considers three types of interactions:

- *Ligand-ligand interactions:* the non-covalent interactions between the ligands of two molecules of catalyst may form a dimer, whose catalytic activity is different compared to the activity show by the parent monomer.

- *Ligand-additive interactions:* when an additive is added to the reaction vessel the catalytic properties of the complex may be modified by means of non-covalent interactions between the ligand and the complementary additive. The interaction between the ligand of the catalyst and the supramolecular additive, is very likely to change the steric and the electronic properties of the catalyst.

- *Ligand-substrate interactions:* the non-covalent interactions between the substrate and one of the ligands of the catalyst may place the substrate in a privileged position from which it can more easily interact with the metal center, and therefore it will be more prone to be activated.
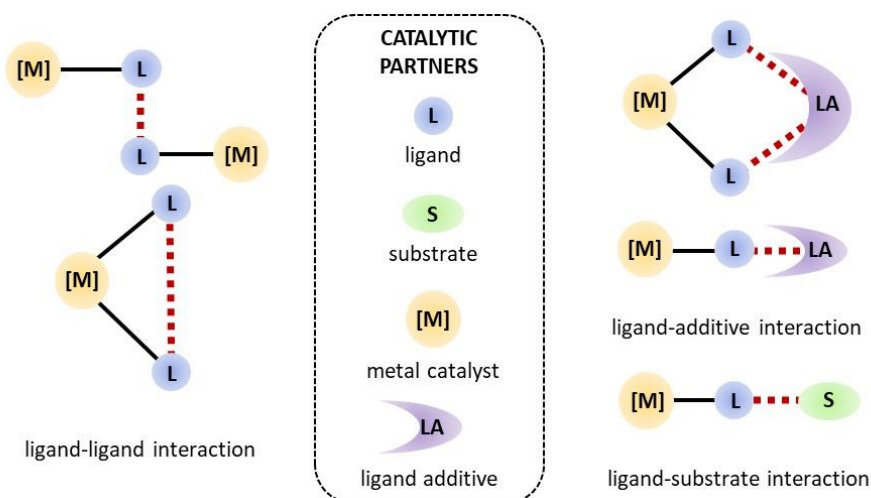
Scheme 13. Usual reaction partners involved in a catalytic process. The dashed red lines represent the non-covalent interaction.

A large number of examples can be found in the literature describing the influence of supramolecular interactions for the improvement of selectivities in homogeneous catalysis. However, much fewer examples have been reported regarding the catalytic consequences related with the modification of the kinetic parameters or activity regarding supramolecular interactions.[6a, 7b, 9c, 12, 66]

Π-stacking, a particular non-covalent interaction, may sometimes play an important role in homogeneously-catalyzed reactions. However, this type of effect may have been unrecognized during decades, until it was systematically studied for the case of NHC-based metal catalysts.[7b, 67] Some early examples of the influence of π-stacking in reactions catalyzed by NHC-based ligand include the works developed by Grela,[68] Blechert,[69] Collins,[70] Verpoort,[71] and Fürstner,[72] but most of them are related with the study of olefin metathesis using modified Ru-Grubbs catalysts. For example, Grela and co-workers showed in 2008[68] that in the olefin metathesis reaction catalysed by a second generation Ru-Grubbs catalyst, the use of fluorinated aromatic solvents had a beneficial influence (Scheme 14). By a combined experimental and theoretical approach, they

hypothesized that $\pi-\pi$ stacking interactions between the fluorinated solvent and the *N*-aromatic substituent of the NHC ligand stabilizes the active ruthenium species and enhances the activity of the catalyst.[66a]
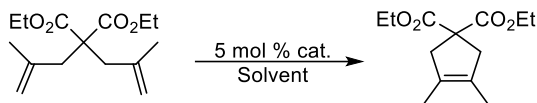
the activity of the catalyst is solvent dependent

$$C_6F_5CF_3 >> C_6H_5CH_3 >> ClCH_2CH_2Cl$$
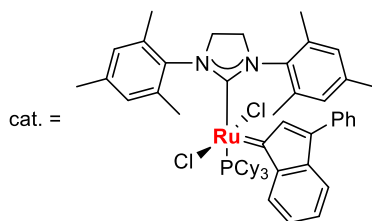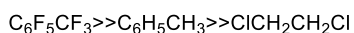
Scheme 14. Influence of fluorinated solvents in the catalyst activity in the olefin metathesis reaction.

Another interesting example regarding the influence of π-stacking interactions on the catalytic activity was described by Peinador and co-workers in 2014.[73] They developed a reusable Pt(II) diazapyrenium-based metallacyclic catalyst for the S_NAr reaction between halodinitrobenzenes and sodium azides. The addition of the appropriate π-stacking additive (in this case pyrene) results in a deactivation of the catalysis as a result of host-guest interactions between the additive and the metallacycle by formation of an inclusion complex. This results in the allosteric inhibition of the S_NAr reaction (Scheme 15).[74] At this point, it may be important to mention that the term *allostery* is originally used in enzymology to refer to the activation or inhibition of an enzyme by a small regulatory molecule that interacts at a site that can be remote with respect to the active site.[75]
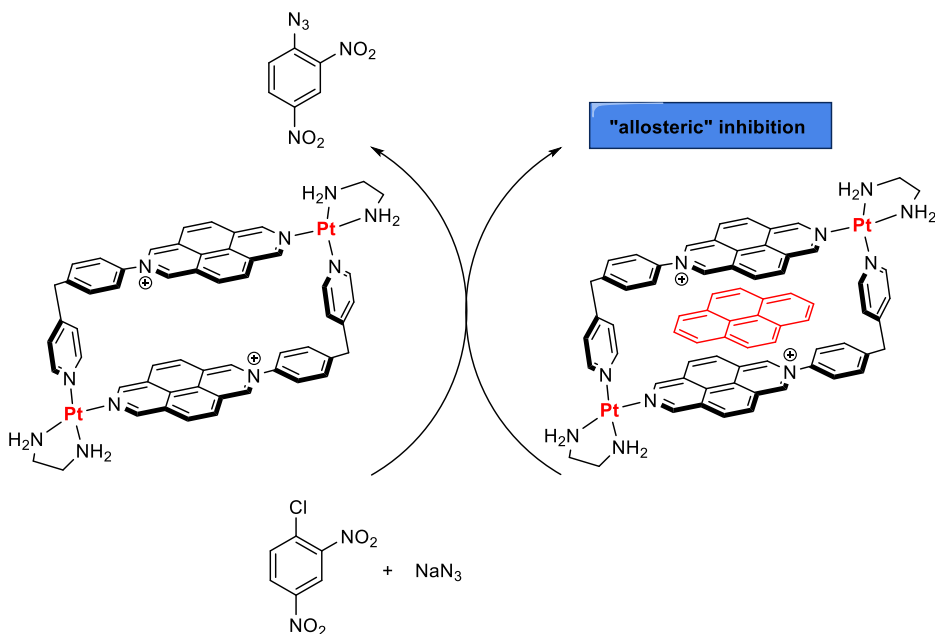
Scheme 15. S$_N$Ar reaction catalyzed by the Pt(II) metallacycle and the "allosteric" inhibition under the presence of an additive.

1.2.1. *Catalysts decorated with π-conjugated polyaromatic systems and their implications in supramolecular catalysis.*

During the last few years, the QOMCAT group was particularly interested in the preparation of polytopic NHC ligands bearing extended polyaromatic systems for the preparation of homogeneous catalysts. The purpose for this was: (1) finding examples for the study of the catalytic cooperativity between the metals comprised in the multimetallic complexes, and (2) preparing heterometallic catalysts for tandem reactions, in which each metal unit catalyses a mechanistically distinct reaction.

1.2.1.1. *Catalytic benefits provided by the ligand-substrate interaction.*
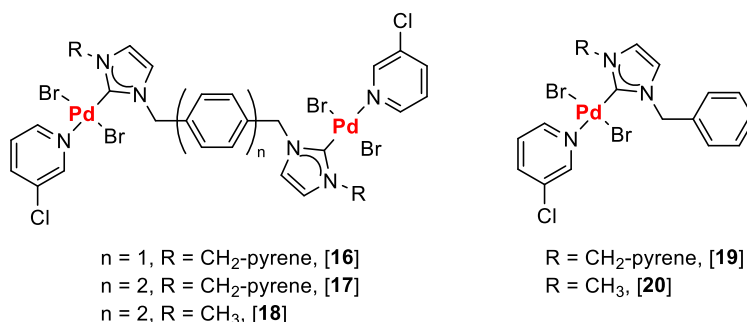
In the course of this research, the QOMCAT group obtained a series of di- and tri-NHCs connected by extended polyaromatic spacers (**A**,[8] **B**,[9c] **C**,[11] **D**,[6a] **F**[14] and **G**[12] in Scheme 2). In principle, the use of these ligands aimed to facilitate the

electronic communication between the metals.[5c, 8, 9c, 12] However, it was shown that the electronic communication was negligible in most of the cases.[76] Nevertheless, detailed studies performed on the catalytic activities shown by catalysts bearing NHC ligands decorated with rigid polyaromatic moieties, demonstrated that these catalysts showed activities essentially different from those catalysts lacking of these systems. One of the earliest evidences of the influence of π-stacking interactions in homogeneous catalysis using NHC ligands decorated with rigid polyaromatic fragments was observed using the triphenylene-tris(imidazolylidene)-based palladium ([**14**]) and gold catalysts ([**15**]) depicted in Scheme 16.[6a] The activity of these trimetallic complexes can be compared with the exact combination of three molecules of their related monometallic benzimidazolylidene analogues, which display exactly the same stereoelectronic properties. The studies were performed by comparing the catalytic efficiency of these catalysts in different reactions. The palladium complex was tested in the α-arylation of propiophenone with aryl bromides, and in the Suzuki–Miyaura coupling between aryl bromides and arylboronic acids. On the other hand, the tri-gold-complex was tested in the hydroamination of phenylacetylene. The results obtained showed that the trimetallic complexes displayed higher activity than the monometallic analogues. The higher activities shown by the trimetallic catalysts were attributed to the π-stacking interactions established between the triphenylene core of the catalysts and the aromatic substrates used in the experiments, which very likely have an influence in the catalytic performance of the catalysts. As an additional study to support this hypothesis, the catalytic experiments were repeated with the addition of catalytic amounts of external π-stacking additives, such as pyrene or hexafluorobenzene. These additives are known to promote π-stacking interactions with polyaromatic surfaces, and therefore should suppress the ability of the aromatic ligands to π -stack with the triphenylene core of the

catalysts. As expected, the addition of any of the additives produced significant changes in the performance of the catalysts.[6a]

Scheme 16. Triphenylene-based NHC complexes of palladium and gold and catalytic reactions tested.

In line with these results, a series of di-NHC-based complexes connected by phenylene or biphenylene were obtained ([**16**]-[**18**] in Scheme 17) to continue studying how π-stacking interactions may influence the activity of catalysts containing rigid polyaromatic functionalities.[77] The *N*-substituents of these ligands were methyl or methyl-pyrene groups, and the related mono-NHCs were also prepared ([**19**]-[**20**] in Scheme 17), in order to evaluate the influence of the presence of two metals in comparison with the monometallic analogue. The studies were performed by comparing the catalytic efficiency of these catalysts in two different reactions, namely, the acylation of arylhalides with

hydrocinnamaldehyde and the Suzuki–Miyaura coupling between arylhalides and arylboronic acids.

n = 1, R = CH$_2$-pyrene, [**16**]
n = 2, R = CH$_2$-pyrene, [**17**]
n = 2, R = CH$_3$, [**18**]

R = CH$_2$-pyrene, [**19**]
R = CH$_3$, [**20**]

Scheme 17. Dimetallic and monometallic palladium complexes tested.

The results showed that the complexes with pyrene tags are slightly more active than those with methyl groups, an observation that becomes more evident when the time-dependent reaction profiles are compared.[77] The dimetallic complexes were also more active than their monometallic analogues. These results were supported by the experimental evidence provided by the addition of catalytic amounts of pyrene to the Suzuki-Miyaura coupling reaction, which produced a partial inhibition of the activity of the pyrene-containing complexes ([**16**], [**17**] and [**19**]), while the activity of the methyl-substituted catalysts ([**18**] and [**20**]) were not affected (Figure 4). Again, the catalytic outcome provided by pyrene-containing catalysts supports the hypothesis of the importance of π-stacking interactions in the overall catalytic reaction. It was supposed that the pyrene-tag of the catalyst and the aromatic substrates established π-stacking interactions that enhanced the catalyst activity.[77]
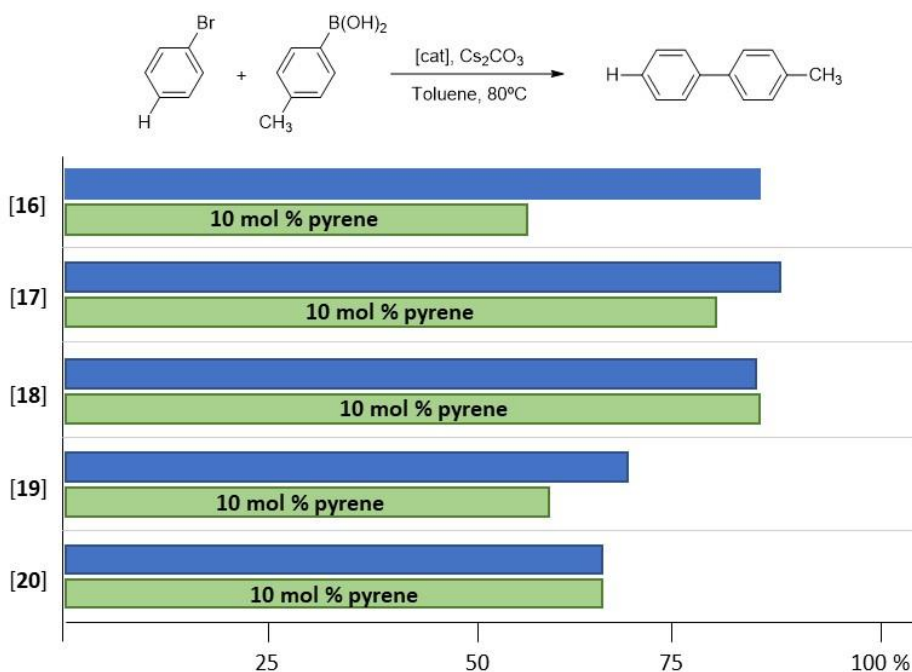
Figure 4. Suzuki-Miyaura coupling between phenyl bromide and 4-tolylboronic acid in the presence and absence of pyrene.

1.2.1.2. The influence of the ligand-additive interactions in the electronic properties of metal complexes with polyaromatic NHC ligands.

To further explore the influence of π-stacking additives on the catalytic activity of NHC-based metal catalysts, a series of NHC ligands decorated with fused polycyclic aromatic hydrocarbons were prepared (Scheme 18).[14, 66b, 66c, 78] The presence of the extended polyaromatic systems should make these systems sensitive to the addition of π-stacking additives, thus magnifying the ligand-additive interactions.
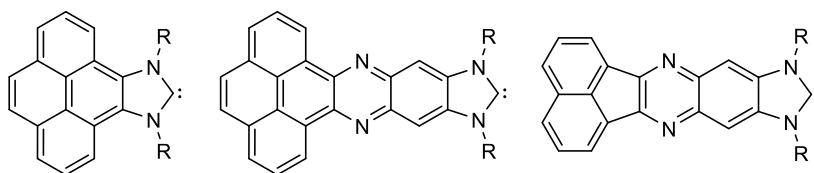
Scheme 18. Monodentate ligands with extended polyaromatic systems.

The influence of the π-stacking interactions on the electronic properties of the ligands was studied by means of four different approaches: (i) electrochemical studies, (ii) DFT calculations, (iii) infrared spectroscopy, and (iv) ^{1}H NMR spectroscopy. It was observed that the electronic properties of these ligands could be modified upon suitable π-stacking additives. In particular, by calculating the Tolman Electronic Parameters (TEPs) of a series of DFT calculated [Ni(NHC)(CO)$_3$] complexes, and by comparing these values with the ones resulting from the optimized structures with a π-stacking additive (pyrene or hexafluorobenzene), a series of important conclusions were extracted. The TEP value for the pyrene-imidazolylidene ligand without any additive was calculated as 2056.1 cm^{-1}, while the values for the system adding pyrene or hexafluorobenzene were 2052.3 cm^{-1} or 2058.4 cm^{-1}, respectively (Figure 5). These results indicate that the formation of the π-stacking complexes induced a significant modification of the TEP value, with values of ΔTEP = -3.8 (pyrene) or 2.3 (hexafluorobenzene) cm^{-1}.[66b] This means that the electrondonating character of the ligand can either be increased, or reduced, by adding pyrene or hexafulorobenzene, respectively.
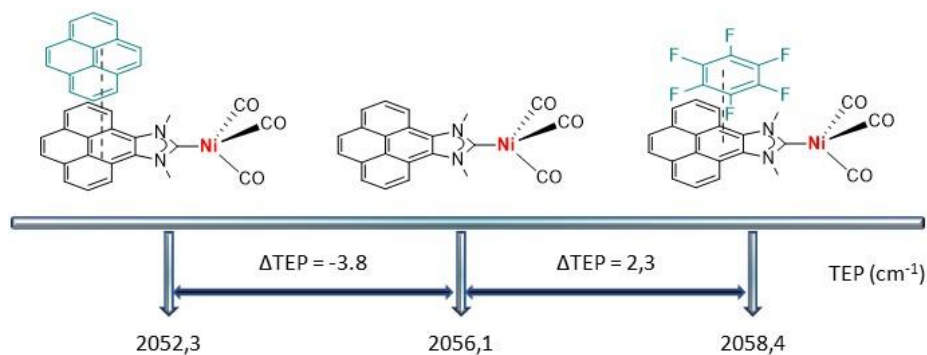

Figure 5. Variaton of the TEP values upon addition of pyrene or hexafluorobenzene of the pyrene-fused NHC ligand.

In order to validate experimentally these results, the variation of the C-O stretching frequencies of the complexes decorated with polyaromatic systems

upon addition of the same π-stacking additives was studied. For this purpose, the IR spectra of a series of [IrCl(NHC)(CO)$_2$] complexes was performed, were NHC is the ligand with the fused polyaromatic moieties. The results indicated clearly that de addition of these π-stacking additives has a significant effect on the variation of the CO stretching frequencies of the complexes, but this clearly depends on the nature of the extended polyconjugated system present in the NHC ligand (Table 1). In all the cases, the addition of pyrene produced an increase of the C-O frequency, while the addition of hexafluorobenzene produced the opposite effect. The largest variation, with an overall value of 2.9 cm^{-1}, was observed for the pyrene-derived-NHC ligand, related to the $\Delta v(CO)_{av}$ observed for the addition of pyrene with respect to the situation generated by addition of hexafluorobenzene.

Table 1. Variation of the IR C-O stretching frequencies of the [IrCl(NHC)(CO)$_2$] complexes upon addition of pyrene or hexafluorobenzene.
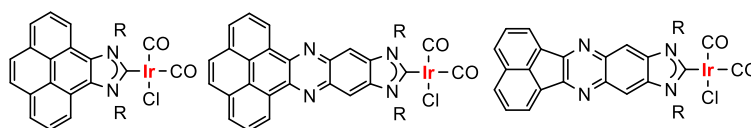
Δv_{av} (CO)(cm^{-1})			
-	0	0	0
pyrene	-1.4	-1.4	-1.4
C$_6$F$_6$	1.5	1.4	0.5

All these results demonstrated that the electron-donating character of a ligand can be postmodified upon addition of the suitable π-stacking additive.[66b]

1.2.1.3. Π-stacking interactions and kinetics.

In order to shed some light onto the influence of the effects produced by π-stacking interactions with additives in the catalytic activity of the complexes, the QOMCAT group synthesized a new family of Ir(I) catalysts (Scheme 19).[14] These

complexes should provide an excellent basis for comparison, with which relevant information could be obtained.
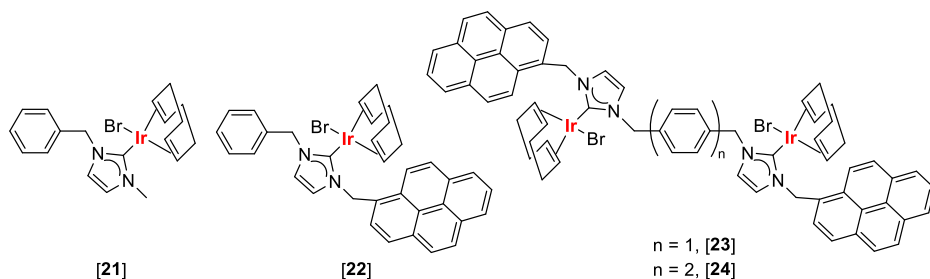
Scheme 19. NHC-based complexes used for the catalytic studies.

The catalytic activity of complexes [**21**]-[**24**] was tested in two typical borrowing hydrogen catalysed processes for which Ir(I) complexes have proven to be very effective catalysts:[79] the reduction of ketones by transfer hydrogenation, and the *β*-alkylation of secondary alcohols with primary alcohols. Particularly, it was important to determine the influence of the additive on the catalytic output of the reactions, and if it has any relation with the nature of the substrates and/or catalysts used. For the transfer hydrogenation process, the reduction of two benchmark ketones, namely acetophenone and cyclohexanone was studied. The results are shown in Figure 6.
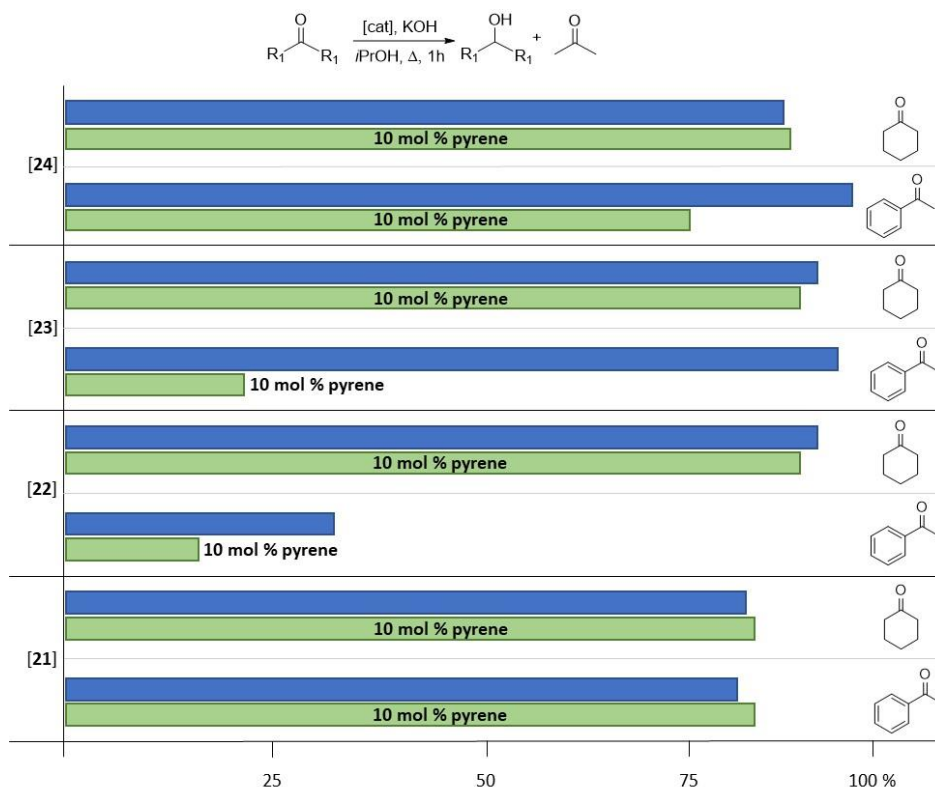
Figure 6. Comparison of the catalytic activities of complexes **10**-**13** in the reduction of acetophenone and cyclohexanone by transfer hydrogenation in isopropanol.

Firstly, all the iridium complexes were very active in the reduction of cyclohexanone to cyclohexanol and the addition of a catalytic amount of pyrene (10 mol % with respect to the substrate) did not produce any measurable modification in the catalytic activity of the catalysts. However, for the reduction of acetophenone to 1-phenylethanol, the addition of the pyrene additive produced an inhibition of the catalytic activity of the catalysts bearing pyrene tags ([**22**]-[**24**]), while the activity shown by [**21**] lacking the polyaromatic system, remained unchanged. These results are in accordance with the previous ones obtained by the QOMCAT group,[6, 77] indicating that only when aromatic substrates and catalysts with polyaromatic tags are used, exist a supramolecular effect capable to influence the activity of the catalyst.[14]

The *β*-alkylation of secondary alcohols with primary alcohols was the other reaction studied to evaluate the catalytic properties of the complexes. In this regard, 1-phenylethanol was coupled with a series of benzyl alcohols (benzyl alcohol, 3-chlorobenzyl alcohol and 4-chlorobenzyl alcohol) and *n*-butanol. All the catalysts ([**21**]-[**24**]) were very selective in the production of the final alcohol, but the phenylene-bridged diiridium complex [**23**] was the most active in all the reactions tested, reaching when the two aromatic alcohols are used almost quantitative conversion.

To further explore the reaction mechanism of the process, especially regarding the interaction of the catalysts with the alcohols in the starting steps, kinetic studies were performed using complexes [**21**] and [**23**] model catalysts, and two primary alcohols (benzyl alcohol and *n*-butanol). The results obtained for these studies are summarized in Scheme 20.
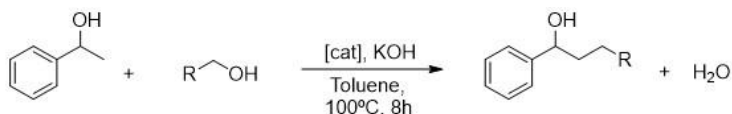
Catalyst used	Primary alcohol	Reaction order
[**21**]	benzyl alcohol	2
[**23**]	benzyl alcohol	0
[**23**]	*n*-butanol	2

Scheme 20. Results obtained for the determination of the reaction orders with respect to the substrates.

The time-dependent reaction profiles for the C-C coupling of the aromatic substrates using the pyrene-tagged catalysts [**23**], followed a zero-order rate in the substrates for all the experiments carried out with different catalyst loadings. This result, which evokes enzymatic catalysis, is suggestive of the catalyst saturation by the substrate all along the reaction course. This situation

should be explained due to non-covalent interactions between the aromatic substrate and the pyrene-tagged catalyst. For all other combinations (non-aromatic substrates or catalyst without pyrene-tags), the reaction followed a second order rate. These results demonstrated the influence of the supramolecular interactions in the kinetics of the reaction when that is carried out with aromatic substrates and catalysts containing polyaromatic fragments.

Finally, other interesting information regarding the supramolecular interactions influencing the catalytic behaviour of [**21**]-[**24**] was obtained from the determination of the rate orders with respect to the concentration of the catalysts. Pyrene-containing catalysts ([**22**] and [**23**]) displayed a fractional rate order < 1 with respect to the catalyst concentration, thus suggesting a monomer-dimer equilibrium,[80] with the monomer acting as the active catalytic species. In contrast, similar studies using the catalyst without the pyrene functionality ([**21**]) derived into a first order dependence on the concentration of catalyst, therefore indicating the monometallic nature of the active catalytic species.[14] This result reveals important implications about the reaction mechanism, pointing at the influence on the kinetics of the process being assigned to a ligand-ligand interaction (self-association of the pyrene-tagged catalysts) and also showed how the presence of polyaromatic fragments modify the reactivity of the catalyst, compared to otherwise identical metal complexes.

2. *Luminescence in transition metal complexes.*

Luminescence is a particular feature of many materials, some plants and animals (Figure 7). It can be defined as the spontaneous emission of light (ultraviolet, visible or infrared) from an electronically excited species. For luminescence to occur, an energy absorption process is previously required, in which electrons go from a ground state, designated as S_0 to either a singlet (S_1, S_2) or triplet (T_1) excited electronic state (see below in Figure 2). Depending on the excitation process involved, luminescence can be classified as photoluminescence, electroluminescence, thermoluminescence, chemiluminescence, radioluminescence, mechanoluminescence, etc.[81]

Figure 7. Fluorite (left) with thermoluminescence. Squid (middle) and fungi (right) with bioluminescence.

Photoluminescence is of particular interest, because it involves the absorption of light (normally UV), which brings the absorbing species into the corresponding electronic excited state that promotes the emission of light. In order to obtain the emission, the absorption of a photon is necessary. Once the molecule is excited, there are several radiative and non-radiative de-excitation pathways that can take place for returning to the ground state. The following is a description of the different types of non-radiative processes:[81-82]

- *Vibrational relaxation:* Occurs when a molecule excited to a higher vibrational level of the target excited state relaxes rapidly to the lowest vibrational level of the excited electronic state. These processes can occur within 10^{-14}-10^{-12} s, shorter time than luminescence lifetimes.

- *Internal conversion:* Rapid relaxation process from a higher-energy excited state (S_2) to a lower-energy excited state (S_1). The molecular spin multiplicity remains the same, differing hereby from the intersystem crossing. The time scale of the process is 10^{-12} s.

- *Intersystem crossing:* Relaxation process that proceeds between excited states of different multiplicity (an example of relaxation from S_1 to T_1 is shown in Figure 8). It is a less likely process than internal conversion, because the spin multiplicity is not conserved (time scale of 10^{-8} s).

- *Non-radiative de-excitation:* The energy is dissipated by the release of infinitesimal amounts of heat (thermal energy), that cannot normally be measured experimentally.

Among all possible de-excitation pathways we will focus this section's attention on two processes for which part of the energy (UV, Visible) absorbed is released in the form of light (radiative processes). These two processes are fluorescence and phosphorescence.

Fluorescence is a spin-allowed process that takes place from a singlet excited state to the ground state ($S_1 \rightarrow S_0$). Therefore, it is a rapid process that yields emission rates in the order of 10 ns. Phosphorescence is a spin-forbidden process in which the energy of the light absorbed is released slowly in form of light. The phosphorescence emission normally takes place from a triplet excited state to a singlet ground state ($T_1 \rightarrow S_0$), thus average lifetimes (τ) range between milliseconds and seconds.[83] These two processes can be graphically depicted using the the Jablonski diagram[84] shown in Figure 8. This graphic shows some of the pathways that a molecule can undertake for returning to the ground state once it absorbed energy from electromagnetic radiation.
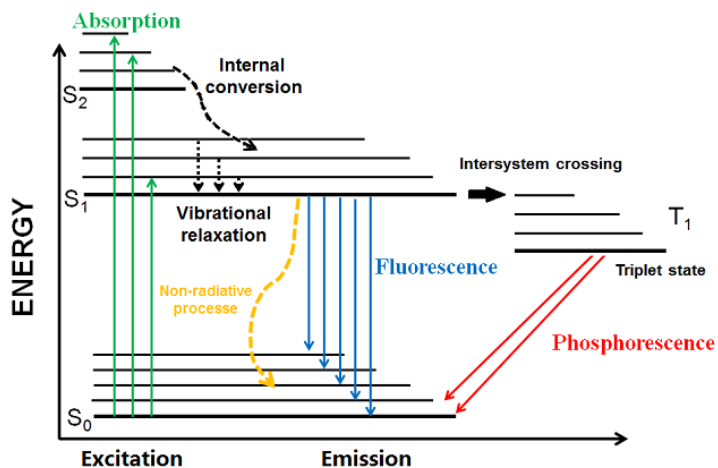
Figure 8. Jablonski diagram, where S_0 is the singlet ground state, S_1 and S_2 are singlet excited states and T_1 is a triplet excited state.

The emission produced after the excitation can be quantified by means of the quantum yield. The quantum yield ($\boldsymbol{\Phi}$), a fundamental property of luminescence, is the ratio between the number of photons emitted and the number of photons absorbed.[83] Therefore, the maximum value of $\boldsymbol{\Phi}$ is 1, for an ideal case in which all photons absorbed produce emission of a photon of lower energy. The quantum yield can also be defined in terms of the rate constants of the radiative (K_{rad}) and non-radiative (K_{nr}) processes[82] according to Equation 1:

$$\boldsymbol{\Phi} = \frac{\sum K_{rad}}{\sum K_{rad} + \sum K_{nr}}$$

Equation 1. Quantum yield calculation, where: K_{rad} includes the rate of fluorescence and phosphorescence and K_{nr} includes the rate constants of all the non-radiative processes.

A variety of factors are believed to influence the luminescence quantum yields of luminophores:[82]

- *The type of transition*: selection rules that apply for luminescence are those that apply for absorption, thus the accomplishment of the selection rules highly influences the quantum yields achieved.

- *Structural rigidity*: molecules that have rigid structures normally exhibit strong luminescence.

- *Composition*: the nature of the substituents may increase or decrease the quantum yield. For example, halogen substituents generally decrease the fluorescence quantum yield while certain aromatic substituents increase this value.

- *Other factors*: temperature, solvent, phase and pH often produce changes in the emission quantum yields.

Since their discovery, the development of materials with emissive properties, due to their applications as fluorescent sensors,[85] organic light-emitting diodes (OLEDs),[86] and bioimaging probes[87] have attracted increasing interest. Attracted by this wide range of features and possibilities, a large variety of luminescent organic devices are continuously developed.[88] Although we can find luminescent materials in every physical state, some of them are preferred over the others depending on the applications that are pursued. For example, films and aggregates are widely used in the fabrication of OLEDs, whereas luminophores for biomedical research are often used in solution. For this reason, it is particularly important to find new materials that show good emission properties in dilute solutions, so that can be visualized by routine techniques, such as fluorescence microscopy. Also important is to develop molecules that are able to combine good emissive properties with chemotherapeutic activity, so that they can be used as *theranostic* agents that provide relevant information about their biological interplay.[89]

Luminescent transition metal complexes have also attracted intense attention during the last two decades.[90] One of the main reasons for the great success of this kind of metal-based luminophores is that intersystem crossing processes (in which relaxation proceeds between excited states of different spin multiplicity)

are very likely to be produced in molecules containing heavy atoms, such as iodine and bromine in organic luminophores and metal ions in inorganic luminophores. In the presence of heavy atoms, the spin–orbit coupling becomes more important and, consequently, a change in spin becomes more likely for improving the emission efficiency from spin-forbidden states.[91] This characteristic allows a fast rate of the intersystem crossing process followed by phosphorescence and, sometimes, high quantum yields.

In transition metal complexes the luminescence transitions may involve the energy levels of the ligand (intra-ligand transitions), the metal (*d–d* transitions), or both the metal and the ligand (charge transfer transitions). Intra-ligand or ligand-centered transitions only involve ligand orbitals, which are almost unaffected by coordination to the metal. The *d–d* transitions are usually forbidden by the Laporte selection rule, so the corresponding absorption and emission bands are generally weak. Conversely, charge-transfer transitions are allowed and can occur either from ligand-to-metal orbitals (ligand-to-metal charge transfer, LMCT) or vice versa (metal-to-ligand charge transfer, MLCT).[82]

Among transition-metal-based luminophores, gold(I)-alkynyls constitute one of the most widely studied systems, probably because acetylides can connect the gold atom to a large variety of organic functions.[92] The origin of the emission is mainly derived from the triplet excited-state of the alkynyl ligand, or from the inter- or intramolecular interactions between gold(I) centers (aurophilicity).[93] However, while highly efficient emissions ($Φ > 85\%$) have been found for a (low) number of gold complexes in the solid or aggregated states,[94] to the best of our knowledge there is only one report describing high quantum yields in solution (Chart 1).[95]
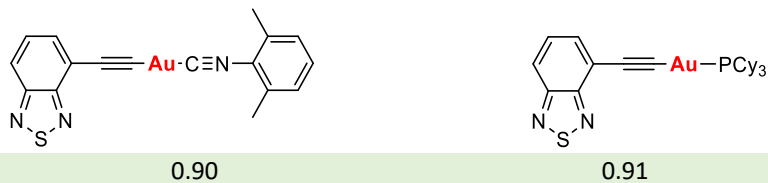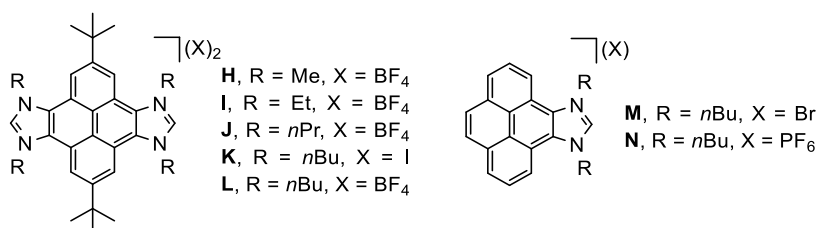
$\Phi_{em}{}^a$	0.90	0.91

Chart 1. Au(I) acetylide complexes. [a]Emission quantum yields (Φ_{em}) were obtained using quinine sulphate in degassed 1N H_2SO_4 (Φ = 0.546) as the standard. Φ_{em} measured in steady state is the overall emission quantum yield.

N-heterocyclic carbene (NHC) ligands have also been extensively used in the preparation of metal complexes with photoluminescent properties.[16] Along with their chemical stability, the wide coordination versatility of NHC ligands has helped to their great development, affording complexes of almost any transition metal in different oxidation states.[16, 96] In addition, the easy preparation of NHC-precursors (commonly azolium-based salts) has allowed access to a wide variety of new topologies.[97] The great versatility of NHC ligands for structural modifications, together with the use of other ancillary ligands, provide numerous possibilities for the synthesis of phosphorescent materials, with emission colours over the entire visible spectra and potential future applications in fields such as photochemical water-splitting,[98] chemosensing,[99] fabrication of dye-sensitised solar cells,[100] and medicine.[101]

Among NHC precursors, benzobisazoliums have been recently proven to represent an interesting class of versatile and robust fluorophores.[102] In this regard, during the last few years, the QOMCAT group reported the photophysical properties of a series of pyrene-containing bisazoliums salts, as well as some complexes showing moderated to good quantum yields.[5b, 9b, 9c] The chromophore of choice was pyrene because is one of the most studied organic materials in the field of photochemistry and photophysics[103] (it is sometimes referred to as the photochemist's fruit fly),[103a] showing unique properties. Moreover, many pyrene-containing complexes are used in fields such as optoelectronics, chemical sensors, and photodynamic therapeutic agents.[104]

The first example reported by the QOMCAT group was a family of *Janus*-type bis-imidazolium salts containing pyrene and different alkyl groups (**H**-**L** in Scheme 21), aiming to obtain materials with interesting physicochemical properties.[9c] The related pyrene-monoazolium salts **M** and **N** (Scheme 21), were also included in the study for comparative purposes.[78] The results showed emissions in the range of 370-440 nm, and emission quantum yields (Φ_{em}) ranging from 0.28 to 0.41 in solution, with **H** being the most efficient fluorophore among all salts studied (Φ_{em} = 0.41).[9c]

H, R = Me, X = BF$_4$
I, R = Et, X = BF$_4$
J, R = nPr, X = BF$_4$
K, R = nBu, X = I
L, R = nBu, X = BF$_4$
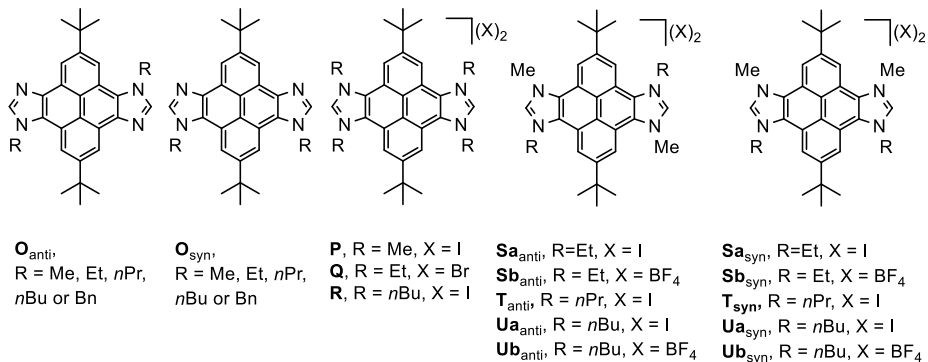
M, R = nBu, X = Br
N, R = nBu, X = PF$_6$

Scheme 21. PBIs (left) and pyrene-monoazoliums (right).

The pyrene-bisazoliums (from now on, PBIs) were used for the preparation of a series of dirhodium and diiridium complexes, but these complexes presented negligible fluorescence emission.[9c] The quenching of this emission was attributed to the heavy-atom perturbation,[105] which is a common effect observed for other NHC complexes of rhodium and iridium.[102e, 105b]

These preliminary results were the basis for the preparation of other pyrene-linked neutral and dicationic bis-azoles with different *N*-substituents depicted in Scheme 22.[9b] The pyrene-based bis-imidazolium salts were used as NHC precursors for the preparation of the related cyclometalated platinum complexes ([**25**]-[**26**] in Scheme 23). The interest of this type of complexes aroused from the fact that similar species have shown a strong potential in highly efficient OLEDs[106] and, in combination with NHC ligands some Pt(II) complexes have provided very interesting luminescent properties.[16] The photophysical studies revealed that, the mother organic molecules of the

related cyclometalated complexes showed fluorescence quantum yields (Φ_f) ranging from 0.14 to 0.75, with emissive properties centered in the pyrene moiety.

O$_{anti}$,
R = Me, Et, *n*Pr,
*n*Bu or Bn

O$_{syn}$,
R = Me, Et, *n*Pr,
*n*Bu or Bn

P, R = Me, X = I
Q, R = Et, X = Br
R, R = *n*Bu, X = I

Sa$_{anti}$, R=Et, X = I
Sb$_{anti}$, R = Et, X = BF$_4$
T$_{anti}$, R = *n*Pr, X = I
Ua$_{anti}$, R = *n*Bu, X = I
Ub$_{anti}$, R = *n*Bu, X = BF$_4$

Sa$_{syn}$, R=Et, X = I
Sb$_{syn}$, R = Et, X = BF$_4$
T$_{syn}$, R = *n*Pr, X = I
Ua$_{syn}$, R = *n*Bu, X = I
Ub$_{syn}$, R = *n*Bu, X = BF$_4$

**Scheme 22.** Pyrene-based bis-imidazolium salts used for the preparation of the platinum complexes.

The introduction of the platinum fragment aroused in a decrease of the emission efficiency, which is suggestive of an increase in the proportion of non-radiative decay processes due to the coordination of the carbene ligand to Pt(II).[107] In addition, the energies associated with the HOMO and LUMO levels suggest that this family of complexes provides versatility in matching the energy levels of a large variety of host materials, an excellent property with potential to be used for the preparation of organic light-emitting devices.[9b]
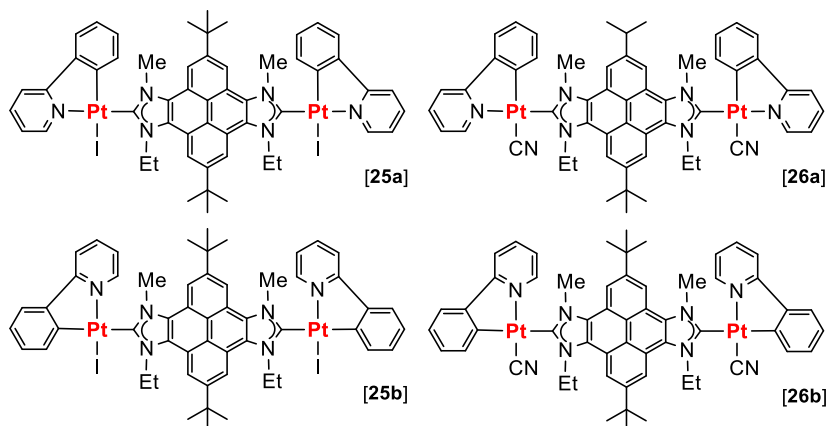
Scheme 23. Pyrene-based bis-NHC diplatinum(II) complexes synthesized by the QOMCAT group.

In line with these results, other platinum(II) and gold(III) complexes[5b] were described by the QOMCAT group (Scheme 24), containing pyrene mono- or bis-NHC, and a CNC pincer ligand (CNC = 2,6-diphenylpyridine).[108] The pyrene-based complexes [**27**]-[**30**] exhibited strong luminescence between 370-440 nm and the emission spectra of the complexes and salts (**V** and **W** in Scheme 24) were superimposable, therefore indicating the predominance of the pyrene moiety in the emission, and the negligible participation of the heterocyclic fragments or the metals. The pyrene-centered emission of complexes ([**27**]-[**30**]) was reduced compared to their pyrene-containing azoliums (**V** and **W**), suggesting again that the coordination of the carbene increases the fraction of non-radiative decay processes.[107] In this regard, the pyrene-based metal complexes displayed quantum yields values in the range of 3.1-6.3 %,[5b] while the quantum yields shown by **V** and **W** were 32 % and 41 %, respectively. However, the Φ_f values shown by [**27**]-[**30**] are rather high when compared with those shown by other complexes with the same pyrene-based bis-NHC ligands.[9b]
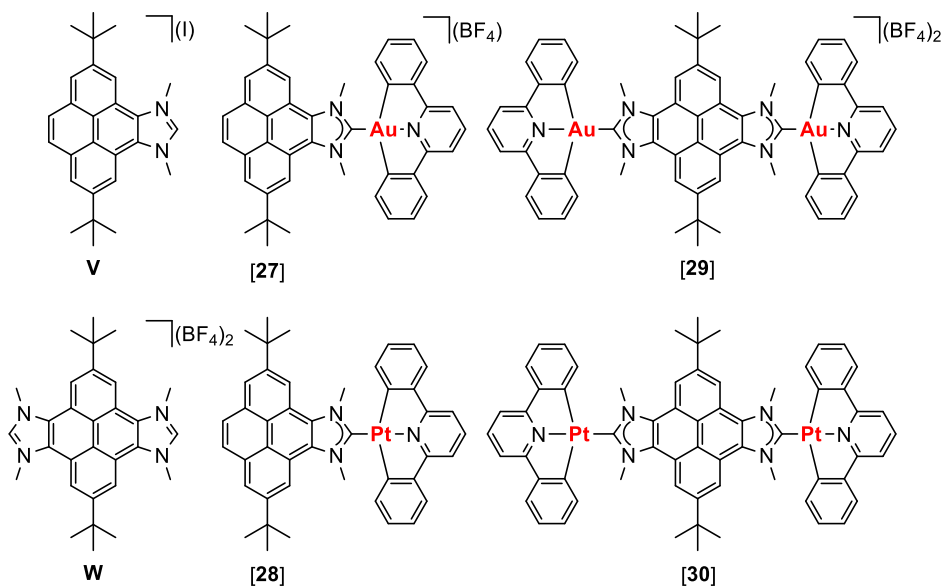
Scheme 24. Pyrene-based (**V** and **W**) and their related Pt(II) and Au(III) complexes ([**27**]-[**30**]) synthesized by the QOMCAT group.

Among all transition metal-NHC complexes with optical properties, those containing a coinage metal (group 11 elements) are the ones that have been most extensively studied, especially those of gold(I).[16, 101c] Since the first report of a luminescent Au(I)-NHC complex by Lin and coworkers,[109] many research groups focussed their efforts on synthesising and studying NHC complexes of Cu, Ag and Au with optical properties, and a large number of luminescent Au(I)-NHC complexes have been described in the literature.[96c, 110]

Luminescent emission, both fluorescence and phosphorescence have been achieved in gold(I)-NHC compounds, depending upon the participation of the metal in the excited states. On the one hand, for complexes bearing organic fluorophores (anthracene, pyrene, coumarin...) in many cases there is a negligible participation of the metal atom in the excited states, but a decrease of the luminescent quantum yields in comparison to the free fluorophore due to deactivation processes is often observed,[111] as mentioned before. On the other hand, the Au(I) atom can impart an important structural influence in the

enhancement of the emission. An example was recently published by Strassert and Hahn,[112] in which an emission enhancement was achieved by rigidification through metal complexation in comparison with the precursor of the NHC ligand (Chart 2). The high luminescence quantum yields for rigid luminophores are probably due to the inhibition of the internal conversion rates and vibrational motion in these complexes.
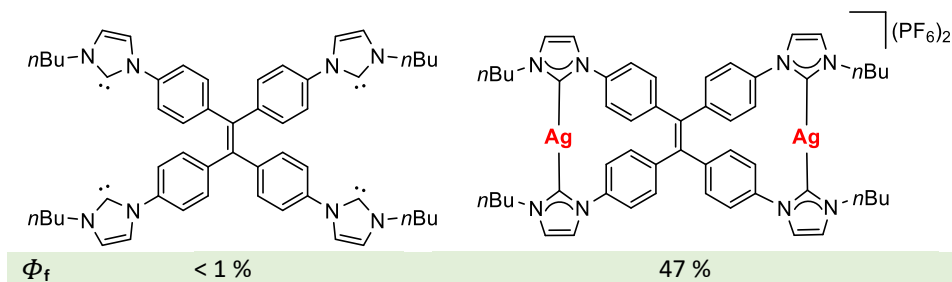

| Φ_f | < 1 % | 47 % |

Chart 2. Fluorescence quantum yields (Φ_f, gives the probability of the excited state being deactivated by fluorescence rather than by another, non-radiative mechanism) were measured in 10^{-6} M acetonitrile solution using a Hamamatsu integrating sphere at excitation wavelength of 315 nm.

As mentioned before, gold(I)-alkynyls constitute an interesting class of complexes with high potential in the field of photoluminescence.[92, 113] Taking this into account, some research groups focussed their efforts on preparing Au(I)-NHC complexes with acetylide ligands,[110j, 114] aiming to obtain complexes with enhanced optical properties. In principle, gold-NHC complexes with acetylide groups are likely to provide high luminescence efficiencies due to the following reasons:

- The electron-donor character of the carbene ligand.
- The presence of a chromophore, or an acetylide ligand directly bound to the gold centre.
- The presence of metallophilic interactions.
- The presence of cyclometallated pincer ligands, in the case of Au(III) complexes

Gold–NHC complexes containing acetylide and chromophore groups bound to the gold centre represent a fascinating class of luminescent materials.[114-115] An interesting example of this type of complexes was reported in 2016 by Mohr and co-workers,[116] who designed a series of luminescent gold(I) complexes combining a benzothiadiazole group (chromophore) through an alkynyl-linker with a gold(I)-NHC unit. The photophysical properties of the resulting gold complexes ([**31**] and [**32**] in Chart 3) together with their TMS-protected alkyne (**X** in Chart 3) were examined in CH_2Cl_2 solutions at room temperature. The luminescence behaviour of the complexes reported was dominated by the benzothiadiazole chromophore, with negligible influence of the gold atom.
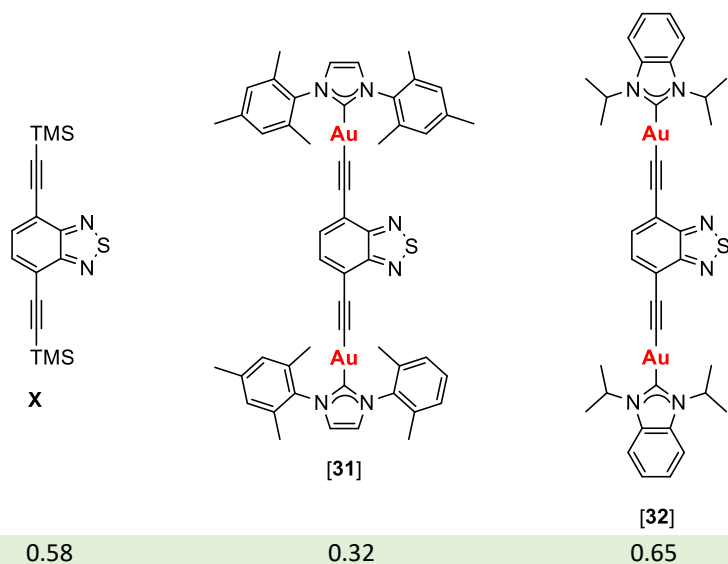
| Φ_f[a] | 0.58 | 0.32 | 0.65 |

Chart 3. TMS-protected alkyne (**X**) and luminescent alkynyl-gold(I)-carbene complexes ([**31**]-[**32**]). [a] Emission quantum yields of **X**, [**31**] and [**32**] were measured in CH_2Cl_2 at room temperature.

Another interesting example was reported recently by Casini and Bonsignore.[117] They synthesized two novel families of gold(I) complexes, including N1-substituted bis-NHC complexes and mixed gold(I) NHC-alkynyl complexes. Among the mixed gold(I) complexes, one features a fluorescent boron-dipyrromethene (BODIPY) fragment (Chart 4, left), which allowed determining

its uptake into the cytoplasm of cancer cells by fluorescence microspcopy. In addition, the quantum yield values shown that the complexation of the fluorophore to the gold(I)-NHC complex through the alkynyl bridge did not quench the fluorescence of the final metal complex, whose quantum yield was found to be 0.74.
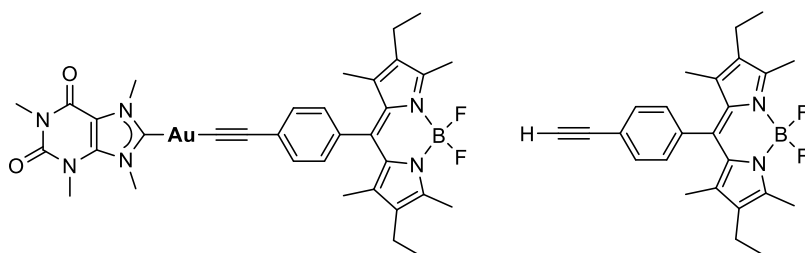
| $\Phi^{[a]}$ | 0.74 | 0.75 |

Chart 4. BODIPY-alkyne (right) and gold(I) NHC complex (left). [a] Emission quantum yield determined in aqueous solution using rhodamine 6G in ethanol (Φ = 0.94) as standard.

In line with this, Tang and co-workers[118] described a series of tetraphenylethene (TPE) modified Au(I)-NHC compounds depicted in Scheme 25, aiming to obtain gold-containing anticancer systems possessing luminescence-guided probing properties. Among all complexes tested, [**33**] achieved the optimal specificity and the most efficient inhibition against various cancer cells with low toxic effects on normal cells. The study demonstrates that the complex possesses great potential as a specific bioimaging and *theranostic* agent for cancer. On the other hand, complex [**36**], which contains an acetylide ligand, showed lower antiproliferative activity than the other gold-NHC complexes and a negligible cancer cell imaging. Nevertheless, this work has a great significance in providing insights into the design of other gold-NHC complexes for their practical application in bioimaging and cancer diagnosis.
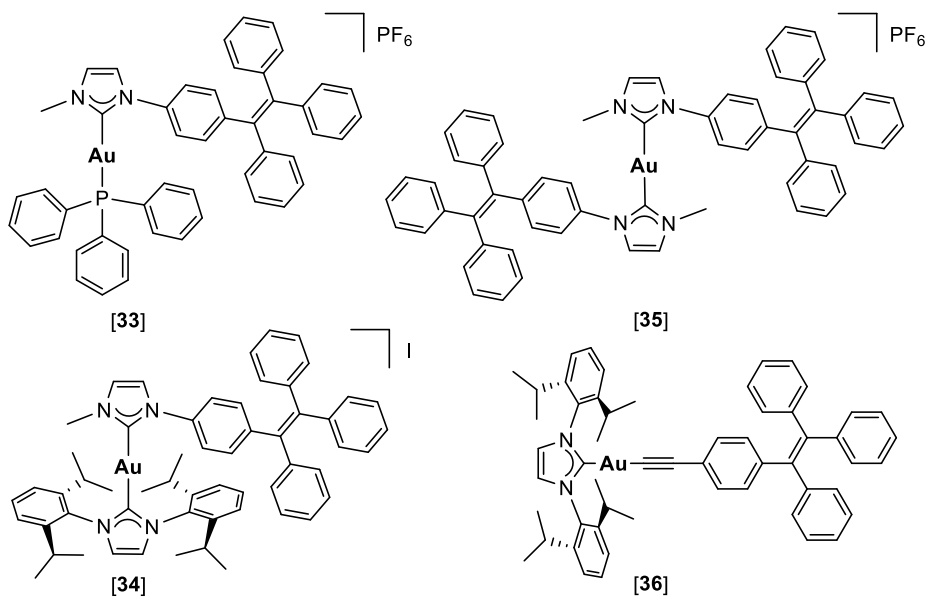
Scheme 25. NHC-based gold(I) complexes ([**33**]-[**36**]) synthesized by Tang's group.

These investigations show that gold-NHC complexes bearing alkynyl and chromophore groups display the potential for the obtention of luminophores with an incredible applicability in medicine, possessing great potential as bioimaging and *theranostic* agents. In conclusion, all these results should be an open door to the development of new Au(I)-NHC complexes containing acetylide ligands and underline them as promising tools for biological applications by appropriate chemical tuning.

References

1.   Berry, J. F.; Thomas, C. M., *Dalton Trans.* **2017,** *46* (17), 5472-5473.

2.   (a) Behlen, M. J.; Zhou, Y.-Y.; Steiman, T. J.; Pal, S.; Hartline, D. R.; Zeller, M.; Uyeda, C., *Dalton Trans.* **2017,** *46* (17), 5493-5497; (b) Mazzacano, T. J.; Leon, N. J.; Waldhart, G. W.; Mankad, N. P., *Dalton Trans.* **2017,** *46* (17), 5518-5521; (c) Nimthong-Roldan, A.; Guillet, J. L.; McNeely, J.; Ozumerzifon, T. J.; Shores, M. P.; Golen, J. A.; Rheingold, A. L.; Doerrer, L. H., *Dalton Trans.* **2017,** *46* (17), 5546-5557; (d) Rosenkoetter, K. E.; Ziller, J. W.; Heyduk, A. F., *Dalton Trans.* **2017,** *46* (17), 5503-5507; (e) Wang, Y.; Hickox, H. P.; Wei, P.; Robinson, G. H., *Dalton Trans.* **2017,** *46* (17), 5508-5512.

3.   Ghosh, P.; Quiroz, M.; Wang, N.; Bhuvanesh, N.; Darensbourg, M. Y., *Dalton Trans.* **2017,** *46* (17), 5617-5624.

4.   (a) Mercs, L.; Neels, A.; Albrecht, M., *Dalton Trans.* **2008,** (41), 5570-5576; (b) Schuster, O.; Mercs, L.; Albrecht, M., *Chimia* **2010,** *64* (3), 184-187; (c) van den Beuken, E. K.; Feringa, B. L., *Tetrahedron* **1998,** *54* (43), 12985-13011.

5.   (a) Böhmer, M.; Kampert, F.; Tan, T. T. Y.; Guisado-Barrios, G.; Peris, E.; Hahn, F. E., *Organometallics* **2018,** *37* (21), 4092-4099; (b) Gonell, S.; Poyatos, M.; Peris, E., *Dalton Trans.* **2016,** *45* (13), 5549-5556; (c) Mas-Marza, E.; Mata, J. A.; Peris, E., *Angew. Chem. Int. Ed.* **2007,** *46* (20), 3729-3731; (d) Mata, J. A.; Hahn, F. E.; Peris, E., *Chem. Sci.* **2014,** *5* (5), 1723-1732; (e) Sabater, S.; Mata, J. A.; Peris, E., *Organometallics* **2012,** *31* (17), 6450-6456; (f) Sabater, S.; Mata, J. A.; Peris, E., *Chem. Eur. J.* **2012,** *18* (20), 6380-6385; (g) Sabater, S.; Mata, J. A.; Peris, E., *Nature Communications* **2013,** *4*; (h) Zanardi, A.; Corberan, R.; Mata, J. A.; Peris, E., *Organometallics* **2008,** *27* (14), 3570-3576; (i) Zanardi, A.; Mata, J. A.; Peris, E., *J. Am. Chem. Soc.* **2009,** *131* (40), 14531-14537.

6.   (a) Gonell, S.; Poyatos, M.; Peris, E., *Angew. Chem. Int. Ed.* **2013,** *52* (27), 7009-7013; (b) Guisado-Barrios, G.; Hiller, J.; Peris, E., *Chem. Eur. J.* **2013,** *19* (31), 10405-10411.

7.   (a) Poyatos, M.; Mata, J. A.; Peris, E., *Chem. Rev.* **2009,** *109* (8), 3677-3707; (b) Peris, E., *Chem. Commun.* **2016,** *52* (34), 5777-5787.

8.   Prades, A.; Peris, E.; Alcarazo, M., *Organometallics* **2012,** *31* (12), 4623-4626.

9.   (a) Gonell, S.; Peris, E., *Acs Catalysis* **2014,** *4* (8), 2811-2817; (b) Ibañez, S.; Guerrero, A.; Poyatos, M.; Peris, E., *Chem. Eur. J.* **2015,** *21* (29), 10566-10575; (c) Gonell, S.; Poyatos, M.; Peris, E., *Chem. Eur. J.* **2014,** *20,* 9716-9724.

10.   Gonell, S.; Alabau, R. G.; Poyatos, M.; Peris, E., *Chem. Commun.* **2013,** *49* (64), 7126-7128.

11.   Mejuto, C.; Guisado-Barrios, G.; Peris, E., *Organometallics* **2014,** *33* (12), 3205-3211.

12.   Valdes, H.; Poyatos, M.; Peris, E., *Organometallics* **2015,** *34* (9), 1725-1729.

13.   Williams, K. A.; Bielawski, C. W., *Chem. Commun.* **2010,** *46* (28), 5166-5168.

14.   Ruiz-Botella, S.; Peris, E., *Chem. Eur. J.* **2015,** *21* (43), 15263-15271.

15.   (a) Gan, M.-M.; Liu, J.-Q.; Zhan, L.; Wang, Y.-Y.; Hahn, F. E.; Han, Y.-F., *Chem. Rev.* **2018,** *118* (19), 9587-9641; (b) Ibañez, S.; Poyatos, M.; Peris, E., *Acc. Chem. Res.* **2020,** *53* (7), 1401-1413; (c) Sinha, N.; Hahn, F. E., *Acc. Chem. Res.* **2017,** *50* (9), 2167-2184.

16.   Visbal, R.; Gimeno, M. C., *Chem. Soc. Rev.* **2014,** *43* (10), 3551-3574.

17.   (a) Li, Z.; Liu, Z.; Sun, H.; Gao, C., *Chem. Rev.* **2015,** *115* (15), 7046-7117; (b) McConnell, A. J.; Wood, C. S.; Neelakandan, P. P.; Nitschke, J. R., *Chem. Rev.* **2015,** *115* (15), 7729-7793; (c) Peng, H.-Q.; Niu, L.-Y.; Chen, Y.-Z.; Wu, L.-Z.; Tung, C.-H.; Yang, Q.-Z., *Chem. Rev.* **2015,** *115* (15), 7502-7542; (d) Sun, X.; James, T. D., *Chem. Rev.* **2015,** *115* (15), 8001-8037; (e) Xue, M.; Yang, Y.; Chi, X.; Yan, X.; Huang, F., *Chem. Rev.* **2015,** *115* (15), 7398-7501; (f) Yu, G.; Jie, K.; Huang, F., *Chem. Rev.* **2015,** *115* (15), 7240-7303.

18.	(a) Lehn, J. M., *Pure Appl. Chem.* **1978,** *50* (9-10), 871-892; (b) Lehn, J. M., *Science* **1985,** *227* (4689), 849-856; (c) Lehn, J. M., *Angew. Chem. Int. Ed.* **1988,** *27* (1), 89-112; (d) Lehn, J. M., *Angew. Chem. Int. Ed.* **1990,** *29* (11), 1304-1319; (e) Fyfe, M. C. T.; Stoddart, J. F., *Acc. Chem. Res.* **1997,** *30* (10), 393-401; (f) Lehn, J. M., *Science* **2002,** *295* (5564), 2400-2403; (g) Oshovsky, G. V.; Reinhoudt, D. N.; Verboom, W., *Angew. Chem. Int. Ed.* **2007,** *46* (14), 2366-2393.

19.	(a) Ariga, K., Kunitake, T., *Supramolecular Chemistry: Fundamentals and Applications*. Springer-Verlag: Berlin, 2006; (b) Cram, D. J., *Angew. Chem. Int. Ed.* **1988,** *27* (8), 1009-1020; (c) Pedersen, C. J., *Angew. Chem. Int. Ed.* **1988,** *27* (8), 1021-1027.

20.	(a) Whitesides, G. M., *Scientific American* **1995,** *273* (3), 146-149; (b) Service, R. F., *Science* **2005,** *309* (5731), 95-95.

21.	(a) Li, W., *Matter* **2020,** *3* (4), 968-969; (b) Whitesides, G. M.; Grzybowski, B., *Science* **2002,** *295* (5564), 2418-2421.

22.	Dydio, P.; Reek, J. N. H., *Chem. Sci.* **2014,** *5* (6), 2135-2145.

23.	(a) Chi, X.; Cen, W.; Queenan, J. A.; Long, L.; Lynch, V. M.; Khashab, N. M.; Sessler, J. L., *J. Am. Chem. Soc.* **2019,** *141* (16), 6468-6472; (b) Choi, H. J.; Park, Y. S.; Song, J.; Youn, S. J.; Kim, H. S.; Kim, S. H.; Koh, K.; Paek, K., *J. Org. Chem.* **2005,** *70* (15), 5974-5981; (c) Serpell, C. J.; Cookson, J.; Thompson, A. L.; Beer, P. D., *Chem. Sci.* **2011,** *2* (3), 494-500.

24.	(a) Castilla, A. M.; Ramsay, W. J.; Nitschke, J. R., *Acc. Chem. Res.* **2014,** *47* (7), 2063-2073; (b) Caulder, D. L.; Raymond, K. N., *Acc. Chem. Res.* **1999,** *32* (11), 975-982; (c) Chakrabarty, R.; Mukherjee, P. S.; Stang, P. J., *Chem. Rev.* **2011,** *111* (11), 6810-6918; (d) Cook, T. R.; Stang, P. J., *Chem. Rev.* **2015,** *115* (15), 7001-7045; (e) Cook, T. R.; Zheng, Y. R.; Stang, P. J., *Chem. Rev.* **2013,** *113* (1), 734-777; (f) Fujita, M., *Chem. Soc. Rev.* **1998,** *27* (6), 417-425; (g) Fujita, M.; Ogura, K., *Coord. Chem. Rev.* **1996,** *148*, 249-264; (h) Gianneschi, N. C.; Masar, M. S.;

Mirkin, C. A., *Acc. Chem. Res.* **2005,** *38* (11), 825-837; (i) Han, M.; Engelhard, D. M.; Clever, G. H., *Chem. Soc. Rev.* **2014,** *43* (6), 1848-1860.

25.   Brown, C. J.; Toste, F. D.; Bergman, R. G.; Raymond, K. N., *Chem. Rev.* **2015,** *115* (9), 3012-3035.

26.   (a) Ahmad, N.; Younus, H. A.; Chughtai, A. H.; Verpoort, F., *Chem. Soc. Rev.* **2015,** *44* (1), 9-25; (b) Cook, T. R.; Vajpayee, V.; Lee, M. H.; Stang, P. J.; Chi, K.-W., *Acc. Chem. Res.* **2013,** *46* (11), 2464-2474; (c) Kumar, A.; Sun, S.-S.; Lees, A. J., *Coord. Chem. Rev.* **2008,** *252* (8-9), 922-939.

27.   Stang, P. J.; Olenyuk, B., *Acc. Chem. Res.* **1997,** *30* (12), 502-518.

28.   (a) Chen, L.-J.; Yang, H.-B.; Shionoya, M., *Chem. Soc. Rev.* **2017,** *46* (9), 2555-2576; (b) Harris, K.; Fujita, D.; Fujita, M., *Chem. Commun.* **2013,** *49* (60), 6703-6712; (c) Lifschitz, A. M.; Rosen, M. S.; McGuirk, C. M.; Mirkin, C. A., *J. Am. Chem. Soc.* **2015,** *137* (23), 7252-7261; (d) Newkome, G. R.; Moorefield, C. N., *Chem. Soc. Rev.* **2015,** *44* (12), 3954-3967.

29.   Lehn, J. M., *Supramolecular Chemistry: Concepts and perspectives*. Wiley-VCH: Weinheim: 1995.

30.   Sauvage, J. P., Dietrich-Buchecker, C., *Molecular Catenanes, Rotaxanes and Knots: A Journey Through the World of Molecular Topology*. Wiley-VCH: Weinheim: 1999.

31.   (a) Leininger, S.; Olenyuk, B.; Stang, P. J., *Chem. Rev.* **2000,** *100* (3), 853-907; (b) Northrop, B. H.; Chercka, D.; Stang, P. J., *Tetrahedron* **2008,** *64* (50), 11495-11503; (c) Olenyuk, B.; Fechtenkotter, A.; Stang, P. J., *Journal of the Chemical Society-Dalton Transactions* **1998,** (11), 1707-1728; (d) Seidel, S. R.; Stang, P. J., *Acc. Chem. Res.* **2002,** *35* (11), 972-983; (e) Stang, P. J., *Chem. Eur. J.* **1998,** *4* (1), 19-27; (f) Stang, P. J., *J. Org. Chem.* **2009,** *74* (1), 2-20.

32.   (a) Caulder, D. L.; Bruckner, C.; Powers, R. E.; Konig, S.; Parac, T. N.; Leary, J. A.; Raymond, K. N., *J. Am. Chem. Soc.* **2001,** *123* (37), 8923-8938; (b)

Caulder, D. L.; Raymond, K. N., *Journal of the Chemical Society-Dalton Transactions* **1999,** (8), 1185-1200.

33.   (a) Fujita, M.; Tominaga, M.; Hori, A.; Therrien, B., *Acc. Chem. Res.* **2005,** *38* (4), 369-378; (b) Fujita, M.; Umemoto, K.; Yoshizawa, M.; Fujita, N.; Kusukawa, T.; Biradha, K., *Chem. Commun.* **2001,** (6), 509-518.

34.   (a) Holliday, B. J.; Mirkin, C. A., *Angew. Chem. Int. Ed.* **2001,** *40* (11), 2022-2043; (b) Oliveri, C. G.; Ulmann, P. A.; Wiester, M. J.; Mirkin, C. A., *Acc. Chem. Res.* **2008,** *41* (12), 1618-1629.

35.   (a) Cotton, F. A.; Lin, C.; Murillo, C. A., *Acc. Chem. Res.* **2001,** *34* (10), 759-771; (b) Cotton, F. A.; Lin, C.; Murillo, C. A., *Proceedings of the National Academy of Sciences of the United States of America* **2002,** *99* (8), 4810-4813.

36.   (a) De, S.; Mahata, K.; Schmittel, M., *Chem. Soc. Rev.* **2010,** *39* (5), 1555-1575; (b) Nitschke, J. R., *Acc. Chem. Res.* **2007,** *40* (2), 103-112; (c) Safont-Sempere, M. M.; Fernandez, G.; Wuerthner, F., *Chem. Rev.* **2011,** *111* (9), 5784-5814.

37.   (a) Cai, J. J.; Sessler, J. L., *Chem. Soc. Rev.* **2014,** *43* (17), 6198-6213; (b) Garcia-Simon, C.; Costas, M.; Ribas, X., *Chem. Soc. Rev.* **2016,** *45* (1), 40-62; (c) Pluth, M. D.; Raymond, K. N., *Chem. Soc. Rev.* **2007,** *36* (2), 161-171; (d) Schneider, H. J.; Yatsimirsky, A. K., *Chem. Soc. Rev.* **2008,** *37* (2), 263-277.

38.   (a) Leenders, S. H. A. M.; Gramage-Doria, R.; de Bruin, B.; Reek, J. N. H., *Chem. Soc. Rev.* **2015,** *44* (2), 433-448; (b) Koblenz, T. S.; Wassenaar, J.; Reek, J. N. H., *Chem. Soc. Rev.* **2008,** *37* (2), 247-262; (c) Chen, L.-J.; Yang, H.-B., *Acc. Chem. Res.* **2018,** *51* (11), 2699-2710; (d) Klosterman, J. K.; Yamauchi, Y.; Fujita, M., *Chem. Soc. Rev.* **2009,** *38* (6), 1714-1725.

39.   (a) Ballester, P.; Fujita, M.; Rebek, J., Jr., *Chem. Soc. Rev.* **2015,** *44* (2), 392-393; (b) Chen, L.; Chen, Q.; Wu, M.; Jiang, F.; Hong, M., *Acc. Chem. Res.* **2015,** *48* (2), 201-210; (c) Constable, E. C., *Chem. Soc. Rev.* **2013,** *42* (4), 1637-1651; (d) Dale, E. J.; Vermeulen, N. A.; Juricek, M.; Barnes, J. C.; Young, R. M.;

Wasielewski, M. R.; Stoddart, J. F., *Acc. Chem. Res.* **2016,** *49* (2), 262-273; (e) Northrop, B. H.; Zheng, Y.-R.; Chi, K.-W.; Stang, P. J., *Acc. Chem. Res.* **2009,** *42* (10), 1554-1563; (f) Smulders, M. M. J.; Riddell, I. A.; Browne, C.; Nitschke, J. R., *Chem. Soc. Rev.* **2013,** *42* (4), 1728-1754; (g) Zarra, S.; Wood, D. M.; Roberts, D. A.; Nitschke, J. R., *Chem. Soc. Rev.* **2015,** *44* (2), 419-432; (h) Zhang, D.; Ronson, T. K.; Nitschke, J. R., *Acc. Chem. Res.* **2018,** *51* (10), 2423-2436.

40.   Han, Y.-F.; Jin, G.-X., *Chem. Soc. Rev.* **2014,** *43* (8), 2799-2823.

41.   Pöthig, A.; Casini, A., *Theranostics* **2019,** *9* (11), 3150-3169.

42.   (a) Garrison, J. C.; Panzner, M. J.; Custer, P. D.; Reddy, D. V.; Rinaldi, P. L.; Tessier, C. A.; Youngs, W. J., *Chem. Commun.* **2006,** (44), 4644-4646; (b) Ghosh, S.; Chakrabarty, R.; Mukherjee, P. S., *Inorg. Chem.* **2009,** *48* (2), 549-556; (c) Jiang, H.; Lin, W. B., *J. Am. Chem. Soc.* **2003,** *125* (27), 8084-8085; (d) Olenyuk, B.; Whiteford, J. A.; Fechtenkotter, A.; Stang, P. J., *Nature* **1999,** *398* (6730), 796-799; (e) Zhao, L.; Ghosh, K.; Zheng, Y.-R.; Stang, P. J., *J. Org. Chem.* **2009,** *74* (22), 8516-8521.

43.   Stang, P. J.; Persky, N. E.; Manna, J., *J. Am. Chem. Soc.* **1997,** *119* (20), 4777-4778.

44.   (a) Boydston, A. J.; Bielawski, C. W., *Dalton Trans.* **2006,** (34), 4073-4077; (b) Hahn, F. E.; Langenhahn, V.; Lugger, T.; Pape, T.; Le Van, D., *Angew. Chem. Int. Ed.* **2005,** *44* (24), 3759-3763.

45.   Li, Y.; An, Y. Y.; Fan, J. Z.; Liu, X. X.; Li, X.; Hahn, F. E.; Wang, Y. Y.; Han, Y. F., *Angew. Chem. Int. Ed.* **2019**.

46.   Boydston, A. J.; Williams, K. A.; Bielawski, C. W., *J. Am. Chem. Soc.* **2005,** *127* (36), 12496-12497.

47.   (a) Ibañez, S.; Poyatos, M.; Peris, E., *Chem. Commun.* **2017,** *53* (26), 3733-3736; (b) Segarra, C.; Linke, J.; Mas-Marza, E.; Kuck, D.; Peris, E., *Chem. Commun.* **2013,** *49* (90), 10572-10574.

48.   Radloff, C.; Weigand, J. J.; Hahn, F. E., *Dalton Trans.* **2009,** (43), 9392-9394.

49.   (a) Schmidtendorf, M.; Brinke, C. S. T.; Hahn, F. E., *J. Organomet. Chem.* **2014,** *751*, 620-627; (b) Sinha, N.; Roelfes, F.; Hepp, A.; Hahn, F. E., *Chem. Eur. J.* **2017,** *23* (25), 5939-5942.

50.   Schmidtendorf, M.; Pape, T.; Hahn, F. E., *Dalton Trans.* **2013,** *42* (45), 16128-16141.

51.   Radloff, C.; Hahn, F. E.; Pape, T.; Frohlich, R., *Dalton Trans.* **2009,** (35), 7215-7222.

52.   (a) Conrady, F. M.; Frohlich, R.; Brinke, C. S. T.; Pape, T.; Hahn, F. E., *J. Am. Chem. Soc.* **2011,** *133* (30), 11496-11499; (b) Schmidtendorf, M.; Pape, T.; Hahn, F. E., *Angew. Chem. Int. Ed.* **2012,** *51* (9), 2195-2198.

53.   (a) Casini, A.; Woods, B.; Wenzel, M., *Inorg. Chem.* **2017**, 14715-14729; (b) Kascatan-Nebioglu, A.; Panzner, M. J.; Tessier, C. A.; Cannon, C. L.; Youngs, W. J., *Coord. Chem. Rev.* **2007,** *251* (5-6), 884-895; (c) Pöthig, A.; Ahmed, S.; Winther-Larsen, H. C.; Guan, S.; Altmann, P. J.; Kudermann, J.; Andresen, A. M. S.; Gjoen, T.; Astrand, O. A. H., *Frontiers in Chemistry* **2018,** *6*.

54.   (a) Baker, M. V.; Barnard, P. J.; Berners-Price, S. J.; Brayshaw, S. K.; Hickey, J. L.; Skelton, B. W.; White, A. H., *J. Organomet. Chem.* **2005,** *690* (24-25), 5625-5635; (b) Lazreg, F.; Cazin, C. S. J., *Medical Applications of NHC-Gold and -Copper Complexes*. 2014; p 173-198; (c) Schuh, E.; Pflueger, C.; Citta, A.; Folda, A.; Rigobello, M. P.; Bindoli, A.; Casini, A.; Mohr, F., *J. Med. Chem.* **2012,** *55* (11), 5518-5528.

55.   Altmann, P. J.; Poethig, A., *J. Am. Chem. Soc.* **2016,** *138* (40), 13171-13174.

56.   Altmann, P. J.; Poethig, A., *Angew. Chem. Int. Ed.* **2017,** *56* (49), 15733-15736.

57.   (a) Martínez-Agramunt, V.; Gusev, D.; Peris, E., *Chem. Eur. J.* **2018,** *24* (55), 14802-14807; (b) Martinez-Agramunt, V.; Ruiz-Botella, S.; Peris, E., *Chem. Eur. J.* **2017,** *23* (27), 6675-6681.

58.   (a) Martinez-Agramunt, V.; Eder, T.; Darmandeh, H.; Guisado-Barrios, G.; Peris, E., *Angew. Chem. Int. Ed.* **2019,** *58* (17), 5682-5686; (b) Martinez-Agramunt, V.; Peris, E., *Chem. Commun.* **2019,** *55* (99), 14972-14975; (c) Martinez-Agramunt, V.; Peris, E., *Inorg. Chem.* **2019,** *58* (17), 11836-11842.

59.   Ibañez, S.; Peris, E., *Angew. Chem. Int. Ed.* **2020,** *59* (17), 6860-6865.

60.   Ibañez, S.; Peris, E., *Angew. Chem. Int. Ed.* **2019,** *58* (20), 6693-6697.

61.   (a) Biz, C.; Ibañez, S.; Poyatos, M.; Gusev, D.; Peris, E., *Chem. Eur. J.* **2017,** *23* (58), 14439-14444; (b) Ibañez, S.; Peris, E., *Chem. Eur. J.* **2018,** *24* (33), 8424-8431; (c) Ibañez, S.; Poyatos, M.; Peris, E., *Angew. Chem. Int. Ed.* **2018,** *57* (51), 16816-16820; (d) Ibañez, S.; Poyatos, M.; Peris, E., *Angew. Chem. Int. Ed.* **2017,** *56* (33), 9786-9790; (e) Ibañez, S.; Peris, E., *Chem. Eur. J.* **2019,** *25* (35), 8254-8258.

62.   (a) Haritash, A. K.; Kaushik, C. P., *J. Hazard. Mater.* **2009,** *169* (1-3), 1-15; (b) Keyte, I. J.; Harrison, R. M.; Lammel, G., *Chem. Soc. Rev.* **2013,** *42* (24), 9333-9391; (c) Lemieux, C. L.; Lambert, A. B.; Lundstedt, S.; Tysklind, M.; White, P. A., *Environ. Toxicol. Chem.* **2008,** *27* (4), 978-990; (d) Srogi, K., *Environmental Chemistry Letters* **2007,** *5* (4), 169-195.

63.   (a) Hardouin-Lerouge, M.; Hudhomme, P.; Salle, M., *Chem. Soc. Rev.* **2011,** *40* (1), 30-43; (b) Harmata, M., *Acc. Chem. Res.* **2004,** *37* (11), 862-873; (c) Klarner, F. G.; Schrader, T., *Acc. Chem. Res.* **2013,** *46* (4), 967-978; (d) Leblond, J.; Petitjean, A., *Chemphyschem* **2011,** *12* (6), 1043-1051.

64.   Leeuwen, P. W. N. M. v., *Supramolecular Catalysis*. Wiley-VCH: Germany, 2008.

65.   (a) Ballester, P.; Vidal-Ferran, A.; van Leeuwen, P. W. N. M., Modern Strategies in Supramolecular Catalysis. In *Advances in Catalysis, Vol 54*, Gates,

B. C.; Knozinger, H., Eds. 2011; Vol. 54, pp 63-126; (b) Hermann, K.; Ruan, Y.; Hardin, A. M.; Hadad, C. M.; Badjic, J. D., *Chem. Soc. Rev.* **2015,** *44* (2), 500-514; (c) Liu, J.; Chen, L.; Cui, H.; Zhang, J.; Zhang, L.; Su, C.-Y., *Chem. Soc. Rev.* **2014,** *43* (16), 6011-6061; (d) Raynal, M.; Ballester, P.; Vidal-Ferran, A.; van Leeuwen, P., *Chem. Soc. Rev.* **2014,** *43* (5), 1660-1733; (e) Raynal, M.; Ballester, P.; Vidal-Ferran, A.; van Leeuwen, P., *Chem. Soc. Rev.* **2014,** *43* (5), 1734-1787.

66.   (a) Samojlowicz, C.; Bieniek, M.; Pazio, A.; Makal, A.; Wozniak, K.; Poater, A.; Cavallo, L.; Wojcik, J.; Zdanowski, K.; Grela, K., *Chem. Eur. J.* **2011,** *17* (46), 12981-12993; (b) Valdes, H.; Poyatos, M.; Peris, E., *Inorg. Chem.* **2015,** *54* (7), 3654-3659; (c) Valdes, H.; Poyatos, M.; Ujaque, G.; Peris, E., *Chem. Eur. J.* **2015,** *21* (4), 1578-1588.

67.   (a) Ibañez, S.; Poyatos, M.; Peris, E., *Organometallics* **2017,** *36* (7), 1447-1451; (b) Nuevo, D.; Poyatos, M.; Peris, E., *Organometallics* **2018,** *37* (20), 3407-3411.

68.   Samojlowicz, C.; Bieniek, M.; Zarecki, A.; Kadyrov, R.; Grela, K., *Chem. Commun.* **2008,** (47), 6282-6284.

69.   Rost, D.; Porta, M.; Gessler, S.; Blechert, S., *Tetrahedron Lett.* **2008,** *49* (41), 5968-5971.

70.   Grandbois, A.; Collins, S. K., *Chem. Eur. J.* **2008,** *14* (30), 9323-9329.

71.   Ledoux, N.; Allaert, B.; Pattyn, S.; Vander Mierde, H.; Vercaemst, C.; Verpoort, F., *Chem. Eur. J.* **2006,** *12* (17), 4654-4661.

72.   Furstner, A.; Ackermann, L.; Gabor, B.; Goddard, R.; Lehmann, C. W.; Mynott, R.; Stelzer, F.; Thiel, O. R., *Chem. Eur. J.* **2001,** *7* (15), 3236-3253.

73.   Lopez-Vidal, E. M.; Fernandez-Mato, A.; Garcia, M. D.; Perez-Lorenzo, M.; Peinador, C.; Quintela, J. M., *J. Org. Chem.* **2014,** *79* (3), 1265-1270.

74.   Fritsky, I. O.; Ott, R.; Kramer, R., *Angew. Chem. Int. Ed.* **2000,** *39* (18), 3255-+.

75. Srinivasan, B.; Forouhar, F.; Shukla, A.; Sampangi, C.; Kulkarni, S.; Abashidze, M.; Seetharaman, J.; Lew, S.; Mao, L.; Acton, T. B.; Xiao, R.; Everett, J. K.; Montelione, G. T.; Tong, L.; Balaram, H., *Febs Journal* **2014,** *281* (6), 1613-1628.

76. Gusev, D. G.; Peris, E., *Dalton Trans.* **2013,** *42*, 7359-7364.

77. Ruiz-Botella, S.; Peris, E., *Organometallics* **2014,** *33* (19), 5509-5516.

78. Valdes, H.; Poyatos, M.; Peris, E., *Organometallics* **2014,** *33* (1), 394-401.

79. (a) Edwards, M. G.; Jazzar, R. F. R.; Paine, B. M.; Shermer, D. J.; Whittlesey, M. K.; Williams, J. M. J.; Edney, D. D., *Chem. Commun.* **2004,** (1), 90-91; (b) Guillena, G.; Ramon, D. J.; Yus, M., *Angew. Chem. Int. Ed.* **2007,** *46* (14), 2358-2364; (c) Hamid, M.; Slatford, P. A.; Williams, J. M. J., *Adv. Synth. Catal.* **2007,** *349* (10), 1555-1575.

80. (a) Hegg, E. L.; Mortimore, S. H.; Cheung, C. L.; Huyett, J. E.; Powell, D. R.; Burstyn, J. N., *Inorg. Chem.* **1999,** *38* (12), 2961-2968; (b) Srivastava, R. S.; Nicholas, K. M., *Organometallics* **2005,** *24* (7), 1563-1568.

81. Valeur, B., *Molecular Fluorescence: Principles and applications*. WILEY-VCH: Weinheim (Germany), 2001.

82. Omary, M. A.; Patterson, H. H., *Luminescence, Theory*. 2017; p 636-653.

83. Lakowicz, J. R., *Principles of Fluorescence Spectroscopy*. Springer US: New York, 2006; p 954.

84. Jablonski, A., *Z. Physik* **1935,** (94), 38-46.

85. (a) Chen, X. Q.; Tian, X. Z.; Shin, I.; Yoon, J., *Chem. Soc. Rev.* **2011,** *40* (9), 4783-4804; (b) Chen, X. Q.; Wang, F.; Hyun, J. Y.; Wei, T. W.; Qiang, J.; Ren, X. T.; Shin, I.; Yoon, J., *Chem. Soc. Rev.* **2016,** *45* (10), 2976-3016; (c) Niu, L. Y.; Chen, Y. Z.; Zheng, H. R.; Wu, L. Z.; Tung, C. H.; Yang, Q. Z., *Chem. Soc. Rev.* **2015,** *44* (17), 6143-6160; (d) Vendrell, M.; Zhai, D. T.; Er, J. C.; Chang, Y. T., *Chem. Rev.* **2012,** *112* (8), 4391-4420; (e) Yang, S. K.; Shi, X. H.; Park, S.; Ha, T.; Zimmerman,

S. C., *Nat. Chem.* **2013,** *5* (8), 692-697; (f) Wu, J. S.; Liu, W. M.; Ge, J. C.; Zhang, H. Y.; Wang, P. F., *Chem. Soc. Rev.* **2011,** *40* (7), 3483-3495.

86.   (a) Dai, X. L.; Zhang, Z. X.; Jin, Y. Z.; Niu, Y.; Cao, H. J.; Liang, X. Y.; Chen, L. W.; Wang, J. P.; Peng, X. G., *Nature* **2014,** *515* (7525), 96-99; (b) Zhu, M. R.; Yang, C. L., *Chem. Soc. Rev.* **2013,** *42* (12), 4963-4976.

87.   (a) Ashton, T. D.; Jolliffe, K. A.; Pfeffer, F. M., *Chem. Soc. Rev.* **2015,** *44* (14), 4547-4595; (b) Yao, J.; Yang, M.; Duan, Y. X., *Chem. Rev.* **2014,** *114* (12), 6130-6178.

88.   (a) Kido, J.; Kimura, M.; Nagai, K., *Science* **1995,** *267* (5202), 1332-1334; (b) Burroughes, J. H.; Bradley, D. D. C.; Brown, A. R.; Marks, R. N.; Mackay, K.; Friend, R. H.; Burn, P. L.; Holmes, A. B., *Nature* **1990,** *347* (6293), 539-541.

89.   Fernández-Moreira, V.; Gimeno, M. C., *Chem. Eur. J.* **2018,** (24), 3345-3353.

90.   (a) Chou, P. T.; Chi, Y.; Chung, M. W.; Lin, C. C., *Coord. Chem. Rev.* **2011,** *255* (21-22), 2653-2665; (b) Heine, J.; Muller-Buschbaum, K., *Chem. Soc. Rev.* **2013,** *42* (24), 9232-9242; (c) Wagenknecht, P. S.; Ford, P. C., *Coord. Chem. Rev.* **2011,** *255* (5-6), 591-616.

91.   (a) Li, P.; Ahrens, B.; Feeder, N.; Raithby, P. R.; Teat, S. J.; Khan, M. S., *Dalton Trans.* **2005,** (5), 874-883; (b) Liu, L.; Wong, W.-Y.; Shi, J.-X.; Cheah, K.-W., *J. Polym. Sci., Part A: Polym. Chem.* **2006,** *44* (19), 5588-5607; (c) Aguilo, E.; Moro, A. J.; Outis, M.; Pina, J.; Sarmento, D.; Seixas de Melo, J. S.; Rodriguez, L.; Carlos Lima, J., *Inorg. Chem.* **2018,** *57* (21), 13423-13430; (d) Vogt, R. A.; Gray, T. G.; Crespo-Hernandez, C. E., *J. Am. Chem. Soc.* **2012,** *134* (36), 14808-14817.

92.   Lima, J. C.; Rodriguez, L., *Chem. Soc. Rev.* **2011,** *40* (11), 5442-5456.

93.   (a) Cheung, K. L.; Yip, S. K.; Yam, V. W. W., *J. Organomet. Chem.* **2004,** *689* (24), 4451-4462; (b) McArdle, C. P.; Van, S.; Jennings, M. C.; Puddephatt, R. J., *J. Am. Chem. Soc.* **2002,** *124* (15), 3959-3965; (c) Tiekink, E. R. T., *Coord. Chem. Rev.* **2014,** *275*, 130-153.

94.   (a) To, W. P.; Chan, K. T.; Tong, G. S. M.; Ma, C. S.; Kwok, W. M.; Guan, X. G.; Low, K. H.; Che, C. M., *Angew. Chem. Int. Ed.* **2013,** *52* (26), 6648-6652; (b) To, W. P.; Zhou, D. L.; Tong, G. S. M.; Cheng, G.; Yang, C.; Che, C. M., *Angew. Chem. Int. Ed.* **2017,** *56* (45), 14036-14041; (c) Wong, B. Y. W.; Wong, H. L.; Wong, Y. C.; Au, V. K. M.; Chan, M. Y.; Yam, V. W. W., *Chem. Sci.* **2017,** *8* (10), 6936-6946.

95.   Chan, K. T.; Tong, G. S. M.; To, W. P.; Yang, C.; Du, L. L.; Phillips, D. L.; Che, C. M., *Chem. Sci.* **2017,** *8* (3), 2352-2364.

96.   (a) Hopkinson, M. N.; Richter, C.; Schedler, M.; Glorius, F., *Nature* **2014,** *510* (7506), 485-496; (b) Danopoulos, A. A.; Simler, T.; Braunstein, P., *Chem. Rev.* **2019,** *119* (6), 3730-3961; (c) Lin, J. C. Y.; Huang, R. T. W.; Lee, C. S.; Bhattacharyya, A.; Hwang, W. S.; Lin, I. J. B., *Chem. Rev.* **2009,** *109* (8), 3561-3598; (d) Bellemin-Laponnaz, S.; Dagorne, S., *Chem. Rev.* **2014,** *114* (18), 8747-8774.

97.   Benhamou, L.; Chardon, E.; Lavigne, G.; Bellemin-Laponnaz, S.; Cesar, V., *Chem. Rev.* **2011,** *111* (4), 2705-2733.

98.   (a) Hansen, S.; Klahn, M.; Beweries, T.; Rosenthal, U., *Chemsuschem* **2012,** *5* (4), 656-660; (b) Park, H.-J.; Kim, W.; Choi, W.; Chung, Y. K., *New J. Chem.* **2013,** *37* (10), 3174-3182.

99.   Liu, Q.-X.; Yao, Z.-Q.; Zhao, X.-J.; Zhao, Z.-X.; Wang, X.-G., *Organometallics* **2013,** *32* (12), 3493-3501.

100.   Park, H.-J.; Kim, K. H.; Choi, S. Y.; Kim, H.-M.; Lee, W. I.; Kang, Y. K.; Chung, Y. K., *Inorg. Chem.* **2010,** *49* (16), 7340-7352.

101.   (a) Bertrand, B.; Citta, A.; Franken, I. L.; Picquet, M.; Folda, A.; Scalcon, V.; Rigobello, M. P.; Le Gendre, P.; Casini, A.; Bodio, E., *J. Biol. Inorg. Chem.* **2015,** *20* (6), 1005-1020; (b) Mui, Y. F.; Fernandez-Gallardo, J.; Elie, B. T.; Gubran, A.; Maluenda, I.; Sanau, M.; Navarro, O.; Contel, M., *Organometallics* **2016,** *35* (9),

1218-1227; (c) Mora, M.; Concepcion Gimeno, M.; Visbal, R., *Chem. Soc. Rev.* **2019,** *48* (2), 447-462.

102.   (a) Boydston, A. J.; Pecinovsky, C. S.; Chao, S. T.; Bielawski, C. W., *J. Am. Chem. Soc.* **2007,** *129* (47), 14550-14551; (b) Boydston, A. J.; Vu, P. D.; Dykhno, O. L.; Chang, V.; Wyatt, A. R., II; Stockett, A. S.; Ritschdbrff, E. T.; Shear, J. B.; Bielawski, C. W., *J. Am. Chem. Soc.* **2008,** *130* (10), 3143-3156; (c) Er, J. A. V.; Tennyson, A. G.; Kamplain, J. W.; Lynch, V. M.; Bielawski, C. W., *Eur. J. Inorg. Chem.* **2009,** (13), 1729-1738; (d) Wiggins, K. M.; Kerr, R. L.; Chen, Z.; Bielawski, C. W., *J. Mater. Chem.* **2010,** *20* (27), 5709-5714; (e) Tennyson, A. G.; Rosen, E. L.; Collins, M. S.; Lynch, V. M.; Bielawski, C. W., *Inorg. Chem.* **2009,** *48* (14), 6924-6933.

103.   (a) Figueira-Duarte, T. M.; Muellen, K., *Chem. Rev.* **2011,** *111* (11), 7260-7314; (b) Winnik, F. M., *Chem. Rev.* **1993,** *93* (2), 587-614.

104.   Howarth, A. J.; Majewski, M. B.; Wolf, M. O., *Coord. Chem. Rev.* **2015,** *282*, 139-149.

105.   (a) Ballardini, R.; Varani, G.; Indelli, M. T.; Scandola, F., *Inorg. Chem.* **1986,** *25* (22), 3858-3865; (b) Tapu, D.; Owens, C.; VanDerveer, D.; Gwaltney, K., *Organometallics* **2009,** *28* (1), 270-276.

106.   (a) Berenguer, J. R.; Lalinde, E.; Teresa Moreno, M., *Coord. Chem. Rev.* **2010,** *254* (7-8), 832-875; (b) Chang, S. Y.; Kavitha, J.; Li, S. W.; Hsu, C. S.; Chi, Y.; Yeh, Y. S.; Chou, P. T.; Lee, G. H.; Carty, A. J.; Tao, Y. T.; Chien, C. H., *Inorg. Chem.* **2006,** *45* (1), 137-146; (c) Cummings, S. D., *Coord. Chem. Rev.* **2009,** *253* (3-4), 449-478; (d) Diez, A.; Lalinde, E.; Teresa Moreno, M., *Coord. Chem. Rev.* **2011,** *255* (21-22), 2426-2447; (e) Mydlak, M.; Yang, C. H.; Polo, F.; Galstyan, A.; Daniliuc, C. G.; Felicetti, M.; Leonhardt, J.; Strassert, C. A.; De Cola, L., *Chem. Eur. J.* **2015,** *21*, 5161-5172; (f) Williams, J. A. G., Photochemistry and photophysics of coordination compounds: Platinum. In *Photochemistry and Photophysics of*

Coordination Compounds Ii, Balzani, V.; Campagna, S., Eds. 2007; Vol. 281, pp 205-268; (g) Williams, J. A. G., *Chem. Soc. Rev.* **2009,** *38* (6), 1783-1801.

107.   Hu, J. J.; Bai, S.-Q.; Yeh, H. H.; Young, D. J.; Chi, Y.; Hor, T. S. A., *Dalton Trans.* **2011,** *40* (17), 4402-4406.

108.   Li, C. K.-L.; Sun, R. W.-Y.; Kui, S. C.-F.; Zhu, N.; Che, C.-M., *Chem. Eur. J.* **2006,** *12* (20), 5253-5266.

109.   Wang, H. M. J.; Chen, C. Y. L.; Lin, I. J. B., *Organometallics* **1999,** *18* (7), 1216-1223.

110.   (a) Carcedo, C.; Knight, J. C.; Pope, S. J. A.; Fallis, I. A.; Dervisi, A., *Organometallics* **2011,** *30* (9), 2553-2562; (b) Concepcion Gimeno, M.; Laguna, A.; Visbal, R., *Organometallics* **2012,** *31* (20), 7146-7157; (c) Dinda, J.; Das Adhikary, S.; Seth, S. K.; Mahapatra, A., *New J. Chem.* **2013,** *37* (2), 431-438; (d) Yam, V. W.-W.; Lee, J. K.-W.; Ko, C.-C.; Zhu, N., *J. Am. Chem. Soc.* **2009,** *131* (3), 912-+; (e) Kriechbaum, M.; List, M.; Berger, R. J. F.; Patzschke, M.; Monkowius, U., *Chem. Eur. J.* **2012,** *18* (18), 5506-5509; (f) Pingxia Guo, R. J., Mengzhu Wang, Qun He, Chunhua Cai, Qiang Zhao, Weifeng Bu, *J. Organomet. Chem.* **2021,** *931*; (g) Baron, M.; Tubaro, C.; Biffis, A.; Basato, M.; Graiff, C.; Poater, A.; Cavallo, L.; Armaroli, N.; Accorsi, G., *Inorg. Chem.* **2012,** *51* (3), 1778-1784; (h) Haziz, U. F. M.; Haque, R. A.; Zhan, S.-Z.; Razali, M. R., *J. Organomet. Chem.* **2020,** *910*; (i) Monticelli, M.; Baron, M.; Tubaro, C.; Bellemin-Laponnaz, S.; Graiff, C.; Bottaro, G.; Armelao, L.; Orian, L., *Acs Omega* **2019,** *4* (2), 4192-4205; (j) Penney, A. A.; Starova, G. L.; Grachova, E. V.; Sizov, V. V.; Kinzhalov, M. A.; Tunik, S. P., *Inorg. Chem.* **2017,** *56* (24), 14771-14787; (k) Visbal, R.; Ospino, I.; Lopez-de-Luzuriaga, J. M.; Laguna, A.; Concepcion Gimeno, M., *J. Am. Chem. Soc.* **2013,** *135* (12), 4712-4715.

111.   Garg, J. A.; Blacque, O.; Heier, J.; Venkatesan, K., *Eur. J. Inorg. Chem.* **2012,** (11), 1750-1763.

112.   Sinha, N.; Stegemann, L.; Tan, T. T. Y.; Doltsinis, N. L.; Strassert, C. A.; Hahn, F. E., *Angew. Chem. Int. Ed.* **2017,** *56* (10), 2785-2789.

113.   Cerrada, E.; Fernandez-Moreira, V.; Gimeno, M. C., Gold and platinum alkynyl complexes for biomedical applications. In *Advances in Organometallic Chemistry, Vol 71*, Perez, P. J., Ed. 2019; Vol. 71, pp 227-258.

114.   Chow, A. L. F.; So, M. H.; Lu, W.; Zhu, N. Y.; Che, C. M., *Chem. Asian J.* **2011,** *6* (2), 544-553.

115.   Gao, L.; Partyka, D. V.; Updegraff, J. B.; Deligonul, N.; Gray, T. G., *Eur. J. Inorg. Chem.* **2009,** (18), 2711-2719.

116.   Moeller, A.; Bleckenwegner, P.; Monkowius, U.; Mohr, F., *J. Organomet. Chem.* **2016,** *813*, 1-6.

117.   Meier-Menches, S. M.; Aikman, B.; Dollerer, D.; Klooster, W. T.; Coles, S. J.; Santi, N.; Luk, L.; Casini, A.; Bonsignore, R., *J. Inorg. Biochem.* **2020,** *202*.

118.   Zhang, J.; Zou, H.; Lei, J.; He, B.; He, X.; Sung, H. H. Y.; Kwok, R. T. K.; Lam, J. W. Y.; Zheng, L.; Tang Ben, Z., *Angew. Chem. Int. Ed.* **2020,** *59* (18), 7097-7105.

2

Objectives

For many years, one of the main targets of the QOMCAT group was the development of new poly-NHC-based ligands decorated with polyaromatic fragments for the preparation of multimetallic catalysts, which displayed improved catalytic activities. The supramolecular interactions between the catalyst and the substrates played a key role in the improvement of the catalytic activity of these systems, when compared to systems lacking this type of interactions. More recently, the research interest of the group moved to the development of supramolecular organometallic assemblies for host-guest chemistry studies. In a continuation of these broad research lines, the general objective of this Ph.D. Thesis is to obtain new poly-NHC-based ligands with extended polyaromatic systems for the preparation of multimetallic complexes with interesting photophysical and catalytic applications. This general objective can be divided in the following more specific objectives, which will be explained in detail in the next chapters:

- Synthesis of three different tetraalkynyl gold(I) complexes containing a pyrene scaffold. The presence of the pyrene fragment (an effective chromophore) should introduce interesting luminescent properties to the metal complexes derived from this type of organic polyaromatic fused core.

- Study of the presence of the metal in the luminescent properties of the complexes obtained. Although in most of the cases the luminescent properties of the resulting complexes may be mainly due to the presence of the organic chromophore, the study of the metal role in the luminescent properties of the complex is of key importance in order to allow a rational design of metal-containing compounds with luminescent properties. The determination of the photophysical

properties in solution and in solid state, including the determination of the corresponding emission quantum yields will be performed.

- Introduction of the new luminescent complexes obtained in healthy living cells. Confocal microscopy studies will be performed in order to monitor the incorporation into the cell of the metal-containing bioimaging probes.

- Preparation of a new pyrene-centered tetra-NHC ligand and study of the catalytic properties of the rhodium and iridium complexes derived. Special attention will be paid to factors that may indicate that supramolecular interactions have a role in the catalytic performance, mainly as a consequence of the incorporation of the pyrene moiety in the core of the complex.

- Synthesis of supramolecular organometallic assemblies using an angular bis-imidazolindi-ylidene ligand previously obtained in the QOMCAT group. The use of this di-NHC ligand for the preparation of unusual supramolecular metallo-cyclophanes may have important implications in the preparation of new NHC-based supramolecular organometallic complexes with interesting host-guest properties.

Objetivos

Durante muchos años, uno de los objetivos principales del grupo QOMCAT fue el desarrollo de nuevos ligandos basados en policarbenos N-heterocíclicos decorados con fragmentos poliaromáticos para la preparación de catalizadores multimetálicos, que mostraron actividades catalíticas mejoradas. Las interacciones supramoleculares entre el catalizador y los sustratos jugaron un papel clave en la mejora de la actividad catalítica de estos sistemas, cuando se compararon con sistemas que carecían de este tipo de interacciones. Mas recientemente, el interés del grupo se desplazó hacia el desarrollo de complejos organometálicos supramoleculares para estudios químicos host-guest. Como continuación de estas amplias líneas de investigación, el objetivo general de esta Tesis Doctoral es la obtención de nuevos ligandos basados en policarbenos N-heterocíclicos con sistemas poliaromáticos extendidos para la preparación de complejos multimetálicos con aplicaciones fotofísicas y catalíticas interesantes. Este objetivo general puede dividirse en los siguientes objetivos más específicos, los cuales serán explicados con detalle en los siguientes capítulos:

- Síntesis de tres complejos de oro(I) tetra-alquinilo diferentes que contienen una base pireno. La presencia del fragmento pireno (un cromóforo muy efectivo) debería introducir propiedades luminiscentes interesantes a los complejos metálicos derivadas de este tipo de núcleo fusionado poliaromático orgánico.

- Estudio de la presencia del metal en las propiedades luminiscentes de los complejos obtenidos. Aunque es muchos de los casos las propiedades luminiscentes de los complejos resultantes puedan deberse principalmente a la presencia de un cromóforo orgánico, el estudio del papel del metal en las propiedades luminiscentes del complejo es de vital importancia para permitir un diseño racional de

compuestos que contienen metales con propiedades luminiscentes. Se lleva a cabo la determinación de las propiedades fotofísicas en disolución y en estado sólido, incluyendo la determinación del correspondiente rendimiento cuántico.

- Introducción de los nuevos complejos luminiscentes obtenidos en células sanas vivas. Se llevan a cabo estudios de microscopía confocal para monitorizar la incorporación dentro de la célula de las sondas de bioimagen que contienen metales.

- Preparación de nuevos ligandos tetra-NHC centrados en pireno y estudio de las propiedades catalíticas de los complejos de rodio e iridio derivados. Se debe prestar especial atención a los factores que pueden indicar que las interacciones supramoleculares juegan un papel en el comportamiento catalítico, principalmente como consecuencia de la incorporación de la molécula de pireno en el núcleo del complejo.

- Síntesis de estructuras organometálicas supramoleculares usando un ligando bis-imidazolindi-ilideno angular previamente obtenido por el grupo QOMCAT. El uso de este ligando di-NHC para la preparación de metalo-ciclofanos supramoleculares inusuales puede tener implicaciones importantes en la preparación de nuevos complejos organometálicos supramoleculares basados en carbenos N-heterocíclicos con interesantes propiedades host-guest.

3

ORGANOMETALLICS

Tetra-Au(I) Complexes Bearing a Pyrene Tetraalkynyl Connector Behave as Fluorescence Torches

Ana Gutiérrez-Blanco,[†] Vanesa Fernández-Moreira,[‡] M. Concepción Gimeno,[‡] Eduardo Peris,[†] and Macarena Poyatos*[,†]

[†]Institute of Advanced Materials (INAM). Universitat Jaume I, Av. Vicente Sos Baynat s/n, E-12071 Castellón, Spain

[‡]Departamento de Química Inorgánica, Instituto de Síntesis Química y Catálisis Homogénea (ISQCH), CSIC-Universidad de Zaragoza, 50009 Zaragoza, Spain

S *Supporting Information*

ABSTRACT: A pyrene tetraalkynyl ligand has been used for the preparation of three different tetraalkynyl Au(I) complexes. Two of these complexes display fluorescent emission in CH_2Cl_2 solution, with quantum yields exceeding 90%. Although the emission is mainly due to ligand-centered excited states, the presence of the metal center is key to reaching such excellent quantum yield values, providing an extra rigidity to the system and therefore, minimizing the nonradiative deactivation pathways. To the best of our knowledge, these quantum yields lie among the highest reported for metal-based luminophores in solution, a quality that makes them resemble molecular torches. Preliminary studies on healthy cheek cells show that one of the complexes is efficiently and rapidly taken up into the cell.

■ INTRODUCTION

Since the discovery of luminescent organic devices,[1] there has been increasing interest in the development of materials with emissive properties, mostly due to their applications as fluorescent sensors,[2] light-emitting diodes (OLEDs),[3] and bioimaging probes.[4] Although luminescent materials may find applications in every physical state, the vast majority are used as films and aggregates, as for example in the fabrication of OLEDs. This justifies why much effort has been directed to the study of the aggregation-induced emission (AIE) phenomenon, a process for which nonemissive luminogens are induced to emit by aggregate formation.[5] However, in the area of biomedical research, luminophores are often used in solution; therefore, it is very important to find new materials that show good emission properties in dilute solutions. If the luminophores are also able to show chemotherapeutic activity, then optical theranostic agents may be obtained, which could provide relevant information about their biological interplay.[6] Luminescent transition-metal compounds have attracted intense attention during the last two decades.[7] One of the main reasons for the great success of metal-based chromophores is that the heavy atom enhances spin−orbit coupling to yield partial mixing between triplet and singlet excited states, allowing a fast rate of intersystem crossing followed by phosphorescence and, sometimes, high quantum yields. Among transition-metal-based luminophores, gold(I) alkynyls constitute one of the most widely studied groups, probably because acetylides can connect the gold atom to a very large variety of organic functions.[8] N-heterocyclic carbene (NHC) ligands have also been extensively used in the preparation of metal complexes with photoluminescent properties, because their strong σ-donating character ensures high-energy emissions that facilitate the desired blue color needed for OLED applications.[9] While highly efficient emissions (ϕ > 85%) have been found for a (low) number of gold complexes in the solid or aggregated states,[10] to the best of our knowledge there is only one report describing comparably high quantum yields in solution.[11] In most cases, the nature of the ligands, the oxidation state, the coordination geometry of the Au complexes, or the presence of metallic interactions determines the nature of the luminescence. Both fluorescence and phosphorescence have been achieved in gold(I) compounds, depending upon the participation of the metal in the excited states. It has been observed that, in complexes bearing organic fluorophores, there is in many cases a negligible participation of the metal atom in the excited states. This is usually translated in a decrease of the luminescent quantum yields in comparison to the fluorophore because of deactivation processes. In some cases, the Au(I) atom can have important structural implications in the enhancement of the emission, as in a recent article published by Strassert and Hahn describing an example of emission enhancement by rigidification through metal complexation.[12]

Herein, we describe three pyrene-based tetraalkynyl Au(I) complexes bearing aromatic NHC or phosphine ligands. Two of these complexes were found to be highly emissive in solution, a property mostly related to the central pyrene core

Tetra-Au(I) Complexes Bearing a Pyrene Tetraalkynyl Connector Behave as Fluorescence Torches

Ana Gutiérrez-Blanco,[a] Vanesa Fernández-Moreira,[b] M. Concepción Gimeno,[b] Eduardo Peris,[a] and Macarena Poyatos[a],*

[a] *Institute of Advanced Materials (INAM). Universitat Jaume I, Av. Vicente Sos Baynat s/n, E-12071 Castellón, Spain*

[b] *Departamento de Química Inorgánica, Instituto de Síntesis Química y Catálisis Homogénea (ISQCH), CSIC-Universidad de Zaragoza, 50009 Zaragoza, Spain*

Email: poyatosd@uji.es

Abstract

A pyrene tetraalkynyl ligand has been used for the preparation of three different tetraalkynyl Au(I) complexes. Two of these complexes display fluorescent emission in CH_2Cl_2 solution, with quantum yields exceeding 90 %. Although the emission is mainly due to ligand-centered excited states, the presence of the metal center is key to reaching such excellent quantum yield values, providing an extra rigidity to the system and therefore, minimizing the nonradiative deactivation pathways. To the best of our knowledge, these quantum yields lie among the highest reported for metal-based luminophores in solution, a quality that makes them resemble molecular torches. Preliminary studies on healthy cheek cells show that one of the complexes is efficiently and rapidly taken up into the cell.

1. Introduction

Since the discovery of luminescent organic devices,[1] there has been increasing interest in the development of materials with emissive properties, mostly due to their applications as fluorescent sensors,[2] light-emitting diodes (OLEDs),[3] and bioimaging probes.[4] Although luminescent materials may find applications in every physical state, the vast majority are used as films and aggregates, as for example in the fabrication of OLEDs. This justifies why much effort has been directed to the study of the aggregation-induced emission (AIE) phenomenon, a process for which nonemissive luminogens are induced to emit by aggregate formation.[5] However, in the area of biomedical research, luminophores are often used in solution; therefore, it is very important to find new materials that show good emission properties in dilute solutions. If the luminophores are also able to show chemotherapeutic activity, then optical theranostic agents may be obtained, which could provide relevant information about their biological interplay.[6] Luminescent transition-metal compounds have attracted intense attention during the last two decades.[7] One of the main reasons for the great success of metal-based chromophores is that the heavy atom enhances spin–orbit coupling to yield partial mixing between triplet and singlet excited states, allowing a fast rate of intersystem crossing followed by phosphorescence and, sometimes, high quantum yields. Among transition-metal-based luminophores, gold(I) alkynyls constitute one of the most widely studied groups, probably because acetylides can connect the gold atom to a very large variety of organic functions.[8] N-Heterocyclic carbene (NHC) ligands have also been extensively used in the preparation of metal complexes with photoluminescent properties, because their strong σ-donating character ensures high-energy emissions that facilitate the desired blue colour needed for OLED applications.[9] While highly efficient emissions ($\phi > 85\%$) have been found for a (low) number of gold complexes in the solid or aggregated states,[10] to the best of our

knowledge there is only one report describing comparably high quantum yields in solution.[11] In most cases, the nature of the ligands, the oxidation state, the coordination geometry of the Au complexes, or the presence of metallic interactions determines the nature of the luminescence. Both fluorescence and phosphorescence have been achieved in gold(I) compounds, depending upon the participation of the metal in the excited states. It has been observed that, in complexes bearing organic fluorophores, there is in many cases a negligible participation of the metal atom in the excited states. This is usually translated in a decrease of the luminescent quantum yields in comparison to the fluorophore because of deactivation processes. In some cases, the Au(I) atom can have important structural implications in the enhancement of the emission, as in a recent article published by Strassert and Hahn describing an example of emission enhancement by rigidification through metal complexation.[12]

In this publication we describe three pyrene-based tetraalkynyl Au(I) complexes bearing aromatic NHC or phosphine ligands. Two of these complexes were found to be highly emissive in solution, a property mostly related to the central pyrene core yet enhanced by the coordination of the metal fragments and consequent rigidification of the final system.

2. Results and discussion

We decided to prepare a series of tetra-Au(I) complexes connected by a pyrene tetraalkynyl ligand. Our initial aim was to combine pyrene (one of the most widely studied organic materials in the field of photochemistry and photophysics[13]) with gold(I) alkynyl compounds bearing NHC ancillary ligands and study their photophysical properties. As will be described below, this combination of components allowed us to obtain two of the most efficient Au-based fluorescence emitters in solution reported to date.

The pyrene-connected Au(I) complexes were synthesized according to the procedure depicted in Scheme 1.
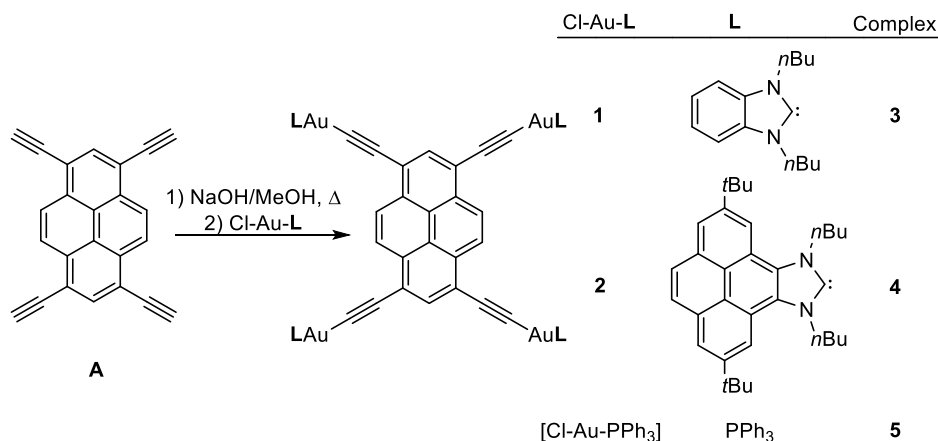
Scheme 1. Preparation of complexes **3**−**5**.

Complexes **3** and **4** were prepared by deprotonating 1,3,6,8-tetraethynylpyrene (**A**) with NaOH in refluxing methanol, followed by the addition of benzimidazolylidene gold(I) complex **1**[14] or pyrene imidazolylidene gold(I) complex **2**,[15] respectively. Following the same synthetic protocol, the triphenylphosphine-based Au(I) complex **5** was prepared by reacting **A** with [AuCl(PPh₃)] in the presence of NaOH. Complexes **3**−**5** were isolated in yields ranging from 40 to 60 %. All three complexes are highly soluble in chlorinated solvents, such as dichloromethane and chloroform, displaying very bright yellow solutions. Complexes **3**−**5** were characterized by NMR spectroscopy and gave satisfactory elemental analysis.

For complexes **3** and **4**, the number and integration of the signals displayed in the ^{1}H NMR spectra are in agreement with the presence of four NHC ligands with respect to the pyrene core. The ^{13}C NMR spectra of **3** and **4** revealed the appearance of signals due to the four equivalent metalated carbene carbons at 194.90 and 193.52 ppm, respectively.

The molecular structure of complex **3** was confirmed by means of X-ray diffraction. As depicted in Figure 1, the molecule consists of four benzimidazolylidene−Au(I) units connected by a pyrene tetraacetylide ligand. Two of the benzimidazolylidene ligands form an angle of 68.38° with respect to the plane of the pyrene linker, while the two remaining ligands are quasi-coplanar with the pyrene linker, as reflected by the small angle formed by the planes of the pyrene and the NHC fragments, 7.06°.
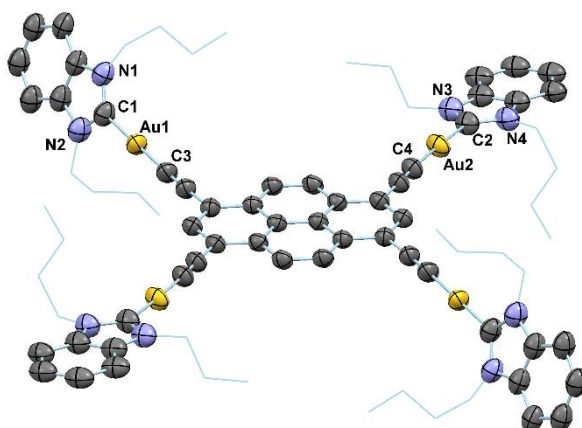
Figure 1. Molecular structure of **3**. Hydrogen atoms are removed for clarity. *n*Bu groups are represented in wireframe form. Selected distances (Å) and angles (deg): Au1−C1 2.027(12), Au1−C3 1.992(11), Au2−C2 2.029(12), Au2−C4 2.015(11); C2− Au2−C4 176.9(5), C3−Au1−C1 177.2(5).

The Au−$C_{carbene}$ bond distances are 2.017−2.029 Å. All other distances and angles are unexceptional. The crystal packing of the molecules shows that there is a two-dimensional array produced by the π-stacking interactions between the pyrene core and the benzene rings of opposite benzimidazolylidene ligands (see Figure S7 of the Supporting Information). The distance between planes is 3.45 Å, which is indicative of a π-stacking interaction. The Au−Au distance is 4.38 Å and therefore greater than the distances that can be considered within the range of aurophilic interactions (2.8−3.5 Å).[16]

The UV−visible absorption and the emission spectra of complexes **3** and **4** were studied in dichloromethane at 298 K (Table 1). The UV−vis spectrum of

compound **A** displays one vibronically resolved band in the region of 350–450 nm, assigned to pyrene-centered transitions. The acetylene-centered π–π^* transitions are observed as intense absorptions between 270 and 320 nm. The UV−vis spectra of complexes **3** and **4** show two intraligand transitions centered at the pyrene and acetylide units, although they are significantly red shifted in comparison to those of compound **A**, as a consequence of the perturbation produced by the coordination to the metal (see Figure S9 of the Supporting Information).

The emission spectra of complexes **3** and **4** in CH_2Cl_2 show a pyrene-centered vibronically resolved band, which is bathochromically shifted ($\Delta\lambda \approx$ +75 nm) in comparison to the emission shown by **A** (Figure 2). Possibly, the coordination of the gold atom to the alkynyl moiety withdraws the electron density of the latter and in consequence, there is a stabilization of the LUMO orbital. Interestingly, the lowest energy emission bands of the Au(I) complexes occurred at 546 nm, well into the visible region, thus justifying their bright visible emission. The excited-state lifetimes of **A**, as well as of complexes **3** and **4**, were found to be monoexponential and to be on the order of nanoseconds, therefore indicating the fluorescence nature of the emission and the apparent lack of participation of the metal in the electronic excited states. This observation is in accordance with the results found by Che and co-workers for their highly emissive Au(I) alkynyl complexes, where very small lifetimes were found, and the emissions are attributable to ligand-centered transitions with a small contribution of MLCT.[11]

Table 1. Photophysical data for **A** and **3−5** in CH_2Cl_2 solution[a]

	λ_{abs} (nm)	$\lambda_{em}{}^a$ (nm)	τ^b (ns)	$\phi_{em}{}^c$	K_r (10^8 s^{-1})	K_{nr} (10^8 s^{-1})
A	416, 391, 371, 306, 294, 255, 246	473 (sh), 445, 422	4	0.58	1.45	1.08
3	471, 441, 415, 342, 290, 282, 238	543 (sh), 507, 481	2	0.90	4.5	0.5
4	472, 442, 416, 342, 282, 253	546 (sh), 508, 481	1	0.38	3.8	6.8
5	469, 441, 413, 336, 268, 228	540 (sh), 505, 476	3	0.92	3.06	0.27

[a]Measurements performed in CH_2Cl_2 solution under ambient conditions (λ_{exc} 345 nm). [b]Excited state lifetime measured in degassed CH_2Cl_2 solution (λ_{exc} 345 nm with prompt use). [c]Quantum yields measured in degassed CH_2Cl_2 solution with excitation at 370 nm (absolute method). Deactivation rate constants were calculated by $K_r = \phi_{em}/\tau$ and $K_{nr} = ((1/\tau) - K_r)$.[17] sh = shoulder.
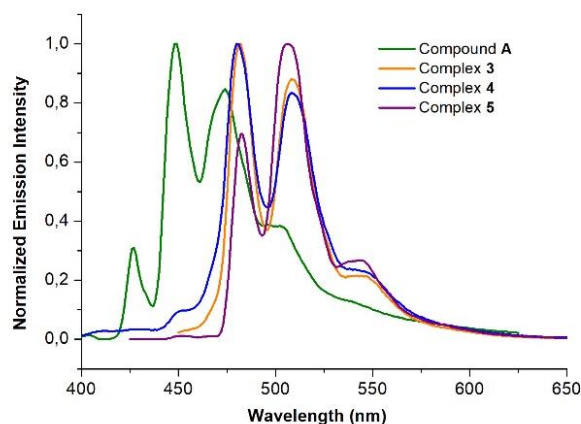
Figure 2. Fluorescence emission spectra of compound **A** and complexes **3−5** in CH_2Cl_2, upon excitation at 345 nm.

Complexes **3** and **4** were found to be remarkably emissive in solution, with fluorescence quantum yields of 0.90 and 0.38, respectively. As previously reported for species **A**, the presence of molecular oxygen barely affects the quantum yield values of **3−5** as consequence of the short excited-state lifetimes.[17] It is worth mentioning that complex **3** has a photoluminescence quantum yield considerably higher than that found for **A** (ϕ_{em} = 0.58).

This places complex **3** among the most emissive gold NHC complexes reported to date in solution. It is also worth mentioning that there is a notable difference between the emission intensity exhibited by complexes **3** and **4** and that of the monometallic Au(I) NHC complexes **1** and **2**, which were found to be nonemissive under the same conditions. In order to assess if the NHC ligand played a role in the emissive properties of complexes **3** and **4**, we also measured the photophysical properties of the phosphine-containing complex **5**, for which an extraordinary high quantum yield of 0.92 was observed (Table 1). This result indicates that both NHC ligands might play a different role in the luminescence efficiency. Whereas in the case of complex **3** a negligible participation of the NHC is observed, the pyrene imidazolylidene NHC derivative in complex **4** might promote an additional nonradiative deactivation pathway because of its extended π-conjugation and higher electron-donating character.[18] Radiative (K_r) and nonradiative (K_{rn}) rate constants were calculated to assess the existence of an additional nonradiative deactivation pathway for complex **4** (see Table 1). In all cases, both rate constants were on the order of 10^8, a much higher value than that of the pyrene itself (10^6 s^{-1}),[19] which is in accordance with their small excited-state lifetime value (1–4 ns).[17] In general, it was observed that the radiative rate constant value was higher than the non-radiative rate constant except for complex **4**, corroborating the extra deactivation pathway for this complex and consequently leading to a smaller quantum yield value. In any case, it seems clear that the gold metal center gives the alkynyl pyrene platform extra rigidity that highly increases the emission efficiency. As an illustrative image of the extraordinary emission properties of these complexes, Figure 3 shows a photograph of solutions of **A** and **3**–**5** in CH$_2$Cl$_2$ and in the solid state, upon irradiation with UV light (λ_{ex} = 365 nm).
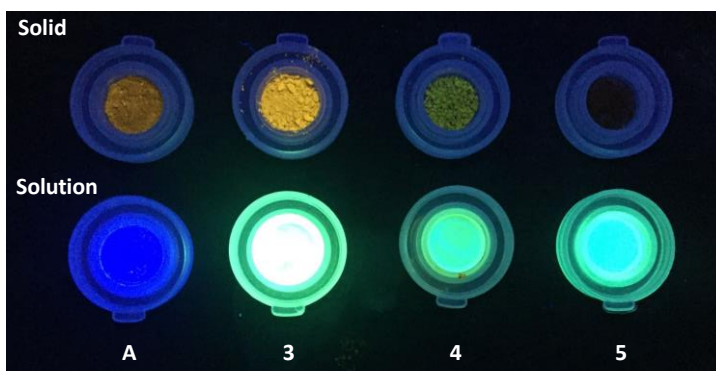
Figure 3. Photograph of **A** and **3**−**5** in the solid state (top) and in CH_2Cl_2 solution (bottom), under UV light at 365 nm.

The emission spectra of complexes **3**−**5** in the solid state at room temperature reveal one broad and featureless band typical of the pyrene excimer emission, with maxima at 585, 541, and 650 nm, respectively (see Figure S10 of the Supporting Information). The excited lifetimes of these bands are on the order of nanoseconds, and the quantum yields are 2.2 % for **3** and < 1 % for **4** and **5**. We attribute the bathochromic shift of the solid-state emission spectra in comparison to those of the solutions to intermolecular $\pi-\pi$ interactions occurring in the solid state, as demonstrated in the X-ray molecular structure of **3**. These $\pi-\pi$ stacking interactions should also justify the quenching of the emission produced by aggregation-caused quenching (ACQ). The low excited-state lifetimes are in accordance with the fluorescent nature of the emission of the solids, therefore discarding the presence of Au···Au interactions in the solid state, which would very likely produce delayed fluorescence or phosphorescence. We were also interested in studying the self-assembly capabilities of complexes **3** and **4** in solution. For this purpose, we obtained a series of ^1H NMR spectra of the two complexes at different concentrations, using $CDCl_3$. The representative concentration-dependent ^1H NMR spectra at room

temperature and labelling of the protons for complex **3** are given in Figure S15 of the Supporting Information.

The analysis of the signals of the spectra indicates that two signals assigned to the aromatic protons of the pyrene scaffold and two signals due to the aromatic protons of the benzimidazolylidene ligands are shifted downfield upon decreasing the concentration of the complex. This behaviour is strongly suggestive of the presence of aggregation driven by intermolecular π–π stacking interactions between these two parts of the molecule, as is also observed in the crystal packing of the molecule. No significant changes were detected in the ^{1}H NMR spectra of **4** in CDCl$_3$ in the range of concentrations studied (0.1–20 mM). A nonlinear regression analysis of the data of this series of spectra allowed us to calculate a self-association constant of 48 M^{-1}, thus demonstrating the propensity of **3** to form π-stacking aggregates.

This self-aggregation is responsible for some interesting photophysical consequences, as self-aggregation is temperature-dependent.

Figure 4. Photograph showing a solution of **3** in CH$_2$Cl$_2$ at 77 K (frozen solution, left) and at room temperature (right), under UV light at 365 nm.

As can be observed in Figure 4, the colour of the emission of a CH$_2$Cl$_2$ solution of **3** can switch from blue to yellow, by freezing the solution at 77 K. It could be suggested that lowering the temperature might prompt the formation of aggregates of **3**, which behave similarly to the solid state.

In view of the supramolecular self-assembly capability of complex **3**, the morphology of the aggregates was studied by scanning electron microscopy (SEM). For comparative purposes, SEM images of a sample of complex **4** were

also recorded. SEM images of **3**, prepared by slow diffusion of MeOH into a saturated solution of the complex in chloroform, show needles with a laminar nanostructure. On the other hand, SEM images of a sample of **4**, prepared by slow diffusion of hexane into a saturated solution of the complex in dichloromethane, show a disordered fiberlike nanostructure (Figure 5).
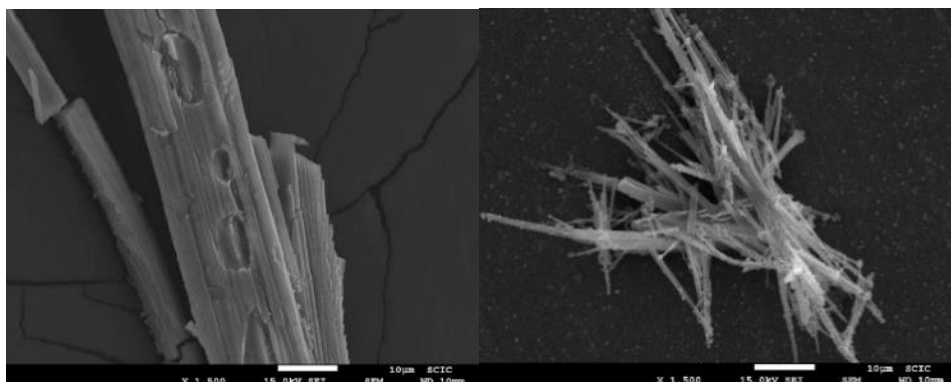
Figure 5: SEM micrographs of **3** (left) and **4** (right) at a magnification value of 1500×.

The combination of the fluorescence properties of complexes **3**−**5** with the well-established therapeutic properties of Au(I)[20] makes these complexes potential candidates as optical theranostic agents.[6] Regardless of their application as diagnostic and/or therapeutic agents, establishing their rapid and efficient cellular uptake is of crucial importance. Given the high quantum yield and stability of **3**, we selected it to monitor its uptake into healthy cheek cells (more details can be found in Figure S20 of the Supporting Information). The actual transport of **3** into the cellular interior, rather than association solely at the membrane surface, is evident by confocal microscopy upon excitation at 405 nm. The colour shown in the confocal microscopy figures is arbitrary. Purple was chosen here to enhance visualization of the emissive zones of the cell. Intense luminescence in the cytoplasm is apparent within 15 min (Figure 6, left).
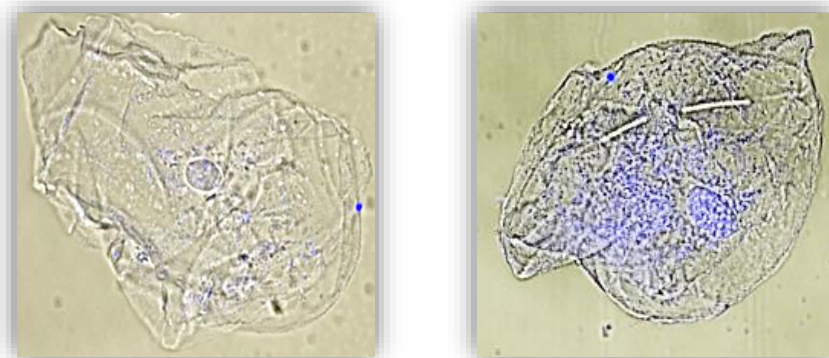
Figure 6. Confocal microscopy of healthy cheek cells treated with complex **3** for 15 min (left) and 30 min (right), excited at 405 nm.

After 30 min, intense luminescence can be also observed in the nucleus (Figure 6, right), thus proving that the uptake of **3** into the cell interior is efficient and rather rapid.

3. Conclusions

In summary, we obtained a series of pyrene tetraalkynyl complexes of Au(I) and studied their photophysical properties. Two of these complexes are among the most emissive Au(I) complexes described to date in solution. Although the origin of the emissions is assigned to an intraligand transition, coordination to the gold centers plays a key role, as it allows a red-shifted displacement of the emissions and an incredible enhancement of the quantum yields. We believe that the excellent emissive properties of these complexes in solution may find applications as bioimaging probes. Indeed, our preliminary studies on healthy cheek cells show that complex **3** is efficiently and rapidly taken up into the cell. Further studies involving cancer cells are currently underway.

4. Experimental section

General Methods. 2,7-Di-*tert*-butylpyrene[21] and 1,3,6,8-tetraethynylpyrene (**A**)[22] were prepared according to literature methods. NHC-based Au(I) complexes **1**[14] and **2**[15] were prepared as previously reported, starting from the corresponding benzimidazolium[14] and pyrene imidazolium[23] iodide salts, respectively. [AuCl(PPh$_3$)] was prepared according to the literature.[24] Anhydrous solvents were dried using a solvent purification system (SPS MBraun) or purchased and degassed prior to use by purging them with dry nitrogen. All of the reagents and solvents were used as received from commercial suppliers. NMR spectra were recorded on a Varian Innova 500 MHz or a Bruker 400/300 MHz instrument, using CDCl$_3$ as solvent. Elemental analyses were carried out on a TruSpec Micro Series apparatus. Infrared spectra (FTIR) were obtained with a FT/IR-6200 (Jasco) spectrometer with a spectral window of 4000–600 cm^{-1}. UV-vis absorption spectra were recorded on a Varian Cary 300 BIO spectrophotometer in CH$_2$Cl$_2$ solution under ambient conditions. Room-temperature steady-state emission and excitation spectra were recorded with a Horiba Jobin Yvon Fluorolog FL3-11 spectrometer fitted with a JY TBX picosecond detection module. Lifetime measurements were recorded with an LED from Horiba Jobin Ybon with a pulse duration of 1.2 ns. LED frequencies were selected attending to excitation energies. A prompt was performed using LUDOX AS-40 colloidal silica, as a 40 wt % suspension in water. Lifetime data were fitted using DAS6 V6.1 software. The quantum yields in solution were measured with an Absolute PL C11437 quantum yield spectrometer (Hamamatsu Photonics KK). The solvent was deaerated by sparging with nitrogen for 15 min prior to performing emission and quantum yield measurements. Scanning electron micrographs were taken with a JEOL Model 7001F field emission gun scanning electron microscope (FEG-SEM), equipped with an energy dispersion X-ray spectrometer (EDS) from Oxford Instruments. Confocal microscopy was

performed on a Leica TCS SP8 inverted microscope using a 20x dry objective. The confocal microscope was equipped with a 405 nm diode.

Healthy cheek cells were collected by buccal smear using a sterile interdental brush. The brush was immediately immersed in a small vial containing 10 mL of saline solution. A few drops of a solution of the metal complex in DMSO were added to the saline solution. Confocal microscopy images were taken after approximately 15 min. For comparative purposes, confocal microscopy images of nontreated cells were also taken, but no fluorescence was observed under the same measurement conditions.

Synthesis of the Au(I) Complexes. *General Procedure*. NaOH (7 equiv.) and 1,3,6,8-tetraethynylpyrene (1 equiv.) were placed together in a Schlenk tube. The tube was evacuated and filled with nitrogen three times. The solids were suspended in degassed MeOH, and the resulting solution was heated at reflux for 4 h. Then, the reaction mixture was allowed to reach room temperature and the corresponding NHC-based Au(I) complex (**1** or **2**, 4.2 equiv.) or [AuCl(PPh$_3$)] was added. The resulting suspension was heated at reflux overnight. The resulting bright suspension was allowed to reach room temperature. After removal of the volatiles, the crude solid was suspended in dichloromethane and filtered through a pad of Celite. The solvent was removed under vacuum. Whereas complexes **3** and **4** were found to be stable in the solid state as well as in solution, complex **5** suffered decomposition in solution within hours, which prevented recording a suitable ^{13}C NMR spectrum.

Synthesis of 3. Complex **1** (200 mg, 0.433 mmol) was added to a suspension of compound **A** (31 mg, 0.104 mmol) and NaOH (30 mg, 0.728 mmol) in MeOH (40 mL). After the general workup, the resulting solid was washed with MeCN and collected by filtration. Complex **3** was isolated as a bright yellow solid. Yield: 108.4 mg (52 %). IR (KBr): v 2102.03 cm^{-1} (C≡C). ^{1}H NMR (300 MHz, CDCl$_3$): δ 8.82 (s, 4H, C*H*$_{pyr}$), 8.38 (s, 2H, C*H*$_{pyr}$), 7.43−7.41 (m, 8H, C*H*$_{benz}$), 7.34−7.32 (m, 8H,

CH_{benz}), 4.60 (t, $^3J_{H–H}$ = 14.6 Hz, 16H, NCH_2CH$_2$CH$_2$CH$_3$), 1.99 (q, 16H, NCH$_2$CH_2CH$_2$CH$_3$), 1.53–1.46 (m, 16H, NCH$_2$CH$_2$CH_2CH$_3$), 1.02 (t, $^3J_{H–H}$ = 14.7 Hz, 24H, NCH$_2$CH$_2$CH$_2$CH_3). ^{13}C{^{1}H} NMR (75 MHz, CDCl$_3$): δ 194.70 (Au-$C_{carbene}$), 135.41 (CH_{pyr}), 135.12 ($C_{q,pyr}$), 133.68 ($C_{q,benz}$), 131.92 ($C_{q,pyr}$), 126.78 (CH_{pyr}), 124.56 ($C_{q,pyr}$), 124.03 (CH_{benz}), 120.40 ($C_{q,acetylide}$), 111.53 (CH_{benz}), 104.59 ($C_{q,acetylide}$), 48.78 (NCH_2CH$_2$CH$_2$CH$_3$), 32.55 (NCH$_2$CH_2CH$_2$CH$_3$), 20.50 (NCH$_2$CH$_2$CH_2CH$_3$), 14.21 (NCH$_2$CH$_2$CH$_2$CH_3). Anal. Calcd. for C$_{84}$H$_{94}$N$_8$Au$_4$: C, 50.36; H, 4.73; N, 5.59. Found: C, 50.47; H, 5.03; N, 5.67.

Synthesis of 4. Complex **2** (190 mg, 0.272 mmol) was added to a suspension of compound **A** (19.4 mg, 0.065 mmol) and NaOH (18 mg, 0.455 mmol) in MeOH (40 mL). Complex **4** was isolated as an orange solid after precipitation from a dichloromethane/diethyl ether mixture. Yield: 117.1 mg (61 %). IR (KBr): v 2095.28 cm^{-1} (C≡C). ^{1}H NMR (400 MHz, CDCl$_3$): δ 8.98 (s, 4H, CH_{pyr}), 8.70 (d, $^3J_{H–H}$ = 1.2 Hz, 8H, CH_{pyr-im}), 8.53 (s, 2H, CH_{pyr}), 8.25 (d, $^3J_{H–H}$ = 1.4 Hz, 8H, CH_{pyr-im}), 8.09 (s, 8H, CH_{pyr-im}), 5.35 (t, $^3J_{H–H}$ = 15.1 Hz, 16H, NCH_2CH$_2$CH$_2$CH$_3$), 2.24 (q, 16H, NCH$_2$CH_2CH$_2$CH$_3$), 1.82–1.76 (m, 16H, NCH$_2$CH$_2$CH_2CH$_3$), 1.63 (s, 72H, C(CH_3)$_3$), 1.11 (t, $^3J_{H–H}$ = 14.7 Hz, 24H, NCH$_2$CH$_2$CH$_2$CH_3). ^{13}C{^{1}H} NMR (100 MHz, CDCl$_3$): δ 193.52 (Au-$C_{carbene}$), 149.22 ($C_{q,pyr-im}$), 134.70 (CH_{pyr}), 133.07 ($C_{q,pyr}$), 131.95 ($C_{q,pyr-im}$), 128.45 ($C_{q,pyr-im}$), 128.04 (CH_{pyr-im}), 126.87 (CH_{pyr}), 122.96 ($C_{q,acetylide}$), 122.89 (CH_{pyr-im}), 121.71 ($C_{q,pyr-im}$), 120.98 ($C_{q,pyr-im}$), 120.94 ($C_{q,pyr}$), 120.43 ($C_{q,pyr}$), 116.86 (CH_{pyr-im}), 104.61 ($C_{q,acetylide}$), 52.36 (NCH_2CH$_2$CH$_2$CH$_3$), 35.62 (C(CH$_3$)), 32.83 (NCH$_2$CH_2CH$_2$CH$_3$), 32.01 (C(CH$_3$)), 20.42 (NCH$_2$CH$_2$CH_2CH$_3$), 14.24 (NCH$_2$CH$_2$CH$_2$CH_3). Anal. Calcd. for C$_{156}$H$_{174}$N$_8$Au$_4$: C, 63.54; H, 5.95; N, 3.80. Found: C, 64.80; H, 5.88; N, 3.84.

Synthesis of 5. [AuCl(PPh$_3$)] (150 mg, 0.303 mmol) was added to a suspension of compound **A** (22.6 mg, 0.076 mmol) and NaOH (21.3 mg, 0.532 mmol) in MeOH (30 mL). After the general workup, complex **5** was isolated as a red solid upon precipitation from a dichloromethane/hexane mixture. The resulting solid was

washed with MeOH and collected by filtration. Complex **5** was isolated as a bright red solid. Yield: 51.0 mg (30 %). IR (KBr): v 2095.28 cm^{-1} (C≡C). ^{1}H NMR (400 MHz, CDCl$_3$): δ 8.83 (s, 4H, CH_{pyr}), 8.36 (s, 2H, CH_{pyr}), 7.65−7.48 (m, 60H, CH_{phenyl}). ^{31}P{^{1}H} NMR (162 MHz, CDCl$_3$): δ 42.30 (P−Au). Anal. Calcd. for C$_{96}$H$_{66}$P$_4$Au$_4$·3CH$_2$Cl$_2$: C, 49.83; H, 3.04. Found: C, 49.77; H, 3.00

Acknowledgments

References

1.   (a) Burroughes, J. H.; Bradley, D. D. C.; Brown, A. R.; Marks, R. N.; Mackay, K.; Friend, R. H.; Burn, P. L.; Holmes, A. B., *Nature* **1990,** *347* (6293), 539-541; (b) Kido, J.; Kimura, M.; Nagai, K., *Science* **1995,** *267* (5202), 1332-1334.

2.   (a) Chen, X. Q.; Tian, X. Z.; Shin, I.; Yoon, J., *Chem. Soc. Rev.* **2011,** *40* (9), 4783-4804; (b) Chen, X. Q.; Wang, F.; Hyun, J. Y.; Wei, T. W.; Qiang, J.; Ren, X. T.; Shin, I.; Yoon, J., *Chem. Soc. Rev.* **2016,** *45* (10), 2976-3016; (c) Niu, L. Y.; Chen, Y. Z.; Zheng, H. R.; Wu, L. Z.; Tung, C. H.; Yang, Q. Z., *Chem. Soc. Rev.* **2015,** *44* (17), 6143-6160; (d) Vendrell, M.; Zhai, D. T.; Er, J. C.; Chang, Y. T., *Chem. Rev.* **2012,** *112* (8), 4391-4420; (e) Yang, S. K.; Shi, X. H.; Park, S.; Ha, T.; Zimmerman, S. C., *Nat. Chem.* **2013,** *5* (8), 692-697; (f) Wu, J. S.; Liu, W. M.; Ge, J. C.; Zhang, H. Y.; Wang, P. F., *Chem. Soc. Rev.* **2011,** *40* (7), 3483-3495.

3.   (a) Dai, X. L.; Zhang, Z. X.; Jin, Y. Z.; Niu, Y.; Cao, H. J.; Liang, X. Y.; Chen, L. W.; Wang, J. P.; Peng, X. G., *Nature* **2014,** *515* (7525), 96-99; (b) Zhu, M. R.; Yang, C. L., *Chem. Soc. Rev.* **2013,** *42* (12), 4963-4976.

4.   (a) Ashton, T. D.; Jolliffe, K. A.; Pfeffer, F. M., *Chem. Soc. Rev.* **2015,** *44* (14), 4547-4595; (b) Yao, J.; Yang, M.; Duan, Y. X., *Chem. Rev.* **2014,** *114* (12), 6130-6178.

5.   (a) Hong, Y. N.; Lam, J. W. Y.; Tang, B. Z., *Chem. Commun.* **2009,** (29), 4332-4353; (b) Hong, Y. N.; Lam, J. W. Y.; Tang, B. Z., *Chem. Soc. Rev.* **2011,** *40* (11), 5361-5388; (c) Mei, J.; Leung, N. L. C.; Kwok, R. T. K.; Lam, J. W. Y.; Tang, B. Z., *Chem. Rev.* **2015,** *115* (21), 11718-11940; (d) Hu, R.; Leung, N. L. C.; Tang, B. Z., *Chem. Soc. Rev.* **2014,** *43* (13), 4494-4562.

6.   Fernández-Moreira, V.; Gimeno, M. C., *Chem. Eur. J.* **2018,** (24), 3345-3353.

7.   (a) Wagenknecht, P. S.; Ford, P. C., *Coord. Chem. Rev.* **2011,** *255* (5-6), 591-616; (b) Chou, P. T.; Chi, Y.; Chung, M. W.; Lin, C. C., *Coord. Chem. Rev.* **2011,**

255 (21-22), 2653-2665; (c) Heine, J.; Muller-Buschbaum, K., *Chem. Soc. Rev.* **2013,** *42* (24), 9232-9242.

8.   Lima, J. C.; Rodriguez, L., *Chem. Soc. Rev.* **2011,** *40* (11), 5442-5456.

9.   Visbal, R.; Gimeno, M. C., *Chem. Soc. Rev.* **2014,** *43* (10), 3551-3574.

10.   (a) Visbal, R.; Ospino, I.; Lopez-de-Luzuriaga, J. M.; Laguna, A.; Gimeno, M. C., *J. Am. Chem. Soc.* **2013,** *135* (12), 4712-4715; (b) To, W. P.; Chan, K. T.; Tong, G. S. M.; Ma, C. S.; Kwok, W. M.; Guan, X. G.; Low, K. H.; Che, C. M., *Angew. Chem. Int. Ed.* **2013,** *52* (26), 6648-6652; (c) To, W. P.; Zhou, D. L.; Tong, G. S. M.; Cheng, G.; Yang, C.; Che, C. M., *Angew. Chem. Int. Ed.* **2017,** *56* (45), 14036-14041; (d) Wong, B. Y. W.; Wong, H. L.; Wong, Y. C.; Au, V. K. M.; Chan, M. Y.; Yam, V. W. W., *Chem. Sci.* **2017,** *8* (10), 6936-6946.

11.   Chan, K. T.; Tong, G. S. M.; To, W. P.; Yang, C.; Du, L. L.; Phillips, D. L.; Che, C. M., *Chem. Sci.* **2017,** *8* (3), 2352-2364.

12.   Sinha, N.; Stegemann, L.; Tan, T. T. Y.; Doltsinis, N. L.; Strassert, C. A.; Hahn, F. E., *Angew. Chem. Int. Ed.* **2017,** *56* (10), 2785-2789.

13.   (a) Figueira-Duarte, T. M.; Muellen, K., *Chem. Rev.* **2011,** *111* (11), 7260-7314; (b) Winnik, F. M., *Chem. Rev.* **1993,** *93* (2), 587-614.

14.   Jahnke, M. C.; Paley, J.; Hupka, F.; Weigand, J. J.; Hahn, F. E., *Z. Naturforsch., B: Chem. Sci.* **2009,** *64* (11-12), 1458-1462.

15.   Ibañez, S.; Poyatos, M.; Peris, E., *Organometallics* **2017,** *36* (7), 1447-1451.

16.   Schmidbaur, H.; Schier, A., *Chem. Soc. Rev.* **2008,** *37* (9), 1931-1951.

17.   Shyamala, T.; Sankararaman, S.; Mishra, A. K., *Chem. Phys.* **2006,** *330* (3), 469-477.

18.   Valdes, H.; Poyatos, M.; Peris, E., *Inorg. Chem.* **2015,** *54* (7), 3654-3659.

19.   Karpovich, D. S.; Blanchard, G. J., *J. Phys. Chem.* **1995,** *99* (12), 3951-3958.

20.   Liu, W.; Gust, R., *Coord. Chem. Rev.* **2016,** *329*, 191-213.

21.   Li, Q.; Li, J. Y.; Ren, H. C.; Gao, Z. X.; Liu, D., *Synth. Commun.* **2011,** *41* (22), 3325-3333.

22.   Venkataramana, G.; Sankararaman, S., *Eur. J. Org. Chem.* **2005,** (19), 4162-4166.

23.   Nuevo, D.; Gonell, S.; Poyatos, M.; Peris, E., *Chem. Eur. J.* **2017,** *23*, 7272-7277.

24.   Bruce, M. I.; Nicholson, B. K.; Binshawkataly, O.; Shapley, J. R.; Henly, T., *Inorg. Synth.* **1989,** *26*, 324-328.

Supporting information for:

Tetra-Au(I) complexes bearing a pyrene-tetra-alkynyl connector behave as fluorescence torches

by

Ana Gutiérrez-Blanco,[a] Vanesa Fernández-Moreira,[b]
M. Concepción Gimeno,[b] Eduardo Peris[a] and Macarena
Poyatos*[a]

[a] Institute of Advanced Materials (INAM). Universitat Jaume I. Av. Vicente Sos Baynat s/n, Castellón, E-12071, Spain.

[b] Departamento de Química Inorgánica, Instituto de Síntesis Química y Catálisis Homogénea (ISQCH), CSIC-Universidad de Zaragoza, 50009 Zaragoza, Spain.

Email: poyatosd@uji.es

1. Spectroscopic data of complexes 3-5
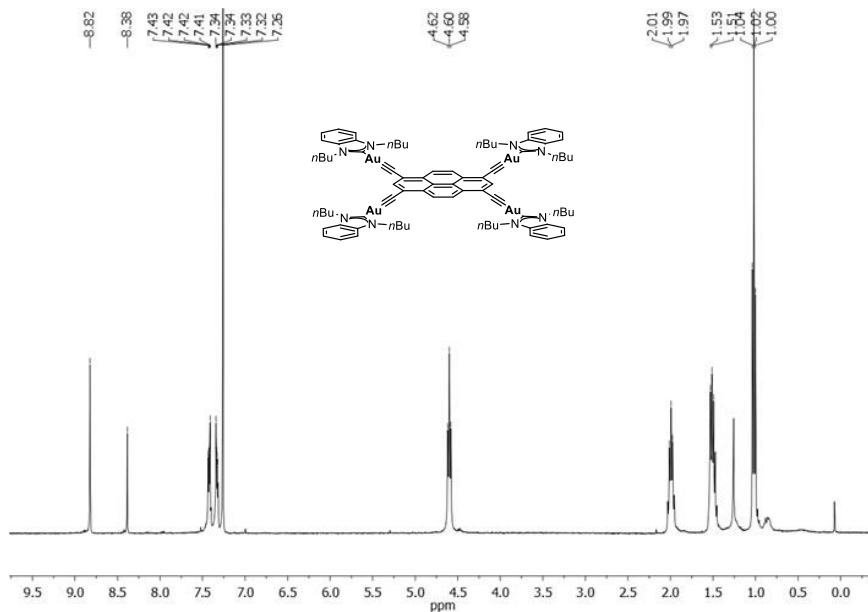
Figure S1. ^{1}H NMR spectrum (300 MHz, CDCl$_3$) of complex **3**.
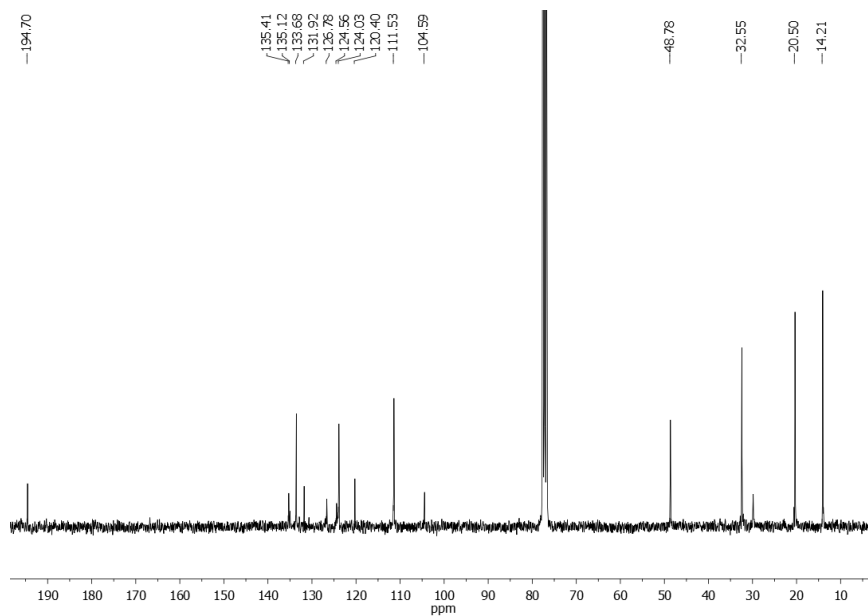
Figure S2. ^{13}C {^{1}H} NMR spectrum (75 MHz, CDCl$_3$) of complex **3**.
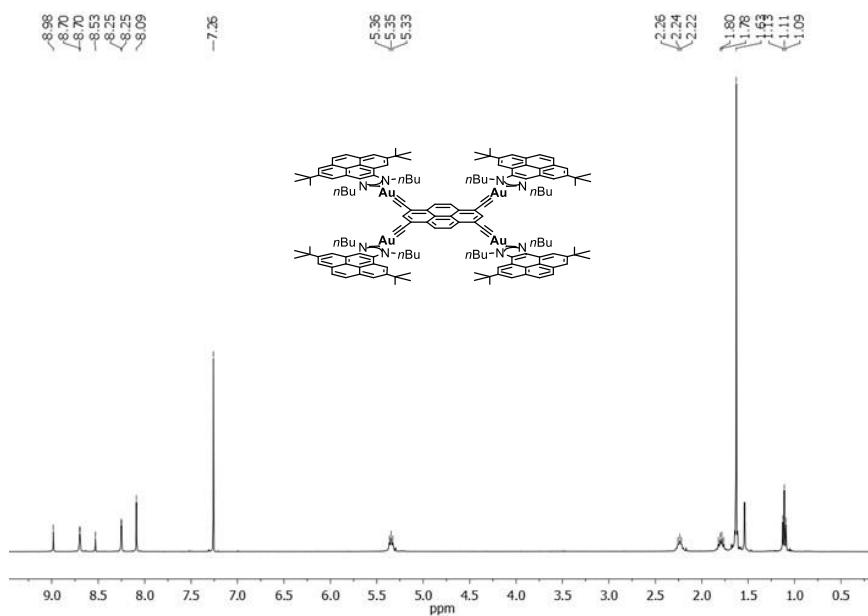
Figure S3. ^{1}H NMR spectrum (400 MHz, CDCl$_3$) of complex **4**.
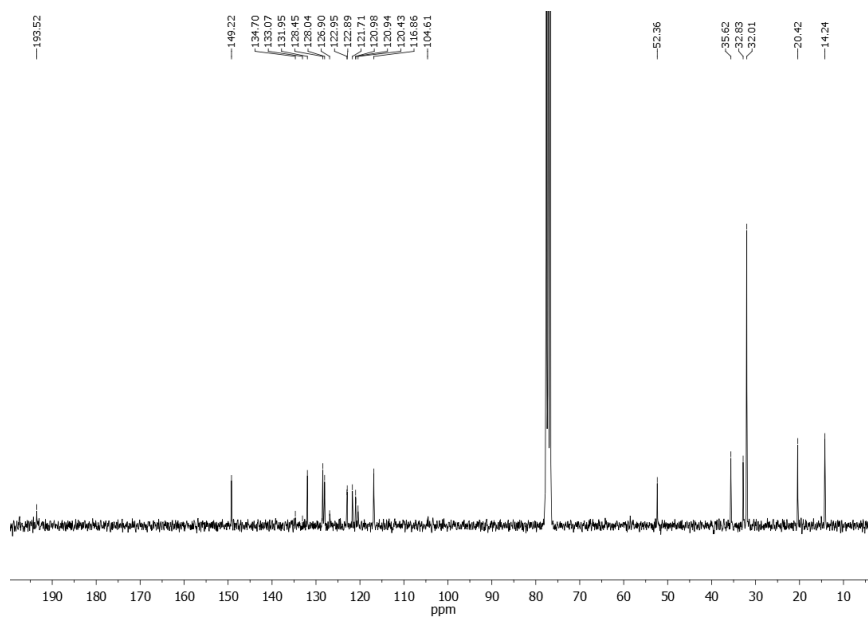
Figure S4. ^{13}C {^{1}H} NMR spectrum (100 MHz, CDCl$_3$) of complex **4**.
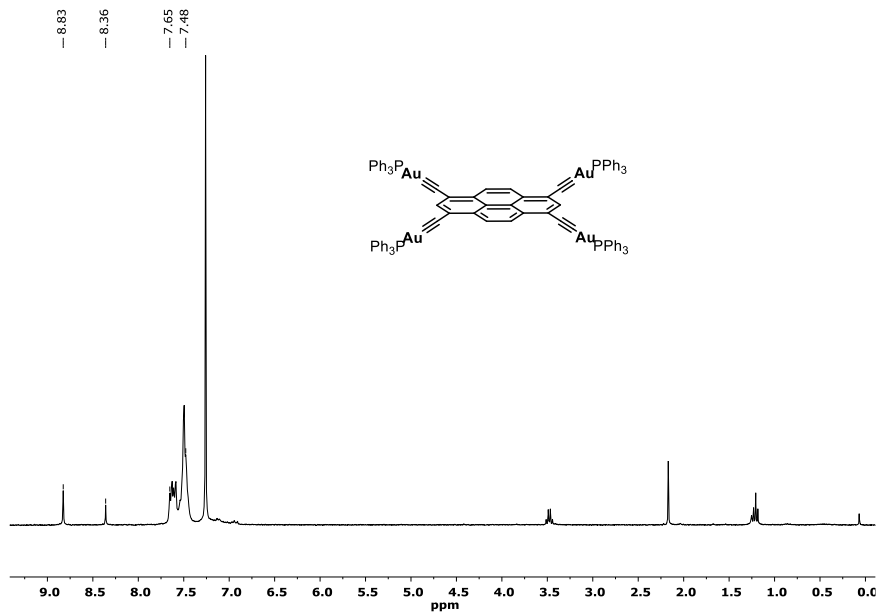
Figure S5. ^{1}H NMR spectrum (400 MHz, CDCl$_3$) of complex **5**.
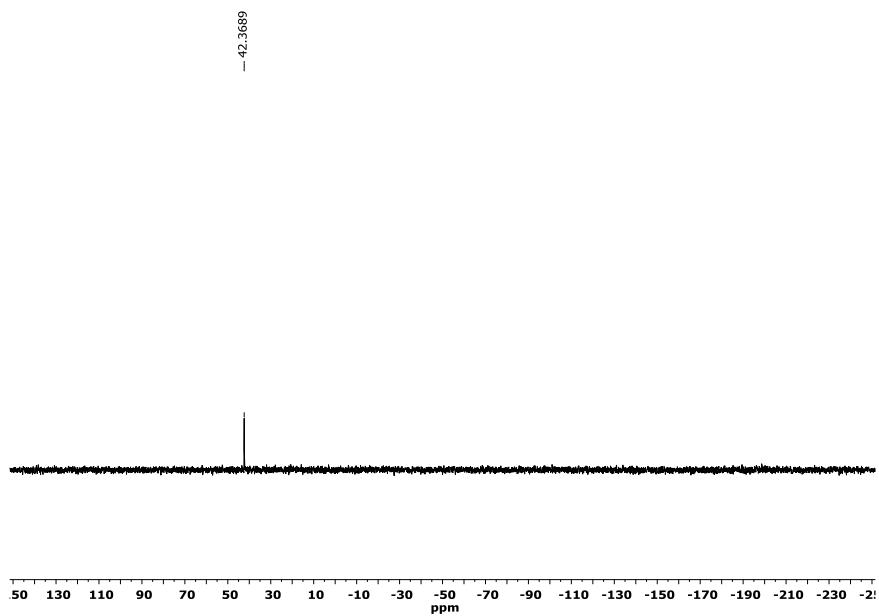
Figure S6. ^{31}P {^{1}H} NMR spectrum (162 MHz, CDCl$_3$) of complex **5**.

2. X-Ray Crystallography

X-Ray Diffraction studies for complex 3. Crystals suitable for X-Ray studies of complex **3** were obtained by slow diffusion of methanol into a concentrated solution of the complex in chloroform. Diffraction data of complex **3** were collected on an Agilent SuperNova diffractometer equipped with an Atlas CCD detector using Mo-Kα radiation (λ = 0.71073 Å). Single crystals were mounted on a MicroMount® polymer tip (MiteGen) in a random orientation. Absorption corrections based on the multi-scan method were applied. Using Olex2,[1] the structure of the complex was solved using Charge Flipping in Superflip[2] and refined with ShelXL[3] refinement package using Least Squares minimization. The structure model of complex **3** exhibits significant disorder in the lattice solvent region. The lattice solvent region has been treated using the PLATON SQUEEZE[4] procedure. H-atoms were introduced in calculated positions and refined on a riding model. Non-hydrogen atoms were refined anisotropically. A global, enhanced rigid bond restraint (SHELX RIGU) was applied. CheckCIF on Platon shows the following A alert for the molecular structure of **3**:

PLAT971_ALERT_2_A Check Calcd. Residual Density 0.95A From Au2 4.42 eA^{-3}

RESPONSE

The following information can be found in the shelx.lst:

Electron density synthesis with coefficients Fo-Fc

Highest peak 4.41 at 0.8772 0.6186 0.9336 [0.99A from AU2]

Deepest hole -1.36 at 0.9609 0.8177 0.6374 [0.07A from C21]

It is normal to expect the largest residual electron density to be associated with heavy metal sites. While this is a larger than expected residual, the data was checked for signs of twinning, using PLATON, and no twin law was detected. Next, we have supporting characterizations to indicate that the metals have been correctly assigned. Finally, given the proximity to the heavy metal, it is not likely that these peaks represent solvent, or other small molecules that have been

missed. Key details of the crystals and structure refinement data are summarized in Supplementary Table S1. Further crystallographic details may be found in the respective CIF, which was deposited at the Cambridge Crystallographic Data Centre, Cambridge, UK. The reference number for **3** is 1824571. Figure S7 shows different perspective views of the X-Ray molecular structure of **3**.
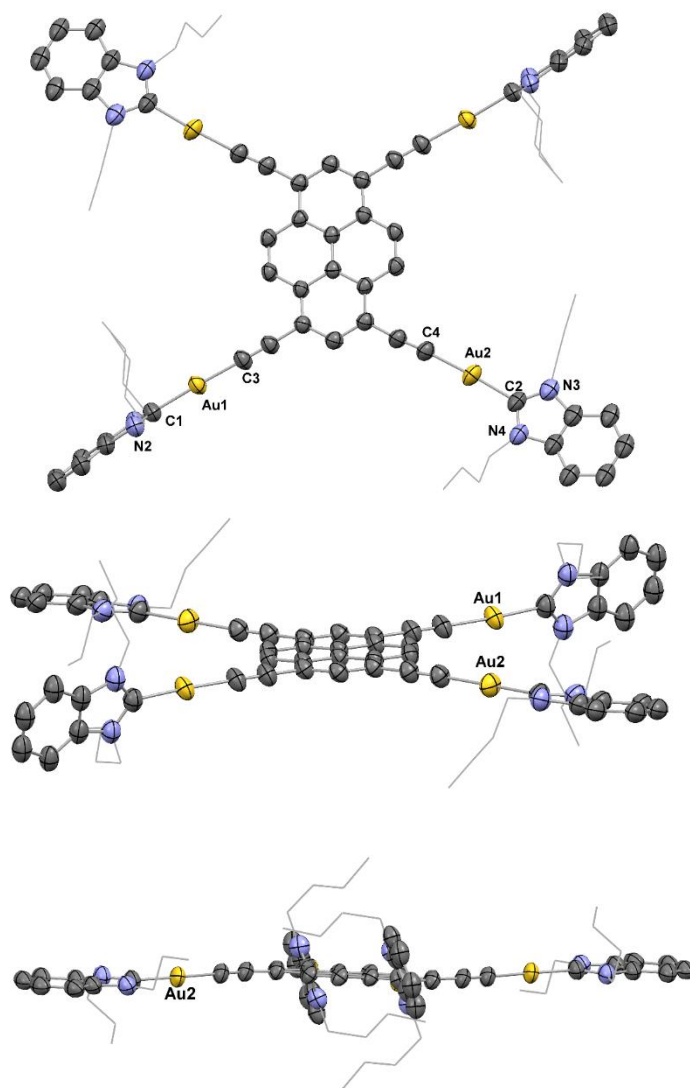
Figure S7. Different perspective views of complex **3**. Hydrogen atoms and solvent molecules (chloroform) have been omitted for clarity. *n*-Butyl groups are represented in the wireframe form.

Table S1. Summary of crystal data, data collection, and structure refinement details of **3**.

	1
Empirical formula	$C_{42}H_{45}Au_2N_4 \cdot CHCl_3$
Formula weight	1120.13
Temperature/K	170(2)
Crystal system	Triclinic
Space group	P-1
a/Å	12.9226(4)
b/Å	13.4575(4)
c/Å	14.9277(5)
α/°	63.719(3)
β/°	79.773(3)
γ/°	68.194(3)
Volume/Å³	2160.87(14)
Z	2
ρ_{calc}mg/mm³	1.722
μ/mm⁻¹	7.001
F(000)	1084.0
Crystal size/mm³	0.701 x 0.218 x 0.125
Radiation	Mo Kα (λ = 0.71073 Å)
2Θ range for data collection/°	6.514 to 46.512
Index ranges	-14 ≤ h ≤ 14, -14 ≤ k ≤ 14, -16 ≤ l ≤ 16
Reflections collected	34407
Independent reflections	6187 [R_{int} = 0.0538, R_{sigma} = 0.0313]
Data/restraints/parameters	6187/678/486
Goodness-of-fit on F²	1.037
Final R indexes [I>=2σ (I)]	R1 = 0.0554, wR2 = 0.1340
Final R indexes [all data]	R1 = 0.0658, wR2 = 0.1451
Largest diff. peak/hole / e Å⁻³	4.41/-1.36
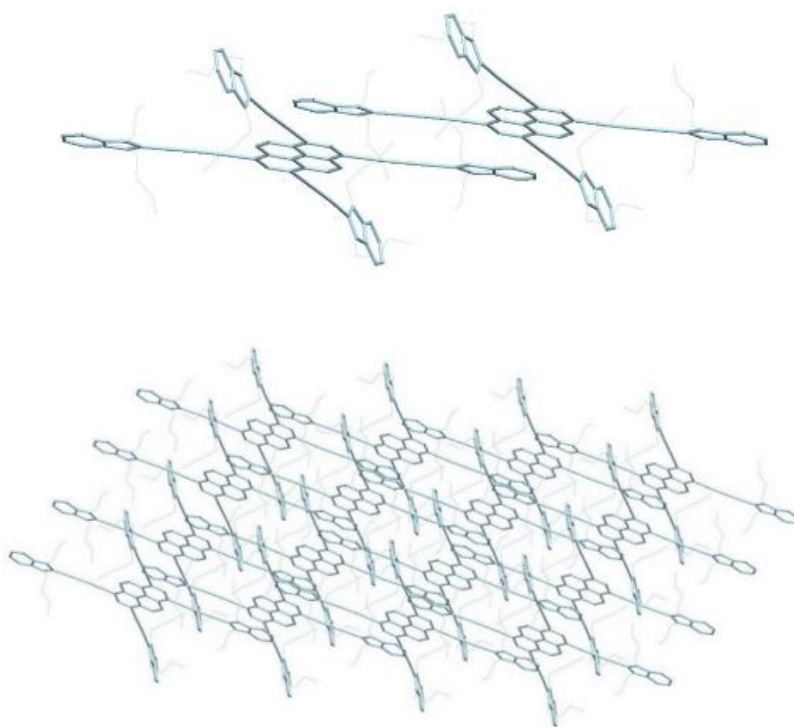
Figure S8. Above: Crystal packing along the *b* axis showing the π-stacking between dissimilar aromatic functionalities. Below: View of the crystal packing of complex **3**. Hydrogen atoms and solvent molecules (chloroform) have been omitted for clarity. *n*-Butyl groups are represented in the wireframe form.

3. Photophysical analisis

3.1. UV-visible absorption spectra
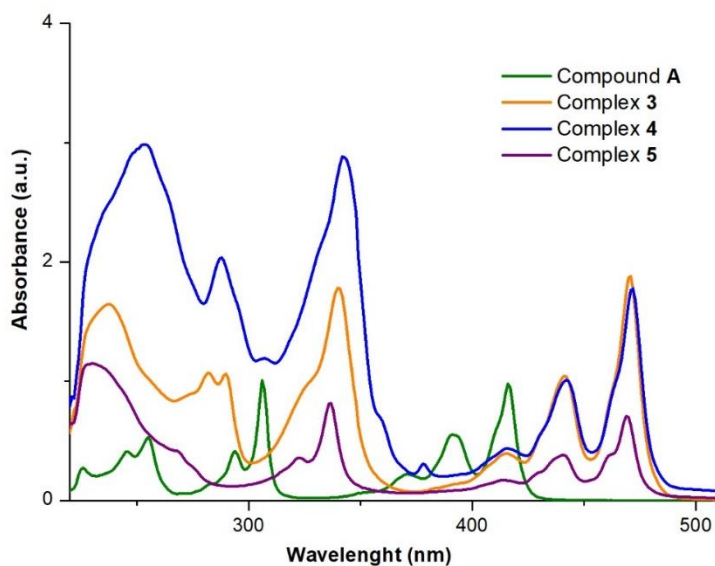
Figure S9. UV-vis spectra of compounds **A** and complexes **3-5**, recorded in CH_2Cl_2 at a concentration of 10^{-5} M, under aerobic conditions at room temperature.

3.2. Emission spectra
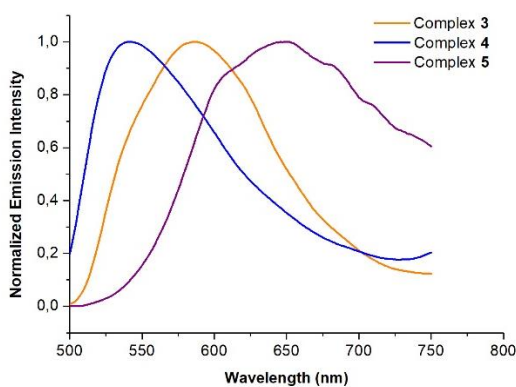
Figure S10. Emission spectra of complexes **3**-**5** at 345 nm in the solid state under aerobic conditions.
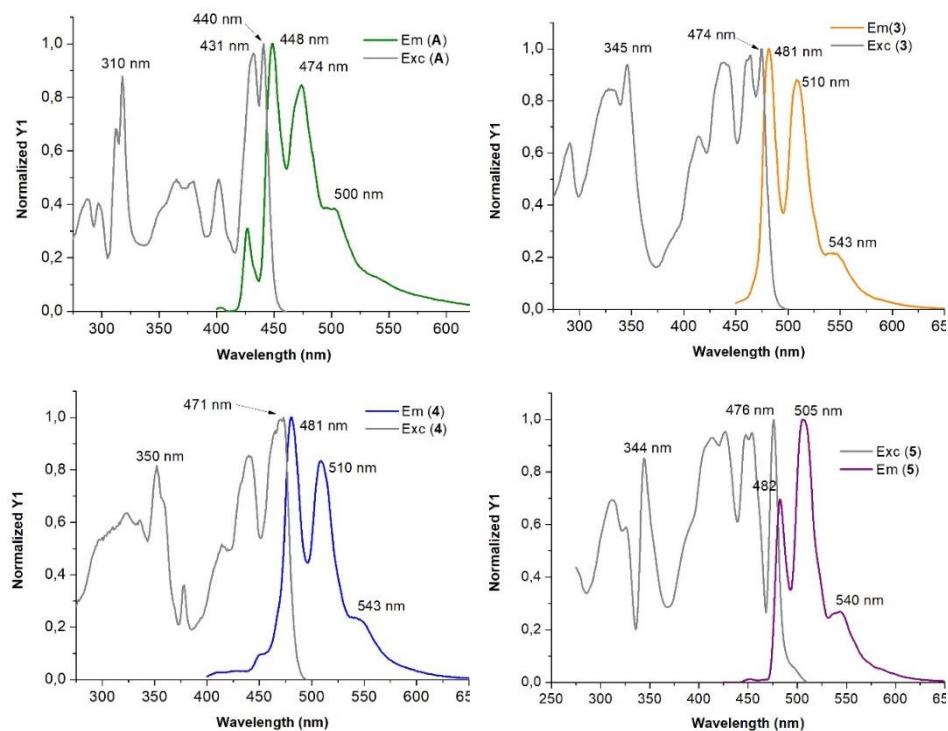
Figure S11. Excitation and emission spectra of compound **A** and complexes **3**-**5** in CH_2Cl_2 solution (1.25×10^{-5} M), under aerobic conditions at room temperature, exciting at 345 nm.
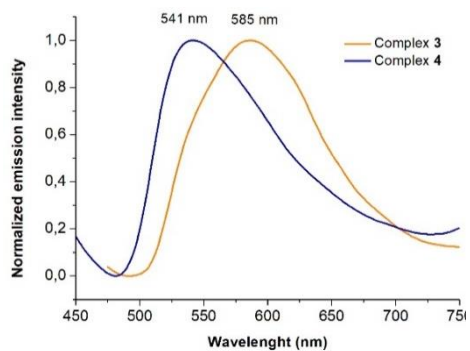
Figure S12. Emission spectra of complexes **3** and **4** in the solid state recorded at room temperature, excited 425 nm.
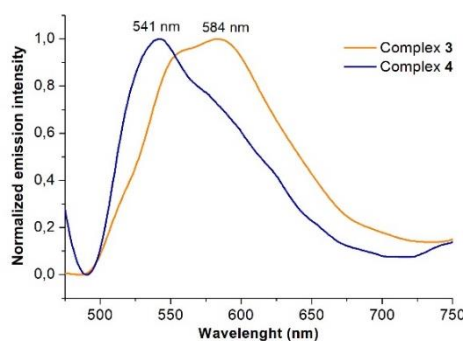
Figure **S13.** Emission spectra of complexes **3** and **4** in the solid state recorded at 77 K, excited at 425 nm.
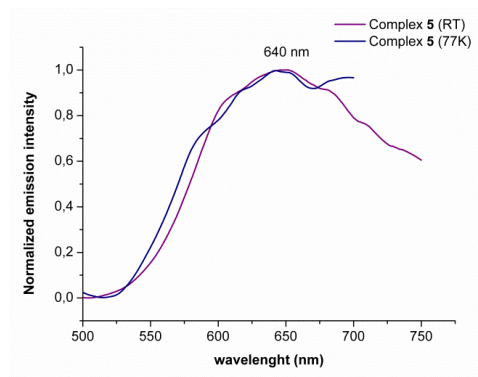
Figure S14. Emission spectra of complex **5** in the solid state recorded at room temperature and at 77 K, excited at 425 nm.

4. Molecular aggregation

4.1. Variable-concentration ^{1}H NMR spectra

The self-aggregation capability of complex **3** was studied by ^{1}H NMR experiments, by decreasing the concentration of the solution of complex **3** adding small amounts of the desired solvent. In our case the experiment was carried out in CDCl$_3$ starting with a concentration of 20 mM. The dilution of **3** produced a perturbation in the signals of the spectra attributed to the aromatic protons H$_a$, H$_b$, H$_c$ and H$_d$ (δ_a, δ_b, δ_c and δ_d in Table S2 and Figure S5). The association constant was obtained by nonlinear least-square analysis by using HypNMR 2008.[5] Figure S6 shows the different representations used for the calculation of the dimerization constant.

Table S2. Data values from the dilution experiment study of **3**.

Experiment	[Host] (mM)	δ_a (ppm)	δ_b (ppm)	δ_c (ppm)	δ_d (ppm)
1	19.98	8.75	8.34	7.30	7.20
2	9.99	8.78	8.36	7.35	7.27
3	6.66	8.79	8.36	7.37	7.29
4	5.00	8.80	8.37	7.38	7.30
5	4.00	8.81	7.37	7.39	7.31
6	2.00	8.83	8.39	7.43	7.36
7	1.33	8.84	8.39	7.44	7.38
8	1.00	8.84	8.39	7.45	7.38
9	0.80	8.85	8.40	7.45	7.39
10	0.67	8.85	8.40	7.46	7.40
11	0.33	8.86	8.40	7.46	7.40
12	0.22	8.86	8.40	7.47	7.41
13	0.17	8.86	8.40	7.47	7.41
14	0.13	8.86	8.41	7.47	7.41
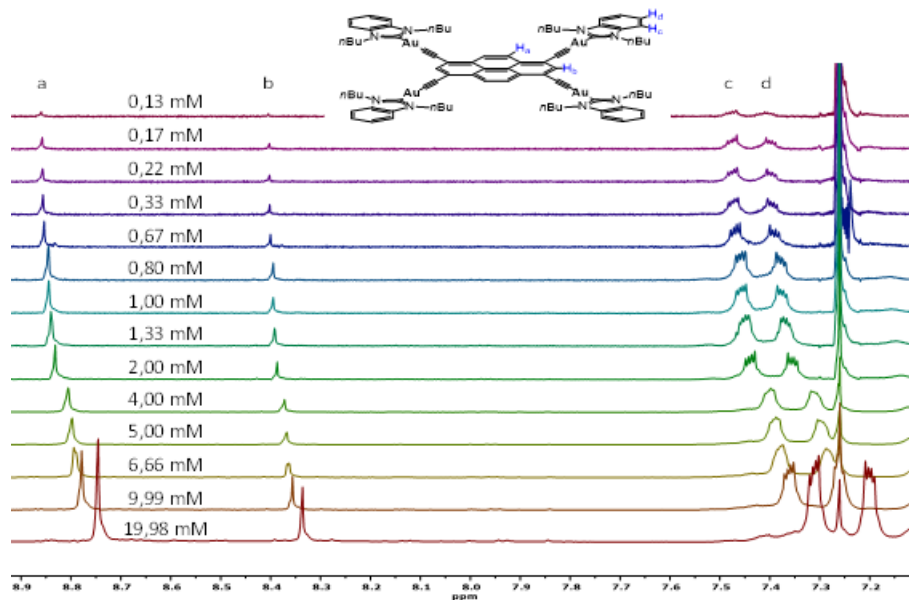
Figure S15. Variable-concentration ^{1}H NMR spectra (500 MHz, CDCl$_3$, 298K) of complex **3**.
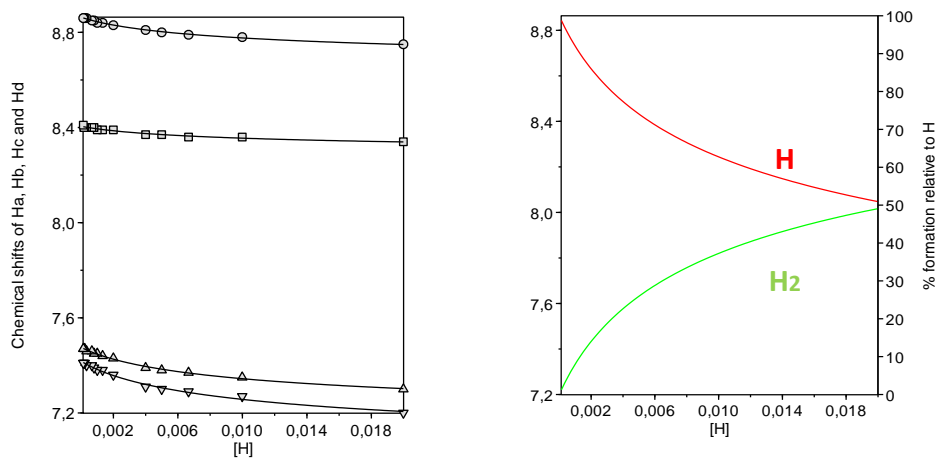
Figure S16. Non-linear least-squares fitting of the chemical shift changes of H$_a$, H$_b$, H$_c$ and H$_d$ during dilution experiments (left) and speciation profiles for the dimerization (right) of complex **3**. HypNMR 2008 refinement K$_{dim}$= (48 ± 8) M^{-1}.
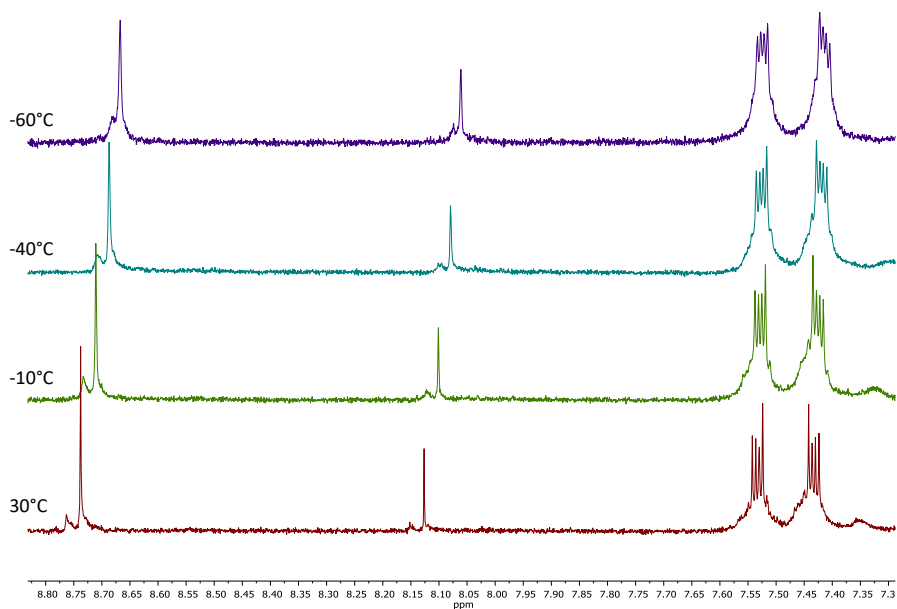
4.2. Variable-temperature ^{1}H NMR spectra

Figure S17. Variable-temperature ^{1}H NMR spectra (500 MHz) of complex **3** in CD$_2$Cl$_2$ 5x10^{-4} M.

5. Scanning Electronic Microscopy (SEM) images
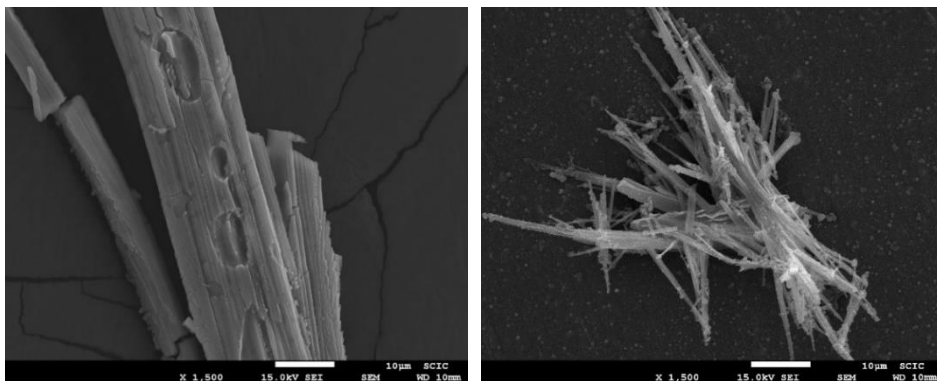
Figure S18. SEM micrographs of **3** (left) and **4** (right) at a magnification value of 1.500x.
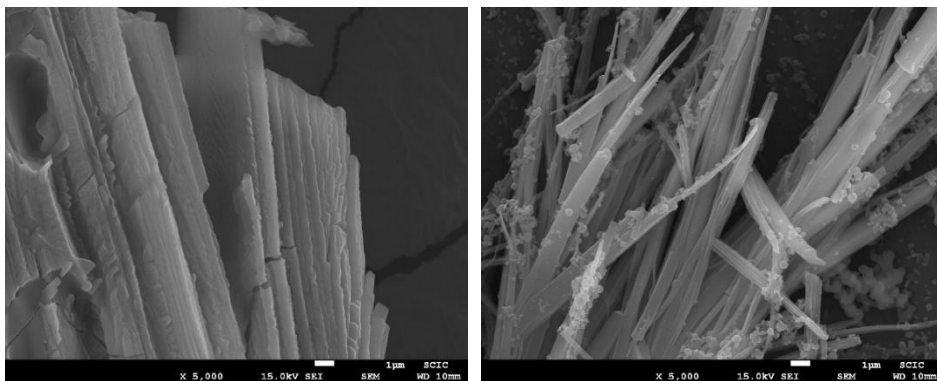
Figure **S19.** SEM micrographs of **3** (left) and **4** (right) at a magnification value of 5.000x

6. Confocal microscopy images
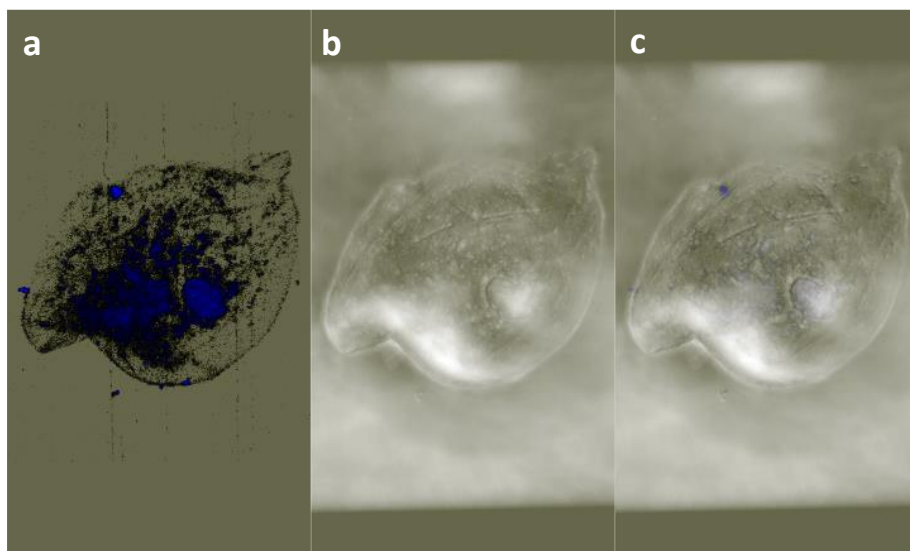
Figure S20. Confocal images of healthy cheek cells treated with complex **3** for 30 minutes, excited at 405 nm: a) fluorescence image; b) transmitted light image; c) merged image

7. References

1.   Dolomanov, O. V.; Bourhis, L. J.; Gildea, R. J.; Howard, J. A. K.; Puschmann, H., *J. Appl. Crystallogr.* **2009,** *42*, 339-341.

2.   Palatinus, L.; Chapuis, G., *J. Appl. Crystallogr.* **2007,** *40*, 786-790.

3.   Sheldrick, G. M., *Acta Crystallogr., Sect. A: Found. Crystallogr.* **2015,** *71*, 3-8.

4.   Vandersluis, P.; Spek, A. L., *Acta Crystallographica Section A* **1990,** *46*, 194-201.

5.   Frassineti, C.; Ghelli, S.; Gans, P.; Sabatini, A.; Moruzzi, M. S.; Vacca, A., *Anal. Biochem.* **1995,** *231* (2), 374-382.

4

Pyrene-Connected Tetraimidazolylidene Complexes of Iridium and Rhodium. Structural Features and Catalytic Applications

Ana Gutiérrez-Blanco, Eduardo Peris,[ ] and Macarena Poyatos*[ ]

Institute of Advanced Materials (INAM), Universitat Jaume I, Av. Vicente Sos Baynat s/n, Castellón, E-12071, Spain

S *Supporting Information*

ABSTRACT: A pyrene-connected tetra-imidazolium salt has been prepared starting from commercially available 1,3,6,8-tetrabromopyrene, and used as tetra-NHC precursor in the preparation of tetranuclear Rh(I) and Ir(I) complexes. The tetra-NHC ligand displays axial chirality upon coordination to the MCl(cod) (M = Rh and Ir) fragments, giving rise to right- and left-handed helix conformations. The catalytic activity of the resulting complexes was studied in two relevant reactions that lead to the formation of five- and six-membered oxygen-containing heterocycles, namely, the cyclization of acetylenic carboxylic acid and the coupling of diphenylcyclopropenone with substituted phenylacetylenes.

INTRODUCTION

The widespread use of N-heterocyclic carbene (NHC) ligands arises from their extraordinary stereoelectronic versatility and their capability to incorporate a wide variety of additional functional groups.[1] The presence of these additional functions makes the resulting complexes good candidates for undergoing supramolecular interactions since they may establish reversible noncovalent interactions with the other reaction partners (substrate, additive, and counterion). The introduction of these interactions by design is an important tool for modifying the properties of a metal-based catalyst, and constitutes the basis of supramolecular catalysis.[2] In addition, over the past years, discrete supramolecular complexes held together by M–C_{NHC} bonds have become of interest, and this required the preparation of poly-NHC ligands with suitable topologies that offer the possibility of forming self-assembled structures.[3]

Our group has been particularly interested in studying the catalytic behavior of NHC-based complexes bearing extended polyaromatic systems as additional functions. We demonstrated that, due to the ability of polyaromatic groups to afford π-stacking noncovalent interactions, their catalytic properties clearly differ from those shown by analogues lacking these polyaromatic systems.[4] In line with this, a series of NHC-based complexes containing pyrene in their structure were prepared. Employing pyrene-containing palladium[5] (**A**, Chart 1), nickel,[5]

rhodium,[6] iridium,[7] and gold[8] complexes, we further explored the importance of π-stacking interactions in homogeneously catalyzed reactions. The inherent capability of pyrene to afford π-stacking interactions with graphitic surfaces also allowed to support pyrene-tagged complexes,[6,7,9] such as complex **B** in Chart 1,[7] onto reduced graphene oxide and to study the activity and recyclability properties of the resulting heterogenized catalysts. Additionally, and taking advantage of the fluorescent properties of pyrene, we prepared NHC-based complexes with interesting photophysical properties.[10]

More recently, we prepared a tetra-Au(I) complex connected by 1,3,6,8-tetraethynylpyrene, which turned out to be one of the most efficient Au-based fluorescence emitters in solution reported to date (**C**, Chart 1).[11]

All of these findings illustrate how pyrene-adorned NHC-metal complexes constitute an interesting family of materials with unusual photophysical and catalytic properties. In this new work, we report the preparation of a pyrene-connected tetra-imidazolium salt and its use as tetra-NHC precursor in the preparation of rhodium and iridium complexes. The catalytic properties of the rhodium and iridium complexes were studied in the cyclization of acetylenic carboxylic acids and in the cycloaddition of diphenylcyclopropenone and alkynes.

RESULTS AND DISCUSSION

The pyrene-tetra-imidazolium salt **2** was prepared by a three-step procedure starting from commercially available 1,3,6,8-tetrabromopyrene, as displayed in Scheme 1. Treatment of 1,3,6,8-tetrabromopyrene with 4 equiv of imidazole in the presence of CuI and K_2CO_3 in refluxing DMF resulted in the formation of neutral tetraimidazolyl-pyrene compound **1**.

Chart 1
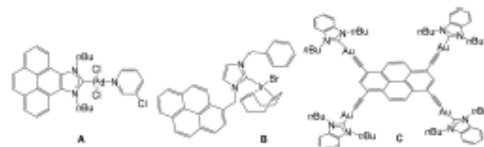
109

Pyrene-Connected Tetraimidazolylidene Complexes of Iridium and Rhodium. Structural Features and Catalytic Applications

Ana Gutiérrez-Blanco, Eduardo Peris, and Macarena Poyatos*

Institute of Advanced Materials (INAM). Universitat Jaume I, Av. Vicente Sos Baynat s/n, E-12071 Castellón, Spain

Email: poyatosd@uji.es

Abstract

A pyrene-connected tetra-imidazolium salt has been prepared starting from commercially available 1,3,6,8-tetrabromopyrene, and used as tetra-NHC precursor in the preparation of tetranuclear Rh(I) and Ir(I) complexes. The tetra-NHC ligand displays axial chirality upon coordination to the MCl(cod) (M = Rh and Ir) fragments, giving rise to right- and left-handed helix conformations. The catalytic activity of the resulting complexes was studied in two relevant reactions that lead to the formation of five- and six-membered oxygen-containing heterocycles, namely, the cyclization of acetylenic carboxylic acid and the coupling of diphenylcyclopropenone with substituted phenylacetylenes.

1. Introduction

The widespread use of N-heterocyclic carbene (NHC) ligands arises from their extraordinary stereoelectronic versatility and their capability to incorporate a wide variety of additional functional groups.[1] The presence of these additional functions makes the resulting complexes good candidates for undergoing

110

supramolecular interactions since they may establish reversible noncovalent interactions with the other reaction partners (substrate, additive, and counterion). The introduction of these interactions by design is an important tool for modifying the properties of a metal-based catalyst and constitutes the basis of supramolecular catalysis.[2] In addition, over the past years, discrete supramolecular complexes held together by M–C$_{NHC}$ bonds have become of interest, and this required the preparation of poly-NHC ligands with suitable topologies that offer the possibility of forming self-assembled structures.[3]

Our group has been particularly interested in studying the catalytic behaviour of NHC-based complexes bearing extended polyaromatic systems as additional functions. We demonstrated that, due to the ability of polyaromatic groups to afford π-stacking noncovalent interactions, their catalytic properties clearly differ from those shown by analogues lacking these polyaromatic systems.[4] In line with this, a series of NHC-based complexes containing pyrene in their structure were prepared.
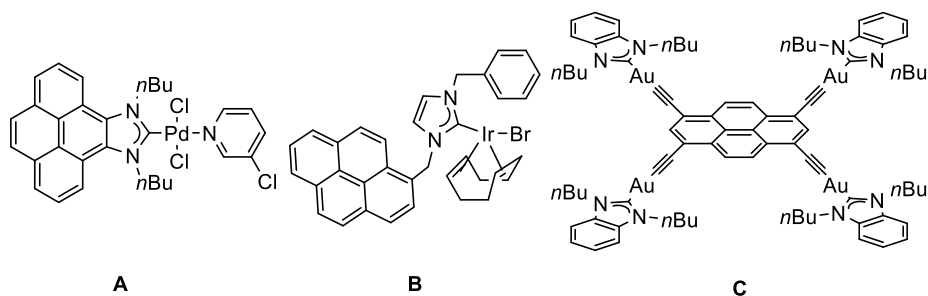
Chart 1

Employing pyrene-containing palladium[5] (**A**, Chart 1), nickel,[5] rhodium,[6] iridium,[7] and gold[8] complexes, we further explored the importance of π-stacking interactions in homogeneously catalyzed reactions. The inherent capability of pyrene to afford π-stacking interactions with graphitic surfaces also allowed to support pyrene-tagged complexes,[6,7,9] such as complex **B** in Chart 1,[7] onto

reduced graphene oxide and to study the activity and recyclability properties of the resulting heterogenized catalysts. Additionally, and taking advantage of the fluorescent properties of pyrene, we prepared NHC-based complexes with interesting photophysical properties.[10]

More recently, we prepared a tetra-Au(I) complex connected by 1,3,6,8-tetraethynylpyrene, which turned out to be one of the most efficient Au-based fluorescence emitters in solution reported to date (**C**, Chart 1).[11]

All of these findings illustrate how pyrene-adorned NHC-metal complexes constitute an interesting family of materials with unusual photophysical and catalytic properties. In this new work, we report the preparation of a pyrene-connected tetra-imidazolium salt and its use as tetra-NHC precursor in the preparation of rhodium and iridium complexes. The catalytic properties of the rhodium and iridium complexes were studied in the cyclization of acetylenic carboxylic acids and in the cycloaddition of diphenylcyclopropenone and alkynes.

2. Results and discussion

The pyrene-tetra-imidazolium salt **2** was prepared by a three-step procedure starting from commercially available 1,3,6,8-tetrabromopyrene, as displayed in Scheme 1. Treatment of 1,3,6,8-tetrabromopyrene with 4 equiv. of imidazole in the presence of CuI and K_2CO_3 in refluxing DMF resulted in the formation of neutral tetraimidazolyl-pyrene compound **1**.
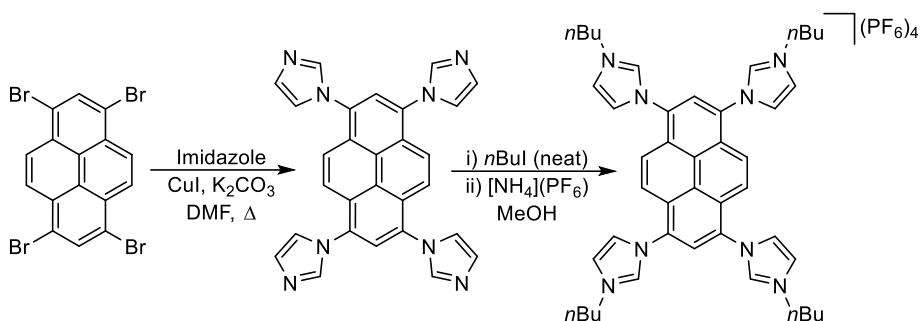
Scheme 1. Synthesis of tetra-imidazolium *salt* **2**.

Compound **1** was isolated as a highly insoluble dark green solid, in almost quantitative yield.

The *N*-quaternization of the four imidazole rings of compound **1** with *n*-BuI and subsequent anion metathesis using [NH$_4$](PF$_6$) in methanol afforded the hexafluorophosphate tetra-imidazolium salt **2**. Compound **2** was isolated as a dark brown solid, in a 65 % overall yield.

The ^{1}H NMR spectrum in acetone-*d$_6$* of the pyrene-containing tetra-imidazolium salt **2** shows the resonance due to the four equivalent acidic protons of the NCHN groups at 9.7 ppm. The ^{13}C NMR spectrum shows the resonance due to the carbon atoms of the NCHN groups at 139.1 ppm. The ESI-MS spectrum (positive ions) of **2** exhibits an intense peak at m/z 279.9, which was assigned to [M − 3(PF$_6$)]$^{3+}$.

We initially considered that compound **2** could be used as the precursor of a bis-C$_{NHC}$CC$_{NHC}$-*pincer* ligand, in which the two potential *pincer* arms are linearly opposed and connected by an aromatic skeleton. However, all our attempts to achieve this coordination mode to Rh(III) and Ir(III) by the metalation/transmetalation strategy using Zr(NMe$_2$)$_4$[12] were unsuccessful. Instead, the reaction of **2** with [MCl(cod)]$_2$ (M = Rh or Ir) afforded the tetrametallic complexes **3** and **4** (Scheme 2).
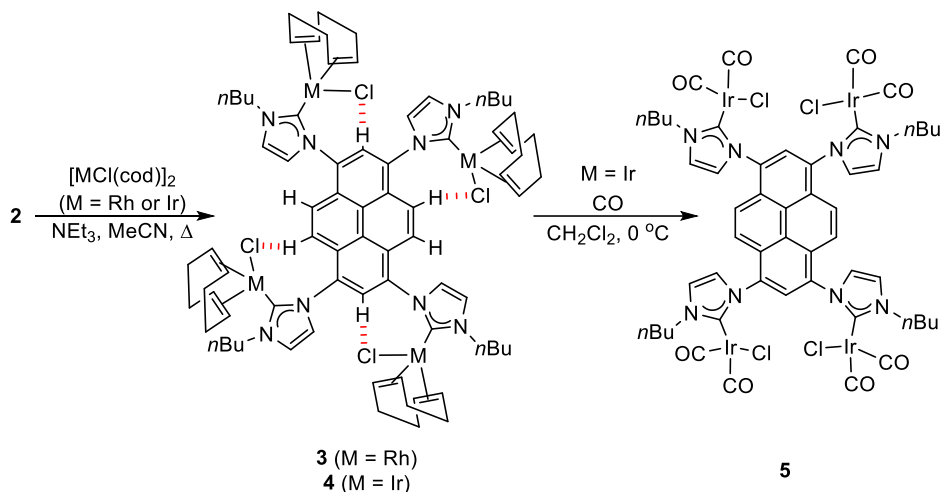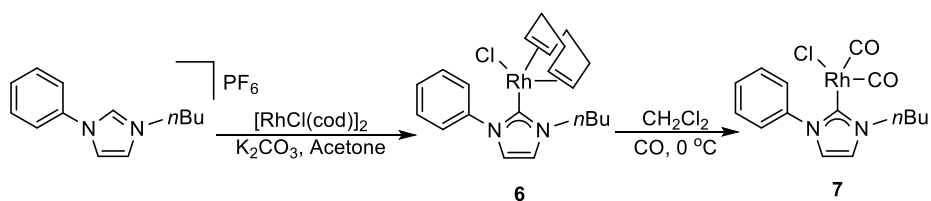
Scheme 2. Synthesis of tetrametallic complexes **3−5**.

Complexes **3** and **4** were characterized by NMR spectroscopy, electrospray mass spectrometry, and elemental analysis. Both the ^{1}H and ^{13}C NMR spectra are in agreement with the two-fold symmetry of the complexes, and with the presence of only one of the possible rotational isomers. The observed tetra-NHC ligand/cod ratio obtained from ^{1}H NMR integration along with the positive ion ESI-MS signals at 802.9 and 981.7 m/z, assigned to [M − 2Cl]$^{2+}$, confirmed the formation of the tetranuclear complexes **3** and **4**, respectively.

Whereas the presence of a singlet at 8.49 ppm indicates the equivalency of four of the protons of the pyrene core of the tetra-imidazolium salt **2**, these protons are no longer equivalent in complexes **3** and **4**, due to the restricted rotation about the C$_{pyr}$−N$_{imid}$ and the M−C$_{carbene}$ bonds, upon coordination of the MCl(cod) fragment. These resonances appear as two doublets at 9.85 and 8.11 ppm (complex **3**) and at 9.35 and 7.97 ppm (complex **4**). One of the two doublets is downfield shifted, thus strongly suggesting the presence of weak hydrogen-bonding interactions with the chloride ligands, as illustrates the drawing of **3** and **4** in Scheme 2. This situation indicates that the symmetry of the complex in solution is C_2, rather than that expected for a 1,3,6,8-(symmetrically)-

tetrasubstituted pyrene (C_{2v}). As a result of this loss of symmetry, complexes **3** and **4** feature two different sets of metalated carbon atoms, thus showing two carbene carbon resonances in their ^{13}C NMR spectra [185.5 and 183.6 ppm ($^{1}J_{Rh-C}$ = 51 Hz) for **3**, and 182.4 and 181.2 ppm for **4**]. We did not observe changes in the ^{1}H NMR spectra of complexes **3** and **4** upon performing VT-NMR experiments in CDCl$_3$.

In order to estimate the electron-donating character of the tetra-NHC ligand, we transformed tetra-iridium complex **4** into its carbonyl derivative **5** (Scheme 2) by bubbling carbon monoxide through a solution of the complex in dichloromethane at 0 °C. Complex **5** displays only one carbene-carbon resonance at 180.7 ppm in the ^{13}C NMR spectrum, indicating that the rotation about the Ir−C$_{carbene}$ bond is no longer restricted, and thus suggesting a pseudo-C_{2v} symmetry for the complex in solution. Complex **5** displays two strong CO stretching bands at 1977 and 2064 cm^{-1}, which allowed us to calculate the Tolman Electronic Parameter (TEP) as 2047 cm^{-1}, by using well-known correlations.[13] For comparative purposes, we prepared the complex [1-*n*-butyl-3-phenylimidazol-2-ylidene]dicarbonylchlororhodium (**7**, Scheme 3), which can be regarded as the mono-rhodium counterpart of **5**.

Scheme 3. Synthesis of monometallic *c*omplexes **6** and **7**.

For this complex, we found a TEP value of 2045 cm^{-1}, thus indicating that the electron-donating strength of the tetra-NHC ligand in **5** is similar to that shown by 1-*n*-butyl-3-phenylimidazol-2-ylidene (in **7**).

The X-ray diffraction studies confirmed the molecular structure of complex **4** and revealed the presence of two independent molecules in the asymmetric unit. Each molecule consists of four *n*-butyl-imidazolylidene-Rh(I)Cl(cod) units connected by the pyrene core. The two molecules are enantiomers as, upon coordination, the tetra-NHC ligand displays axial chirality. The top view of one of the enantiomers is given in Figure 1 (top), and shows a helical (or screw-shaped) geometry, giving rise to a left-handed helix conformation.

As can be observed from the side view of the molecular structure of **4** (Figure 1, bottom), the two metal units at the pyrene 1- and 6-positions are above the plane formed by the pyrene central unit, placing the chloride ligands in close proximity to the protons at the 2- and 7-positions, at an average distance of 2.84 Å. In a similar manner, the two metal units at the pyrene 3- and 8-positions are below the pyrene plane, placing the chloride atoms in close proximity to the protons at the 4- and 9-positions, at an average distance of 2.90 Å. This is in agreement with our observations in the ^{1}H NMR of complexes **3** and **4**, and indicate the presence of weak hydrogen-bonding interactions, which are also evident in the solid state. The imidazolylidene rings deviate from the plane of the pyrene core by an average angle of 64°. The Supporting Information (See Figure S20) includes different perspective views of the other enantiomer of **4**.
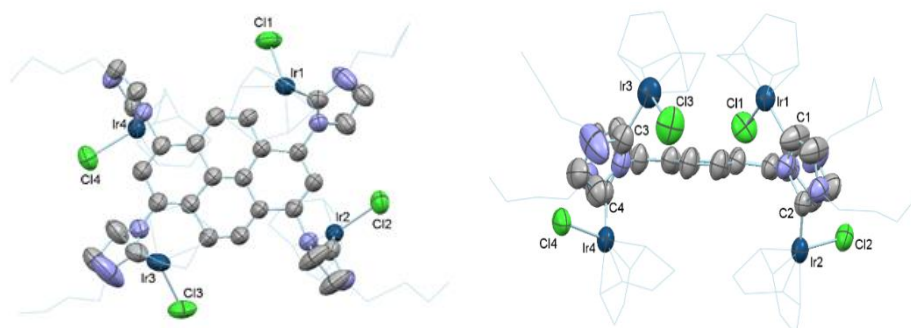

Figure 1. Top and side views of one of the enantiomers of **4**. Solvent (CHCl$_3$ and CH$_2$Cl$_2$) and hydrogen atoms have been removed for clarity. n-Butyl substituents and 1,5-cylooctadiene ligands are shown in the wireframe form. Selected distances (Å): Ir1−C1 2.07(4), Ir2− C2 1.84(4), Ir3−C3 2.07(5), Ir4−C4 1.88(4).

In order to evaluate the catalytic activity of the isolated complexes, we selected organic transformations typically catalysed by Rh(I), namely, the cyclization of acetylenic carboxylic acids[14] and the synthesis of cyclopentadienones.[15] These two reactions are of practical relevance to the pharmaceutical industry because they allow the formation of five- and six-membered oxygen-containing heterocycles. We believe that these two reactions constitute two excellent models for the comparison of the activity of our new complexes with the related mononuclear ones, in order to evaluate if the presence of the four metal units in the catalyst, or the presence of the pyrene core, have any relevant role in the activity of our systems. Complexes **3** and **4** were first tested in the intramolecular cyclization of 4-pentynoic and 5-hexynoic acid, which leads to the formation of five- and six-membered rings, respectively. The reactions were performed in an NMR tube containing 0.75 mL of CD_3CN with different catalyst loadings (10^{-3}–1 mol %), at 80 °C.

The results shown in

Table **1**, indicate that the iridium complex outperforms the rhodium one, both in the cyclization of 4-pentynoic and 5-hexynoic acids. Complexes **3** and **4** achieved full conversion to *γ*-methylene-*γ*-butyrolactone after 2.5 h, using a catalyst loading of 1 mol %. With a catalyst loading of 0.1 mol % (0.4 mol % based on the concentration of metal), full conversion was achieved by complex **4** in 4 h, whereas a longer reaction time (21 h) was required for complex **3** (compare entries 2 and 6). At a catalyst loading of 0.01 mol % (0.04 mol % based on metal), the iridium complex achieved full conversion after 21 h (entry 7). In agreement with previous reports,[14c, 14d, 16] the cyclization of 5-hexynoic acid resulted much less efficient; complexes **3** and **4** required 8 days of reaction to afford 80 % conversion (entries 12 and 14).

Table 1. Catalytic cyclization of acetylenic carboxylic acids[a]
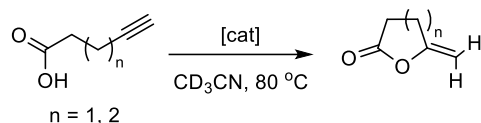
Entry	Substrate	Cat.	Cat. loading (mol %)	Time (h)	Conversion (%)[b]
1	4-pentynoic acid	**3**	1	2.5	>99
2		**3**	0.1	21	>99
3		**3**	0.01	21	35
4		**3**	0.001	21	16
5		**4**	1	2.5	>99
6		**4**	0.1	4	>99
7		**4**	0.01	21	>99
8		**4**	0.001	21	9
9		**6**	0.4	21	>99
10		**6**	0.04	21	>99
11		**6**	0.004	21	12
12	5-hexynoic acid	**3**	0.1	192	93
13		**3**	0.01	216	0
14		**4**	0.1	192	79
15		**4**	0.01	192	21
16		**6**	0.4	192	31
17		**6**	0.04	216	0

[a]Reaction conditions: in an NMR tube, 0.5 mmol acetylenic acid, catalyst **3**, **4**, or **6**, CD$_3$CN (0.75 mL), 80 °C. [b]Conversions were determined by ^{1}H NMR spectroscopy using 1,3,5-trimethoxybenzene as internal standard.

In order to study if the use of tetrametallic complexes produced an improvement in the catalytic efficiencies compared to those provided by their monometallic analogues, we employed the mono-rhodium complex [1-*n*-butyl-3-phenylimidazol-2-ylidene](1,5-cyclooctadiene)chlororhodium, **6** (Scheme 3).

Unfortunately, our attempts to isolate a pure sample of the mono-iridium complex were unsuccessful.

In the cyclization of 4-pentynoic acid, the mono-rhodium complex **6** performed better than its tetrametallic counterpart (complex **3**) when using catalyst loadings of 0.4 and 0.04 mol % based on the concentration of the metal. Nevertheless, using a catalyst loading of 0.004 mol %, the two catalysts led to similar outcomes (compare entries 4 and 11). In order to explain this behaviour, we studied the time-dependent reaction profiles of the cyclization of 4-pentynoic acid using different concentrations of **3**, and we determined the reaction order with respect to the catalyst, by plotting the concentration of the product against a normalized time scale $t[cat]^n$ (being n the order of the catalyst).[17] The power value gives the right reaction order with respect to the catalyst when the corrected conversion curves overlay. Four catalyst loadings of 1, 0.1, 0.01, and 0.001 mol % were employed to determine the reaction order in catalyst. Visual analysis of the reaction profiles depicted in Figure 2 indicates that the order in catalyst is 1 (Figure 2b), although the curve for the higher concentration (1 mol %) is clearly out of the fit. This result is explained as a consequence of the low solubility of catalyst **3** in acetonitrile (the same applies to the iridium catalyst **4**; see the Figure S27 of the Supporting Information for details), and therefore, once the saturation concentration has been reached, increasing the amount of catalyst added to the reaction media does not produce any improvement in the reaction rate. This result clearly contrasts with our previous findings using other pyrene-containing ligands, for which fractional reaction orders were observed, as a consequence of the formation of nonactive dimers by π-stacking self-association of the catalyst.[7,8] The different solubility of **3** and **6** explains why, at higher concentrations, the monometallic complex outperforms the tetrametallic one, while, at lower concentrations, both catalysts display similar activity, as expected for two complexes with quasi-identical stereoelectronic properties.

Furthermore, the first-order reaction found with respect to the concentration of **3** (and **4**) suggests that the cooperativity between the metal units in both tetrametallic catalysts is negligible.
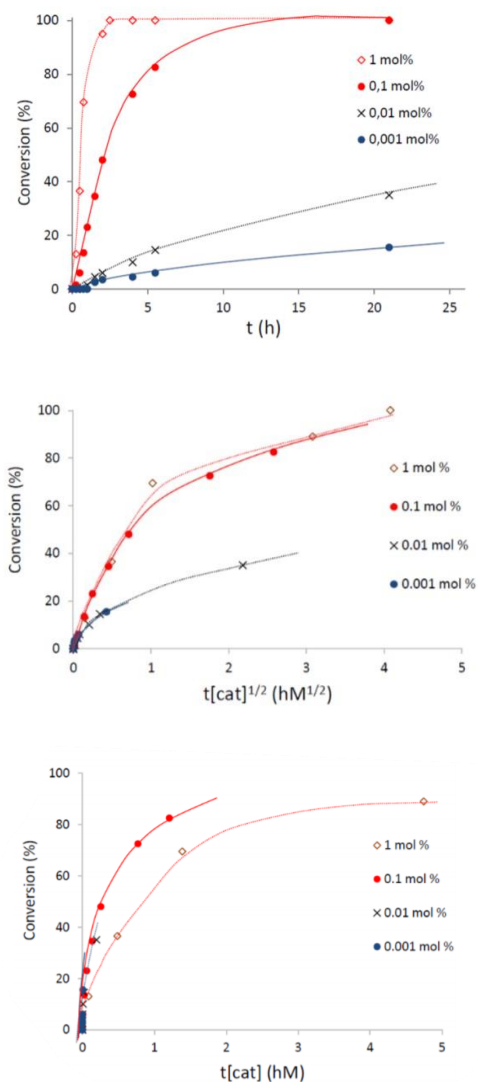

Figure 2. (a) Time-dependent reaction profile of the cyclization reaction of 4-pentynoic acid using catalyst **3**. (b) Reaction profile with normalized time scale assuming a catalyst order of 1/2. (c) Reaction profile with normalized time scale assuming a catalyst order of 1. Reaction conditions are the same as those shown in **Table 1**. In all three graphics, the evolution is shown as consumption of 4-pentynoic acid. Lines are only to guide the eye.

In order to widen the study on the catalytic activities of complexes **3** and **4**, we decided to test them in the [3 + 2] cycloaddition reaction of cyclopropenones and alkynes (Table 2). This reaction, first reported by Wenders and co-workers, constitutes a selective and high-yielding route to valuable cyclopentadienones (CPDs).[15]

Table 2. [3 + 2] Cycloaddition Reactions of Diphenylcyclopropenone with Substituted Phenylacetylenes[a]
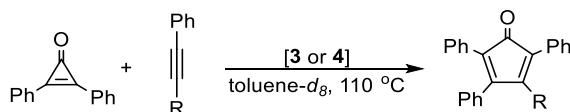
Entry	R	Cat.	Cat. loading (mol %)	Time (h)	Conversion (%)[b]
1	CO_2Et	**3**	1	24	72
2	CO_2Et	**3**	0.5	24	60
3	CO_2Et	**3**	0.1	48	71
4	CH_3	**3**	0.1	48	64
5	H	**3**	0.1	48	30
6	CO_2Et	**4**	1	24	95
7	CO_2Et	**4**	0.5	24	75
8	CO_2Et	**4**	0.1	24	92
9	CH_3	**4**	0.1	24	44
10	H	**4**	0.1	24	30

[a]Reaction conditions: 0.225 mmol of diphenylcyclopropenone, 0.15 mmol of alkyne, catalyst **3** or **4**, toluene-d_8 (0.3 M), 110 °C. [b]Conversions were determined by ^{1}H NMR spectroscopy using 1,3,5-trimethoxybenzene as internal standard.

Using 1 mol % of Rh(I) complex **3**, the [3 + 2] cycloaddition of diphenylcyclopropenone and ethylpropionate gave the corresponding CPD in 72 % after 24 h at 110 °C (entry 1). The catalytic activity of **3** compares well with those given by other Rh(I) complexes described in the literature, bearing NHC[15b] and cyclic(amino)- (aryl)carbene ligands.[15c]

In all cases, the tetra-iridium complex **4** showed higher catalytic activity than **3** in the reaction of diphenylcyclopropenone with ethylphenylpropiolate (compare entries 1−3 and 6−8), and constitutes one of the best catalysts described to date

for this type of transformation. As well as **3**, **4** showed moderate catalytic activity in the reactions using 1-phenyl-1-propyne and phenylacetylene.

3. Conclusions

In summary, we described a new pyrene-tetra-imidazolium salt that we used for the preparation of a series of Rh(I) and Ir(I) pyrene-tetra-NHC complexes. The coordination of MCl(cod) units results in the formation of helix-type structures dominated by the restricted rotation about the $C_{pyr}–N_{imid}$ and $M–C_{NHC}$ bonds, which yield hydrogen-bonding interactions between the chloride ligands and the protons of the pyrene connector. The two complexes were tested in the cyclization of acetylenic carboxylic acids, and in the reaction of diphenylcyclopropenone with substituted phenylacetylenes to form cyclopentadienones. In the first of these two reactions, the activity of the tetrametallic catalysts is similar to the activity shown by a monometallic analogue, only at low concentrations. At higher concentrations, the monometallic complex outperforms the tetrametallic one. This behaviour is explained as a consequence of the low solubility of the tetrametallic catalyst, which leads to a maximum concentration of the catalyst when the saturation of the solution has been reached. In the coupling of diphenylcyclopropenone with substituted phenylacetylenes, the tetra-iridium complex (**4**) shows higher activity than the tetra-rhodium one (**3**). Although there is clearly room for improvement, to the best of our knowledge, complex **4** is the first iridium complex tested in this reaction.

4. Experimental section

General Considerations. Anhydrous solvents were dried using a solvent purification system (SPS M BRAUN) or purchased and degassed prior to use by purging them with dry nitrogen. All the reagents and solvents were used as received from commercial suppliers. Column chromatography was performed on silica gel Merck 60, 62–200 mm unless otherwise stated, using mixtures of solvents. NMR spectra were recorded on a Varian Innova 500 MHz or on a Bruker 400/300 MHz, using DMSO-d_6, acetone-d_6, toluene- d_8, or CDCl$_3$ as solvent. Elemental analyses were carried out on a TruSpec Micro Series. Infrared spectra (FT-IR) were performed on a Bruker EQUINOX 55 spectrometer with a spectral window of 4000–600 cm^{-1}. Electrospray Mass Spectra (ESI-MS) were recorded on a Micromass Quatro LC instrument. MeOH, CH$_3$CN, or CH$_2$Cl$_2$ was used as mobile phase, and nitrogen was employed as the drying and nebulizing gas.

Synthesis of the Rh(I) and Ir(I) Complexes. *Synthesis of 1-n-butyl-3-phenylimidazolium hexafluorophosphate.* Imidazole (1.3 g, 19.6 mmol, 4 equiv.), CuSO$_4$ (196 mg, 1.23 mmol, 0.25 equiv.), and K$_2$CO$_3$ (2 g, 14.7 mmol, 3 equiv.) were placed together in a high pressure Schlenk tube fitted with a Teflon cap. The tube was evacuated and filled with nitrogen three times. Iodobenzene (0.56 mL, 4.9 mmol, 1 equiv.) was added, and the resulting suspension was heated at 150 °C for 24 h. After this time, the resulting solid was washed with water (3 × 40 mL) and filtrated using a Büchner funnel. The solid was extracted with MeOH (3 × 20 mL). 1-Phenylimidazole, which was isolated as an oil after removal of the volatiles, was employed in the next step without further purification. Yield: 400 mg (57 %). A mixture of 1-phenylimidazole (400 mg, 2.8 mmol, 1 equiv.) and *n*-BuI (0.3 mL, 2.8 mL, 1 equiv.) in dry THF (20 mL) was heated at 110 °C in a high pressure Schlenk tube fitted with a Teflon cap, during 12 h. After removal of the volatiles, 1-*n*-butyl-3-phenylimidazolium was isolated as a brown oil. A mixture

of 1-*n*-butyl-3-phenylimidazolium (885 mg, 2.7 mmol, 1 equiv.) and [NH$_4$](PF$_6$) (550 mg, 3.4 mmol, 1.25 equiv.) in MeOH (15 mL) was heated at 40 °C overnight. After removal of the volatiles, the crude was washed with CH$_2$Cl$_2$ and the insoluble salts were separated by filtration. The desired product was isolated as an off-white solid after precipitation from a mixture dichloromethane/diethyl ether. Yield: 900 mg (93 %). ^{1}H NMR (400 MHz, CDCl$_3$): δ 9.08 (s, 1H, NC*H*N), 7.61–7.48 (m, 7H; 5H, C*H*$_{phenyl}$ and 2H, C*H*$_{im}$), 4.36 (t, $^3J_{H-H}$ = 8 Hz, 2H, NC*H*$_2$CH$_2$CH$_2$CH$_3$), 1.98–1.91 (m, 2H, NCH$_2$C*H*$_2$CH$_2$CH$_3$), 1.46–1.40 (m, 2H, NCH$_2$CH$_2$C*H*$_2$CH$_3$), 0.98 (t, $^3J_{H-H}$ = 8 Hz, 3H, NCH$_2$CH$_2$CH$_2$C*H*$_3$). ^{19}F{^{1}H} NMR (376 MHz, CDCl$_3$): δ −72.3 (d). ^{31}P{^{1}H} NMR (162 MHz, CDCl$_3$): δ −144.32 (m). ^{13}C{^{1}H} NMR (100 MHz, CDCl$_3$): δ 134.4 (NC*H*N), 134.3 (*C*$_{q,phenyl}$), 130.7 (*C*H$_{phenyl}$), 127.8 (*C*H$_{phenyl}$), 123.1 (*C*H$_{im}$), 122.3 (*C*H$_{phenyl}$), 121.5 (*C*H$_{im}$), 50.6 (N*C*H$_2$CH$_2$CH$_2$CH$_3$), 31.9 (NCH$_2$*C*H$_2$CH$_2$CH$_3$), 19.5 (NCH$_2$CH$_2$*C*H$_2$CH$_3$), 13.4 (NCH$_2$CH$_2$CH$_2$*C*H$_3$). Electrospray MS (cone 20 V) (m/z, fragment): 201.2 [M − PF$_6$]$^+$ (Calcd. for [M − PF$_6$]$^+$: 201.3). Anal. Calcd. for C$_{13}$H$_{17}$N$_2$PF$_6$·CH$_2$Cl$_2$ (431.18): C, 39.00; H, 4.44; N, 6.50. Found: C, 39.42; H, 4.18; N, 6.99.

Synthesis of the neutral precursor 1. A mixture of 1,3,6,8-tetrabromopyrene (500 mg, 0.97 mmol, 1 equiv.), imidazole (265.6 mg, 3.86 mmol, 4 equiv.), K$_2$CO$_3$ (1079 mg, 7.73 mmol, 8 equiv.), and CuI (73.6 mg, 0.39 mmol, 0.4 equiv.) were placed together in a high pressure Schlenk tube fitted with a Teflon cap. The tube was evacuated and filled with nitrogen three times. The solids were suspended in anhydrous DMF (12 mL), and the resulting solution was heated at 160 °C for 72 h. Then, the reaction mixture was allowed to reach room temperature. Distilled water (75 mL) was added, and the suspension was stirred for 2 h. The resulting solid was collected by filtration using a Büchner and washed with water. Compound **1** was isolated as a highly insoluble dark green solid. Yield: 452.0 mg (>99 %). ^{1}H NMR (500 MHz, DMSO-*d$_6$*): δ 8.43 (br s, 2H, C*H*$_{pyr}$), 8.27 (br s, 4H, NC*H*N), 8.08 (br s, 4H, C*H*$_{pyr}$), 7.85 (br s, 2H, C*H*$_{im}$), 7.36 (br s, 2H, C*H*$_{im}$).

Electrospray MS (cone 20 V) (m/z, fragment): 467.2 [M + H]$^+$ (Calcd. for [M + H]$^+$: 467.2).

*Synthesis of the tetra-imidazolium salt **2**.* Under aerobic conditions, a mixture of compound **1** (517 mg, 1.11 mmol, 1 equiv.) and *n*-BuI (16 mL, 89 mmol, 80 equiv.) was heated in a thick walled Schlenk tube fitted with a Teflon cap at 100 °C for 72 h. After cooling at room temperature, the excess of *n*-BuI was distilled under vacuum. The resulting black solid residue was washed several times with diethyl ether and ethyl acetate and collected by filtration. The iodide salt (500 mg, 0.42 mmol, 1 equiv.) was dissolved in MeOH (15 mL) and treated with [NH$_4$](PF$_6$) (342.3 mg, 2.10 mmol, 5 equiv.). The suspension was heated at 40°C overnight. Compound **2** was collected by filtration as a brown solid. Yield: 885 mg (71 %). ^{1}H NMR (400 MHz, acetone-*d$_6$*): δ 9.72 (s, 4H, NC*H*N), 9.06 (s, 2H, C*H*$_{pyr}$), 8.49 (s, 4H, C*H*$_{pyr}$), 8.31 (s, 4H, C*H*$_{im}$), 8.26 (s, 4H, C*H*$_{im}$), 4.62 (t, $^3J_{H-H}$ = 8 Hz, 8H, NC*H$_2$*CH$_2$CH$_2$CH$_3$), 2.18−2.10 (m, 8H, NCH$_2$C*H$_2$*CH$_2$CH$_3$), 1.58−1.49 (m, 8H, NCH$_2$CH$_2$C*H$_2$*CH$_3$), 1.02 (t, $^3J_{H-H}$ = 8 Hz, 12H, NCH$_2$CH$_2$CH$_2$C*H$_3$*). ^{19}F{^{1}H} NMR (376 MHz, acetone-*d$_6$*): δ −72.3 (d). ^{31}P{^{1}H} NMR (162 MHz, acetone-*d$_6$*): δ −144.4 (m). ^{13}C{^{1}H} NMR (101 MHz, acetone-d6): δ 139.1 (N*C*HN), 131.2 (*C*$_{q,pyr}$), 128.8 (*C*$_{q,pyr}$), 126.9 (*C*H$_{pyr}$), 126.4 (*C*H$_{pyr}$), 125.9 (*C*H$_{im}$), 125.2 (*C*$_{q,pyr}$), 124.8 (*C*H$_{im}$), 51.3 (N*C*H$_2$CH$_2$CH$_2$CH$_3$), 32.5 (NCH$_2$*C*H$_2$CH$_2$CH$_3$), 20.2 (NCH$_2$CH$_2$*C*H$_2$CH$_3$), 13.7 (NCH$_2$CH$_2$CH$_2$*C*H$_3$). Electrospray MS (cone 20 V) (m/z, fragment): 173.7 [M − 4(PF$_6$)]$^{4+}$, 279.9 [M − 3(PF$_6$)]$^{3+}$, 492.3 [M − 2(PF$_6$)]$^{2+}$ (Calcd. for [M − 4(PF$_6$)]$^{4+}$: 173.6, [M − 3(PF$_6$)]$^{3+}$: 279.8, [M − 2(PF$_6$)]$^{2+}$: 492.2). Anal. Calcd. for C$_{44}$H$_{54}$N$_8$P$_4$F$_{24}$·2CH$_2$Cl$_2$ (1444.68): C, 38.24; H, 4.05; N, 7.76. Found: C, 38.43; H, 3.92; N, 7.82.

*Synthesis of the tetrametallic complexes **3**−**5**. General procedure for complexes **3** and **4**.* Compound **2** (1 equiv.) was placed in a Schlenk tube. The tube was evacuated and filled with nitrogen three times. The solid was suspended in dry CH$_3$CN and NEt$_3$ (50 equiv.) was added to the suspension. The resulting solution

was heated at 40 °C for 45 min. The corresponding metal precursor (2.2 equiv. of [RhCl(cod)]$_2$ or [IrCl(cod)]$_2$) was placed in a second Schlenk tube. The tube was evacuated and filled with nitrogen three times. The solid was then suspended in dry CH$_3$CN and subsequently cannulated over the first Schlenk. The resulting mixture was heated under reflux overnight. Once at room temperature, the resulting yellow precipitate was collected by filtration. The crude product was purified by column chromatography. Elution with a 9:1 CH$_2$Cl$_2$/acetone mixture afforded a bright red band that contained the desired complex.

Synthesis of 3. A mixture of [RhCl(cod)]$_2$ (127.8 mg, 0.260 mmol) in dry CH$_3$CN (10 mL) was cannulated to a suspension of **2** (150 mg, 0.118 mmol) and NEt$_3$ (0.82 mL, 5.9 mmol) in dry CH$_3$CN (30 mL). After the general workup, complex **3** was isolated as a bright yellow solid. Yield: 107.1 mg (54 %). ^{1}H NMR (300 MHz, CDCl$_3$): δ 9.86 (d, $^3J_{H-H}$ = 7 Hz, 2H, CH_{pyr}), 8.98 (s, 2H, CH_{pyr}), 8.15 (d, $^3J_{H-H}$ = 1.5 Hz, 2H, CH_{im}), 8.11 (d, $^3J_{H-H}$ = 7 Hz, 2H, CH_{pyr}), 7.40 (d, $^3J_{H-H}$ = 1.5 Hz, 2H, CH_{im}), 7.21 (d, $^3J_{H-H}$ = 1.5 Hz, 2H, CH_{im}), 7.20 (d, $^3J_{H-H}$ = 1.5 Hz, d, 2H, CH_{im}), 5.27−5.21 (m, 4H, NCH_2CH$_2$CH$_2$CH$_3$), 4.88−4.78 (m, 8H, CH_{cod}), 4.71−4.61 (m, 8H, CH_{cod}), 4.50−4.43 (m, 4H, NCH_2CH$_2$CH$_2$CH$_3$), 3.35 (q, 3H, C$H_{2\ cod}$), 3.29 (q, 3H, C$H_{2\ cod}$). The rest of the signals corresponding to the *n*-butyl and cod ligands are displayed in the region between 2.50 and 0.30 ppm. ^{13}C{^{1}H} NMR (75 MHz, CDCl$_3$): δ 185.5 (d, Rh-$C_{carbene}$, $^1J_{Rh-C}$ = 51 Hz), 183.6 (d, Rh-$C_{carbene}$, $^1J_{Rh-C}$ = 51 Hz), 134.4 ($C_{q,pyr}$), 134.4 ($C_{q,pyr}$), 128.1 ($C H_{im}$), 127.6 (CH_{im}), 127.3 ($C_{q,pyr}$), 127.0 ($C_{q,pyr}$), 125.5 (CH_{im}), 125.1 ($C_{q,pyr}$), 123.9 (CH_{im}), 122.1 (CH_{pyr}), 121.8 (CH_{pyr}), 121.7 (CH_{pyr}), 98.3 (d, Rh-CH_{cod}, $^1J_{Rh-C}$ = 6.75 Hz), 98.1 (d, Rh-CH_{cod}, $^1J_{Rh-C}$ = 6.75 Hz), 97.5 (d, Rh-CH_{cod}, $^1J_{Rh-C}$ = 7.5 Hz), 96.9 (d, Rh-CH_{cod}, $^1J_{Rh-C}$ = 7.5 Hz), 69.7 (d, Rh-CH_{cod}, $^1J_{Rh-C}$ = 14.25 Hz), 69.4 (d, Rh-CH_{cod}, $^1J_{Rh-C}$ = 14.25 Hz), 68.7 (d, Rh-CH_{cod}, $^1J_{Rh-C}$ = 13.5 Hz), 66.6 (d, Rh-CH_{cod}, $^1J_{Rh-C}$ = 13.5 Hz), 52.0 (NCH_2CH$_2$CH$_2$CH$_3$), 51.1 (NCH_2CH$_2$CH$_2$CH$_3$), 35.06 ($CH_{2\ cod}$), 33.1 (NCH$_2$$CH_2CH_2CH_3$), 33.1 (NCH$_2$$CH_2CH_2CH_3$), 31.5 ($CH_{2\ cod}$), 31.0 ($CH_{2\ cod}$), 30.5 ($CH_{2\ cod}$), 29.7 ($CH_{2\ cod}$), 28.6 ($CH_{2\ cod}$), 28.4 ($CH_{2\ cod}$), 27.1 ($CH_{2\ cod}$), 20.3

(NCH$_2$CH$_2$*C*H$_2$CH$_3$), 20.3 (NCH$_2$CH$_2$*C*H$_2$CH$_3$), 14.1 (NCH$_2$CH$_2$CH$_2$*C*H$_3$), 14.0 (NCH$_2$CH$_2$CH$_2$*C*H$_3$). Electrospray MS (cone 20 V) (m/z, fragment): 802.9 [M − 2Cl]$^{2+}$ (Calcd. for [M − 2Cl]$^{2+}$: 802.2). Anal. Calcd. for C$_{76}$H$_{98}$N$_8$Rh$_4$Cl$_4$·CH$_2$Cl$_2$ (1762.03): C, 52.49; H, 5.72; N, 6.36. Found: C, 51.95; H, 5.86; N, 6.97.

Synthesis of 4. A mixture of [IrCl(cod)]$_2$ (137.6 mg, 0.173 mmol) in dry CH$_3$CN (8 mL) was cannulated to a suspension of **2** (100 mg, 0.079 mmol) and NEt$_3$ (0.55 mL, 3.925 mmol) in dry CH$_3$CN (20 mL). After the general workup, complex **4** was isolated as a bright orange solid. Yield: 87.7 mg (54 %). ^{1}H NMR (300 MHz, CDCl$_3$): δ 9.36 (d, $^3J_{\text{H-H}}$ = 9.5 Hz, 2H, C*H*$_{\text{pyr}}$), 8.82 (s, 2H, C*H*$_{\text{pyr}}$), 7.98 (d, $^3J_{\text{H-H}}$ = 9.5 Hz, 2H, C*H*$_{\text{pyr}}$), 7.92 (d, $^3J_{\text{H-H}}$ = 1.5 Hz, 2H, C*H*$_{\text{im}}$), 7.41 (d, $^3J_{\text{H-H}}$ = 1.5 Hz, 2H, C*H*$_{\text{im}}$), 7.23 (d, $^3J_{\text{H-H}}$ = 1.5 Hz, 2H, C*H*$_{\text{im}}$), 7.20 (d, $^3J_{\text{H-H}}$ = 1.5 Hz, 2H, C*H*$_{\text{im}}$), 5.01−4.94 (m, 4H, NC*H*$_2$CH$_2$CH$_2$CH$_3$), 4.55−4.44 (m, 8H, C*H*$_{\text{cod}}$ and 4H, NC*H*$_2$CH$_2$CH$_2$CH$_3$), 4.32−4.27 (m, 8H, C*H*$_{\text{cod}}$), 3.03−3.00 (m, 3H, C*H*$_{2\ \text{cod}}$), 2.92−2.88 (m, 3H, C*H*$_{2\ \text{cod}}$). The rest of the signals corresponding to the *n*-butyl and cod ligands are displayed in the region between 2.15 and 0.10 ppm. ^{13}C{^{1}H} NMR (101 MHz, CDCl$_3$): δ 182.4 (Ir-*C*$_{\text{carbene}}$), 181.2 (Ir-*C*$_{\text{carbene}}$), 133.7 (*C*$_{\text{q,pyr}}$), 133.5 (*C*$_{\text{q,pyr}}$), 128.4 (*C*H$_{\text{im}}$), 127.7 (*C*H$_{\text{im}}$), 127.4 (*C*$_{\text{q,pyr}}$), 126.8 (*C*$_{\text{q,pyr}}$), 124.8 (*C*H$_{\text{im}}$), 124.7 (*C*$_{\text{q,pyr}}$), 123.4 (*C*H$_{\text{im}}$), 121.4 (*C*H$_{\text{pyr}}$), 121.4 (*C*H$_{\text{pyr}}$), 121.1 (*C*H$_{\text{pyr}}$), 84.3 (*C*H$_{\text{cod}}$), 84.2 (*C*H$_{\text{cod}}$), 84.0 (*C*H$_{\text{cod}}$), 82.5 (*C*H$_{\text{cod}}$), 53.4 (*C*H$_{\text{cod}}$), 53.1 (*C*H$_{\text{cod}}$), 52.6 (*C*H$_{\text{cod}}$), 51.7 (N*C*H$_2$CH$_2$CH$_2$CH$_3$), 50.8 (N*C*H$_2$CH$_2$CH$_2$CH$_3$), 50.4 (*C*H$_{\text{cod}}$), 35.8 (*C*H$_{2\ \text{cod}}$), 33.6 (*C*H$_{2\ \text{cod}}$), 33.1 (NCH$_2$*C*H$_2$CH$_2$CH$_3$), 32.9 (NCH$_2$*C*H$_2$CH$_2$CH$_3$), 32.3 (*C*H$_{2\ \text{cod}}$), 31.2 (*C*H$_{2\ \text{cod}}$), 30.5 (*C*H$_{2\ \text{cod}}$), 29.4 (*C*H$_{2\ \text{cod}}$), 29.0 (*C*H$_{2\ \text{cod}}$), 27.6 (*C*H$_{2\ \text{cod}}$), 20.2 (NCH$_2$CH$_2$*C*H$_2$CH$_3$), 20.2 (NCH$_2$CH$_2$*C*H$_2$CH$_3$), 14.0 (NCH$_2$CH$_2$CH$_2$*C*H$_3$), 14.0 (NCH$_2$CH$_2$CH$_2$*C*H$_3$). Electrospray MS (cone 20 V) (m/z, fragment): 981.7 [M − 2Cl]$^{2+}$ (Calcd. for [M − 2Cl]$^{2+}$: 981.3). Anal. Calcd. for C$_{76}$H$_{98}$N$_8$Ir$_4$Cl$_4$ (2034.34): C, 44.87; H, 4.86; N, 5.51. Found: C, 45.16; H, 5.62; N, 5.13.

Synthesis of 5. CO gas was passed through a solution of complex **4** (30 mg, 0.015 mmol) in CH$_2$Cl$_2$ (10 mL) at 0 °C, for 30 min. After this time, the solution was

concentrated under reduced pressure and precipitated with hexane. The corresponding carbonyl derivative precipitated as a pale-yellow solid in quantitative yield. IR (KBr): v 2064 cm^{-1} (C=O), v 1977 cm^{-1} (C=O). ^{1}H NMR (400 MHz, CDCl$_3$): δ 8.36 (br, 2H, CH_{pyr}), 8.03 (br, 4H, CH_{pyr}), 7.49 (s, 4H, CH_{im}), 7.33 (s, 4H, CH_{im}), 4.57 (br, 4H, NCH_2CH$_2$CH$_2$CH$_3$), 4.46 (br, 4H, NCH_2CH$_2$CH$_2$CH$_3$), 2.07−2.02 (m, 8H, NCH$_2$CH_2CH$_2$CH$_3$), 1.54−1.51 (m, 8H, NCH$_2$CH$_2$CH_2CH$_3$), 1.06 (t, $^3J_{\text{H-H}}$ = 9.5 Hz, 12H, NCH$_2$CH$_2$CH$_2$CH_3). ^{13}C{^{1}H} NMR (101 MHz, CDCl$_3$): δ 180.7 (Ir-$C_{carbene}$), 175.6 (Ir-CO), 168.1 (Ir-CO), 133.3 ($C_{q,pyr}$), 129.0 ($C_{q,pyr}$), 125.4 (CH$_{pyr}$), 125.0 (CH$_{pyr}$), 125.0 (CH$_{im}$), 124.8 ($C_{q,pyr}$), 122.0 (CH$_{im}$), 51.6 (NCH$_2$CH$_2$CH$_2$CH$_3$), 32.9 (NCH$_2$$CH_2CH_2CH_3$), 20.0 (NCH$_2CH_2$$CH_2CH_3$), 13.9 (NCH$_2CH_2CH_2$$CH_3$). Electrospray MS (cone 20 V) (m/z, fragment): 1791.3 [M − Cl]$^+$ (Calcd. for [M − Cl]$^+$: 1789.1). Anal. Calcd. for C$_{52}$H$_{50}$N$_8$O$_8$Ir$_4$Cl$_4$·CH$_2$Cl$_2$ (1910.62): C, 33.32; H, 2.74; N, 5.86. Found: C, 33.25; H, 2.96; N, 6.21.

*Synthesis of the monometallic complexes **6** and **7**. Synthesis of **6**.* 1-*n*-Butyl-3-phenylimidazolium hexafluorophosphate (50 mg, 0.144 mmol, 1 equiv.), [RhCl(cod)]$_2$ (35.5 mg, 0.072 mmol, 0.5 equiv.), and K$_2$CO$_3$ (60 mg, 0.432 mmol, 3 equiv.) were placed together in a high pressure Schlenk. The resulting mixture was dissolved in acetone (3 mL) and stirred for 20 h at 60 °C. After this time, the mixture was cooled to room temperature. The solution was then filtered, and the volatiles were removed under vacuum. The resulting solid was dissolved in CH$_2$Cl$_2$, filtered through a pad of Celite, and the solvent was removed under vacuum. The crude solid was purified by column chromatography. Elution with CH$_2$Cl$_2$ afforded a bright orange band that contained the desired complex. Yield: 53.5 mg (83.5 %). ^{1}H NMR (400 MHz, CDCl$_3$): δ 8.22−8.20 (m, 2H, CH_{Ph}), 7.55−7.50 (m, 2H, CH_{Ph}), 7.45−7.40 (m, 1H, CH_{Ph}), 7.17 (d, $^3J_{\text{H-H}}$ = 2 Hz, 1H, CH_{im}), 7.02 (d, $^3J_{\text{H-H}}$ = 2 Hz, 1H, CH_{im}), 5.26−5.22 (m, 1H, CH_{cod}), 5.18− 5.11 (m, 1H, CH_{cod}), 4.87−4.77 (m, 1H, NCH_2CH$_2$CH$_2$CH$_3$), 4.44− 4.34 (m, 1H, NCH_2CH$_2$CH$_2$CH$_3$), 3.42−3.37 (m, 1H, CH_{cod}), 2.78− 2.73 (m, 1H, CH_{cod}), 2.32−2.22 (m, 2H, C$H_{2\ cod}$), 2.11−1.99 (m, 2H,

C$H_{2\ cod}$), 1.96–1.71 (m, 4H, C$H_{2\ cod}$ and 2H, NCH$_2$CH_2CH$_2$CH$_3$), 1.57–1.46 (m, 2H, NCH$_2$CH$_2$CH_2CH$_3$), 1.06 (t, $^3J_{H-H}$ = 12 Hz, 3H, NCH$_2$CH$_2$CH$_2$CH_3). ^{13}C{^{1}H} NMR (101 MHz, CDCl$_3$): δ 182.2 (d, Rh-$C$$_{carbene}$, $^1J_{Rh-C}$ = 49 Hz), 140.5 ($C_{q,Ph}$), 128.8 (CH$_{Ph}$), 127.9 (CH$_{Ph}$), 124.7 (CH$_{Ph}$), 121.9 (CH$_{im}$), 120.9 (CH$_{im}$), 95.7 (d, Rh-CH$_{cod}$, $^1J_{Rh-C}$ = 7 Hz), 72.1 (d, Rh-CH$_{cod}$, $^1J_{Rh-C}$ = 14 Hz), 71.3 (d, Rh-CH$_{cod}$, $^1J_{Rh-C}$ = 14 Hz), 52.0 (NCH$_2$CH$_2$CH$_2$CH$_3$), 33.0 (CH$_{2\ cod}$), 32.4 (NCH$_2$$CH_2CH_2CH_3$), 31.2 ($CH_{2\ cod}$), 29.8 ($CH_{2\ cod}$), 29.2 ($CH_{2\ cod}$), 20.3 (NCH$_2CH_2$$CH_2CH_3$), 14.1 (NCH$_2CH_2CH_2$$CH_3$). Electrospray MS (cone 20 V) (m/z, fragment): 411.3 [M − Cl]$^+$ (Calcd. for [M − Cl]$^+$: 411.1). Anal. Calcd. for C$_{21}$H$_{28}$N$_2$RhCl·2CH$_2$Cl$_2$ (616.68): C, 44.80; H, 5.23; N, 4.54. Found: C, 44.67; H, 5.39; N, 4.83.

Synthesis of 7. CO gas was passed through a solution of complex **6** (33 mg, 0.074 mmol) in CH$_2$Cl$_2$ (10 mL) at 0 °C, for 30 min. After this time, the solvent was removed under vacuum. The corresponding carbonyl derivative was obtained as a yellow solid in quantitative yield. Complex **7** was found unstable in solution as well as in the solid state, which prevented a correct elemental analysis. IR (KBr): v 2067 cm^{-1} (C=O), 1997 cm^{-1} (C=O). ^{1}H NMR (300 MHz, CDCl$_3$): δ 7.73–7.71 (m, 2H, CH_{Ph}), 7.51–7.44 (m, 3H, CH_{Ph}), 7.28–7.27 (d, $^3J_{H-H}$ = 2 Hz, 1H, CH_{im}), 7.17–7.16 (d, $^3J_{H-H}$ = 2 Hz, 1H, CH_{im}), 4.61–4.52 (m, 1H, NCH_2CH$_2$CH$_2$CH$_3$), 4.19– 4.10 (m, 1H, NCH_2CH$_2$CH$_2$CH$_3$), 1.98–1.88 (m, 2H, NCH$_2$CH_2CH$_2$CH$_3$), 1.46–1.39 (m, 2H, NCH$_2$CH$_2$CH_2CH$_3$), 1.00 (t, $^3J_{H-H}$ = 7.3 Hz, 3H, NCH$_2$CH$_2$CH$_2$CH_3). ^{13}C{^{1}H} NMR (75 MHz, CDCl$_3$): δ 187.2 (d, Rh-$C$$_{carbene}$, $^1J_{Rh-C}$ = 53.25 Hz), 181.2 (d, Rh-CO, $^1J_{Rh-C}$ = 77.25 Hz), 172.66 (d, Rh-CO, $^1J_{Rh-C}$ = 41.25 Hz), 139.8 ($C_{q,Ph}$), 129.3 (CH$_{Ph}$), 128.9 (CH$_{Ph}$), 125.5 (CH$_{Ph}$), 122.9 (CH$_{im}$), 122.3 (CH$_{im}$), 52.1 (NCH$_2$CH$_2$CH$_2$CH$_3$), 32.3 (NCH$_2$$CH_2CH_2CH_3$), 19.9 (NCH$_2CH_2$$CH_2CH_3$), 13.9 (NCH$_2CH_2CH_2$$CH_3$).

References

1.   Peris, E., *Chem. Rev.* **2017,** *118* (19), 9988–10031.

2.   (a) Leeuven, P. W. N. M. V., *Supramolecular Catalysis*. Wiley-VCH: Weinheim, Germany, 2008; (b) Raynal, M.; Ballester, P.; Vidal-Ferran, A.; van Leeuwen, P., *Chem. Soc. Rev.* **2014,** *43* (5), 1734-1787; (c) Raynal, M.; Ballester, P.; Vidal-Ferran, A.; van Leeuwen, P., *Chem. Soc. Rev.* **2014,** *43* (5), 1660-1733.

3.   Sinha, N.; Hahn, F. E., *Acc. Chem. Res.* **2017,** *50* (9), 2167-2184.

4.   Peris, E., *Chem. Commun.* **2016,** *52* (34), 5777-5787.

5.   Valdes, H.; Poyatos, M.; Ujaque, G.; Peris, E., *Chemistry-a European Journal* **2015,** *21* (4), 1578-1588.

6.   Ruiz-Botella, S.; Peris, E., *Chemcatchem* **2018,** *10* (8), 1874-1881.

7.   Ruiz-Botella, S.; Peris, E., *Chemistry-a European Journal* **2015,** *21* (43), 15263-15271.

8.   Ibañez, S.; Poyatos, M.; Peris, E., *Organometallics* **2017,** *36* (7), 1447-1451.

9.   (a) Sabater, S.; Mata, J. A.; Peris, E., *Acs Catalysis* **2014,** *4* (6), 2038-2047; (b) Sabater, S.; Mata, J. A.; Peris, E., *Organometallics* **2015,** *34* (7), 1186-1190; (c) Ventura-Espinosa, D.; Vicent, C.; Baya, M.; Mata, J. A., *Catalysis Science & Technology* **2016,** *6* (22), 8024-8035.

10.   (a) Ibañez, S.; Guerrero, A.; Poyatos, M.; Peris, E., *Chemistry-a European Journal* **2015,** *21* (29), 10566-10575; (b) Gonell, S.; Poyatos, M.; Peris, E., *Dalton Transactions* **2016,** *45* (13), 5549-5556.

11.   Gutiérrez-Blanco, A.; Fernández-Moreira, V.; Gimeno, M. C.; Peris, E.; Poyatos, M., *Organometallics* **2018,** *37*, 1795–1800.

12.   Rubio, R. J.; Andavan, G. T. S.; Bauer, E. B.; Hollis, T. K.; Cho, J.; Tham, F. S.; Donnadieu, B., *J. Organomet. Chem.* **2005,** *690* (23), 5353-5364.

13.   (a) Kelly, R. A.; Clavier, H.; Giudice, S.; Scott, N. M.; Stevens, E. D.; Bordner, J.; Samardjiev, I.; Hoff, C. D.; Cavallo, L.; Nolan, S. P., *Organometallics*

2008, *27* (2), 202-210; (b) Droge, T.; Glorius, F., *Angewandte Chemie-International Edition* **2010,** *49* (39), 6940-6952; (c) Chianese, A. R.; Li, X. W.; Janzen, M. C.; Faller, J. W.; Crabtree, R. H., *Organometallics* **2003,** *22* (8), 1663-1667.

14.   (a) Wei, S. P.; Pedroni, J.; Meissner, A.; Lumbroso, A.; Drexler, H. J.; Heller, D.; Breit, B., *Chemistry-a European Journal* **2013,** *19* (36), 12067-12076; (b) Man, B. Y. W.; Bhadbhade, M.; Messerle, B. A., *New J. Chem.* **2011,** *35* (8), 1730-1739; (c) Elgafi, S.; Field, L. D.; Messerle, B. A., *J. Organomet. Chem.* **2000,** *607* (1-2), 97-104; (d) Mas-Marza, E.; Sanau, M.; Peris, E., *Inorg. Chem.* **2005,** *44*, 9961-9967.

15.   (a) Wender, P. A.; Paxton, T. J.; Williams, T. J., *J. Am. Chem. Soc.* **2006,** *128* (46), 14814-14815; (b) Peng, H. M.; Webster, R. D.; Li, X. W., *Organometallics* **2008,** *27* (17), 4484-4493; (c) Rao, B.; Tang, H. R.; Zeng, X. M.; Liu, L.; Melaimi, M.; Bertrand, G., *Angewandte Chemie-International Edition* **2015,** *54* (49), 14915-14919.

16.   Chan, D. M. T.; Marder, T. B.; Milstein, D.; Taylor, N. J., *J. Am. Chem. Soc.* **1987,** *109* (21), 6385-6388.

17.   (a) Bures, J., *Angewandte Chemie-International Edition* **2016,** *55* (6), 2028-2031; (b) Bures, J., *Angewandte Chemie-International Edition* **2016,** *55* (52), 16084-16087.

Supporting information for:

Tetra-Au(I) Complexes Bearing a Pyrene Tetraalkynyl Connector Behave as Fluorescence Torches

by

Ana Gutiérrez-Blanco, Eduardo Peris and Macarena Poyatos*

Institute of Advanced Materials (INAM). Universitat Jaume I. Av. Vicente Sos Baynat s/n, Castellón, E-12071, Spain.

Email: poyatosd@uji.es

1. Spectroscopic data
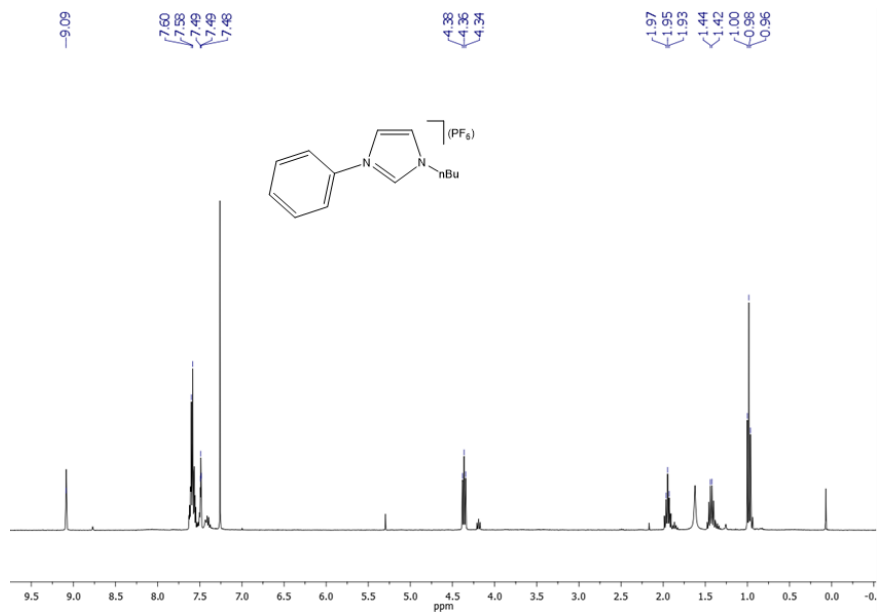
Figure S1. ^{1}H NMR spectrum (400 MHz, CDCl$_3$) of 1-n-butyl-3-phenylimidazolium hexafluorophosphate.
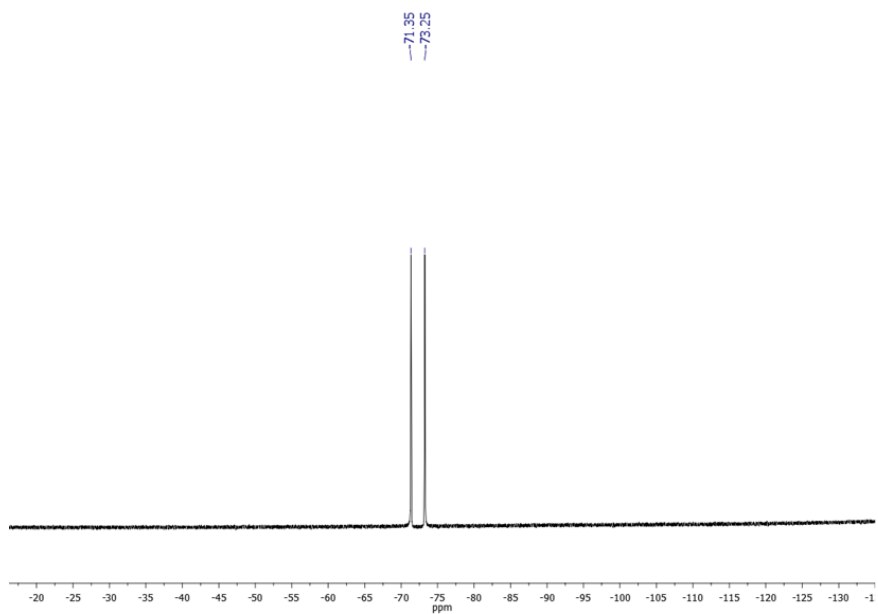
Figure S2. ^{19}F {^{1}H} NMR spectrum (376 MHz, CDCl$_3$) of 1-*n*-butyl-3- phenylimidazolium hexafluorophosphate.
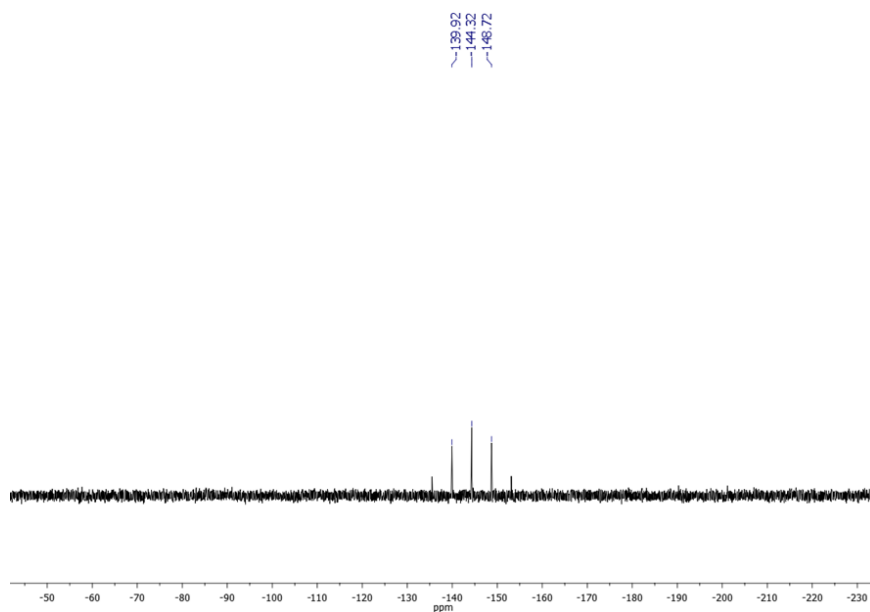
Figure S3. ^{31}P {^{1}H} NMR spectrum (162 MHz, CDCl₃) of 1-*n*-butyl-3- phenylimidazolium hexafluorophosphate.
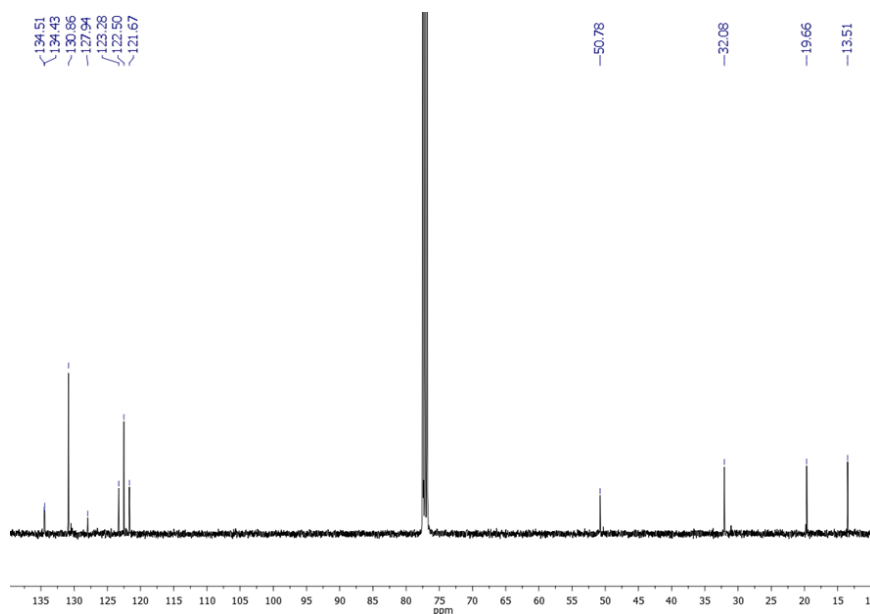
Figure S4. ^{13}C {^{1}H} NMR spectrum (100 MHz, CDCl₃) of 1-*n*-butyl-3- phenylimidazolium hexafluorophosphate.
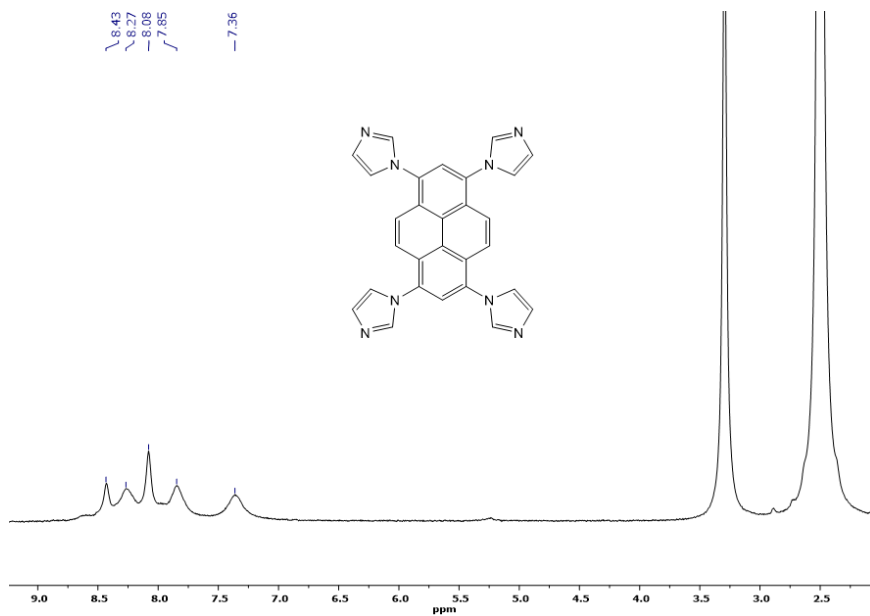
Figure S5. ^{1}H NMR spectrum (500 MHz, DMSO-d_6) of compound **1**.
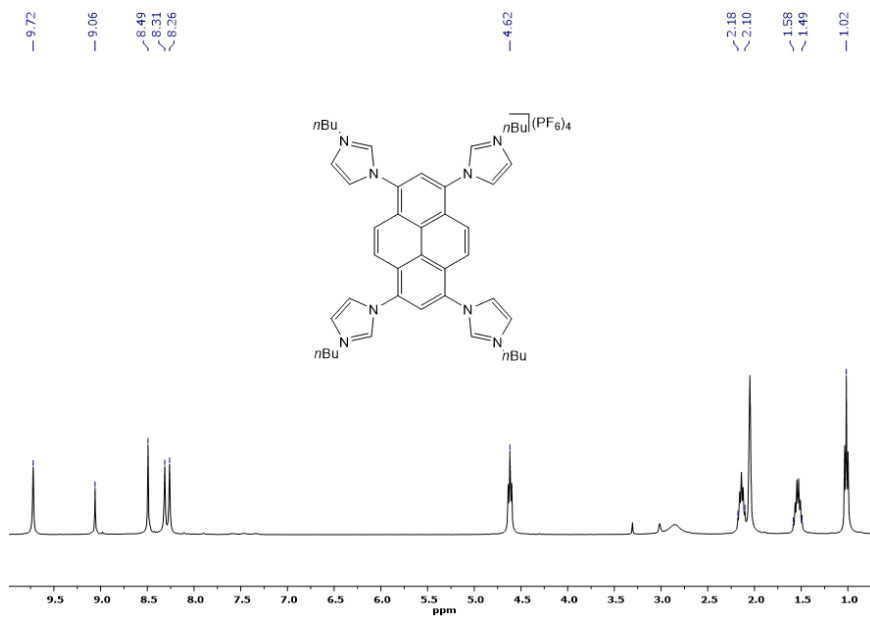
Figure S6. ^{1}H NMR spectrum (400 MHz, acetone-d_6) of **2**.
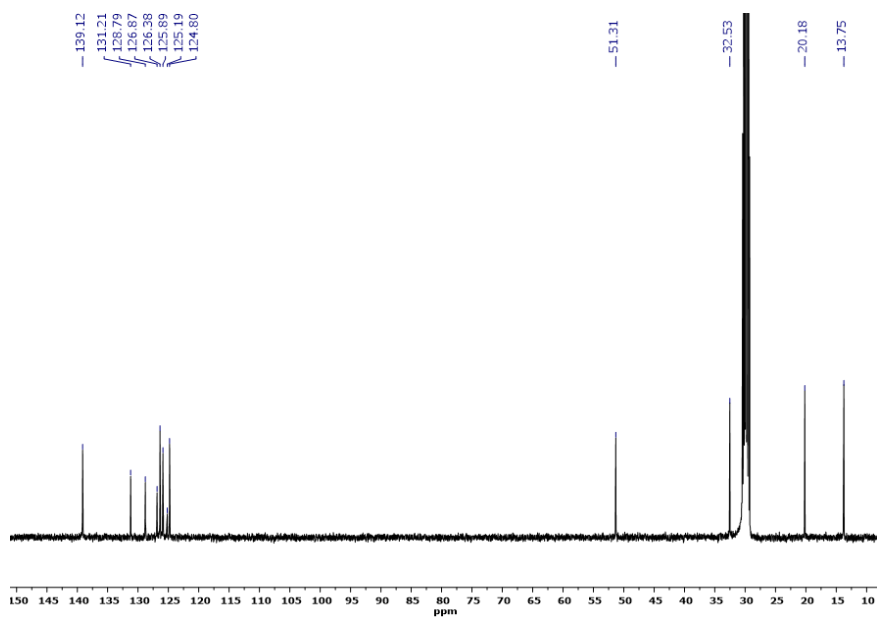
Figure S7. ^{13}C {^{1}H} NMR spectrum (100 MHz, acetone-d_6) of **2**.
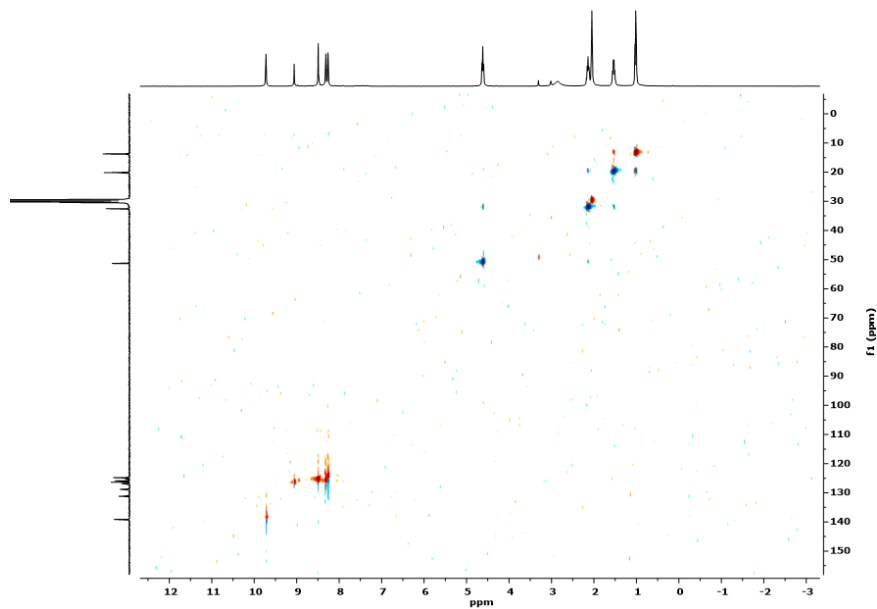
Figure S8. HSQC spectrum (100 MHz, acetone-d_6) of **2**.
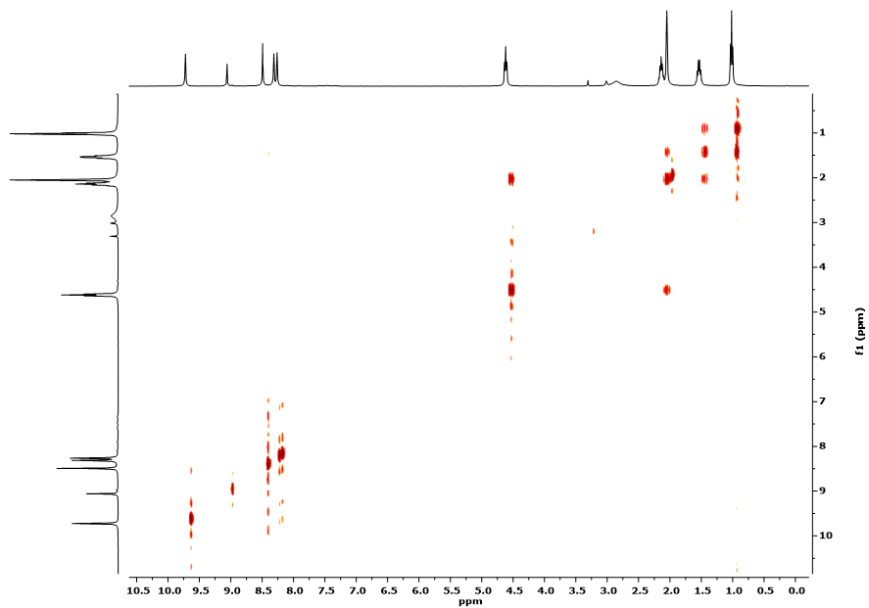
Figure S9. COSY spectrum (400 MHz, acetone-*d₆*) of **2**.
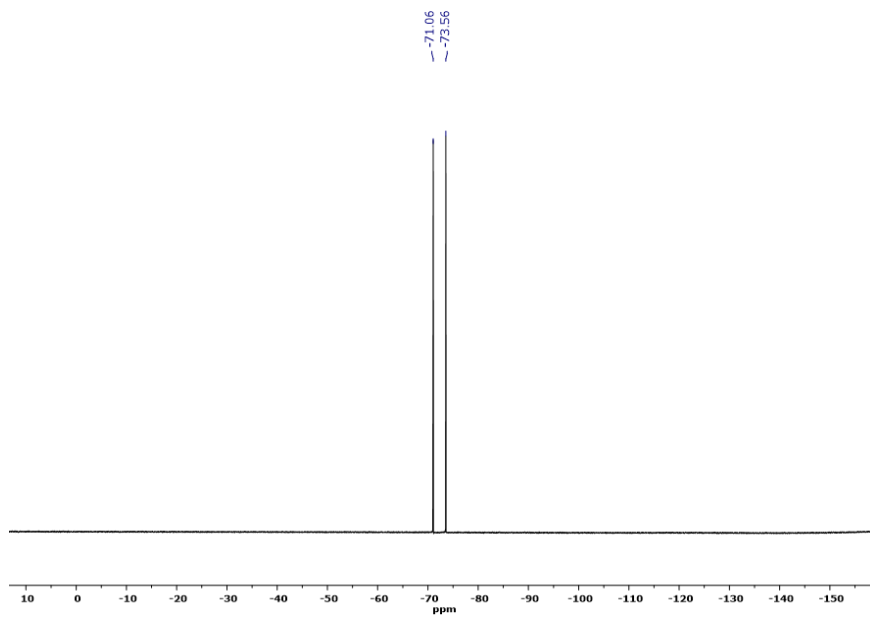
Figure S10. ¹⁹F {¹H} NMR spectrum (376 MHz, acetone-*d₆*) of **2**.
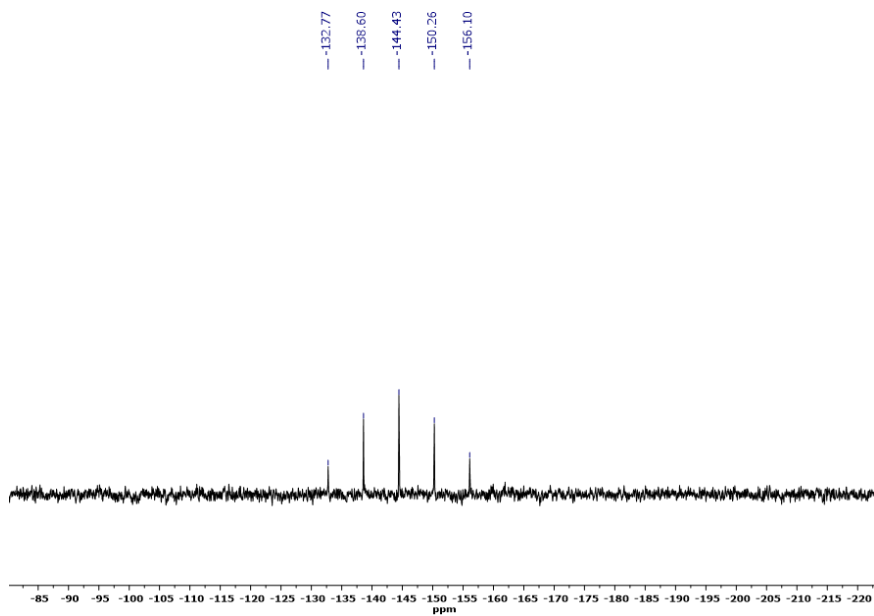
Figure S11. ^{31}P {^{1}H} NMR spectrum (162 MHz, acetone-d_6) of **2**.
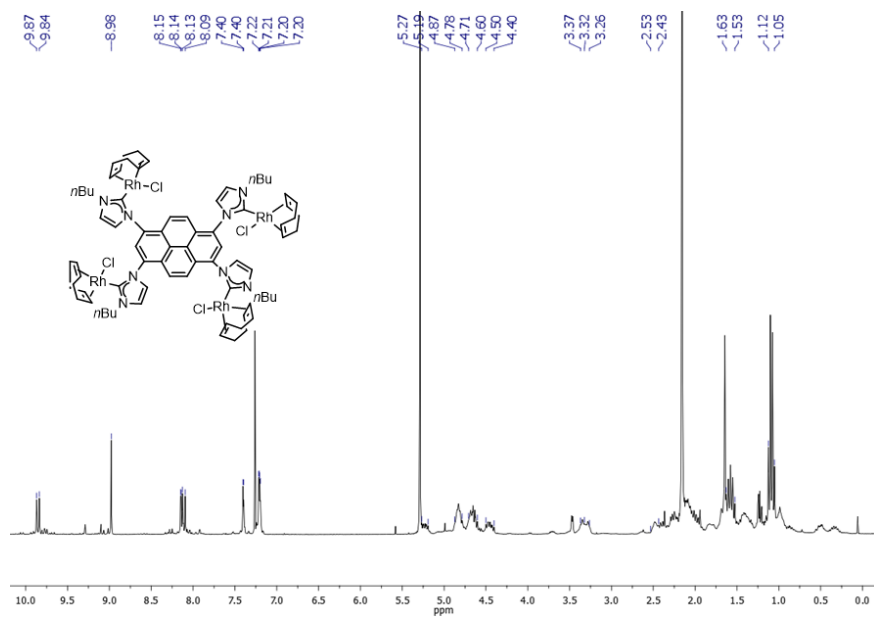
Figure S12. ^{1}H NMR spectrum (300 MHz, CDCl$_3$) of **3**.
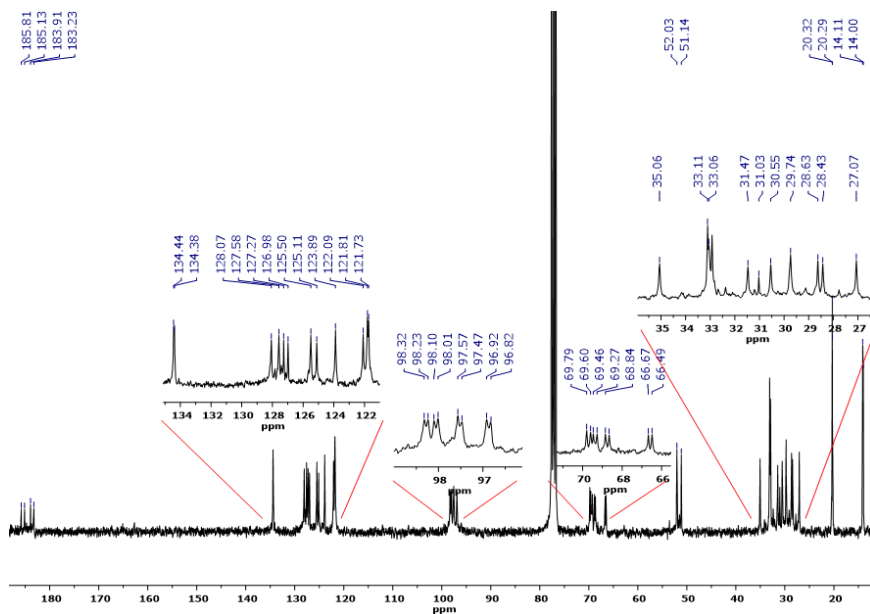
Figure S13. ^{13}C {^{1}H} NMR spectrum (75 MHz, CDCl$_3$) of **3**.
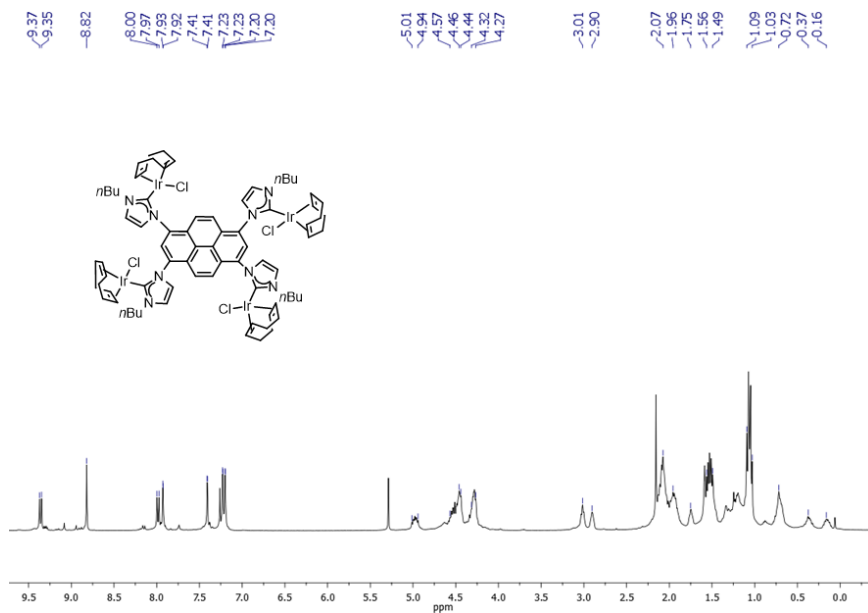
Figure S14. ^{1}H NMR spectrum (400 MHz, CDCl3) of **4**.
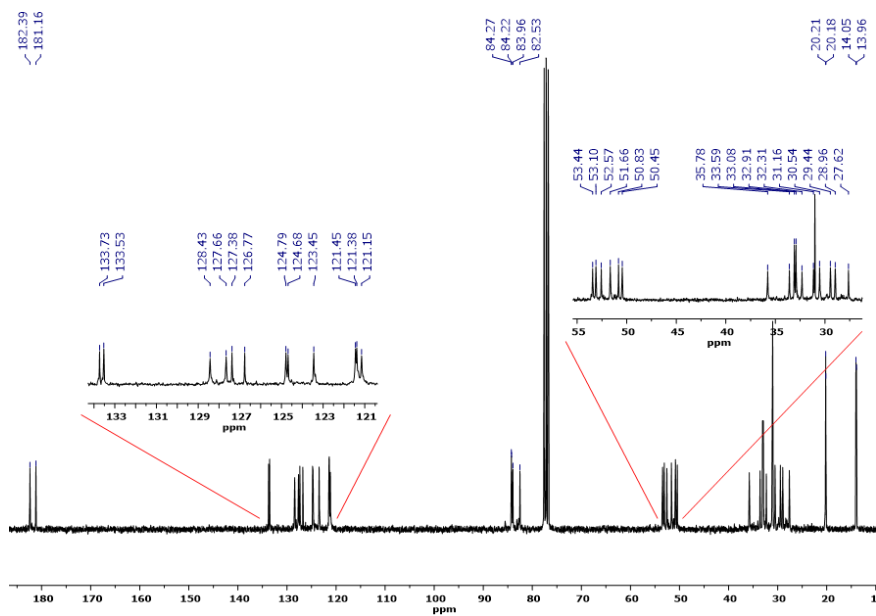
Figure S15. ^{13}C {^1H} NMR spectrum (100 MHz, CDCl$_3$) of **4**.
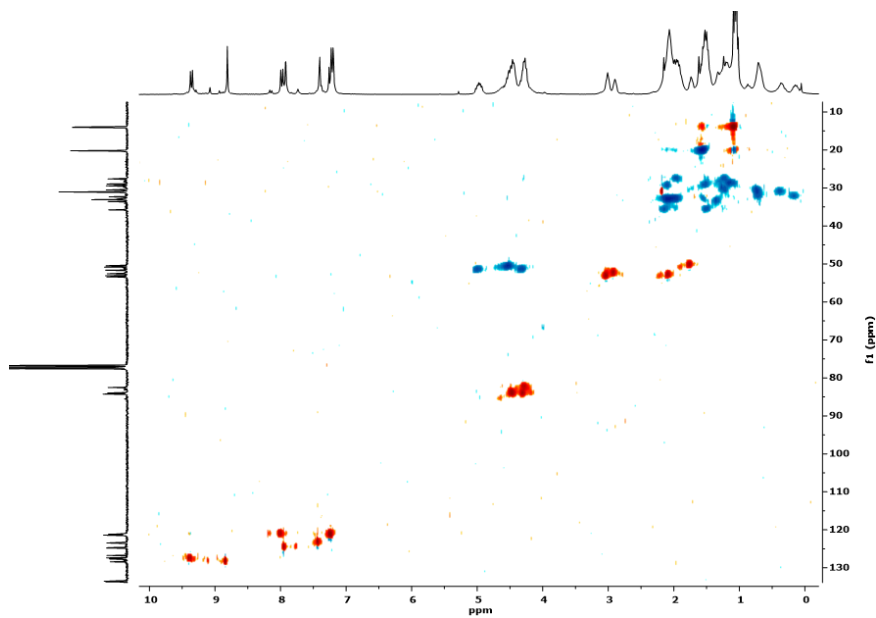
Figure S16. HSQC spectrum (75 MHz, CDCl$_3$) of **4**.
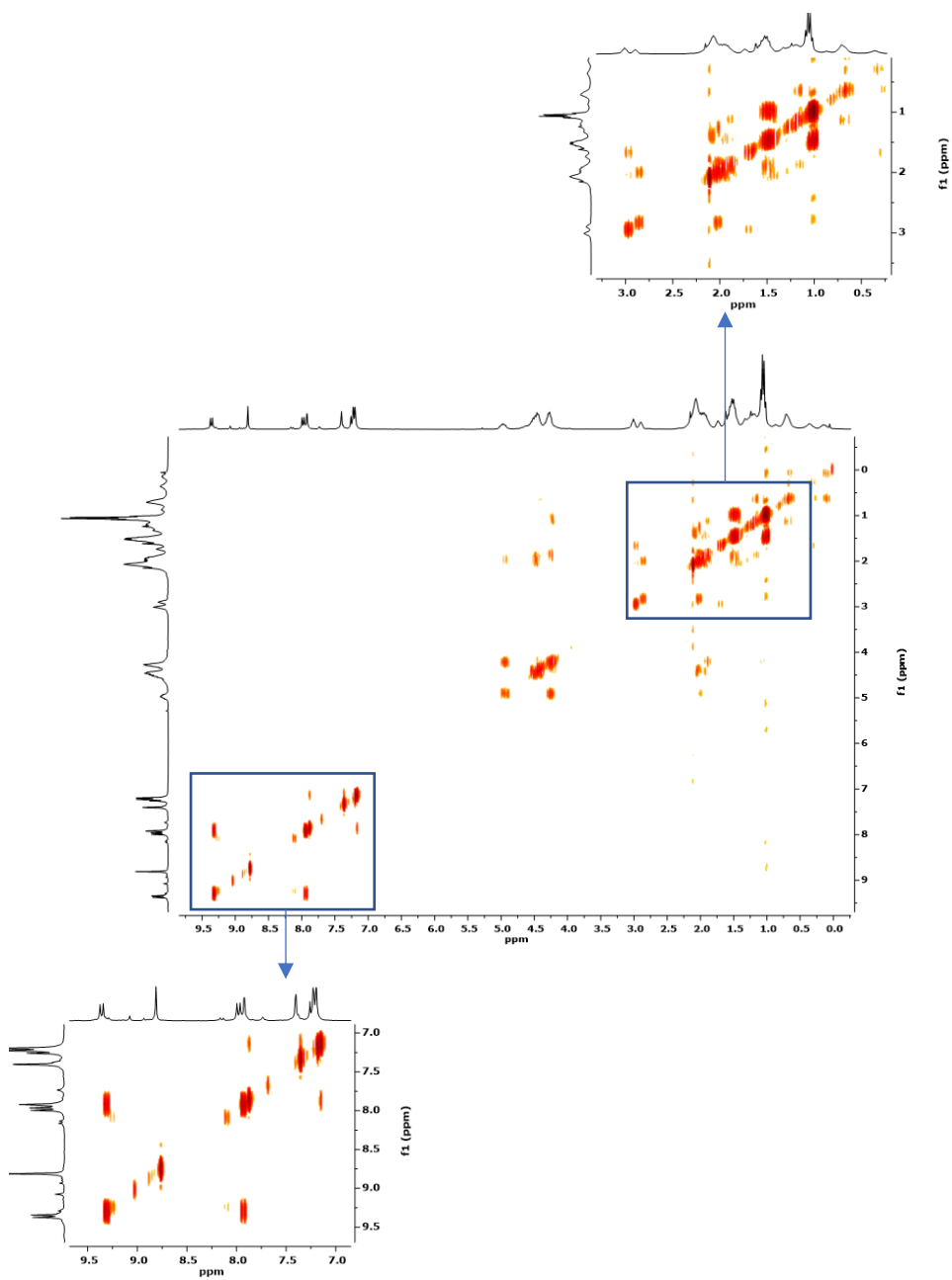
Figure S17. COSY spectrum (300 MHz, CDCl₃) of **4**.
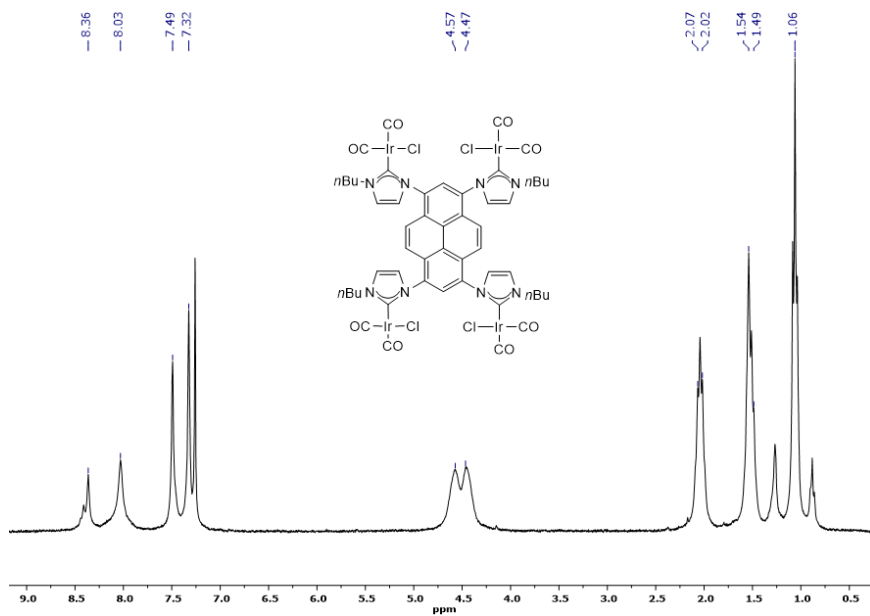
Figure S18. ^{1}H NMR spectrum (400 MHz, CDCl$_3$) of **5**.

Figure S19. ^{13}C{^{1}H} NMR spectrum (100 MHz, CDCl$_3$) of **5**.
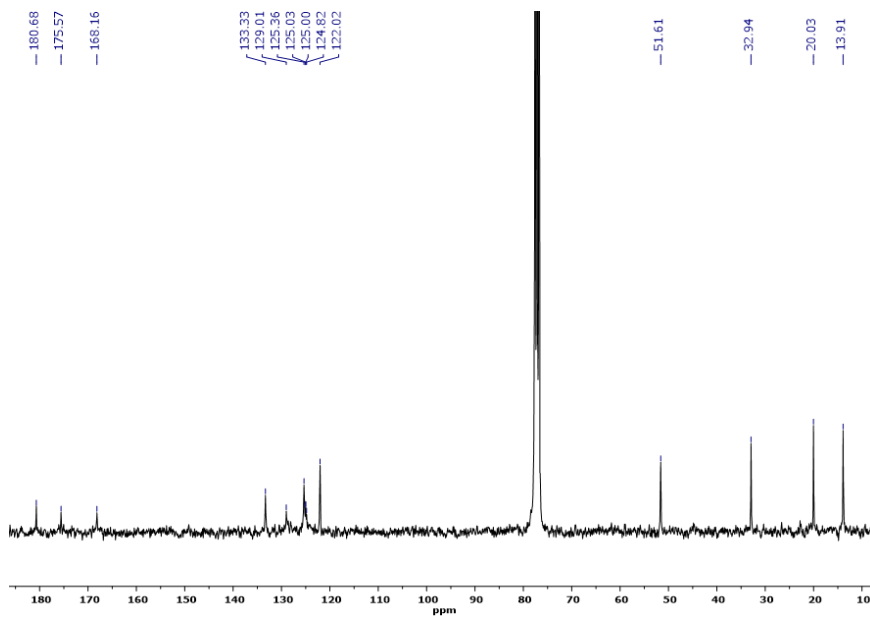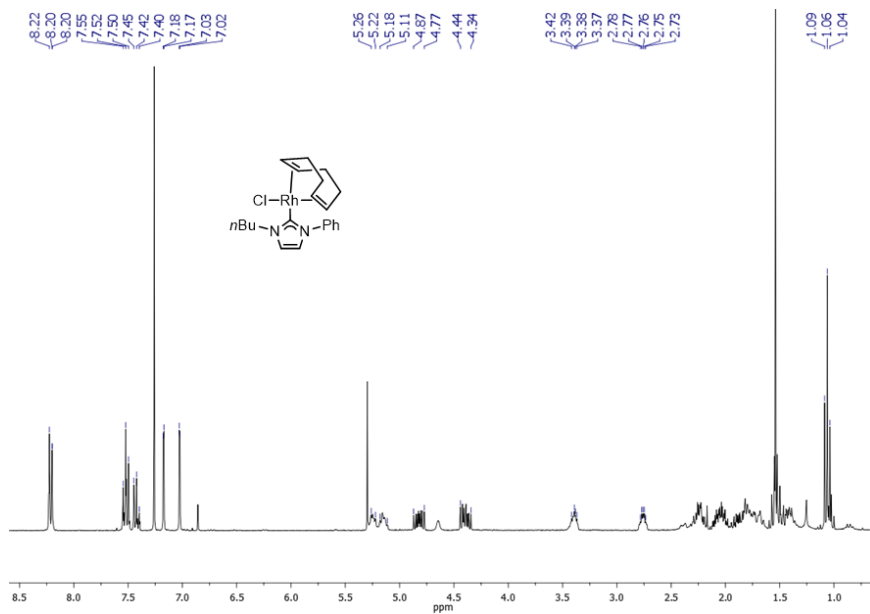
Figure S20. ^{1}H NMR spectrum (400 MHz, CDCl$_3$) of **6**.
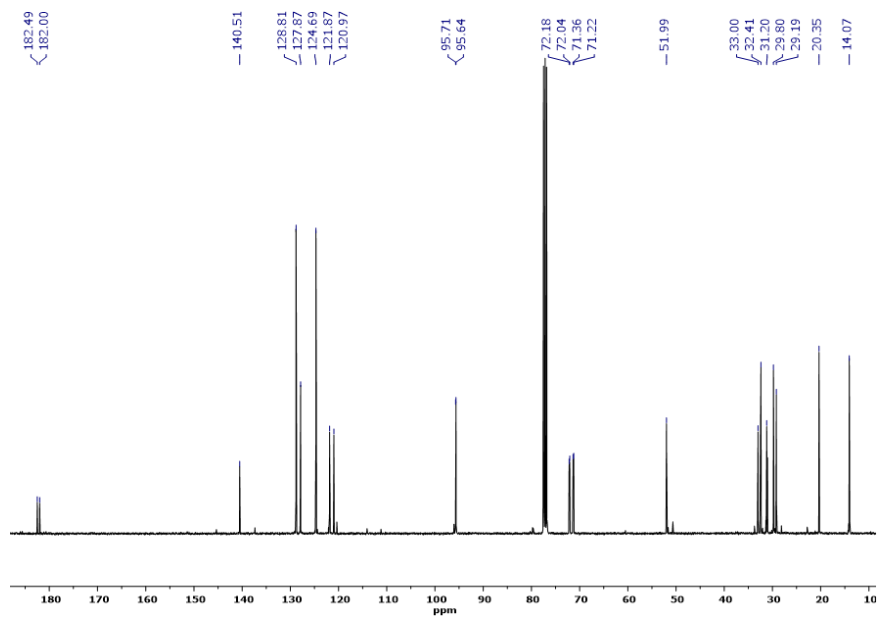
Figure S21. ^{13}C{^{1}H} NMR spectrum (100 MHz, CDCl$_3$) of **6**.
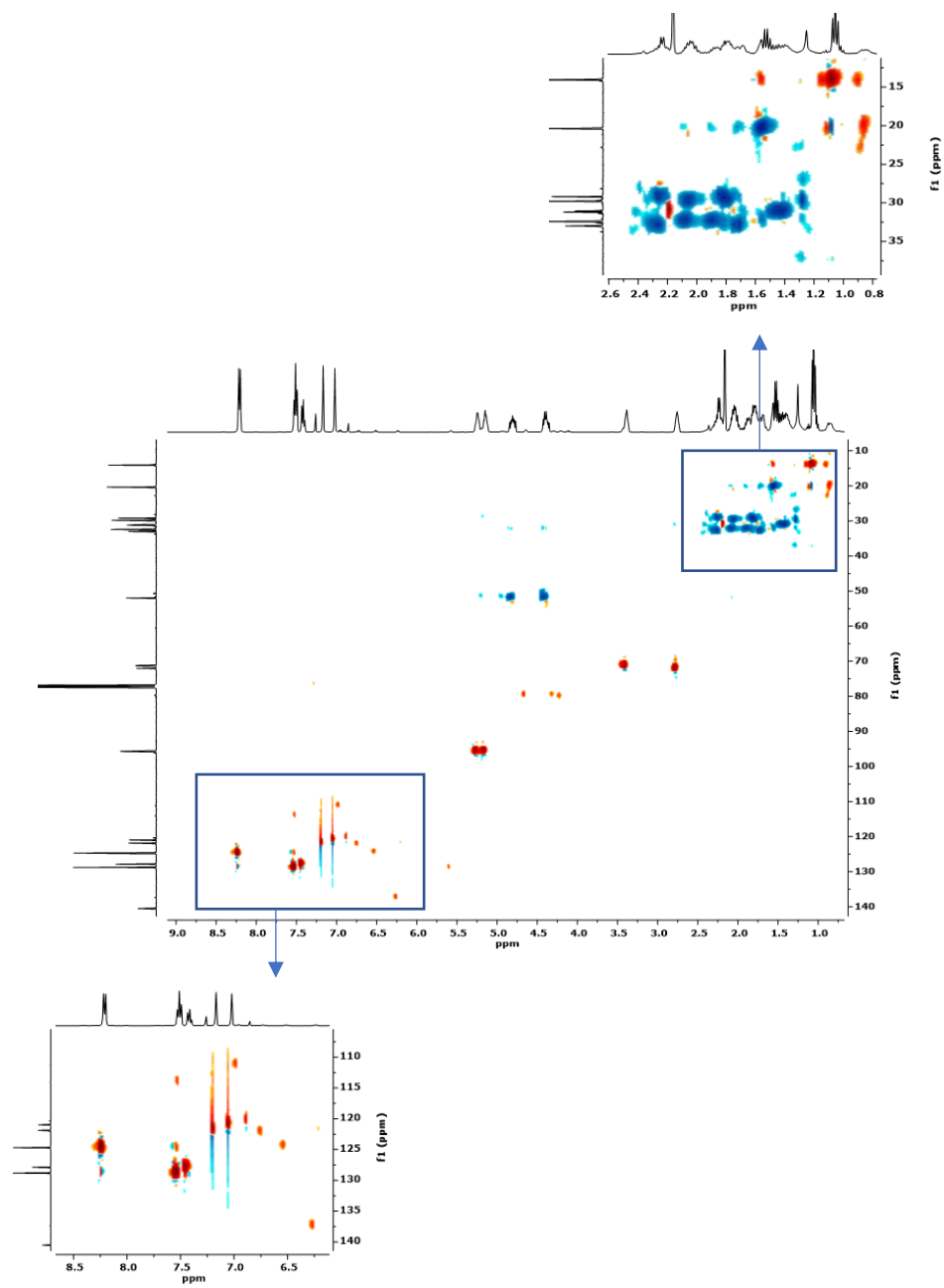
Figure S22. HSQC spectrum (100 MHz, CDCl₃) of **6**.
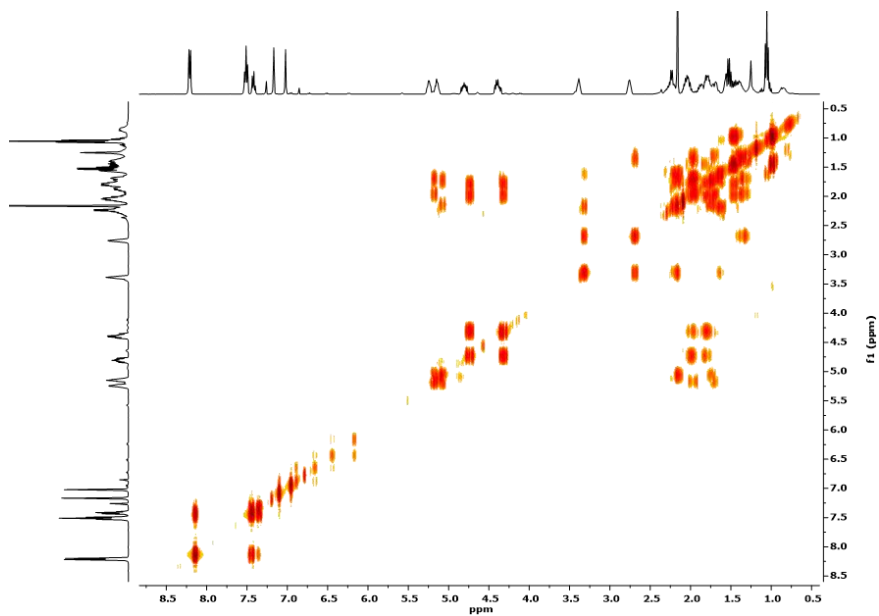
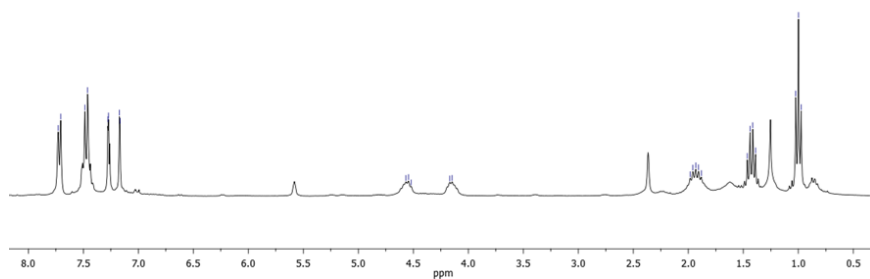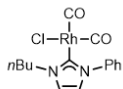**Figure S23.** COSY spectrum (400 MHz, CDCl$_3$) of **6**.

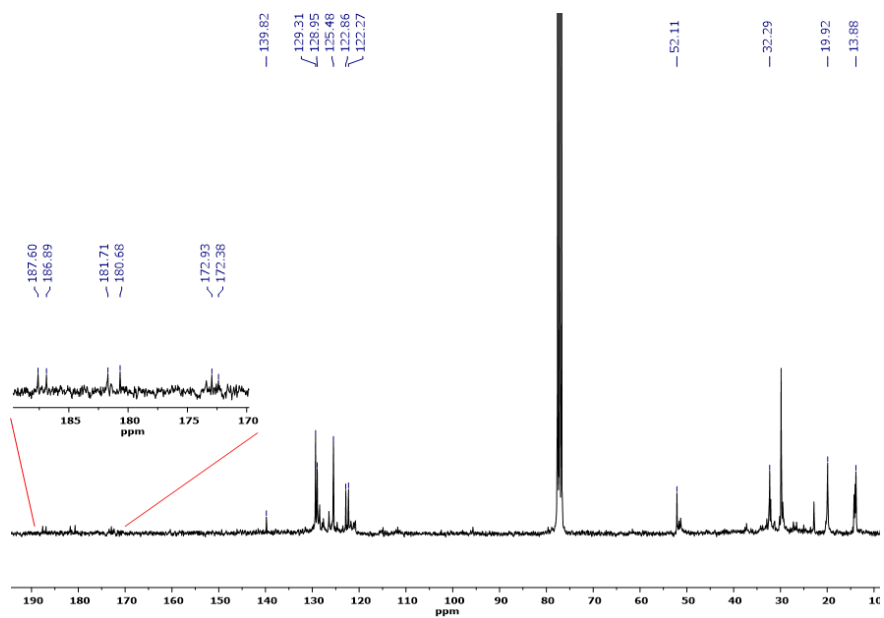**Figure S24.** ^{1}H NMR spectrum (300 MHz, CDCl$_3$) of **7**.

Figure S25. ^{13}C{^{1}H} NMR spectrum (75 MHz, CDCl$_3$) of **7**.

2. X-Ray Crystallography

X-Ray Diffraction studies for complex 4. Crystals suitable for X-Ray studies of complex **4** were obtained by slow diffusion of hexane into a concentrated solution of the complex in chloroform and dichloromethane. Diffraction data of complex **4** were collected on an Agilent SuperNova diffractometer equipped with an Atlas CCD detector using Mo-Kα radiation (λ = 0.71073 Å). Single crystals were mounted on a MicroMount® polymer tip (MiteGen) in a random orientation. Absorption corrections based on the multi-scan method were applied. Using Olex2,[1] the structure of the complex was solved using Charge Flipping in Superflip[2] and refined with ShelXL[3] refinement package using Least Squares minimization.

If we analyze the 'I/sigma vs. resolution' graph in Olex2, which defines noise as anything below the 3sigma line, it suggests that all our data above 40 degrees in 2theta is very weak, indicating that our single-crystal diffracted very poorly. Unfortunately, we were not able to grow better single crystals and to collect better data.

This problem was complicated by the fact that the data was twinned, and the data processing software would have struggled to separate intensities for possibly overlapping reflections because the intensities were very low.

Consequently, we encountered many difficulties (mainly related to disorder) when refining this structure. The structure model of complex **4** exhibits significant disorder in the lattice solvent region and in some of the *n*-butyl chains. The lattice solvent region has been treated using the PLATON SQUEEZE[4] procedure. Hydrogen atoms were introduced in calculated positions and refined on a riding model. Non-hydrogen atoms were refined anisotropically. A global, enhanced rigid bond restraint (SHELX RIGU) was applied.

Despite all the above problems and the obvious limitations of our model, we decided to include it to establish connectivity, since the composition of this

complex is supported by NMR spectroscopy, mass spectrometry and elemental analysis. Key details of the crystals and structure refinement data are summarized in Supplementary Table S1.

Further crystallographic details can be found in the CIF file, which was deposited at the Cambridge Crystallographic Data Centre, Cambridge, UK. The reference number for complex **4** was assigned as 1864607.

Table S1. Summary of crystal data, data collection, and structure refinement details of **4**

|	Complex 4
Empirical formula	$C_{77}H_{87}Cl_{6.5}Ir_4N_8$
Formula weight	2131.33
Temperature/K	293(2)
Crystal system	Monoclinic
Space group	P21/c
a/Å	42.0613(19)
b/Å	27.2586(12)
c/Å	14.5192(5)
$\alpha/°$	90
$\beta/°$	92.320(3)
$\gamma/°$	90
Volume/Å^3	16633.1(12)
Z	8
ρ_{calc}mg/mm^3	1.702
μ/mm^{-1}	6.633
F(000)	8248.0
Crystal size/mm^3	0.345 x 0.094 x 0.076
Radiation	Mo Kα (λ = 0.71073 Å)
2Θ range for data collection/°	4.96 to 46.514
Index ranges	$-46 \leq h \leq 46, 0 \leq k \leq 30, 0 \leq l \leq 16$
Reflections collected	23859
Independent reflections	23859
Data/restraints/parameters	23859/1857/1582
Goodness-of-fit on F^2	1.075
Final R indexes [I>=2σ (I)]	$R_1 = 0.1079, wR_2 = 0.2164$
Final R indexes [all data]	$R_1 = 0.1845, wR_2 = 0.2566$
Largest diff. peak/hole / e Å^{-3}	3.28/-1.91
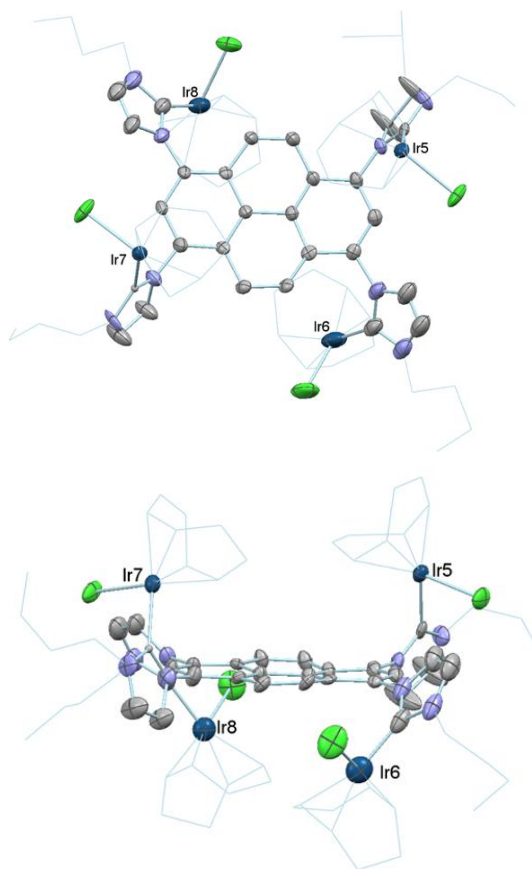
Figure S26. Different perspective views of the other enantiomer of **4**. The top view shows a right-handed conformation. Solvent (CHCl$_3$ and CH$_2$Cl$_2$) and hydrogen atoms have been removed for clarity. *n*-Butyl substituents and 1,5-cylooctadiene ligands are shown in the wireframe form. Selected distances (Å): Ir5-C5 2.14(2), Ir6-C6 1.98(3), Ir7-C7 2.11(18), Ir8-C8 2.02(3).

3. Catalytic studies: cyclization of acetylenic carboxylic acids
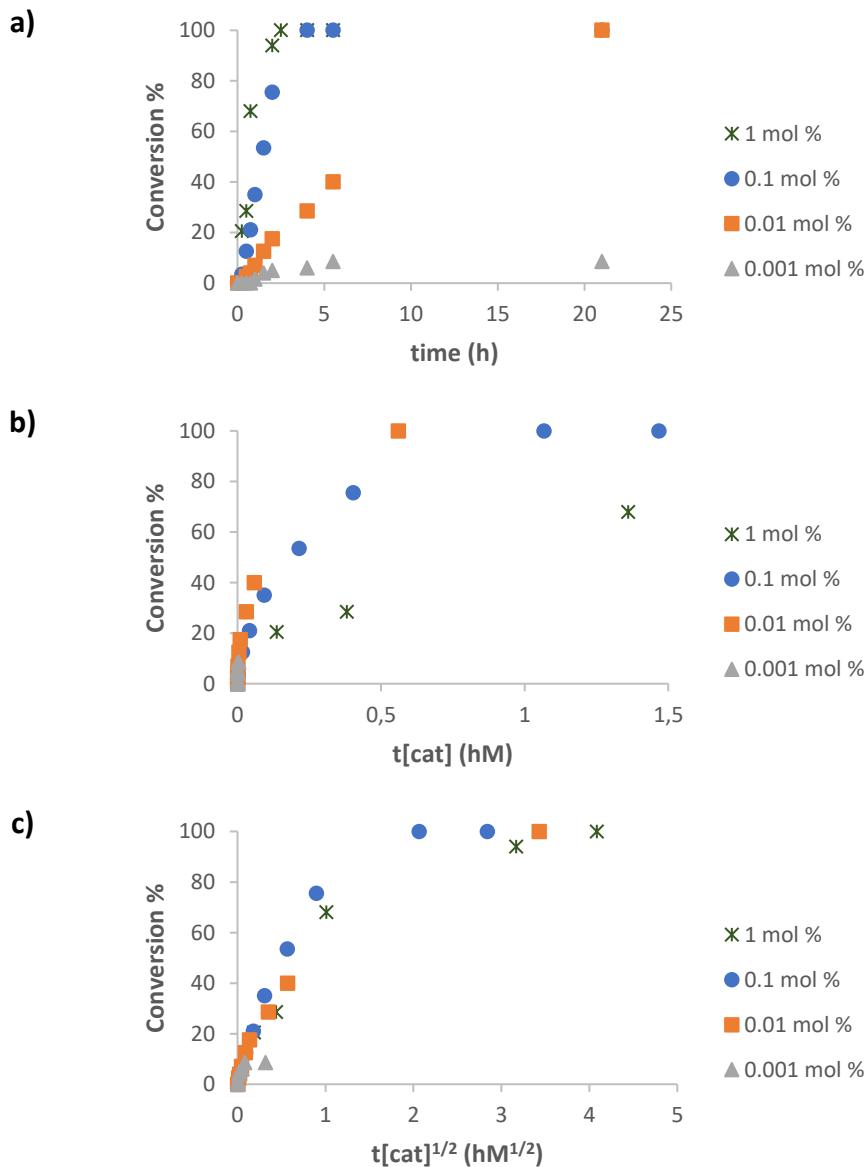
a)

b)

c)

Figure S27. (a) Time-dependent reaction profile of the cyclization reaction of 4-pentynoic acid using catalyst **4**. (b) Reaction profile with normalized time scale assuming a catalyst order of 1. (c) Reaction profile with normalized time scale assuming a catalyst order of 1/2. Reaction conditions are the same as those shown in Table 1 of the manuscript. In all three graphics the evolution is shown as consumption of 4-pentynoic acid.

4. References

1. Dolomanov, O. V.; Bourhis, L. J.; Gildea, R. J.; Howard, J. A. K.; Puschmann, H., OLEX2: a complete structure solution, refinement and analysis program. *Journal of Applied Crystallography* **2009,** *42*, 339-341.

2. Palatinus, L.; Chapuis, G., SUPERFLIP - a computer program for the solution of crystal structures by charge flipping in arbitrary dimensions. *Journal of Applied Crystallography* **2007,** *40*, 786-790.

3. Sheldrick, G. M., SHELXT - Integrated space-group and crystal-structure determination. *Acta Crystallographica a-Foundation and Advances* **2015,** *71*, 3-8.

4. Vandersluis, P.; Spek, A. L., BYPASS - AN EFFECTIVE METHOD FOR THE REFINEMENT OF CRYSTAL-STRUCTURES CONTAINING DISORDERED SOLVENT REGIONS. *Acta Crystallographica Section A* **1990,** *46*, 194-201.
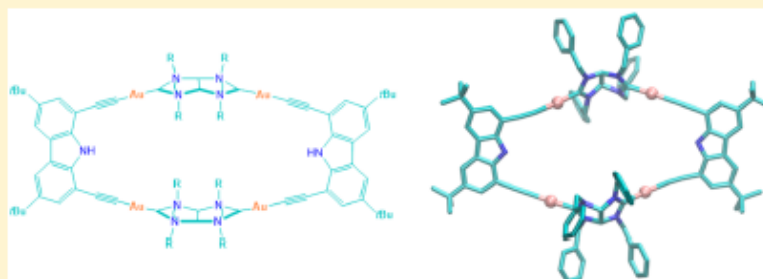
5

A Twisted Tetragold Cyclophane from a Fused Bis-Imidazolindiylidene

Ana Gutiérrez-Blanco,[†,‡] Susana Ibáñez,[‡] F. Ekkehardt Hahn,[†] Macarena Poyatos,*[,‡] and Eduardo Peris*[,‡]

[†]Institut für Anorganische und Analytische Chemie, Westfälische Wilhelms-Universität Münster, Corrensstraße 28-30, 48149 Münster, Germany

[‡]Institute of Advanced Materials (INAM), Centro de Innovación en Química Avanzada (ORFEO−CINQA), Universitat Jaume I, Avda. Vicente Sos Baynat s/n, Castellón E-12071, Spain

⑤ *Supporting Information*

ABSTRACT: The reaction between an angular bis-imidazolidinium salt and [AuCl(SMe)$_2$] allowed the preparation of a discrete digold complex, with a rigid angular bridging bis-imidazolindiylidene ligand. This complex reacts with a diethynylcarbazole to afford a tetragold cyclophane that contains two bis-imidazolindiylidenes and two carbazolyl-diethynyl ligands. Both the dimetallic and the tetrametallic complexes have been characterized by spectroscopic techniques and by single-crystal X-ray diffraction. Due to the geometric constraints of the ligands, the cyclophane deviates from the expected planarity and shows a twisted structure. The work demonstrates that the rigid angular di-NHC ligand is a suitable scaffold for the reliable construction of organometallic-based metallosupramolecular assemblies.

Coordination-driven self-assembly constitutes an effective tool for the rational design of discrete supramolecular coordination compounds (SCCs),[1] ranging from two-dimensional (2-D) polygons to three-dimensional (3-D) polyhedra. The transformation of the different modular building blocks into predesigned assemblies takes advantage of the predictable nature of the metal−ligand coordination sphere and ligand lability to encode directionality. The construction of the supramolecular architectures requires that the complementary building blocks must be structurally rigid with predefined angles, because the symmetry of the individual building units and the overall shape of the resulting assembly are the most important factors to be considered in the design of discrete metallosupramolecular assemblies. From a design perspective, the ligand is arguably considered as the most important block, because its topological features and binding abilities determine the geometry, size, and functionality of the resulting assemblies. It should be mentioned that this field of research is strongly dominated by Werner-type ligands, although in recent years the use of carbon-donor ligands is gaining popularity,[2] probably as a consequence of the structural

diversity that can be achieved by the plethora of poly-N-heterocyclic carbene ligands that can now be found in the literature.[3]

During the last three years, we contributed to the field of organometallic supramolecular chemistry by preparing a series of NHC-based assemblies that we used as hosts for the recognition of organic and inorganic guests. For the design of these supramolecular assemblies, we took advantage of our experience in preparing rigid planar poly-NHC ligands with polyaromatic linkers, which we found particularly useful for the preparation of molecular squares,[4] rectangles,[5] and trigonal prisms.[6] In the course of our most recent research, we also prepared a series of Au-based metallotweezers by using rigid bis-alkynyl connectors combined with a pyrene-imidazolylidene ligand. These metallotweezers were used for the recognition of "naked" metal cations[7] and polycyclic aromatic hydrocarbons.[8] A feature that captured our attention is that, despite its apparent rigidity, the use of a carbazolyl-bis-alkynyl

A Twisted Tetragold Cyclophane from a Fused Bis-Imidazolindiylidene

Ana Gutiérrez-Blanco,[a,b] Susana Ibáñez,[a] F. Ekkehardt Hahn,[b] Macarena Poyatos,[a,*] and Eduardo Peris[a,*]

[a] *Institute of Advanced Materials (INAM). Universitat Jaume I, Av. Vicente Sos Baynat s/n, E-12071 Castellón, Spain*

[b] *Institut für Anorganische und Analytische Chemie, Westfalische Wilhelms-Universität Münster, Corrensstraße 28-30, 48149 Münster, Germany*

Email: poyatosd@uji.es, eperis@uji.es

Abstract

The reaction between an angular bis-imidazolidinium salt and [AuCl(SMe₂)] allowed the preparation of a discrete digold complex, with a rigid angular bridging bis-imidazolindiylidene ligand. This complex reacts with a diethynylcarbazole to afford a tetragold cyclophane that contains two bis-imidazolindiylidenes and two carbazolyl-diethynyl ligands. Both the dimetallic and the tetrametallic complexes have been characterized by spectroscopic techniques and by single-crystal X-ray diffraction. Due to the geometric constraints of the ligands, the cyclophane deviates from the expected planarity and shows a twisted structure. The work demonstrates that the rigid angular di-NHC ligand is a suitable scaffold for the reliable construction of organometallic-based metallosupramolecular assemblies.

1. Introduction

Coordination-driven self-assembly constitutes an effective tool for the rational design of discrete supramolecular coordination compounds (SCCs),[1] ranging from two-dimensional (2D) polygons to three-dimensional (3D) polyhedra. The transformation of the different modular building blocks into predesigned assemblies takes advantage of the predictable nature of the metal–ligand coordination sphere and ligand lability to encode directionality. The construction of the supramolecular architectures requires that the complementary building blocks must be structurally rigid with predefined angles, because the symmetry of the individual building units and the overall shape of the resulting assembly are the most important factors to be considered in the design of discrete metallosupramolecular assemblies. From a design perspective, the ligand is arguably considered as the most important block, because its topological features and binding abilities determine the geometry, size, and functionality of the resulting assemblies. It should be mentioned that this field of research is strongly dominated by Werner-type ligands, although in recent years the use of carbon-donor ligands is gaining popularity,[2] probably as a consequence of the structural diversity that can be achieved by the plethora of poly-N-heterocyclic carbene ligands that can now be found in the literature.[3]

During the last three years, we contributed to the field of organometallic supramolecular chemistry by preparing a series of NHC-based assemblies that we used as hosts for the recognition of organic and inorganic guests. For the design of these supramolecular assemblies, we took advantage of our experience in preparing rigid planar poly-NHC ligands with polyaromatic linkers, which we found particularly useful for the preparation of molecular squares,[4] rectangles,[5] and trigonal prisms.[6] In the course of our most recent research, we also prepared a series of Au-based metallotweezers by using rigid bis-alkynyl connectors combined with a pyrene-imidazolylidene ligand. These metallotweezers were

used for the recognition of "naked" metal cations[7] and polycyclic aromatic hydrocarbons.[8] A feature that captured our attention is that, despite its apparent rigidity, the use of a carbazolyl-bis-alkynyl linker could provide structures in which the angle defined by the two alkynyl–Au axes could vary between 30.2° for the open metallotweezer **A** (Figure 1) and 23.9° for the closed trigonal-prismatic structure **B** (Figure 1).
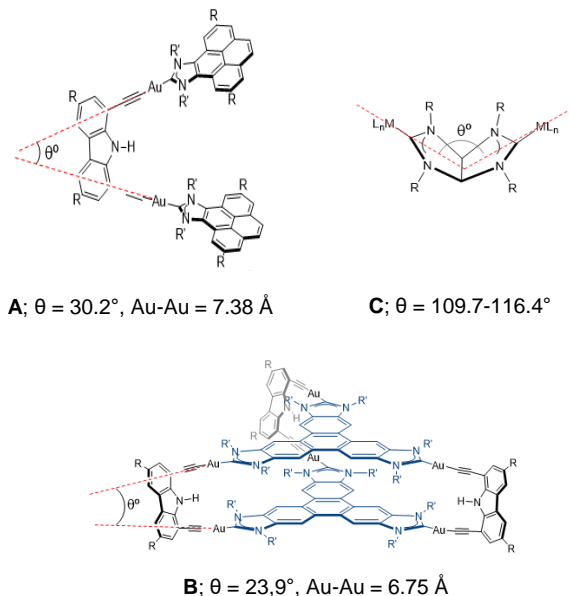
A; θ = 30.2°, Au-Au = 7.38 Å   **C**; θ = 109.7-116.4°

B; θ = 23,9°, Au-Au = 6.75 Å

Figure 1. Flexibility shown by the coordination angle (θ) of a carbazolyl-bis-alkynyl ligand in supramolecular coordination compounds (**A** and **B**) and a bis-imidazolindiylidene-based complex (**C**).

This rendered Au–Au distances between the gold centers bound to the bis-alkynyl ligand ranging from 6.75 to 7.38 Å. The flexibility of this apparently rigid connector made us think that the carbazolyl-bis-alkynyl unit could be used as a versatile and adaptable building block for the construction of supramolecular structures combined with other rigid, yet not planar, di-NHC ligands. Rigid angular di-NHC ligands are rare, but some years ago we described a bis-imidazolindiylidene ligand (in complex **C**) that was coordinated to rhodium and iridium[9] and then to palladium.[10] Depending on the steric congestion brought

about the metal coordination sphere, the angle between the planes of the two fused NHC rings could vary in the range of 109.7–116.4°.

2.   Results and discussion

On the basis of these previous findings, we now report the preparation of a bis-imidazolindiylidene complex of digold(I), which we used as a building unit for the preparation of a cyclic assembly in combination with a carbazolyl-bis-alkynyl ligand. The formation of a "twisted" metallocyclophane reveals unusual features that will be discussed in detail.

The reaction of the bis-imidazolidinium salt **1** with [AuCl(SMe$_2$)] in THF in the presence of potassium bis(trimethylsilyl)amide (KHMDS) afforded a bis-imidazolindiylidene complex of digold(I) (**2**) in 69 % yield after purification (Scheme 1).
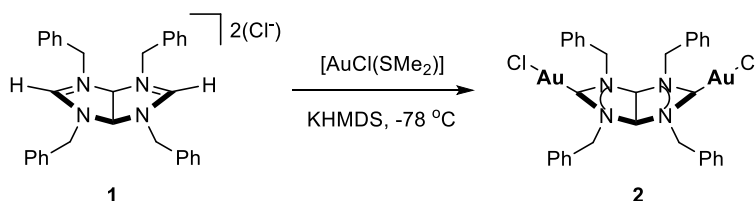
Scheme 1. Preparation of the digold(I) complex **2**.

Both the ^{1}H and the ^{13}C NMR spectra of the complex are consistent with the 2-fold symmetry of its structure. The ^{13}C NMR spectrum displays distinctive resonances due to the carbene carbon atoms at 198.40 ppm.

The molecular structure of complex **2** was determined by means of single-crystal X-ray diffraction studies (Figure 2). The structure confirms that the tetracyclic bis-NHC ligand is bridging the two gold atoms, which complete their linear coordination sphere with a chloro ligand. The coordination about the Au atoms is quasi-linear, with an average Cl–Au–C angle of 178.05°. The average distance of the Au–C bond is 1.994 Å. The through-space distance between the two gold atoms is 7.362 Å. The angular nature of the rigid fused bis-NHC ligand is reflected

by the angle formed by the two Cl–Au–C axes, 126.7°, which is significantly larger than the largest angle reported for this type of ligand so far (116.4°).[9]
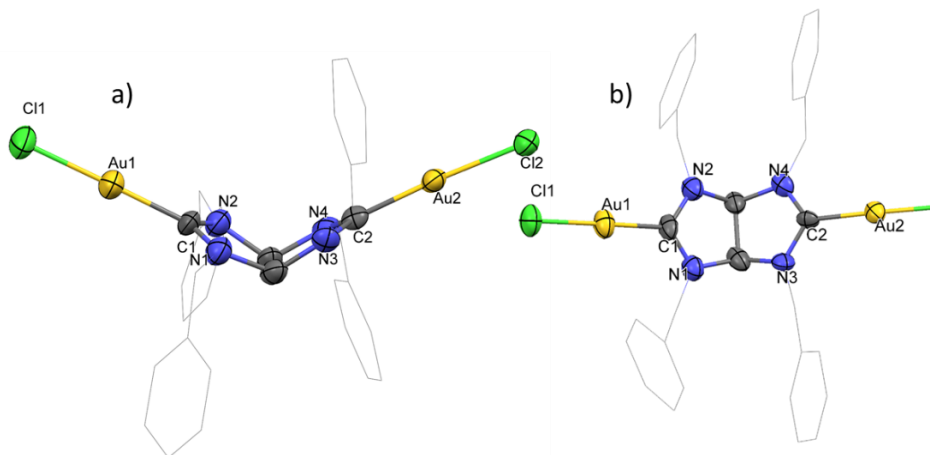

Figure 2. Two perspectives of the molecular structure (50% displacement ellipsoids) of complex **2**. Hydrogen atoms and solvent (CH_2Cl_2) have been omitted for clarity. The benzyl groups are shown in wireframe form. Selected bond distances (Å) and angles (deg): Au1–C1 1.997(15), Au1–Cl1 2.268(4), Au2–C2 1.991(16), Au2– Cl2 2.89(4), Cl1–Au1–C1 179.2(5), Cl2–Au2–C2 176.9(4).

Once complex **2** was structurally characterized, we decided to study its potential use as a building unit for the construction of a metallocyclophane by reaction with a carbazolyl-bis-alkynyl ligand. By following simple geometry rules, we were aware that the angle of 126.7° provided by the structure of **2** should need a building block with an angle of about 53° to facilitate the construction of a simple rhombohedral two-dimensional structure. However, this angle is far from the maximum angle that we have observed for the coordination of the carbazolyl-bis-alkynyl unit in our previously published structures. Therefore, it is expected that the target cyclophane, if formed, should render a structure in which either the angles of the building units significantly deviate from those shown in our previous structures or the structure deviates from a simple 2-D architecture.

The tetragold(I) cyclophane **3** was obtained by deprotonating 3,6-di-*tert*-butyl-1,8-diethynyl-9H-carbazole with sodium hydroxide in MeOH, followed by addition of the bis-imidazolindiylidene complex of digold(I), **2** (Scheme 2). After

purification, compound **3** was obtained as a yellow solid in 62 % yield. The new complex was characterized by NMR spectroscopy, mass spectrometry, and elemental analysis. The ^{13}C NMR spectrum shows a signal due to the four magnetically equivalent carbene carbon atoms at 189.92 ppm.
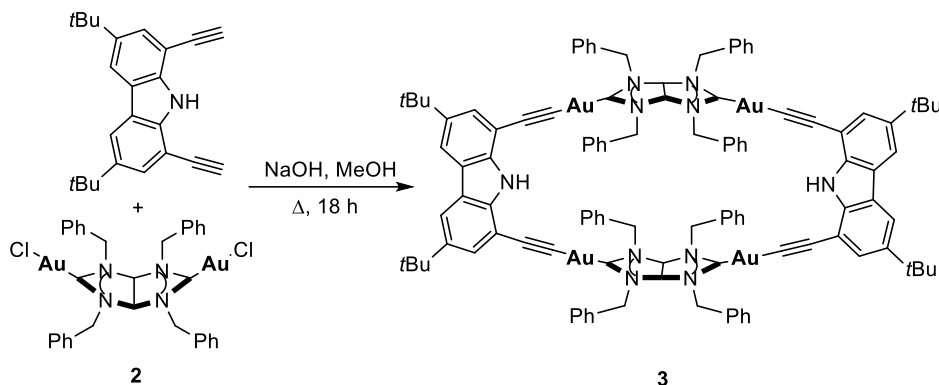
Scheme 2. Preparation of the metallocyclophane **3**.

The diffusion-ordered NMR spectrum (DOSY) showed that all proton resonances display the same diffusion coefficient in CDCl$_3$ (4.5×10^{-10} m^2 s^{-1}, see the Figure S8 of the Supporting Information for details), indicating the presence of a single assembly. By using the Stokes–Einstein equation, this coefficient provides an average hydrodynamic radius of 8.9 Å.

The molecular structure of **3** was confirmed by single-crystal X-ray diffraction studies (Figure 3). The C$_{2h}$-symmetric structure contains four gold atoms, bridged by two bis-imidazolindiylidene ligands and two carbazolyl-diethynyl ligands. This nanosized molecule measures 24.4 Å, calculated from the distance between the quaternary carbons of the *tert*-butyl groups of opposite carbazolyl-diethynyl ligands. The average distance of the Au–C$_{carbene}$ bonds is 2.025 Å, thus slightly longer than the Au–C$_{carbene}$ distance in **2**, likely due to the strong trans influence generated by the Au–C$_{C≡C}$ bond. The distance between the gold atoms bound by the same bis-NHC ligand is 7.491 Å, and the distance between the gold atoms bound by the same carbazolyl-diethynyl ligand is 7.757 Å; therefore, the four

gold centers constitute the corners of an almost regular square, with all four gold atoms in the same plane.
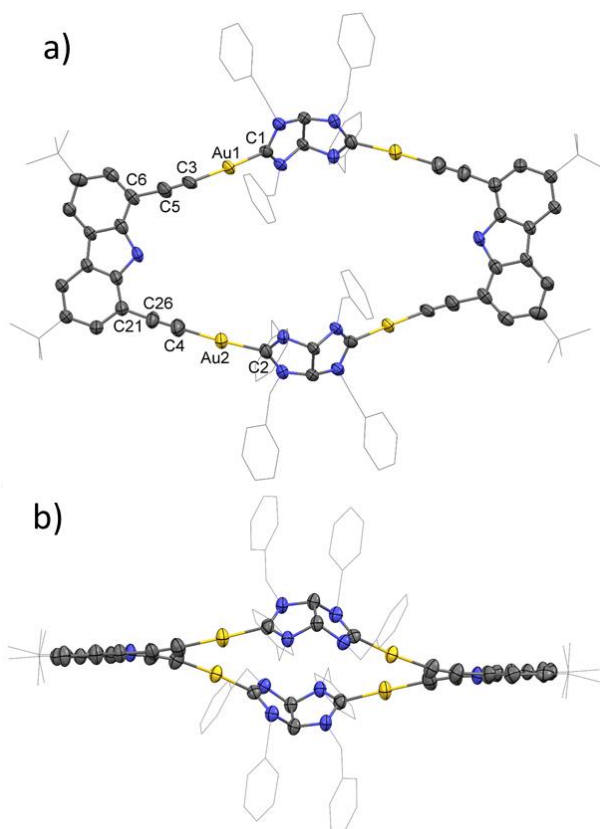

Figure 3. Two perspectives of the molecular structure (50% displacement ellipsoids) of complex **3**. Hydrogen atoms and solvent (CHCl$_3$) have been omitted for clarity. Benzyl and *tert*-butyl groups are shown in wireframe form. Selected bond distances (Å) and angles (deg): Au1–C1 2.020(13), Au1–C3 1.994(15), Au2–C2 2.029(13), Au2–C4 2.013(16), C3–Au1–C1 174.7(6), C4–Au2–C2 176.0(6).

The angle established between the $C_{C\equiv C}$–Au–$C_{carbene}$ axes that diverge from the bis-NHC ligand is 128.6°, slightly larger than the angle found for the open structure of **2**. The angle formed by the two Au–C≡C axes that converge at the carbazolyl moiety is 32.9°, again larger than the largest angle found for the binding of other related complexes with this carbazolyl-dialkynyl ligand (the largest angle found is 30.2°, as shown in Figure 1). These parameters reflect that the structure is geometrically constrained. The side-on view of the structure

(Figure 3b) shows that the four gold centers and the two di-NHC ligands are out of the plane formed by the two carbazolyl moieties, thus rendering a twisted structure that deviates from a simple 2D structure, as we previously predicted. This deviation is well reflected by the Au2−C21−C6−Au1 torsion angle of 20°. The determination of this molecular structure also allows determining the volume of the internal cavity formed inside the cyclophane structure of **3**. This volume is 115 Å^3, as can be observed from the volume diagrams shown in Figure 4.

Internal accesible volumen = 115 Å^3
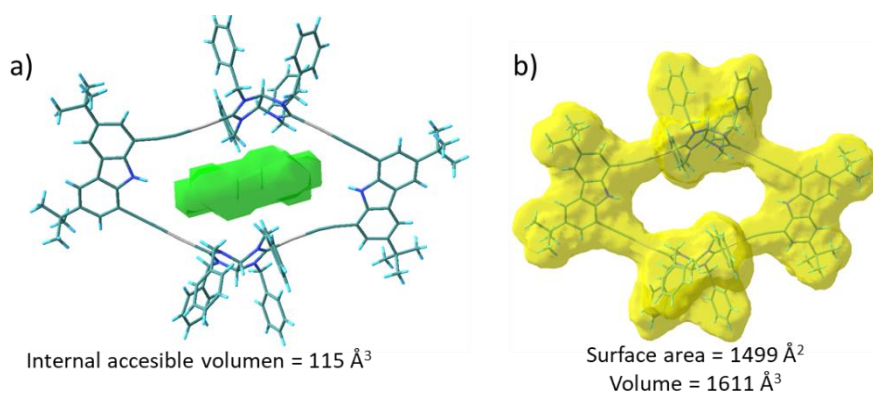
Surface area = 1499 Å^2
Volume = 1611 Å^3

Figure 4. Internal accessible volume (a) and effective surface and volume (b) of **3**. The estimation of volume was made using the swisspdb software, available at http://www.expasy.org/spdbv/.[11]

We also obtained the UV−vis and emission spectra of **3**. The emission spectrum of **3** (Figure S10 in the Supporting Information) shows two short-lived broad featureless bands at 400 and 575 nm. The fluorescence quantum yield is low (ϕ = 0.027). The longest wavelength can be attributed to the arylacetylide ligand, with participation of the Au(I) atom in the population of the triplet state.[12] The higher energy band is coincident with the monomer emission of 3,6-di-*tert*-butyl-1,8-diethynyl-9H-carbazole.[13]

Finally, we performed preliminary experiments in order to test if the gold-based cyclophane could be used as a supramolecular receptor for organic substrates bearing hydrogen bonding functionalities that could interact with the protic N−H

group of the carbazole units. Unfortunately, these experiments failed, most likely due to the lack of other effective receptor sites at the molecule.

3. Conclusions

In summary, we described the preparation of a new tetra-Au-based cyclophane using an angular bis-imidazolindiylidene ligand. The use of this rigid angular di-NHC ligand constitutes a reliable approach to new organometallic-based metallosupramolecular structures, not accessible with other known poly-NHC ligands. Although our new gold-based cyclophane did not behave as an effective supramolecular receptor in its present form, we are convinced that the synthetic procedure described and the use of our digold hinge-shaped building block have the potential to be used for the preparation of further assemblies that incorporate polyaromatic panels and other effective receptor sites, which will easily produce receptors with interesting host–guest chemistry properties. Research in this direction is underway in our laboratories.

Acknowledgments

References

1.   (a) Cook, T. R.; Stang, P. J., *Chem. Rev.* **2015,** *115* (15), 7001-7045; (b) Cook, T. R.; Zheng, Y. R.; Stang, P. J., *Chem. Rev.* **2013,** *113* (1), 734-777; (c) Gianneschi, N. C.; Masar, M. S.; Mirkin, C. A., *Acc. Chem. Res.* **2005,** *38* (11), 825-837; (d) Caulder, D. L.; Raymond, K. N., *Acc. Chem. Res.* **1999,** *32* (11), 975-982; (e) Chakrabarty, R.; Mukherjee, P. S.; Stang, P. J., *Chem. Rev.* **2011,** *111* (11), 6810-6918; (f) Castilla, A. M.; Ramsay, W. J.; Nitschke, J. R., *Acc. Chem. Res.* **2014,** *47* (7), 2063-2073; (g) McConnell, A. J.; Wood, C. S.; Neelakandan, P. P.; Nitschke, J. R., *Chem. Rev.* **2015,** *115* (15), 7729-7793; (h) Fujita, M.; Ogura, K., *Coord. Chem. Rev.* **1996,** *148*, 249-264; (i) Fujita, M., *Chem. Soc. Rev.* **1998,** *27* (6), 417-425; (j) Han, M.; Engelhard, D. M.; Clever, G. H., *Chem. Soc. Rev.* **2014,** *43* (6), 1848-1860; (k) Sun, Y.; Chen, C.; Stang, P. J., *Acc. Chem. Res.* **2019,** *52* (3), 802-817; (l) Saha, S.; Regeni, I.; Clever, G. H., *Coord. Chem. Rev.* **2018,** *374*, 1-14; (m) Constable, E. C., *Coord. Chem. Rev.* **2008,** *252* (8-9), 842-855.

2.   (a) Han, Y.-F.; Jin, G.-X., *Chem. Soc. Rev.* **2014,** *43* (8), 2799-2823; (b) Gan, M.-M.; Liu, J.-Q.; Zhan, L.; Wang, Y.-Y.; Hahn, F. E.; Han, Y.-F., *Chem. Rev.* **2018,** *118* (19), 9587-9641; (c) Sinha, N.; Hahn, F. E., *Acc. Chem. Res.* **2017,** *50* (9), 2167-2184; (d) Jahnke, M. C.; Hahn, F. E., *Coord. Chem. Rev.* **2015,** *293*, 95-115.

3.   (a) Poyatos, M.; Mata, J. A.; Peris, E., *Chem. Rev.* **2009,** *109* (8), 3677-3707; (b) Tennyson, A. G.; Khramov, D. M.; Varnado, C. D., Jr.; Creswell, P. T.; Kamplain, J. W.; Lynch, V. M.; Bielawski, C. W., *Organometallics* **2009,** *28* (17), 5142-5147; (c) Williams, K. A.; Boydston, A. J.; Bielawski, C. W., *Chem. Soc. Rev.* **2007,** *36* (5), 729-744; (d) Boydston, A. J.; Bielawski, C. W., *Dalton Trans.* **2006,** (34), 4073-4077.

4.   Martinez-Agramunt, V.; Eder, T.; Darmandeh, H.; Guisado-Barrios, G.; Peris, E., *Angew. Chem. Int. Ed.* **2019,** *58* (17), 5682-5686.

5.   Martinez-Agramunt, V.; Ruiz-Botella, S.; Peris, E., *Chem. Eur. J.* **2017,** *23* (27), 6675-6681.

6.   (a) Ibañez, S.; Peris, E., *Angew. Chem. Int. Ed.* **2019,** *58* (20), 6693-6697; (b) Martínez-Agramunt, V.; Gusev, D.; Peris, E., *Chem. Eur. J.* **2018,** *24* (55), 14802-14807.

7.   (a) Ibanez, S.; Peris, E., *Chem. Eur. J.* **2018,** *24* (33), 8424-8431; (b) Ibanez, S.; Poyatos, M.; Peris, E., *Angew. Chem. Int. Ed.* **2018,** *57* (51), 16816-16820; (c) Ibañez, S.; Poyatos, M.; Peris, E., *Angew. Chem. Int. Ed.* **2017,** *56* (33), 9786-9790.

8.   Biz, C.; Ibáñez, S.; Poyatos, M.; Gusev, D.; Peris, E., *Chem. Eur. J.* **2017,** *23* (58), 14439-14444.

9.   Prades, A.; Poyatos, M.; Mata, J. A.; Peris, E., *Angew. Chem. Int. Ed.* **2011,** *50* (33), 7666-7669.

10.   Valdes, H.; Poyatos, M.; Peris, E., *Organometallics* **2013,** *32* (21), 6445-6451.

11.   Guex, N.; Peitsch, M. C., *Electrophoresis* **1997,** *18* (15), 2714-2723.

12.   Lima, J. C.; Rodriguez, L., *Chem. Soc. Rev.* **2011,** *40* (11), 5442-5456.

13.   Hwang, I.-h.; Hong, K.-I.; Jeong, K.-S.; Jang, W.-D., *Rsc Advances* **2015,** *5* (2), 1097-1102.

Supporting information for:

A twisted tetra-gold cyclophane from a fused bis-imidazolin-di-ylidene

by

Ana Gutiérrez-Blanco,[a,b] Susana Ibáñez Maella,[b] F. Ekkehardt Hahn,[a] Macarena Poyatos*[,b] and Eduardo Peris*[,b]

[a] *Institut für Anorganische und Analytische Chemie, Westfälische Wilhelms-Universität Münster, Corrensstraße 28-30, 48149 Münster, Germany*

[b] *Institute of Advanced Materials (INAM). Centro de Innovación en Química Avanzada (ORFEO-CINQA), Universitat Jaume I. Av. Vicente Sos Baynat s/n, Castellón, E-12071, Spain.*

Email: poyatosd@uji.es, eperis@uji.es

General considerations. 2,4,6,8-Tetraazabicyclo[3.3.0]octane,[1] [AuCl(SMe₂)][2] and 3,6-di-*tert*-butyl-1,8-diethynyl-9H-carbazole[3] were prepared according to the reported literature methods. All other reagents were used as received from commercial suppliers. NMR spectra were recorded on a Bruker 400 or 300 MHz, using $CDCl_3$ or DMSO-d_6 as solvents. Infrared spectra (FTIR) were performed on a Bruker Equinox 55 spectrometer equipped with a Pro One ATR (Jasco) with a spectral window of 4000-400 cm^{-1}. Electrospray mass spectra (ESI-MS) were recorded on a Micromass Quatro LC instrument; nitrogen was employed as drying and nebulizing gas. High Resolution Mass Spectra (HRMS) were recorded on a Q-TOF Premier mass spectrometer (Waters) with an electrospray source operating in the V-mode. Nitrogen was used as the drying and cone gas at flow rates of 300 and 30 Lh^{-1}, respectively. The temperature of the source block was set to 120 °C, and the desolvation temperature was set to 150 °C. Capillary voltage of 3.5 kV was used in the positive scan modes and the cone voltage was adjusted typically to 20 V. Mass calibration was performed by using solutions of NaI in isopropanol/water (1:1) from *m/z* 50 to 3000. Elemental analyses were carried out on a TruSpec Micro Series. UV-Visible absorption spectra were recorded on a Varian Cary 300 BIO spectrophotometer using dichloromethane under ambient conditions. Emission spectra were recorded on a modular Horiba FluoroLog-3 spectrofluorometer employing dichloromethane. PLQY was measured using a Hamamatsu integrating sphere at excitation wavelength of 315 nm.

1. Synthesis of the Au(I) complexes

1.1.   Synyhesis of the bis-imidazolidinium salt 1. N-Chlorosuccinimide (0.8 g, 6.3 mmol, 3 equiv.) was slowly added to a solution of 2,4,6,8-tetraazabicyclo[3.3.0]octane (1.0 g, 2.1 mmol, 1 equiv.) in degassed 1,2-dimethoxyethane (DME, 15 mL) at 0 °C. The resulting solution was allowed to

reach room temperature and then stirred for 18 h under the exclusion of light. The solid so formed was filtrated and washed subsequently with cold dichloromethane, THF and acetone. Yield: 77.8 mg (68 %). Electrospray MS (20 V, *m/z*): 503.5 [**1** − (2Cl) + OMe]$^+$ (calcd. for [1 − (2Cl) + OMe]$^+$: 503.3), 236.2 [1 − (2Cl)]$^{2+}$ (calcd. for [1 − (2Cl)]$^{2+}$: 236.1). Anal. Calcd. for $C_{32}H_{32}N_4Cl_2$ (542.9): C, 70.71; H, 5.93; N, 10.31. Found: C, 69.98; H, 5.90; N, 10.28. ^{1}H NMR (300 MHz, 298 K, DMSO-d_6): δ 9.51 (s, 2H, C*H*), 7.42-7.38 (m, 20H, C*H*$_{Ph}$), 6.53 (s, 2H, C*H*$_{bridge}$), 5.03 (d, $^2J_{H-H}$ = 15 Hz, 4H, C*H*$_{2\,Ph}$), 4.86 (d, $^2J_{H-H}$ = 15 Hz, 4H, C*H*$_{2\,Ph}$). ^{13}C{^{1}H} NMR (75 MHz, 298 K, DMSO-d_6): δ 162.32 (N*C*HN), 132.55 ($C_{q\,Ph}$), 128.92 (*C*H$_{Ph}$), 128.83 (*C*H$_{Ph}$), 128.63 (*C*H$_{Ph}$), 81.65 (*C*H$_{bridge}$), 51.03 (*C*H$_{2\,Ph}$).

1.2.   Synthesis of di-Au(I) complex 2. KHMDS (0.5M in toluene, 0.8 mL, 0.405 mmol, 2.2 equiv.) was added dropwise to a suspension of compound **1** (100.0 mg, 0.184 mmol, 1 equiv.) in THF (5 mL) at -78 °C. After stirring at that temperature for 30 minutes, the resulting solution was transferred *via* an oven dried cannula to a stirred THF solution (10 mL) of [AuCl(SMe$_2$)] (119.2 mg, 0.405 mmol, 2.2 equiv.). The temperature was allowed to reach – 20 °C, and then the volatiles were removed under reduced pressure. The resulting solid was suspended in dichloromethane. Under air, a spatula of charcoal was added, and the mixture was stirred for 30 minutes. The suspension was then filtered through oven dried Celite, washed with dichloromethane and the solvent was removed under vacuum. The solid was dissolved in the minimum amount of dichloromethane and precipitated with diethyl ether to afford the desired gold(I) complex as a white solid. Yield: 122.0 mg (69 %). Complex **2** was found light sensitive, which prevented a correct elemental analysis. ^{1}H NMR (400 MHz, 298 K, CDCl$_3$): δ 7.38-7.31 (m, 14H, C*H*$_{Ph}$), 7.13-7.06 (m, 6H, C*H*$_{Ph}$), 5.56 (d, $^2J_{H-H}$ = 16 Hz, 4H, C*H*$_{2\,Ph}$), 5.35 (s, 2H, C*H*$_{bridge}$), 4.54 (d, $^2J_{H-H}$ = 16 Hz, 4H, C*H*$_{2\,Ph}$). ^{13}C{^{1}H} NMR

(100 MHz, 298 K, CDCl$_3$): δ 198.40 (Au-$C_{carbene}$), 133.01 ($C_{q\ Ph}$), 129.71 (CH_{Ph}), 129.38 (CH_{Ph}), 127.38 (CH_{Ph}), 79.72 (CH_{bridge}), 54.20 ($CH_{2\ Ph}$).

1.3.   Synthesis of tetra-Au(I) complex 3. NaOH (22.45 mg, 0.561 mmol, 3.5 equiv.) and 3,6-di-*tert*-butyl-1,8-diethynyl-9H-carbazole (52.5 mg, 0.160 mmol, 1 equiv.) were placed together in a Schlenk tube. The tube was evacuated and filled with nitrogen three times. The solids were suspended in degassed MeOH (50 mL), and the resulting solution was refluxed for 2 h. After this time, the solution was allowed to reach room temperature. Complex **2** (150.0 mg, 0.160 mmol, 1equiv.) was added to the latter solution and the resulting suspension was refluxed overnight. The suspension was allowed to reach room temperature. After removal of the volatiles, the crude solid was suspended in dichloromethane and filtered through oven dried Celite. Complex **3** was isolated as a yellow solid. Yield: 129.4 mg (62 %). IR (ATR): ν(C≡C): 2099, 2090 cm^{-1}. HRMS ESI-TOF-MS (positive mode): 2381.0 [**3** + H]$^+$. (Calcd. for [**3** + H]$^+$: 2380.7). Anal. Calcd. for C$_{112}$H$_{106}$N$_{10}$Au$_4$ (2379.72): C, 56.52; H, 4.49; N, 5.89. Found: C, 56.62; H, 4.70; N, 5.92. ^{1}H NMR (400 MHz, 298 K, CDCl$_3$): δ 8.81 (s, 2H, N*H*), 7.87 (d, $^4J_{H-H}$ = 1.7 Hz, 4H, C*H*$_{carb}$), 7.58 (d, $^4J_{H-H}$ = 1.7 Hz, 4H, C*H*$_{carb}$), 7.38-7.36 (dd, $^2J_{H-H}$ = 3 Hz, 28H, C*H*$_{Ph}$), 7.20-7.18 (m, 12H, C*H*$_{Ph}$), 5.89 (d, $^2J_{H-H}$ = 16 Hz, 8H, C*H*$_{2\ Ph}$), 5.35 (s, 4H, C*H*$_{bridge}$), 4.62 (d, $^2J_{H-H}$ = 16 Hz, 8H, C*H*$_{2\ Ph}$), 1.36 (s, 36H, C(C*H*$_3$)$_{3\ carb}$). ^{13}C{^{1}H} NMR (75 MHz, 298 K, CDCl$_3$): δ 189.92 (Au-$C_{carbene}$), 141.90 ($C_{q\ carb}$), 139.09 ($C_{q\ carb}$), 133.38 ($C_{q\ Ph}$), 129.61 (CH_{Ph}), 129.22 (CH_{Ph}), 128.93 ($C_{q\ carb}$), 128.08 (CH_{carb}), 127.68 (CH_{Ph}), 122.94 ($C_{q\ acetyl}$), 118.03 ($C_{q\ acetyl}$), 115.64 (CH_{carb}), 107.12 ($C_{q\ carb}$), 79.79 (CH_{bridge}), 53.90 ($CH_{2\ Ph}$), 34.76 (C(CH$_3$)$_{3\ carb}$), 32.08 (C(CH$_3$)$_{3\ carb}$).
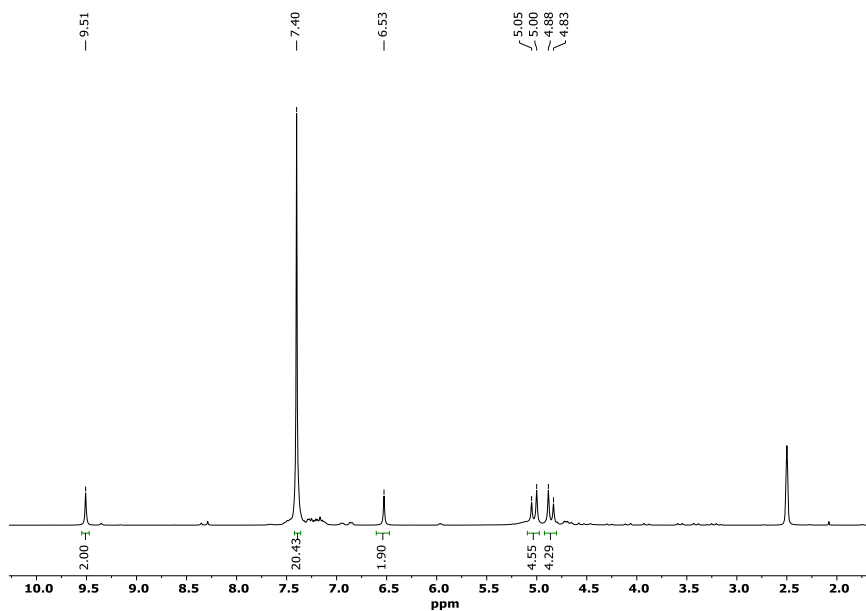
2. Spectroscopic data

Figure S1. ^{1}H NMR spectrum (300 MHz, DMSO-d_6) of bis-imidazolidinium salt **1**.

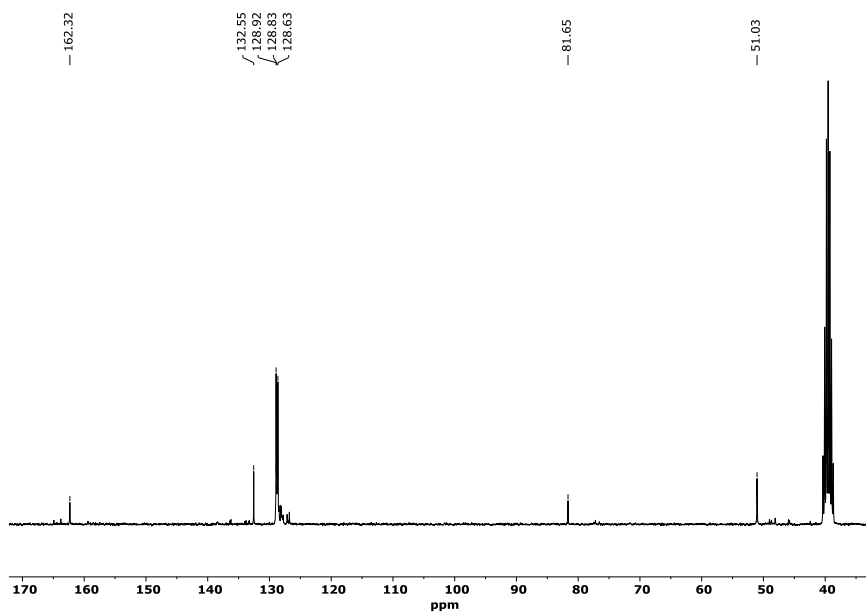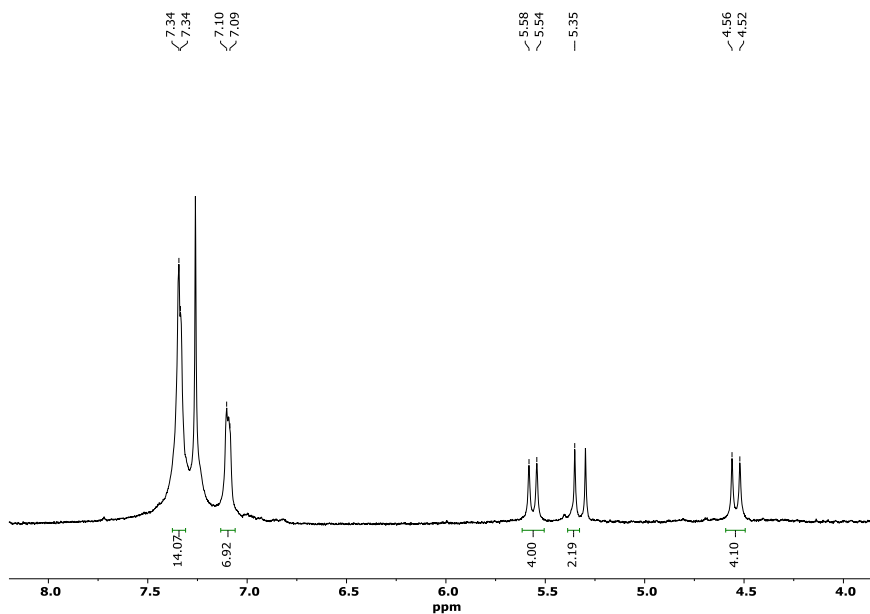**Figure S2.** ^{13}C {^{1}H} NMR spectrum (75 MHz, DMSO-d_6) of bis-imidazolidinium salt **1**.

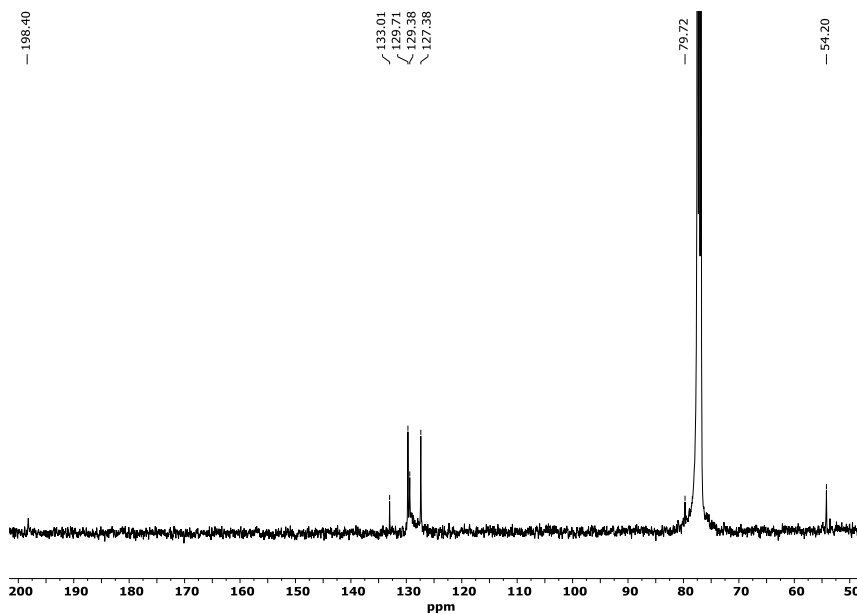**Figure S3.** ^{1}H NMR spectrum (400 MHz, CDCl$_3$) of di-Au(I) complex **2**.

Figure S4. ^{13}C {^{1}H} NMR spectrum (100 MHz, CDCl$_3$) of di-Au(I) complex **2**.
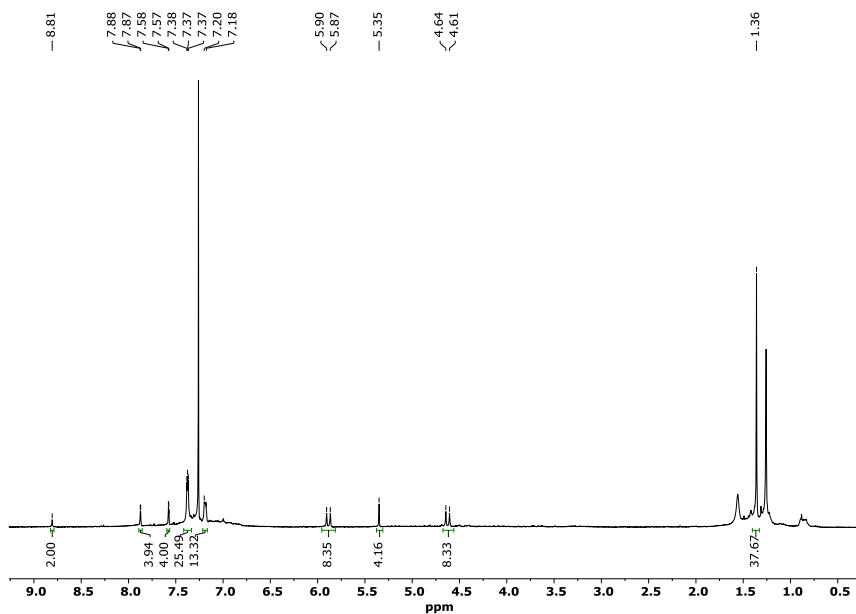
Figure S5. ^{1}H NMR spectrum (400 MHz, CDCl$_3$) of tetra-Au(I) complex **3**.
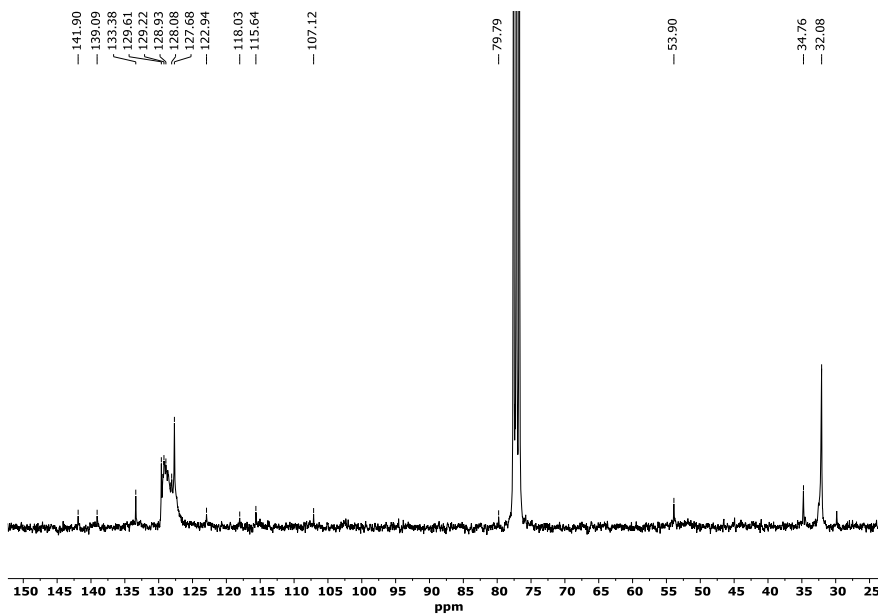

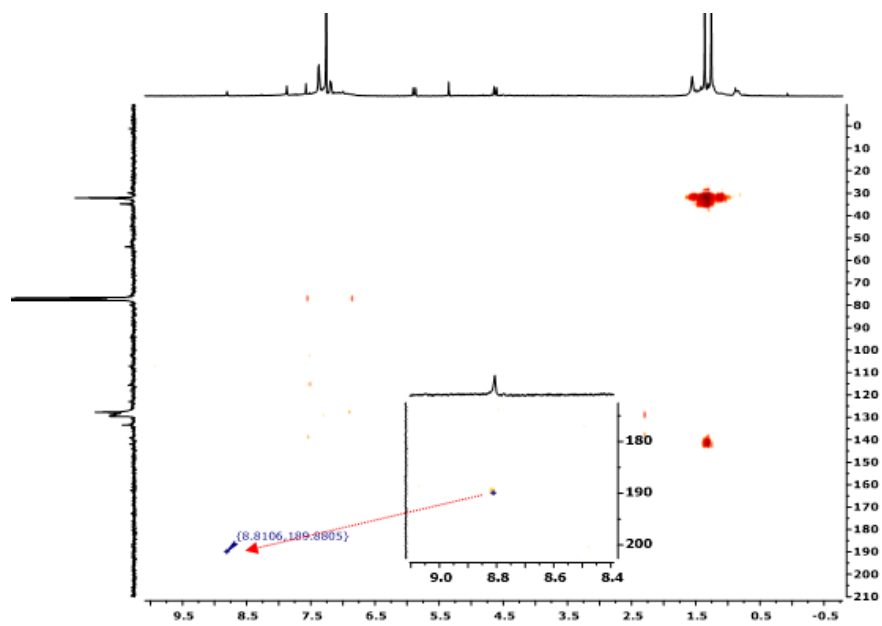**Figure S6.** ^{13}C {^{1}H} NMR spectrum (100 MHz, CDCl$_3$) of tetra-Au(I) complex **3**.

Figure S7. HMBC spectrum (400 MHz, CDCl$_3$) of tetra-Au(I) complex **3**.

3. X-Ray Crystallography

X-Ray Diffraction studies for complexes 2 and 3. Crystals suitable for X-Ray studies of complex **2** were obtained by slow evaporation of a concentrated solution of the complex in chloroform. Suitable crystals of complex **3** were obtained by slow diffusion of hexane into a concentrated solution of the complex in dichlorometane. Diffraction data of complexes were collected on an Agilent SuperNova diffractometer equipped with an Atlas CCD detector using Mo-Kα radiation (λ = 0.71073 Å). Single crystals were mounted on a MicroMount® polymer tip (MiteGen) in a random orientation. Absorption corrections based on the multi-scan method were applied. Using Olex2,[4] the structure of the two complexes was solved using Charge Flipping in Superflip[5] and refined with ShelXL[6] refinement package using Least Squares minimisation. Key details of the crystals and structure refinement data are summarized in Supplementary Table S1. Further crystallographic details can be found in the CIF files, which were deposited at the Cambridge Crystallographic Data Centre, Cambridge, UK. The reference number for complexes **2** and **3** were assigned as 1961185 and 1961186 respectively.

Table S1. Summary of crystal data, data collection, and structure refinement details

|	13	14
Empirical formula	$C_{132}H_{30}Au_2N_4Cl_2 \cdot 2/3CH_2Cl_2$	$C_{112}H_{106}Au_4N_{10} \cdot 11CHCl_3$
Formula weight	963.73	3692.98
Temperature/K	200(2)	200(4)
Crystal system	Monoclinic	Triclinic
Space group	$P2_1/n$	P-1
a/Å	13.9652(8)	11.6839(5)
b/Å	28.6096(19)	14.7840(7)
c/Å	16.5811(13)	22.4048(8)
α/°	90	86.592(3)
β/°	101.169(7)	75.809(3)
γ/°	90	81.581(4)
Volume/Å³	6499.3(8)	3710.4(3)
Z	8	1
ρ_{calc}mg/mm³	1.970	1.653
μ/mm⁻¹	9.266	4.583
F(000)	3648.0	1802.0
Crystal size/mm³	0.585 x 0.12 x 0.098	0.691 x 0.064 x 0.053
Radiation	Mo Kα (λ = 0.71073 Å)	Mo Kα (λ = 0.71073 Å)
2Θ range for data collection	5.11 to 52.744	5.018 to 52.68
Index ranges	-17 ≤ h ≤ 17, -34 ≤ k ≤ 35, -20 ≤ l ≤ 20	-14 ≤ h ≤ 14, -18 ≤ k ≤ 18, -27 ≤ l ≤ 24
Reflections collected	56401	29024
Independent reflections	56401 [R_{int} = 0.0467, R_{sigma} = 0.0953]	29024 [R_{int} = 0.0252, R_{sigma} = 0.1300]
Data/restraints/parameters	56401/12/748	29024/654/817
Goodness-of-fit on F²	1.031	1.016
Final R indexes [I>=2σ (I)]	R_1 = 0.0787, wR_2 = 0.1917	R_1 = 0.0895, wR_2 = 0.2301
Final R indexes [all data]	R_1 = 0.1249, wR_2 = 0.2323	R_1 = 0.1268, wR_2 = 0.2673
Largest diff. peak/hole / e Å⁻³	9.56/-4.82	4.48/-2.92

4. DOSY experiment
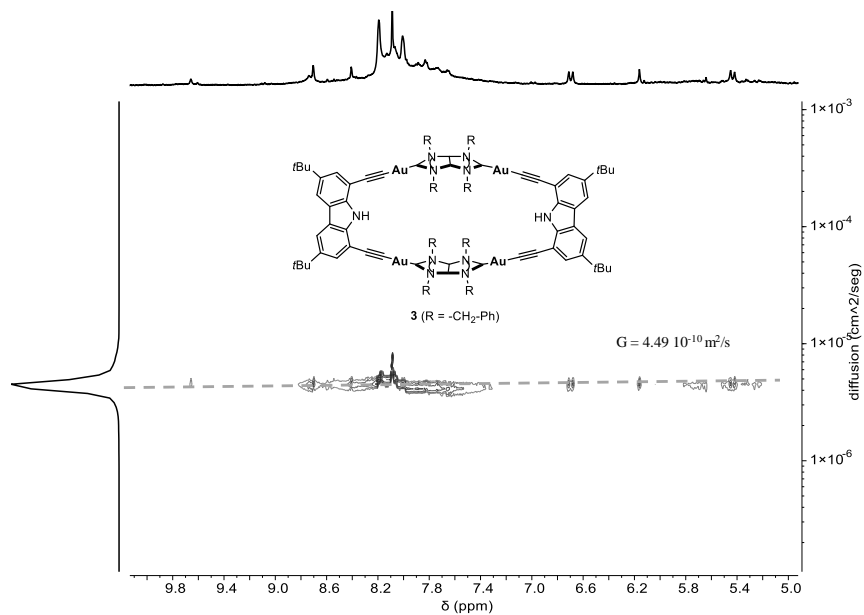
Figure S8. Diffusion Ordered NMR Spectrum (DOSY) of complex **3** (5 mM) in CDCl$_3$.

5. Photophysical studies

5.1. UV-visible spectra of complex 3
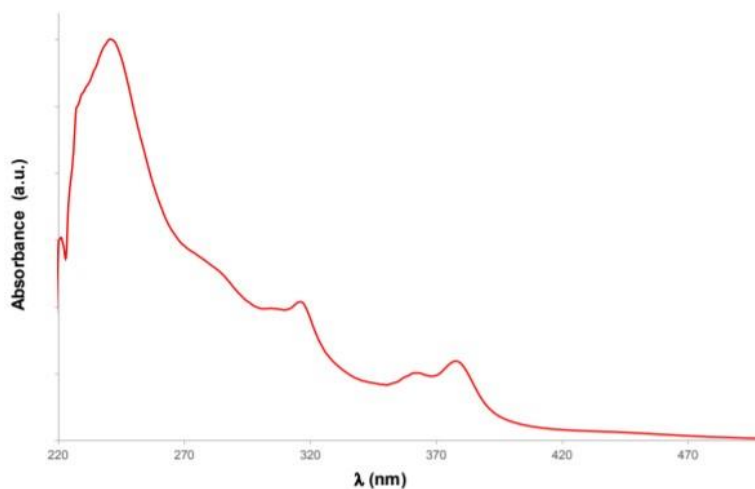

Figure S9. UV-vis spectra of complex **3**, recorded in dichloromethane at a concentration of 10^{-5} M, under aerobic conditions.
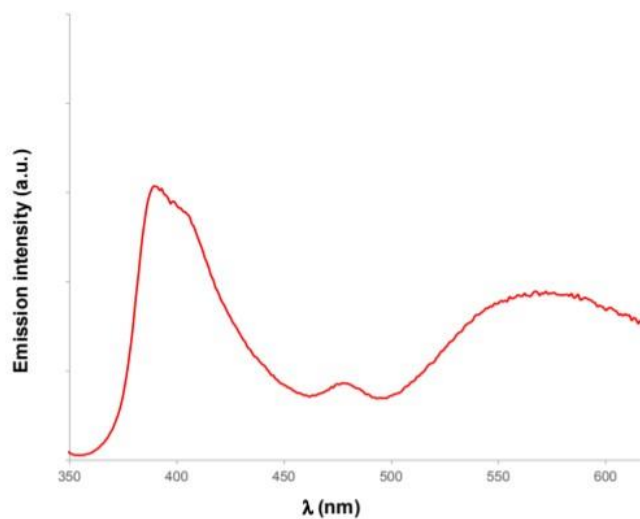
5.2. Emission spectra of complex 3

Figure S10. Emission spectra of complex **3** in dichloromethane (10^{-5} M under aerobic conditions) at 315 nm.

6. References

1.   Nielsen, A. T.; Nissan, R. A.; Chafin, A. P.; Gilardi, R. D.; George, C. F., *J. Org. Chem.* **1992,** *57* (25), 6756-6759.

2.   Uson, R.; Laguna, A.; Vicente, J., *J. Organomet. Chem.* **1977,** *131* (3), 471-475.

3.   Gee, H. C.; Lee, C. H.; Jeong, Y. H.; Jang, W. D., *Chem. Commun.* **2011,** *47* (43), 11963-11965.

4.   Dolomanov, O. V.; Bourhis, L. J.; Gildea, R. J.; Howard, J. A. K.; Puschmann, H., *J. Appl. Crystallogr.* **2009,** *42*, 339-341.

5.   (a) Palatinus, L.; Chapuis, G., *J. Appl. Crystallogr.* **2007,** *40*, 786-790; (b) Palatinus, L.; Steurer, W.; Chapuis, G., *J. Appl. Crystallogr.* **2007,** *40*, 456-462.

6.   Sheldrick, G. M., *Acta Crystallogr., Sect. A: Found. Crystallogr.* **2015,** *71*, 3-8.

6

Conclusions

In this final chapter of the Thesis are presented the conclusions of the attached publications, which have been published in renowned international journals.

Publication 1:

- A series of pyrene tetraalkynyl Au(I) complexes were synthesized and their photophysical properties studied.

- Two of these complexes have present quantum yields upper than 90% in CH_2Cl_2, placing them among the most emissive Au(I) complexes described to date in solution.

- The origin of the emissions is due to an intraligand transition. However, the introduction of gold atoms plays a key role allowing a bathochromic shift of the emissions and an astonishing enhancement of the quantum yields.

- Preliminary studies with one of the complexes on healthy cheek cells shown rapid and efficient taken up into the cells.

Publication 2:

- We report a new pyrene-tetra-imidazolium salt that was used for the preparation of tetrametallic (rhodium and iridium) complexes.

- The catalytic activity of the complexes was evaluated in two organic reactions of practical relevance to the pharmaceutical industry namely, the cyclization of acetylenic carboxylic acids and the reaction of diphenylcyclopropenone with substituted phenylacetylenes to form cyclopentadienones.

- The tetra-iridium complex is the first example tested in the coupling of diphenylcyclopropenone with substituted phenylacetylenes, showing higher activity than the tetra-rhodium one.

Publication 3:

- A novel tetra-Au-based cyclophane using an angular bis-imidazolindiylidene ligand was synthesized.

- The use of the rigid angular di-NHC ligand constitutes the basis to new Supramolecular Organometallic Complexes (SOCs) with different geometries not accessible with other poly-NHC ligands.

- We described a new synthetic procedure using the hinge-shaped ligand as building block. This methodology has the potential to produce new assemblies that incorporate polyaromatic panels and other effective sites, which will allow the production of receptors with interesting host-guest chemistry properties.

To sum up, different tetrametallic (gold, rhodium or iridium) complexes were synthesized. These new systems shown interesting results in different application fields, ranging from catalysis, luminescence and supramolecular chemistry. The obtention of these assemblies is a springboard for the synthesis of similar families of complexes which may present improved characteristics and in some of the cases, create the basis for an innovative research line.

Conclusiones

En este capítulo final de la Tesis se presentan las conclusiones de las publicaciones adjuntas, las cuales han sido publicadas en revistas de renombre internacional.

Publicación 1:

- Fueron sintetizados una serie de complejos de Au(I) pireno tetra-alquinilo y sus propiedades fotofísicas fueron estudiadas.

- Dos de esos complejos han presentado rendimientos cuánticos superiores al 90 % en CH_2Cl_2, colocándolos entre los complejos de Au(I) más emisivos en disolución descritos hasta la fecha.

- El origen de las emisiones es debido a una transición intraligando. Sin embargo, la introducción de los átomos de oro juega un papel clave permitiendo un desplazamiento batocrómico de las emisiones y un asombroso incremento del rendimiento cuántico.

- Estudios preliminares con uno de los complejos en células sanas de la mejilla mostraron un absorción rápida y eficiente dentro de las células.

Publicación 2:

- Hemos reportado una nueva sal de pireno tetra-imidazolio, la cual fue usada para la preparación de complejos tetra-metálicos (rodio e iridio).

- Se evaluó a actividad catalítica de los complejos en dos reacciones orgánicas de relevancia práctica para la industria farmacéutica llamadas, la ciclación de ácidos carboxílicos acetilénicos y la reacción de difenilciclopropenonas con fenilacetilenos sustituidos para formar ciclopentadienonas.

- El complejo de tetra-iridio es el primer ejemplo probado en el acoplamiento de difenilciclopropenona con fenilacetilenos sustituidos, mostrando una actividad catalítica mayor que el de tetra-rodio.

Publicación 3:

- Se sintetizó un nuevo ciclofano de tetra-oro usando un ligando bis-imidazolin-di-ilideno angular.

- El uso del ligando angular di-NHC rígido constituye las bases de nuevos Complejos Organometálicos Supramoleculares (SOCs) con diferentes geometrías que no son son accesibles con otro tipo de ligandos poli-NHC.

- Hemos descrito un nuevo procedimiento sintético usando un ligando con forma de bisagra como bloque de construcción. Esta metodología tiene el potencial de producir nuevas arquitecturas que incorporen paneles poliaromáticos y otro sitios eficaces, que permitirían la producción de receptores con propiedades químicas host-guest interesantes.

Para recapitular, fueron sintetizados diferentes complejos tetra-metálicos (oro, rodio o iridio). Estos nuevos sistemas muestran resultados interesantes en diferentes campos de aplicación, que van desde catálisis, luminiscencia y química supramolecular. La obtención de estas construcciones es un trampolín para la síntesis de familias de complejos similares que puedan presentar características mejoradas y en alguno de los casos, crear las bases para una línea de investigación innovadora.